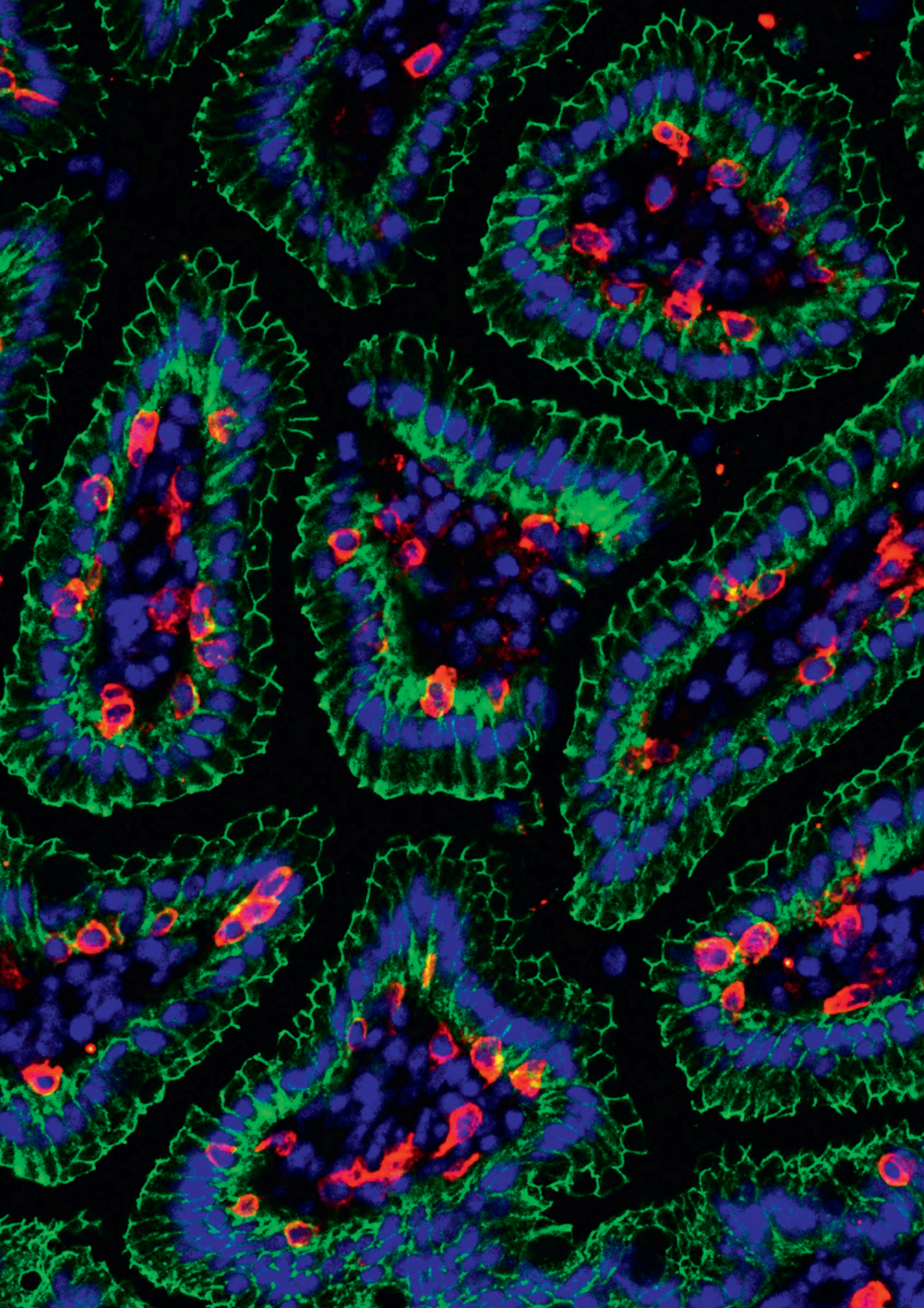


# Protecting intestinal epithelial integrity by galacto-oligosaccharides:

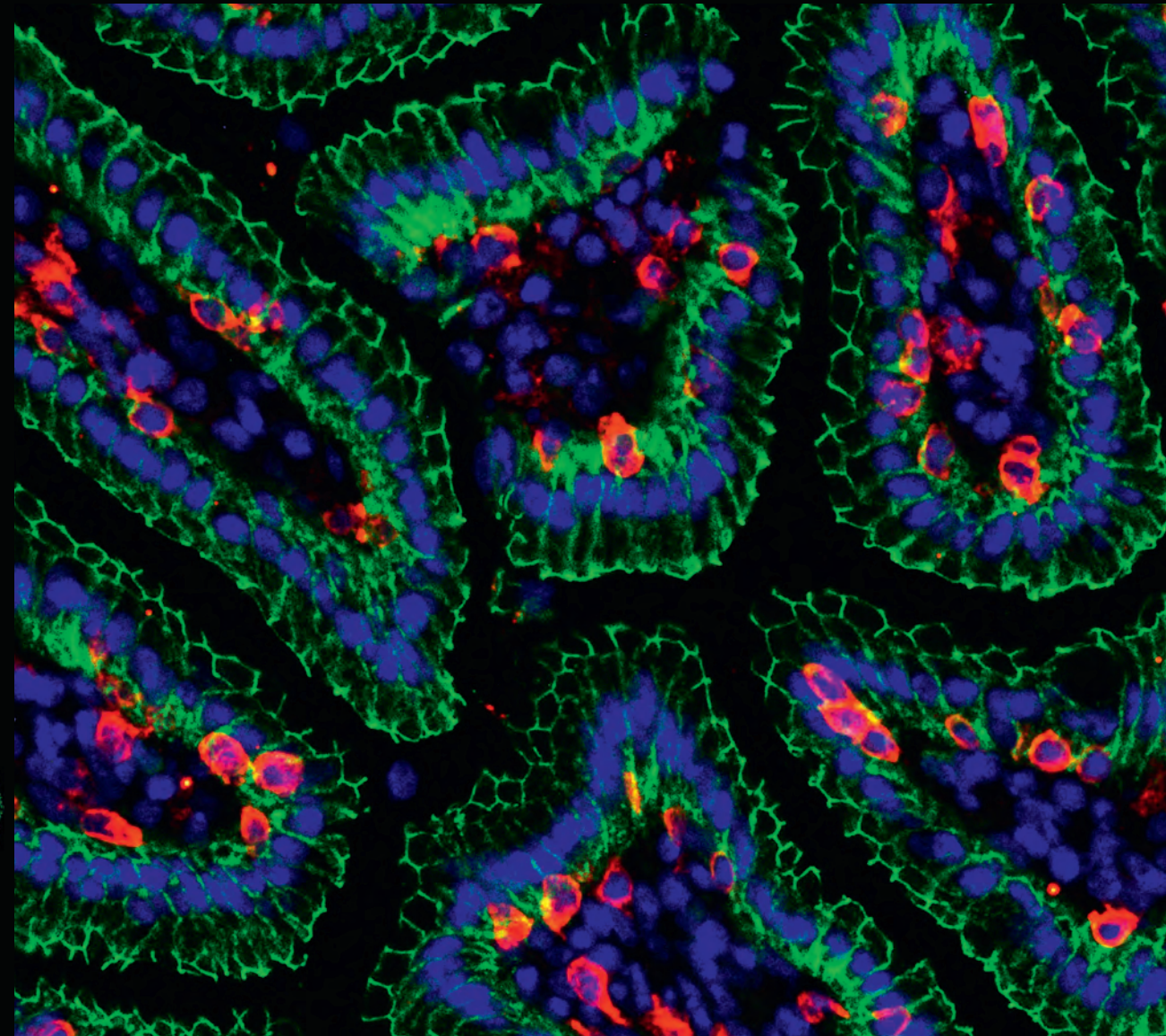
Keeping it tight



Protecting intestinal epithelial integrity by galacto-oligosaccharides: Keeping it tight



Peyman Akbari



Peyman Akbari



Protecting intestinal epithelial integrity  
by galacto-oligosaccharides:  
Keeping it tight

Peyman Akbari



The work of this thesis was carried out in close cooperation with Nutricia Research and FrieslandCampina and was part of the CCC WP-25 program: Immunomodulating properties of oligosaccharides from various sources.

The author gratefully acknowledges the generous support of the Nutricia Research.

Printing of this thesis was financially supported by: Nutricia Research, FrieslandCampina and Utrecht Institute for Pharmaceutical Sciences (UIPS).

Cover: Double-immunofluorescence staining using anti-E-cadherin (green) and anti-CD103 (red) antibodies on a mouse duodenal cryosection with DAPI counterstaining (blue). The image was taken by Rob Bleumink using the Olympus BX60 fluorescence microscope equipped with a Leica DFC450C camera at the Center for Cell Imaging from the Faculty of Veterinary Medicine, Utrecht University, Utrecht, The Netherlands.

Cover design: Ferdinand van Nispen and Peyman Akbari

Layout: Peyman Akbari

Printed by: GVO drukkers & vormgevers B.V. | Ponsen & Looijen, Ede, The Netherlands

ISBN: 978-90-6464-970-7

Copyright © 2016 Peyman Akbari

All rights reserved. No part of this thesis may be reproduced or transmitted in any form, by any means, without prior written permission of the author.



# Protecting intestinal epithelial integrity by galacto-oligosaccharides: Keeping it tight

De beschermende effecten van galacto-oligosacchariden  
op de integriteit van het darmepitheel

*(met een samenvatting in het Nederlands)*

## **Proefschrift**

ter verkrijging van de graad van doctor aan de Universiteit Utrecht  
op gezag van de rector magnificus, prof. dr. G. J. van der Zwaan,  
ingevolge het besluit van het college voor promoties  
in het openbaar te verdedigen op  
woensdag 23 maart 2016 des middags te 4.15 uur

door

**Peyman Akbari**

geboren op 17 september 1985  
te Tabriz, Iran



Promotoren: Prof. dr. J. Garssen

Prof. dr. J. Fink-Gremmels

Copromotoren: Dr. S. Braber

Dr. A. D. Kraneveld



To accomplish great things,  
we must not only act, but also dream;  
not only plan, but also believe.

*Anatole France*





*To children who have never had the opportunity to go to  
school*

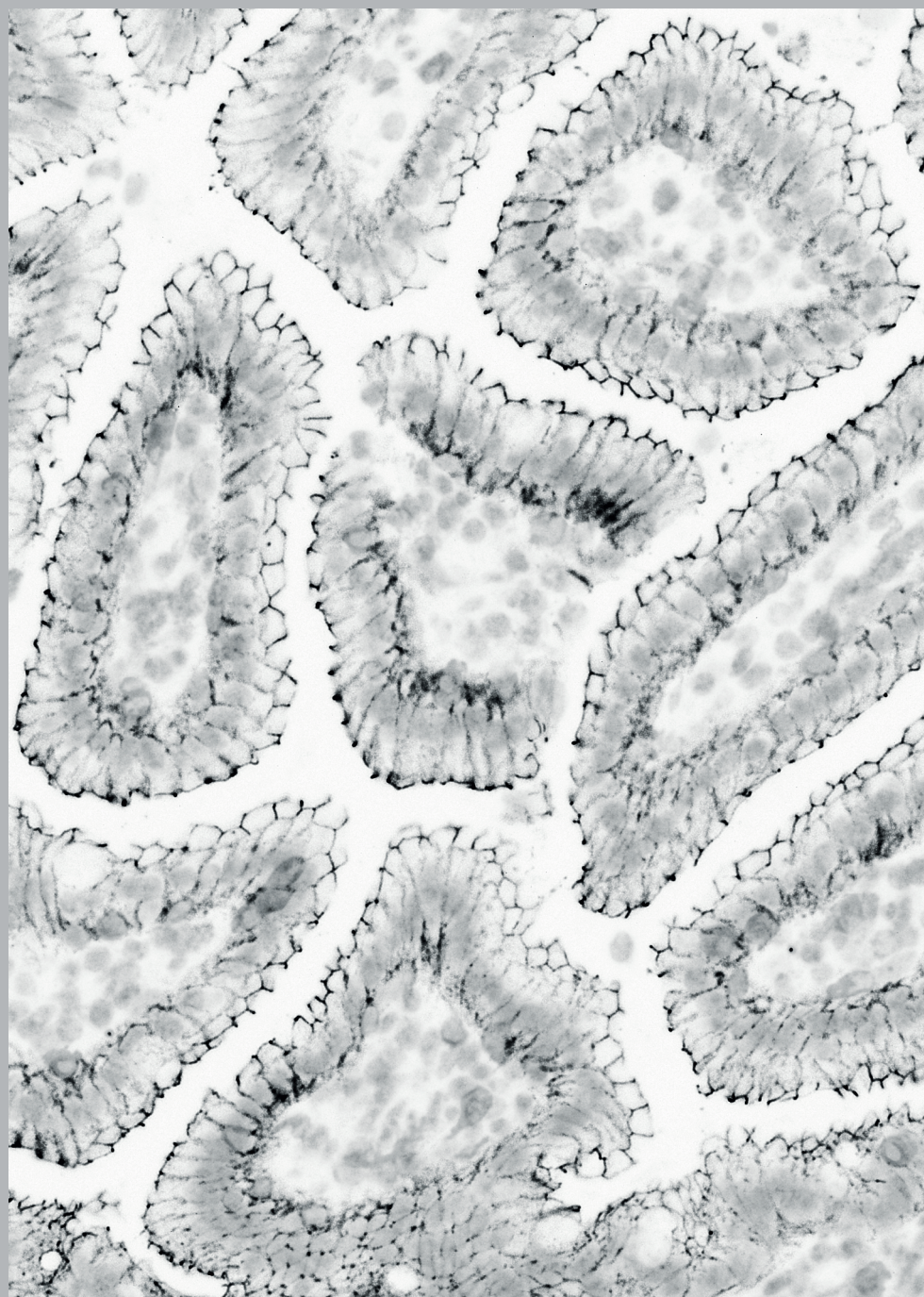
*To my great family for their love, inspiration and support  
throughout my life*



# Contents

Chapter 1	General introduction	11
Chapter 2	Intestinal epithelial tight junctions: molecular structure and importance in gut barrier integrity	19
Chapter 3	The intestinal barrier as an emerging target in the toxicological assessment of mycotoxins: a review	41
Chapter 4	Deoxynivalenol: a trigger for intestinal integrity breakdown	77
Chapter 5	Galacto-oligosaccharides protect the intestinal barrier by maintaining the tight junction network and modulating the inflammatory responses after a challenge with the mycotoxin deoxynivalenol in human Caco-2 cell monolayers and B6C3F <sub>1</sub> mice	115
Chapter 6	Characterizing microbiota-independent effects of oligosaccharides in intestinal epithelial cells: insight into the role of structure and size	147
Chapter 7	Inflammation-induced expression of the alarmin interleukin-33 can be suppressed by galacto-oligosaccharides	173
Chapter 8	General summary	193
Chapter 9	General discussion	205
Appendices	Nederlandse samenvatting	225
	Acknowledgements	231
	Curriculum Vitae	237
	List of publications & Awards	239





# *Chapter 1*



General introduction

The gastrointestinal tract harbours a dense and complex microbiota, which is colonized by various microbes during and immediately after birth. Gut colonization is a life-long process, however the early postnatal period is the most critical phase in the establishment of the gut microbial communities and an increasing body of evidence suggests that the initial colonization of the gut determines the development and reactivity of the immune system in later phases of life (1-5). For example, an early exposure of the gut to so-called “beneficial bacteria” is thought to significantly reduce the incidence of inflammatory, autoimmune and atopic diseases (6-9). Physiologically, a healthy gut flora is achieved by contact between the mother (skin) and the neonate and is supported by functional ingredients in breast milk (5).

In real life, however, the intestinal mucosa is also inevitably exposed to undesirable and potentially harmful substances ingested with food, including natural antigens, pathogens and toxins (10-12). Mycotoxins are the most frequent natural food contaminants occurring in the daily diet, and the structurally very diverse group of fungal metabolites, which has been associated with various adverse effects on human and animal health. Among them, the mycotoxin deoxynivalenol (DON), a member of the trichothecene family, is of specific concern and occurs in many staple foods such as cereals and grains, in particular wheat and wheat-based products. As a small, heat stable molecule, DON resists the technical processes of milling and food processing and can be detected in ready-to-consume food commodities (11, 13-15). DON has recently gained much attention, as it directly affects the intestinal barrier integrity (12, 16).

The intestinal barrier serves as a first line of host defense against potentially harmful stressors from the environment, ingested with food. It is primarily formed by epithelial cells, which are connected to each other by tight junction (TJ) proteins. TJ proteins form an anastomosing network sealing adjacent epithelial cells near the luminal surface, thus preventing a paracellular transport of luminal antigens into the systemic circulation. In addition, the intestinal epithelium contains mucus-secreting goblet cells and Paneth cells that actively secrete anti-microbial peptides (17, 18). Another line of defense is the lamina propria of the intestinal wall, which hosts the majority of mucosal immune cells of the body. The intestinal epithelial cells (IEC) can sense and respond to different stimuli to reinforce their barrier function and to participate in the coordination of appropriate immune responses, ranging from tolerance to the commensal bacteria to anti-pathogen immunity. IEC maintain a fundamental immunoregulatory function that influences the development and homeostasis of mucosal immune cells (17-22).

In neonates, the gastrointestinal barrier is immature in the first period of life and hence an increased epithelial permeability makes the infant very susceptible to natural antigens, pathogens and toxins. Exposure to these harmful stressors can result in nutrient malabsorption and immediate local inflammatory reactions, and even more important, there is increasing evidence that such challenges to the epithelial barrier in early phases



of life can lead to increased prevalence of many chronic inflammatory conditions, such as allergies and auto-immune diseases (9, 18, 23).

Human milk oligosaccharides (HMOs), a major component of colostrum, play an essential role in the postnatal growth and development of the intestinal and immune system (24, 25). As the sufficient supply of the neonate with HMOs cannot always be guaranteed (mastitis and other diseases of the nursing mother impairing full breast feeding), various attempts have been made to design alternative prebiotic oligosaccharides that mimic the health promoting effects of HMOs. At present, a mixture of non-digestible oligosaccharides, including galacto-oligosaccharides (GOS) and fructo-oligosaccharides (FOS), is widely used in infant formula aiming to provide an optimal alternative for HMOs. Although, these neutral oligosaccharides are structurally different from HMOs, they have prebiotic activities and clinical investigations have confirmed that infants given such a formula containing GOS/FOS achieve an intestinal microbiota composition comparable to that of breastfed infants (26-30).

Recent studies also indicate that health promoting effects of GOS/FOS are not limited to shaping of the intestinal microbiota and the microbiota associated immune responses (31-34). Hence, the investigations in this thesis aim to gain more insight into direct, microbiota-independent effects of non-digestible oligosaccharides on epithelial integrity and function. The mycotoxin DON was used as a model compound mimicking intestinal integrity breakdown in the *in vitro* and *in vivo* models described in this thesis.

### **Aims and outline of the thesis:**

The main aim of this thesis is to expand current knowledge regarding the gut health promoting effects of non-digestible oligosaccharides focusing on the protection of the intestinal barrier integrity and subsequent modulation of the associated immune responses.

### ***The following main objectives were addressed in this thesis:***

1. To assess the effects of non-digestible oligosaccharides on the intestinal integrity, a reproducible model that can be applied in comparative *in vitro* and *in vivo* studies is required. Taking into account that natural challenges can occur in real life, the mycotoxin DON was selected as a model compound to impair intestinal integrity and to study intervention strategies to prevent such a breakdown of the barrier function.
2. To determine and compare the protective effects of different non-digestible oligosaccharides against intestinal barrier disruption and to provide more insight into the role of oligosaccharides structure and size composition related to the direct, microbiota-independent interaction with intestinal epithelial cells.
3. To investigate the effect of non-digestible oligosaccharides on the immune system, in particular on the epithelial cell-derived cytokines, as well as on the Th2 mediated immune responses (IL-33/ST2 system) induced by epithelial damage.

***In line with these objectives, the following investigations are presented:***

**Chapter 1:** General introduction, describing the aims and outline of this thesis.

**Chapter 2:** Presents an overview of the importance of TJ proteins in maintaining the intestinal barrier function. In particular, the current knowledge on molecular structure, expression alongside the gastrointestinal tract and clinical relevance of different intestinal TJ proteins are summarized.

**Chapter 3:** Provides a summary of the available evidences regarding direct effects of various mycotoxins on the intestinal barrier integrity as dietary exposure of humans and animals to mycotoxins is of growing concern due to the apparently still increasing prevalence of these fungal toxins in food and feed commodities.

**Chapter 4:** This chapter focuses on the adverse effect of the mycotoxin DON, which triggers an intestinal integrity breakdown through a cascade of events eventually leading to the loss of epithelial barrier integrity as demonstrated by *in vitro* and *in vivo* experiments.

**Chapter 5:** The investigations described in this chapter demonstrate that GOS facilitate TJs reassembly and prevent the DON-induced intestinal (epithelial) barrier disruption and the related immune responses.

**Chapter 6:** In this chapter the hypothesis that the structure and size of individual oligosaccharides may determine the different effects, is investigated. The microbiota-independent effects of different oligosaccharides on the dysregulated intestinal epithelial barrier function and the related inflammatory response are compared. The investigations are conducted with Vivinal® GOS syrup and purified Vivinal GOS, fructo-oligosaccharides and Inulin as well as individual degree of polymerization (DP) fractions.

**Chapter 7:** This chapter aims to enhance our understanding of the immunomodulatory capacity of GOS, demonstrating the impact of dietary GOS intervention on IL-33 and ST2 expression in a murine model for intestinal barrier dysfunction.

**Chapter 8:** A comprehensive summary of the major findings obtained in this thesis is presented.

**Chapter 9:** In the general discussion, the most relevant findings of this thesis are discussed in terms of their clinical relevance and suggestions are presented for future research activities that can lead to the closer understanding of the complex mechanisms involved in the health-promoting effects of dietary non-digestible oligosaccharides.

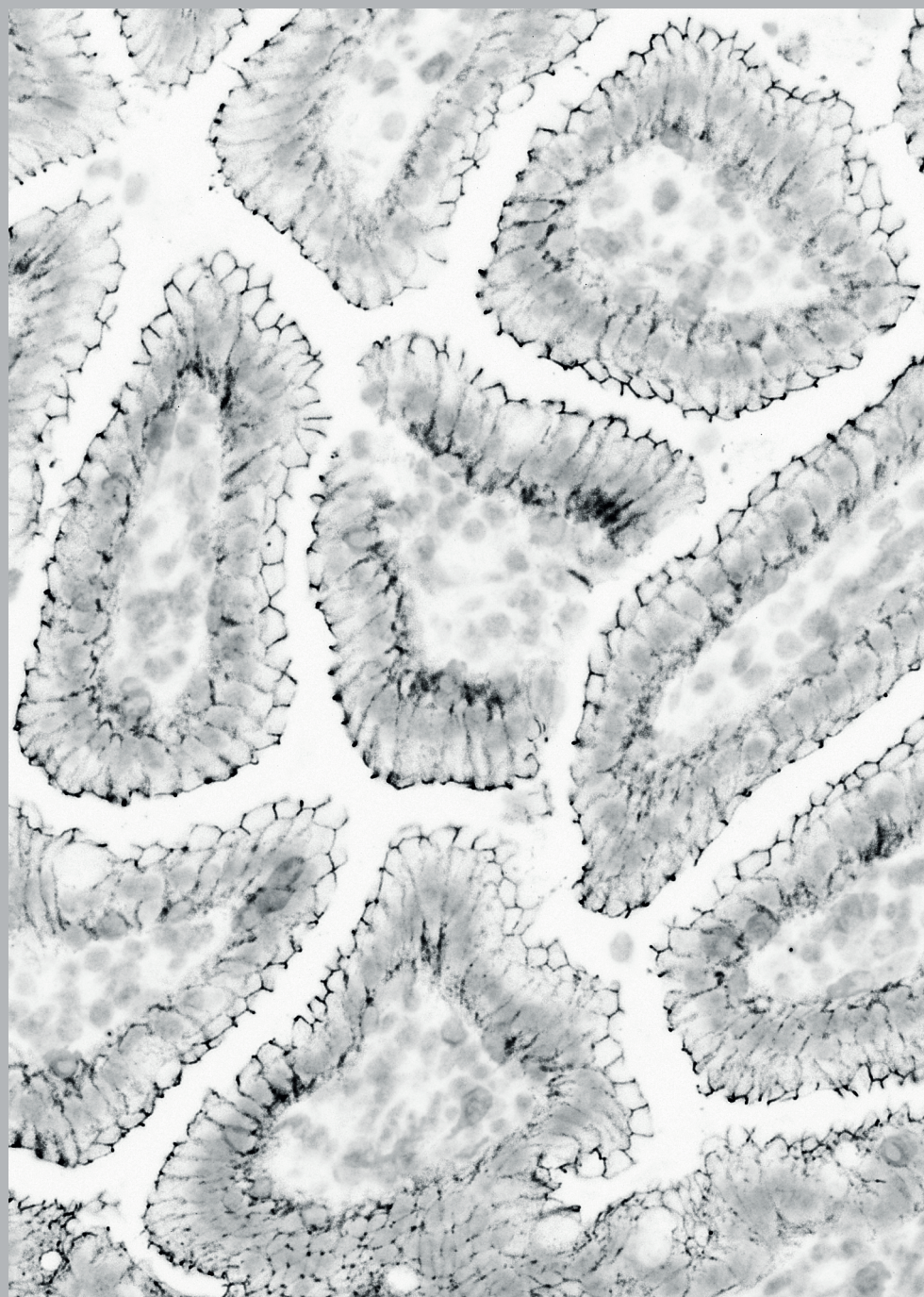
## References

1. Clemente JC, Ursell LK, Parfrey LW, Knight R. The impact of the gut microbiota on human health: an integrative view. *Cell* 2012;148:1258-1270.
2. O'Hara AM, Shanahan F. The gut flora as a forgotten organ. *EMBO Rep* 2006;7:688-693.
3. Mackie RI, Sghir A, Gaskins HR. Developmental microbial ecology of the neonatal gastrointestinal tract. *Am J Clin Nutr* 1999;69:S1035-S1045.
4. Round JL, Mazmanian SK. The gut microbiota shapes intestinal immune responses during health and disease. *Nat Rev Immunol* 2009;9:313-323.
5. Nicholson JK, Holmes E, Kinross J, Burcelin R, Gibson G, Jia W, Pettersson S. Host-gut microbiota metabolic interactions. *Science* 2012;336:1262-1267.
6. Wall R, Ross RP, Ryan CA, Hussey S, Murphy B, Fitzgerald GF, Stanton C. Role of gut microbiota in early infant development. *Clin Med Pediatr* 2009;3:45-54.
7. Sjogren YM, Jenmalm MC, Bottcher MF, Bjorksten B, Sverremermark-Ekstrom E. Altered early infant gut microbiota in children developing allergy up to 5 years of age. *Clin Exp Allergy* 2009;39:518-526.
8. Hooper LV. Bacterial contributions to mammalian gut development. *Trends Microbiol* 2004;12:129-134.
9. Martin R, Nauta AJ, Ben Amor K, Knippels LM, Knol J, Garssen J. Early life: gut microbiota and immune development in infancy. *Benef Microbes* 2010;1:367-382.
10. Berkes J, Viswanathan VK, Savkovic SD, Hecht G. Intestinal epithelial responses to enteric pathogens: effects on the tight junction barrier, ion transport, and inflammation. *Gut* 2003;52:439-451.
11. Bhat R, Rai RV, Karim AA. Mycotoxins in Food and Feed: Present Status and Future Concerns. *Compr Rev Food Sci Food Saf* 2010;9:57-81.
12. Pinton P, Oswald IP. Effect of deoxynivalenol and other Type B trichothecenes on the intestine: a review. *Toxins* 2014;6:1615-1643.
13. Pestka JJ. Deoxynivalenol: mechanisms of action, human exposure, and toxicological relevance. *Arch Toxicol* 2010;84:663-679.
14. Wu F, Groopman JD, Pestka JJ. Public health impacts of foodborne mycotoxins. *Annu Rev Food Sci Technol* 2014;5:351-372.
15. Sobrova P, Adam V, Vasatkova A, Beklova M, Zeman L, Kizek R. Deoxynivalenol and its toxicity. *Interdiscip Toxicol* 2010;3:94-99.
16. Pierron A, Mimoun S, Murate LS, Loiseau N, Lippi Y, Bracarense AF, Liaubet L, Schatzmayr G, Berthiller F, Moll WD, *et al.* Intestinal toxicity of the masked mycotoxin deoxynivalenol-3-beta-D-glucoside. *Arch Toxicol* 2015.
17. Peterson LW, Artis D. Intestinal epithelial cells: regulators of barrier function and immune homeostasis. *Nat Rev Immunol* 2014;14:141-153.
18. Groschwitz KR, Hogan SP. Intestinal barrier function: molecular regulation and disease pathogenesis. *J Allergy Clin Immunol* 2009;124:3-20.
19. Bischoff SC. 'Gut health': a new objective in medicine? *BMC Med* 2011;9:24.
20. Mowat AM. Anatomical basis of tolerance and immunity to intestinal antigens. *Nat Rev Immunol* 2003;3:331-341.
21. Vaishnava S, Yamamoto M, Severson KM, Ruhn KA, Yu X, Koren O, Ley R, Wakeland EK, Hooper LV. The antibacterial lectin RegIIIgamma promotes the spatial segregation of microbiota and host in the intestine. *Science* 2011;334:255-258.
22. Schenk M, Mueller C. The mucosal immune system at the gastrointestinal barrier. *Best Pract Res Clin Gastroenterol* 2008;22:391-409.
23. O'Connell EJ. Pediatric allergy: a brief review of risk factors associated with developing allergic disease in childhood. *Ann Allergy Asthma Immunol* 2003;90:53-58.
24. Bode L. Human milk oligosaccharides: every baby needs a sugar mama. *Glycobiology* 2012;22:1147-1162.
25. Donovan SM, Wang M, Li M, Friedberg I, Schwartz SL, Chapkin RS. Host-microbe interactions in the neonatal intestine: role of human milk oligosaccharides. *Adv Nutr* 2012;3:S450-S455.



26. Bode L. The functional biology of human milk oligosaccharides. *Early Hum Dev* 2015;91:619-622.
27. Boehm G, Stahl B. Oligosaccharides from milk. *J Nutr* 2007;137:S847-S849.
28. Fanaro S, Boehm G, Garssen J, Knol J, Mosca F, Stahl B, Vigi V. Galacto-oligosaccharides and long-chain fructo-oligosaccharides as prebiotics in infant formulas: a review. *Acta Paediatr* 2005;94:22-26.
29. Moro G, Minoli I, Mosca M, Fanaro S, Jelinek J, Stahl B, Boehm G. Dosage-related bifidogenic effects of galacto- and fructooligosaccharides in formula-fed term infants. *J Pediatr Gastroenterol Nutr* 2002;34:291-295.
30. Boehm G, Moro G. Structural and functional aspects of prebiotics used in infant nutrition. *J Nutr* 2008;138:S1818-S1828.
31. Varasteh S, Braber S, Garssen J, Fink-Gremmels J. Galacto-oligosaccharides exert a protective effect against heat stress in a Caco-2 cell model. *J Funct Foods* 2015;16:265-277.
32. Bhatia S, Prabhu PN, Benefiel AC, Miller MJ, Chow J, Davis SR, Gaskins HR. Galacto-oligosaccharides may directly enhance intestinal barrier function through the modulation of goblet cells. *Mol Nutr Food Res* 2015;59:566-573.
33. de Kivit S, Kraneveld AD, Knippels LM, van Kooyk Y, Garssen J, Willemsen LE. Intestinal epithelium-derived galectin-9 is involved in the immunomodulating effects of nondigestible oligosaccharides. *J Innate Immun* 2013;5:625-638.
34. Zenhom M, Hyder A, de Vrese M, Heller KJ, Roeder T, Schrezenmeir J. Prebiotic oligosaccharides reduce proinflammatory cytokines in intestinal Caco-2 cells via activation of PPARgamma and peptidoglycan recognition protein 3. *J Nutr* 2011;141:971-977.





# Chapter 2



## Intestinal epithelial tight junctions: molecular structure and importance in gut barrier integrity

Peyman Akbari<sup>1,2</sup>, Saskia Braber<sup>1</sup>, Johan Garssen<sup>2,3</sup>, Johanna Fink-Gremmels<sup>1</sup>

<sup>1</sup> Division of Veterinary Pharmacology, Pharmacotherapy and Toxicology, Institute for Risk Assessment Sciences, Utrecht University, Utrecht, The Netherlands

<sup>2</sup> Division of Pharmacology, Utrecht Institute for Pharmaceutical Sciences, Faculty of Science, Utrecht University, Utrecht, The Netherlands

<sup>3</sup> Nutricia Research, Utrecht, The Netherlands

## **Abstract**

The gut mucosa is continuously challenged by a diverse microbial community, foreign antigens as well as toxic molecules. Therefore, the regulation of the intestinal barrier appears to be crucial for gut immune homeostasis and its impairment results in increased exposure of the mucosal innate and acquired immune system to the pro-inflammatory molecules. The intestinal barrier is primarily formed by epithelial cells, connected by tight junctions, which form an anastomosing network sealing adjacent epithelial cells near the luminal surface, thus preventing a paracellular transport of luminal antigens into the systemic circulation. Tight junctions are dynamic structures with a complex architecture and are composed of different transmembrane and cytoplasmic scaffolding proteins. Transmembrane tight junction proteins form a linear barrier at the apical-lateral membrane of the cell and consist of occludin, claudins, junctional adhesion molecules and tricellulin. The cytoplasmic scaffolding proteins, including zonula occludens proteins, cingulin and afadin, provide a direct link between transmembrane tight junction proteins and the intracellular cytoskeleton, which plays a crucial role in regulating the tight junctions-based integrity. Each individual component of the tight junction network is structurally and functionally different, but closely interacts with each other to form an efficient intestinal barrier. This review aims to describe the molecular structure and expression of intestinal epithelial tight junction proteins and to characterize the detailed architecture, organization and interaction of some of the key tight junction proteins.



## Introduction

The interplay between the host and environment holds the key to health and well-being. A major unit of this interaction is the gastrointestinal tract due to I) the large surface area of approximately 400 m<sup>2</sup>, which may be exposed to foreign antigens and toxic molecules, II) its diverse microbial community, and III) the complex system of mucosal immune cells that facilitate the major innate and adaptive defense mechanisms (1-5). Maintenance of gut immune homeostasis depends on the capacity of the intestinal barrier to create the separation between luminal antigens, including microbial communities, and mucosal immune cells.

Increased epithelial permeability to food-born allergens, pathogens and toxins leads to local inflammatory reactions and nutrient malabsorption, which are considered not only in terms of immediate disease conditions, but more importantly as factors increasing the prevalence of many chronic inflammatory conditions, auto-immune diseases as well as allergies (6-11).

Maintenance of the intestinal barrier is acquired by a variety of specific and non-specific mechanisms, but intestinal epithelial cells form a first line of host defense against potentially harmful stressors reaching the luminal environment (1, 5, 7, 11).

The lining epithelial cells are connected by multiple protein structures denoted as apical junctional complexes, including tight junctions (TJs), adherens junctions and desmosomes (Figure 1) (12). Adherens junctions play a role in initiation and stabilization of cell-cell contacts through a family of intercellular adhesion molecules and consist of transmembrane proteins, including E-cadherin and nectin as well as associated cytoplasmic proteins catenins, which are directly connected to the actin cytoskeleton (13). Desmosomes are patch-like intercellular junctions at the lateral sides of plasma membranes that join adjacent cells together and provide anchoring sites for intermediate filaments (14).

TJ proteins are thought to be the most essential components of these multiple structures and it is now well-established that the mucosal barrier function cannot be maintained without a well-organized pattern of this anastomosing network of sealing strands comprising over 50 proteins. The intercellular space completely disappears at the level of TJs, whereas in adherens junctions and desmosomes, the adjacent membranes are 15-20 nm apart (Figure 1) (12-16). Each individual component of the TJ network is structurally and functionally different, but closely interacts with each other to form an efficient and functional barrier.

This review aims to describe the molecular structure and expression of intestinal epithelial TJ proteins and to characterize the detailed architecture, organization and interaction of some of the key TJ proteins.

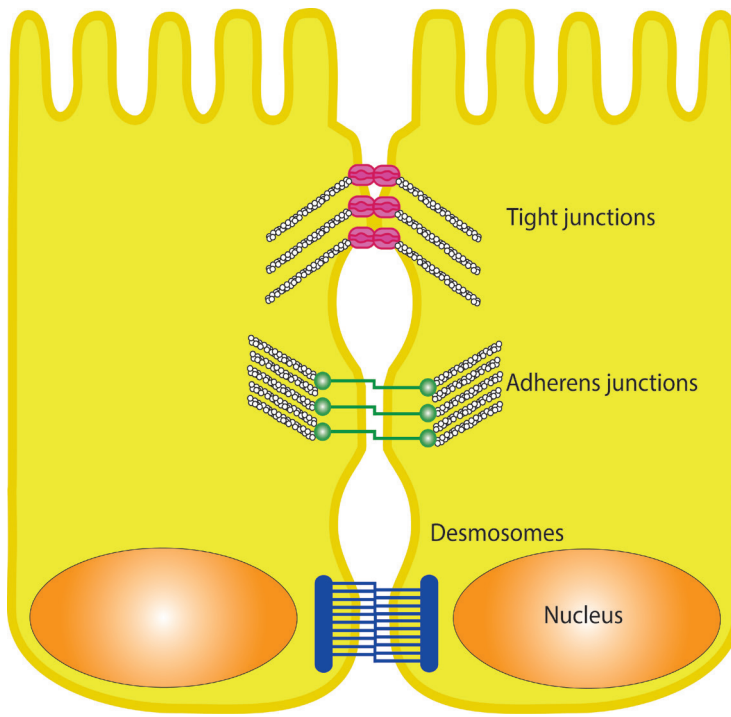


**Figure 1.** Schematic illustration of the epithelial junctional complexes. The intestinal epithelial barrier is primarily regulated by the junctional complexes consisting of tight junctions (TJs), adherens junctions and desmosomes. TJs are the most apical structures, followed by adherens junctions and desmosomes that are located along the lateral membrane. In contrast to TJs, the intercellular space does not completely disappear at the level of adherens junctions and desmosomes. TJs and adherens junctions are linked to the actin filaments (white circles). The illustration is reproduced from Terry *et al.* (17).

### Molecular architecture of TJs

TJs are dynamic structures with a complex architecture that seal adjacent epithelial cells near the luminal surface and thus prevent a paracellular transport of luminal antigens. TJ proteins are composed of I) transmembrane proteins whose extracellular domains cross the plasma membrane and interact with their partners on the adjacent cells and II) cytoplasmic scaffolding proteins, which are entirely located on the intracellular side of the plasma membrane. Transmembrane TJ proteins form a linear barrier at the apical-lateral membrane of the cell and consist of occludin (OCLN), claudins (CLDNs), junctional adhesion molecules (JAMs) and tricellulin. The cytoplasmic scaffolding proteins, including zonula occludens (ZO) proteins, cingulin and afadin, provide a direct link between transmembrane TJ proteins and the intracellular cytoskeleton. The cytoskeleton plays a crucial role in the regulation of TJ-based integrity (14, 18-20). TJ proteins are differentially expressed along the gastrointestinal tract, and this expression pattern is probably related

to the differences in accessibility to luminal substances between individual intestinal segments. As an example, it has been shown that TJ proteins are less expressed in crypts compared to the expression pattern in villi, hence, intercellular tightness is increasing from the crypt to the villus (19, 21-24). The molecular structure, the expression pattern and the function as well as clinical relevance of each TJ proteins will be separately explained in the following section.

### **Occludin (OCLN)**

#### ***Molecular Structure***

OCLN (~65 kDa) is the first discovered TJ protein with a critical role in sealing the adjacent cells and contains one intracellular, two neutral extracellular loops, four transmembrane domains, a short NH<sub>2</sub>-terminal cytoplasmic domain and a long COOH-terminal cytoplasmic domain (Figure 2) (22).

#### ***Expression***

It has been shown that OCLN has a consistent expression throughout the entire mouse intestine and appears as distinct dot-like or line-forming structures at the apical region of the lateral plasma membrane of the epithelial cells of a villus (25-28). However, only the phosphorylated form of OCLN is subjected into the intracellular junctional complexes, whereas the non-phosphorylated OCLN is distributed in an erratic expression pattern along the basolateral plasma membrane and therefore this form does not regulate barrier integrity (15, 20, 29).

#### ***Intestinal barrier function***

Homophilic interaction between the extracellular loops of OCLN with the identical loops originating from OCLN in the adjacent cells seems to form a barrier against macromolecules, but not against small ions (15, 20, 29, 30). The COOH-terminal cytoplasmic domain has been shown to be required for correct targeting of OCLN to the TJ network. The link between OCLN and the intracellular cytoskeleton is also documented through the interaction of COOH terminus with several cytoplasmic scaffolding TJ proteins, such as ZO proteins (Figure 2 and Figure 4) (22). Controversial findings have been reported regarding the role of OCLN in the regulation of paracellular permeability, since OCLN knockout mice showed well-organized TJ architecture and a normal barrier function comparable to those observed in wild type mice. On the other hand, different *in vivo* studies support the concept that OCLN is a functional component of the TJ network and has a convincing role in the regulation of paracellular permeability (15, 20, 31-33). It is further shown that OCLN has a role in TJs reassembly since the absence of OCLN in canine MDCK epithelial cells causes a pronounced decrease in expression of CLDNs and transepithelial electrical resistance (TEER) recovery. However, the expression of ZOs and JAM-A are not affected in OCLN knockdown MDCK cells (34).

### Clinical relevance

Decreased protein expression and redistribution of OCLN have been observed in the intestines of patients with Crohn's disease, ulcerative colitis, coeliac disease and irritable bowel syndrome (7, 35-38). In addition, small intestinal biopsy specimens of patients with food allergy exposed to food allergens showed a decreased protein expression of OCLN compared to those from normal subjects (39).

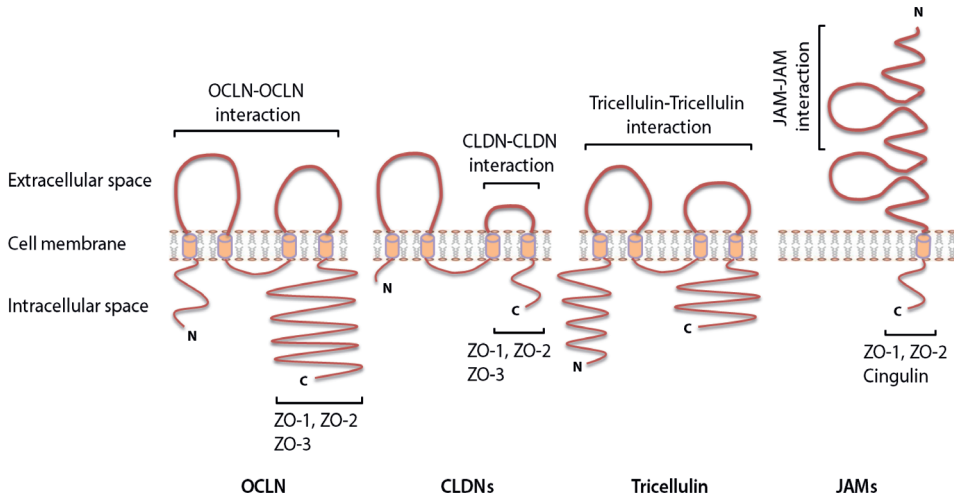


**Figure 2.** Schematic representation of the molecular structure of different transmembrane tight junction (TJ) proteins and the related direct interaction with different transmembrane as well as cytoplasmic scaffolding proteins. OCLN, CLDNs and tricellulin have similar topography, with one intracellular, two extracellular loops, four transmembrane domains, cytoplasmic N- and C-terminal domains. JAMs are characterized by two extracellular Ig-like domains, a transmembrane domain and a C-terminal cytoplasmic domain. The C-terminal cytoplasmic domain has been shown to be crucial in membrane targeting of OCLN, CLDNs and JAMs to the TJ network, whereas both N- and C-terminal domains of tricellulin seem to play a relevant role in tricellulin localization at the TJ network. Homophilic interactions of different transmembrane TJ proteins from adjacent cells (between proteins of the same kind) are mediated through the two extracellular loops (OCLN and tricellulin), second extracellular loop (CLDNs) or membrane-distal extracellular Ig-like domains (JAMs). The C-terminal domain of OCLN, CLDNs and JAMs interact with different cytoplasmic scaffolding TJ proteins, including ZO-1 and ZO-2, by which they are connected to the actin cytoskeleton. C, COOH-terminal domain; CLDNs, claudins; JAMs, junctional adhesion molecules; N, NH<sub>2</sub>-terminal domain; OCLN, occludin; ZO-1, zonula occludens-1.

## **Claudins (CLDNs)**

### ***Molecular Structure***

CLDNs (~20-27 kDa) consist of one intracellular loop, two extracellular loops, four transmembrane domains, a short NH<sub>2</sub>-terminal cytoplasmic domain together with a longer COOH-terminal cytoplasmic domain (Figure 2); however a few members of the CLDN family exhibit a different structure (22, 40). CLDN5, -16 and -25, for example, have a higher molecular mass owing to the long NH<sub>2</sub> terminus (40). It is well known that the half-life of CLDNs mainly depends on length and relevant amino acid sequences of the COOH-terminal cytoplasmic domain (19, 41). A strong correlation has been previously reported between length of the cytoplasmic domains of CLDNs and their half-lives; for example, the cytoplasmic domain of CLDN2 is two times as long as the cytoplasmic domain of CLDN4, whereas the half-life of CLDN2 is more than 3-fold higher compared to CLDN4 (41). The first extracellular loop of CLDNs is recognized by well-conserved charged amino acids, although the number, nature and orientation of charges are different depending on the CLDN type (40, 42, 43). In this respect, CLDN10b, -13 and -17 possess positively charged residues and CLDN2, -7, -10a, -12 and -15 carry negatively charged residues. The charge selective properties of the first extracellular loop enable CLDNs to create paracellular pores for small ions. It is shown that positively and negatively charged CLDNs act as anion and cation pores, respectively (22, 29, 40, 44, 45).

### ***Expression***

Twenty-seven members of the CLDN family are recognized so far in rodents, however their expression in humans is not identical. Twenty-six CLDNs have been discovered by genomic cloning in humans, but the rodent CLDN13 does not have a human homolog (40, 46). Gene expression of CLDN1-27 is profiled and all members, except CLDN6, -9, -11, -16, -19 and -22, have also been distinguished throughout the mouse intestine (25, 40, 46-48). However, the majority of the CLDNs show an inconstant expression pattern throughout the different segments of the gastrointestinal tract. For example, the expression pattern of the different CLDNs along the entire mouse intestine is summarized in Table 1. In addition, CLDNs show a different subcellular distribution alongside the intestinal epithelium. For example, CLDN1 and CLDN3 are expressed laterally between adjacent cells along the crypt-to-villus axis, whereas CLDN2 distribution is mainly restricted to the crypts of the entire intestine. CLDN4 is predominantly expressed in the upper part of the villi alongside the entire intestine. On the contrary, CLDN7 is more expressed on the basolateral surfaces of the intestinal epithelium compared to the apical surfaces (19, 25, 47, 49-51).

### ***Intestinal barrier function***

CLDNs appear to be the major structural components of the TJ proteins and are known as the backbone of the TJ network (52). It has been previously discovered that the second extracellular loop of CLDNs is critically involved in homo- and heterophilic interactions between CLDNs. These interactions among CLDN members are previously claimed to be

much stronger than those of the other TJ proteins, including OCLN-OCLN interaction or tricellulin-tricellulin interaction (Figure 2) (40, 53). The COOH-terminal cytoplasmic domain has been shown to be crucial in membrane targeting of CLDNs to the TJ network and mutations in this domain result in internalization and subsequent degradation of CLDNs (19, 40). In addition, the COOH-terminus of all CLDNs (with the exception of CLDN12, -16, -19a, -21 and -24 to -27) ends in PDZ-binding motifs interacting with PDZ domains of scaffolding protein, including ZO-1, ZO-2 and ZO-3, which are subsequently connected to the intracellular cytoskeleton (Figure 2 and Figure 4) (40, 54, 55). The phenotypes of CLDN knockout mice reveal the importance of specific CLDNs for development, viability and intestinal integrity. For example, CLDN1 and CLDN5 knockout mice die shortly after birth; whereas CLDN7 knockout mice have severe intestinal defects, including mucosal ulcerations, epithelial cell sloughing, villi disruption, significant intercellular gaps between adjacent epithelial cells, enhanced paracellular permeability and colonic inflammation (40, 51, 56).

**Table 1.** The expression pattern of different CLDNs along the mouse intestine (19, 25, 49, 51)

	Duodenum	Jejunum	Ileum	Colon
<b>CLDN3</b>	+	++	+++	++++
<b>CLDN4</b>	++++	+++	++	+
<b>CLDN7</b>	++++	++++	++++	++++
<b>CLDN8</b>	-	-	+	++
<b>CLDN12</b>	+	+++	++++	++
<b>CLDN13</b>	-	-	-	++
<b>CLDN15</b>	+++	++++	++	+

The degree of the expression is defined as ranging from not expressed (-) to strongly expressed (++++)

### **Clinical relevance**

Clinical studies show decreased protein expression and redistribution of CLDN3, CLDN5 and CLDN8 in the intestine of Crohn's disease patients, whereas in the intestine of ulcerative colitis patients decreased protein expression and redistribution of CLDN1 and CLDN4 has been reported. Furthermore, protein expression of CLDN2 is consistently increased in the intestine of patients with Crohn's disease as well as in patients suffering from ulcerative colitis. The protein expression of CLDN1 is decreased in irritable bowel syndrome patients and is irregularly distributed in the colonic mucosa (7, 35-38, 57). Increased protein expression of CLDN2 and CLDN3 is observed in the intestine of patients with coeliac disease (37, 58). In addition, small intestinal biopsy specimens of patients



with food allergy exposed to food allergens showed a decreased protein expression of CLDN1 compared to those from normal subjects (39).

### **Junctional adhesion molecules (JAMs)**

#### ***Molecular Structure***

JAMs (~30-40 kDa) belong to the immunoglobulin (Ig) superfamily of proteins characterized by two extracellular Ig-like domains, a transmembrane domain and a short COOH-terminal cytoplasmic domain (Figure 2) (59). Based on sequence similarities in the cytoplasmic domain, JAMs are classified into two subfamilies. The first subfamily consists of JAM-A, JAM-B and JAM-C, with a class II PDZ binding motifs at their COOH-terminal ends, that directly interact with TJ scaffolding proteins, including ZO-1, ZO-2 and cingulin (Figure 2) (24, 60-62). The second subfamily consists of coxsackie and adenovirus receptor (CAR), endothelial selective adhesion molecule (ESAM) and JAM-4 containing class I PDZ binding motifs (19, 29, 63). Within the JAM family, the role of JAM-A is of particular interest in the regulation of barrier function, which will be discussed in more detail below.

#### ***Expression***

Like OCLN, JAM-A is also constantly expressed throughout the mouse intestine and is localized laterally between adjacent epithelial cells (25, 26, 64).

#### ***Intestinal barrier function***

JAM-A is generally believed to have dual functions. Within the immune system, it has been implicated to control the recruitment of leukocytes to the site of inflammation, whereas along intestinal epithelial cells, dominant expression of JAM-A has been observed in the region of TJs, suggesting a critical role in barrier function (53, 59, 65, 66). Homophilic interaction of JAM-A between adjacent cells is mediated through membrane-distal extracellular Ig-like domains (Figure 2) forming a barrier against luminal substances. The short cytoplasmic domain of JAM-A terminates with PDZ-binding motifs that interact with different cytoplasmic scaffolding proteins, including ZO-1, ZO-2 and cingulin (Figure 2 and Figure 4) by which it is linked to the intracellular cytoskeleton (53, 59, 67). Although, JAM-A knockout mice display a normal epithelial architecture, intestinal integrity tests confirm an increased gut permeability to different paracellular markers and a decreased TEER in mucosal tissue samples obtained from these animals (65, 68). In addition, it has been shown that JAM-A is involved in the recovery of epithelial barrier function after disruption of TJs by transient calcium depletion, since inhibition of JAM-A leads to retarded TJs reassembly in human T84 epithelial cells shown by disrupted redistribution of OCLN and decreased TEER recovery (66).

#### ***Clinical relevance***

Decreased protein expression of JAM-A is observed in the intestines of patients with Crohn's disease and in patients suffering from ulcerative colitis (68).

## **Tricellulin**

### ***Molecular Structure***

Tricellulin (~64 kDa) shares a few structural characteristics with OCLN, including one intracellular, two extracellular loops, four transmembrane domains, a cytoplasmic COOH-terminal domain and a cytoplasmic NH<sub>2</sub>-terminal domain, which is longer compared to the NH<sub>2</sub>-terminal domain of OCLN (Figure 2) (24, 69).

### ***Expression***

Although the above mentioned transmembrane TJ proteins are mainly involved in sealing the intercellular space between two adjacent cells (known as bicellular junctions), tricellulin is the first TJ protein identified at tricellular junctions between three adjacent epithelial cells (Figure 3A, B) (69, 70). Tricellulin is differentially expressed throughout the mouse intestine (strongly expressed in the small intestine, but weakly expressed in the large intestine) and appears as dot-like structures in the corners where three adjacent epithelial cells meet (70, 71). However, it has been shown that tricellulin overexpression directs this protein into both bicellular as well as tricellular junctions (72). Although, there is no evidence showing direct and physical interaction between tricellulin and OCLN, it is proposed that these two proteins may affect each other's cellular distribution (71). For example, *in vitro* studies using MDCK cells showed that knockdown of OCLN results in mislocalization of tricellulin from tricellular to bicellular junctions, whereas tricellulin deficiency causes thinner and disrupted continuity of OCLN distribution at bicellular junctions with teardrop-shaped accumulation of OCLN at tricellular junctions (70, 73).

### ***Intestinal barrier function***

Homophilic interaction of extracellular loops with the identical loops originating from tricellulin in the adjacent cells form a barrier against macromolecules (Figure 2). Unlike OCLN, both NH<sub>2</sub>- and COOH-terminal domains of tricellulin seem to play a relevant role in tricellulin localization at the TJ network (69). Tricellulin appears to be directly involved in the establishment of a barrier at the tricellular junctions, since strands of bicellular TJs are not continuous at tricellular junctions. Although tricellulin knockout mice have not been described yet, a few *in vitro* studies have highlighted the importance of tricellulin. For example, the inhibition of tricellulin in mouse Eph4 epithelial cells severely compromise the epithelial barrier function observed by a decrease in TEER and increase in fluorescein isothiocyanate-dextran permeability (69, 70). In addition, tricellulin has been shown to play a role in TJs reassembly and its role is not restituted by other TJ proteins, since tricellulin knockdown Caco-2 cells show a delay in TJs reassembly and barrier development (71).

### ***Clinical relevance***

Decreased protein expression of tricellulin is observed in the intestines of patients with ulcerative colitis (74).

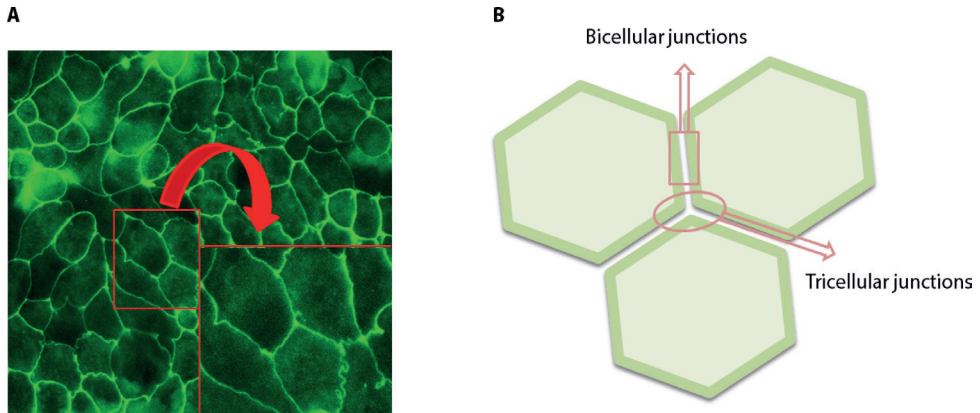


**Figure 3.** Immunofluorescence picture (A) and schematic drawing (B) of the bicellular junctions (contact sites between two adjacent cells) and tricellular junctions (contact sites between three adjacent cells).

## Zonula occludens (ZOs)

### *Molecular Structure*

The family of ZOs are comprised of three closely related isomers known as ZO-1 (~220 kDa), ZO-2 (~160 kDa) and ZO-3 (~130 kDa), belonging to the membrane associated guanylate kinase-like homologs (MAGUK) family (75). The MAGUK family is mainly referred to a group of proteins found at the sites of cell-cell contacts and they function as molecular adaptors in different cellular processes, including cell-cell communications, epithelial polarization and signal transduction (76, 77). Similar to the other MAGUK members, ZO proteins carry a Src homology 3 (SH3) domain, a guanylate-kinase homology (GUK) domain, proline-rich (PR) region and in this case three PDZ domains (Figure 4) (75, 76).

### *Expression*

Consistent expression of ZO-1 has been shown throughout the mouse intestine and appears as distinct line-forming structures at the apical region of the plasma membrane of the epithelial cells along the crypt-to-villus axis (26, 27, 78). Further studies are needed to compare the level of expression of ZO-2 and ZO-3 along the mouse intestine.

### *Intestinal barrier function*

ZO proteins directly interact with both transmembrane TJ proteins (such as OCLN, CLDNs and JAM-A) as well as with adherens junctions (such as  $\alpha$ -catenin and E-cadherin), thus provide the structural basis for the formation of apical junctional complexes and link them to the actin cytoskeleton (75, 76). The PDZ2 domain of ZO-1 appears to be crucial for both homodimerization (ZO-1/ZO-1 dimer) and heterodimerization (ZO-1/ZO-2 dimer or ZO-1/ZO-3 dimer) of this protein, while no direct binding has been reported between ZO-2 and ZO-3 (Figure 4) (75, 79). The GUK domain and the PDZ3 domain of ZO-1 have been proved to interact with OCLN and JAM-A, respectively, whereas PDZ1 of all three

ZO proteins are able to bind to the COOH-terminus of CLDNs and induce independent regulation of both polymerization and localization of CLDNs in epithelial cells. The PDZ2 domain of ZO-2 interacts with JAM-A, while no binding has been reported between ZO-3 and JAM-A (Figure 4) (15, 59, 75, 76, 80).

Both ZO-1 and ZO-2 proteins appear to play a crucial role in maintaining the epithelial barrier function. Early embryonic lethality of mice lacking ZO-1 and ZO-2 reveals the importance of these proteins for development and viability. *In vitro* data using MDCK and Eph4 cells confirm the functional role of ZO-1 and ZO-2 in the intestinal integrity, since inhibition of either ZO-1 or ZO-2 triggers atypical monolayer architecture and alters expression of apical junctional complexes, such as decreasing the amount of OCLN and E-cadherin (81-86). In addition, ZO-1 is shown to be essential for TJs reassembly, since knockout of ZO-1 in MDCK and Eph4 cells causes a pronounced delay in the recruitment of CLDNs and OCLN, after calcium switch assay, to the newly formed apical junctional complexes (87, 88). ZO-3 seems to be unessential for the regulation of intestinal integrity and viability, since ZO-3 deficiency displays no apparent phenotype neither in mice nor in epithelial cells (86, 89).

### ***Clinical relevance***

Decreased protein expression of ZO-1 is observed in the intestines of patients with coeliac disease (37).

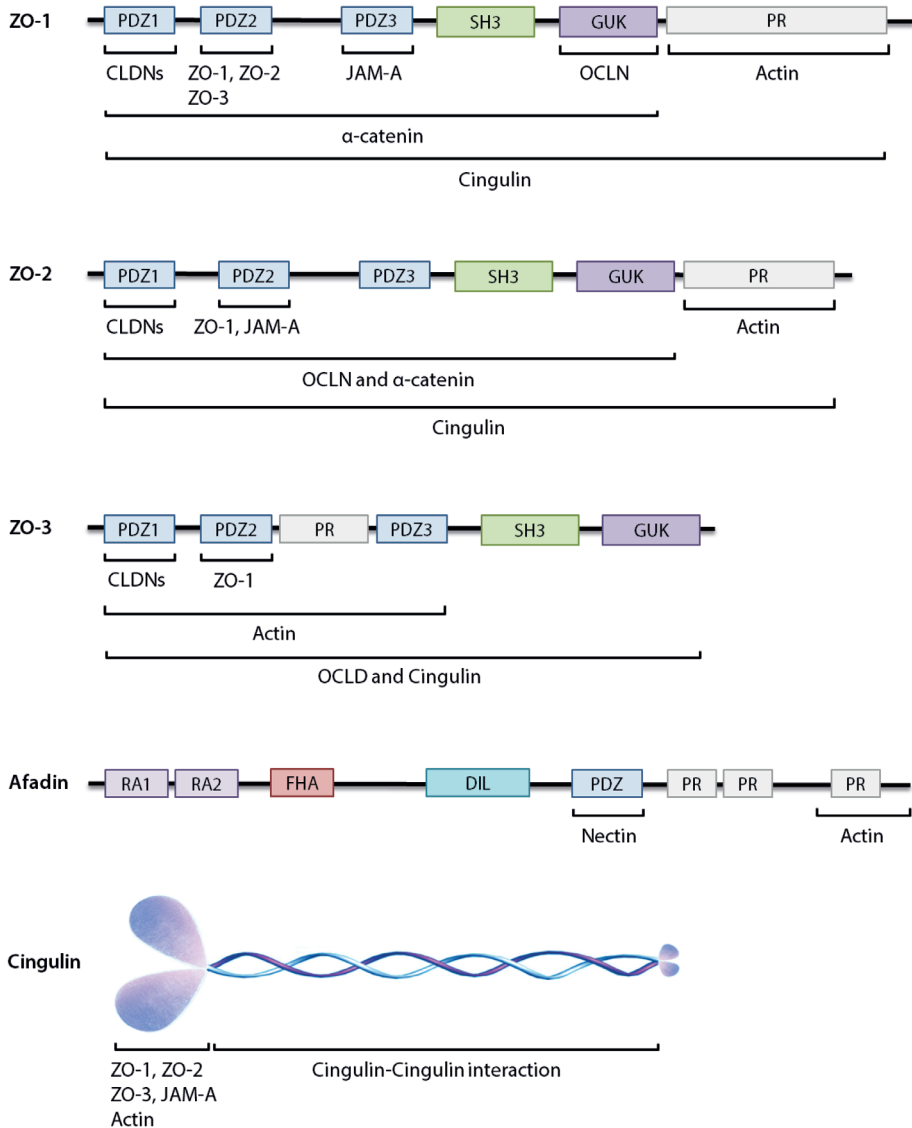


**Figure 4.** Schematic diagrams of the structural organization of individual cytoplasmic scaffolding proteins and the related direct interaction with different tight junctions (TJs) as well as adherens junctions. ZO proteins carry three PDZ domains, a Src homology 3 (SH3) domain, a guanylate-kinase homology (GUK) domain and proline-rich (PR) region. Afadin consists of two Ras-binding domains (RA1 and RA2), a forkhead-associated (FHA) domain, a diluted (DIL) domain, a PDZ domain and three proline-rich (PR) domains. Cingulin exists as a parallel homodimer of two subunits, each comprised of a N-terminal globular head region, a long  $\alpha$ -helical coiled-coil rod region and a small globular tail. CLDNs, claudins; JAM-A, junctional adhesion molecule-A; OCLN, occludin; ZOs, zonula occludens.

## **Afadin**

### ***Molecular Structure***

Afadin (~206 kDa) is a multi-domain protein and consists of two Ras-binding domains (RA1 and RA2), a forkhead-associated (FHA) domain, a diluted (DIL) domain, a PDZ domain and three proline-rich (PR) domains (Figure 4) (24, 90-92).

### ***Expression***

Afadin is expressed throughout the mouse intestine and is localized at both TJs and adherens junctions. Afadin appears as distinct dot-like or line-forming structures at the apical region of the plasma membrane of the epithelial cells along the crypt-to-villus axis (91, 93).

### ***Intestinal barrier function***

The PDZ and proline-rich domains of afadin have been associated with either direct or indirect interaction of afadin with different cell adhesion proteins, including nectin, E-cadherin, JAM-A, ZOs and CLDNs (Figure 4) (53, 62, 90, 94-96). It is already known that afadin plays a crucial role in establishment and proper organization of the apical junctional complexes as well as providing a physical link between different components of apical junctional complexes and the intracellular cytoskeleton (90, 91, 97). It has been reported that the architecture of epithelial apical junctions in both the small and large intestines are preserved in afadin-knockout mice, however, this lack of afadin results in impaired intestinal homeostasis and increased intestinal permeability (93). In addition, it is believed that afadin has a crucial role in recruitment of different TJ proteins to the apical side of the cell-cell adherens junctions, since afadin-depleted MDCK cells show a significant delay in the reassembly of TJs and it subsequently enhances epithelial permeability (53, 94, 95, 98, 99).

### ***Clinical relevance***

Nothing is known about the clinical relevance of afadin-related barrier defects in human diseases.

## **Cingulin**

### ***Molecular Structure***

Cingulin (~140 kDa) is a non-PDZ cytoplasmic scaffolding TJ protein and exists as a parallel homodimer of two subunits, each comprised of a N-terminal globular head region, a long  $\alpha$ -helical coiled-coin rod region and a small globular tail (Figure 4) (100).

### ***Expression***

Cingulin is expressed throughout the mouse intestine, however, subcellular distribution and differences in level of expression alongside the mouse intestine has not been fully investigated (101, 102).

**Intestinal barrier function**

The head domain of cingulin appears to control the efficient recruitment of cingulin into cell-cell junctions through its interaction with ZO<sub>s</sub>, JAM-A and actin, whereas the rod domain is essential for dimerization of cingulin (60, 61, 100, 103, 104). It is still not clear whether cingulin plays a fundamental role in barrier function, since different *in vitro* and *in vivo* studies showed that neither depletion nor overexpression of cingulin (full-length or the head domain of cingulin) cause obvious changes in the molecular organization of the TJ network. In addition, cingulin knockdown MDCK cells show normal TJs reassembly and barrier development (61, 101, 105, 106). In addition, the *in vivo* functional intestinal barrier can be formed in the absence of cingulin. A study by Guillemot *et al.* (101) showed that cingulin is involved in signaling networks that regulate the CLDN2 expression and cingulin knockout mice show a two-fold increase in the level of CLDN2 proteins in the duodenum. However, this CLDN2 effect is not sufficient to induce intestinal barrier breakdown.

**Clinical relevance**

Nothing is known about the clinical relevance of cingulin-related barrier defects in human diseases.

**Conclusions**

It is well accepted that regulation of TJ proteins are indispensable to maintain the healthy intestinal barrier function. Here, we have summarized the relevant knowledge about the molecular structure and the expression patterns of different transmembrane (discriminating between bicellular and tricellular TJs) and cytoplasmic scaffolding TJ proteins. TJs are dynamic structures with a complex architecture and are composed of series of different proteins. The direct interaction among different TJ proteins is essential for the establishment of an efficient paracellular barrier against luminal harmful substances and the impairment of this biological barrier is considered to be one of the predisposing factors leading to various chronic intestinal inflammatory diseases.



## References

1. Peterson LW, Artis D. Intestinal epithelial cells: regulators of barrier function and immune homeostasis. *Nat Rev Immunol* 2014;14:141-153.
2. Clemente JC, Ursell LK, Parfrey LW, Knight R. The impact of the gut microbiota on human health: an integrative view. *Cell* 2012;148:1258-1270.
3. Ley RE, Peterson DA, Gordon JI. Ecological and evolutionary forces shaping microbial diversity in the human intestine. *Cell* 2006;124:837-848.
4. Schenk M, Mueller C. The mucosal immune system at the gastrointestinal barrier. *Best Pract Res Clin Gastroenterol* 2008;22:391-409.
5. Bischoff SC, Barbara G, Buurman W, Ockhuizen T, Schulzke JD, Serino M, Tilg H, Watson A, Wells JM. Intestinal permeability-a new target for disease prevention and therapy. *BMC Gastroenterol* 2014;14:189.
6. Heyman M, Desjeux JF. Cytokine-induced alteration of the epithelial barrier to food antigens in disease. *Ann NY Acad Sci* 2000;915:304-311.
7. Groschwitz KR, Hogan SP. Intestinal barrier function: molecular regulation and disease pathogenesis. *J Allergy Clin Immunol* 2009;124:3-20.
8. O'Connell EJ. Pediatric allergy: a brief review of risk factors associated with developing allergic disease in childhood. *Ann Allergy Asthma Immunol* 2003;90:53-58.
9. DeMeo MT, Mutlu EA, Keshavarzian A, Tobin MC. Intestinal permeation and gastrointestinal disease. *J Clin Gastroenterol* 2002;34:385-396.
10. Pastorelli L, De Salvo C, Mercado JR, Vecchi M, Pizarro TT. Central role of the gut epithelial barrier in the pathogenesis of chronic intestinal inflammation: lessons learned from animal models and human genetics. *Front Immunol* 2013;4:280.
11. Menard S, Cerf-Bensussan N, Heyman M. Multiple facets of intestinal permeability and epithelial handling of dietary antigens. *Mucosal Immunol* 2010;3:247-259.
12. Balda MS, Matter K. Epithelial cell adhesion and the regulation of gene expression. *Trends Cell Biol* 2003;13:310-318.
13. Niessen CM. Tight junctions/adherens junctions: basic structure and function. *J Invest Dermatol* 2007;127:2525-2532.
14. Tsukita S, Furuse M, Itoh M. Multifunctional strands in tight junctions. *Nat Rev Mol Cell Biol* 2001;2:285-293.
15. Denker BM, Nigam SK. Molecular structure and assembly of the tight junction. *Am J Physiol* 1998;274:F1-F9.
16. Perez-Moreno M, Jamora C, Fuchs E. Sticky business: orchestrating cellular signals at adherens junctions. *Cell* 2003;112:535-548.
17. Terry S, Nie M, Matter K, Balda MS. Rho signaling and tight junction functions. *Physiology* 2010;25:16-26.
18. Ivanov AI, Parkos CA, Nusrat A. Cytoskeletal regulation of epithelial barrier function during inflammation. *Am J Pathol* 2010;177:512-524.
19. Chiba H, Osanai M, Murata M, Kojima T, Sawada N. Transmembrane proteins of tight junctions. *Biochim Biophys Acta* 2008;1778:588-600.
20. Schneeberger EE, Lynch RD. The tight junction: a multifunctional complex. *Am J Physiol Cell Physiol* 2004;286:C1213-C1228.
21. Fihn BM, Sjoqvist A, Jodal M. Permeability of the rat small intestinal epithelium along the villus-crypt axis: effects of glucose transport. *Gastroenterology* 2000;119:1029-1036.
22. Hu YJ, Wang YD, Tan FQ, Yang WX. Regulation of paracellular permeability: factors and mechanisms. *Mol Biol Rep* 2013;40:6123-6142.
23. Mitic LL, Van Itallie CM, Anderson JM. Molecular physiology and pathophysiology of tight junctions I. Tight junction structure and function: lessons from mutant animals and proteins. *Am J Physiol Gastrointest Liver Physiol* 2000;279:G250-G254.
24. Van Itallie CM, Anderson JM. Architecture of tight junctions and principles of molecular composition. *Semin Cell Dev Biol* 2014;36:157-165.
25. Holmes JL, Van Itallie CM, Rasmussen JE, Anderson JM. Claudin profiling in the mouse during postnatal

- intestinal development and along the gastrointestinal tract reveals complex expression patterns. *Gene Expr Patterns* 2006;6:581-588.
26. Hwang I, An BS, Yang H, Kang HS, Jung EM, Jeung EB. Tissue-specific expression of occludin, zona occludens-1, and junction adhesion molecule A in the duodenum, ileum, colon, kidney, liver, lung, brain, and skeletal muscle of C57BL mice. *J Physiol Pharmacol* 2013;64:11-18.
27. Akbari P, Braber S, Gremmels H, Koelink PJ, Verheijden KA, Garssen J, Fink-Gremmels J. Deoxynivalenol: a trigger for intestinal integrity breakdown. *FASEB J* 2014;28:2414-2429.
28. Chung CY, Alden SL, Funderburg NT, Fu P, Levine AD. Progressive proximal-to-distal reduction in expression of the tight junction complex in colonic epithelium of virally-suppressed HIV+ individuals. *PLoS Pathog* 2014;10:e1004198.
29. Suzuki T. Regulation of intestinal epithelial permeability by tight junctions. *Cell Mol Life Sci* 2013;70:631-659.
30. Al-Sadi R, Khatib K, Guo S, Ye D, Youssef M, Ma T. Occludin regulates macromolecule flux across the intestinal epithelial tight junction barrier. *Am J Physiol Gastrointest Liver Physiol* 2011;300:G1054-G1064.
31. Rao R. Occludin phosphorylation in regulation of epithelial tight junctions. *Ann N Y Acad Sci* 2009;1165:62-68.
32. Saitou M, Furuse M, Sasaki H, Schulzke JD, Fromm M, Takano H, Noda T, Tsukita S. Complex phenotype of mice lacking occludin, a component of tight junction strands. *Mol Biol Cell* 2000;11:4131-4142.
33. Schulzke JD, Gitter AH, Mankertz J, Spiegel S, Seidler U, Amasheh S, Saitou M, Tsukita S, Fromm M. Epithelial transport and barrier function in occludin-deficient mice. *Biochim Biophys Acta* 2005;1669:34-42.
34. Yu AS, McCarthy KM, Francis SA, McCormack JM, Lai J, Rogers RA, Lynch RD, Schneeberger EE. Knockdown of occludin expression leads to diverse phenotypic alterations in epithelial cells. *Am J Physiol Cell Physiol* 2005;288:C1231-C1241.
35. Zeissig S, Burgel N, Gunzel D, Richter J, Mankertz J, Wahnschaffe U, Kroesen AJ, Zeitz M, Fromm M, Schulzke JD. Changes in expression and distribution of claudin 2, 5 and 8 lead to discontinuous tight junctions and barrier dysfunction in active Crohn's disease. *Gut* 2007;56:61-72.
36. Heller F, Florian P, Bojarski C, Richter J, Christ M, Hillenbrand B, Mankertz J, Gitter AH, Burgel N, Fromm M, *et al.* Interleukin-13 is the key effector Th2 cytokine in ulcerative colitis that affects epithelial tight junctions, apoptosis, and cell restitution. *Gastroenterology* 2005;129:550-564.
37. Drago S, El Asmar R, Di Pierro M, Grazia Clemente M, Tripathi A, Sapone A, Thakar M, Iacono G, Carroccio A, D'Agate C, *et al.* Gliadin, zonulin and gut permeability: Effects on celiac and non-celiac intestinal mucosa and intestinal cell lines. *Scand J Gastroenterol* 2006;41:408-419.
38. Bertiaux-Vandaele N, Youmba SB, Belmonte L, Lecleire S, Antonietti M, Gourcerol G, Leroi AM, Dechelotte P, Menard JF, Ducrotte P, *et al.* The expression and the cellular distribution of the tight junction proteins are altered in irritable bowel syndrome patients with differences according to the disease subtype. *Am J Gastroenterol* 2011;106:2165-2173.
39. Pizzuti D, Senzolo M, Buda A, Chiarelli S, Giacomelli L, Mazzon E, Curioni A, Faggian D, De Lazzari F. *In vitro* model for IgE mediated food allergy. *Scand J Gastroenterol* 2011;46:177-187.
40. Gunzel D, Yu AS. Claudins and the modulation of tight junction permeability. *Physiol Rev* 2013;93:525-569.
41. Van Itallie CM, Colegio OR, Anderson JM. The cytoplasmic tails of claudins can influence tight junction barrier properties through effects on protein stability. *J Membr Biol* 2004;199:29-38.
42. Colegio OR, Van Itallie CM, McCrea HJ, Rahner C, Anderson JM. Claudins create charge-selective channels in the paracellular pathway between epithelial cells. *Am J Physiol Cell Physiol* 2002;283:C142-C147.

43. Krause G, Winkler L, Piehl C, Blasig I, Piontek J, Muller SL. Structure and function of extracellular claudin domains. *Ann NY Acad Sci* 2009;1165:34-43.
44. Krug SM, Gunzel D, Conrad MP, Rosenthal R, Fromm A, Amasheh S, Schulzke JD, Fromm M. Claudin-17 forms tight junction channels with distinct anion selectivity. *Cell Mol Life Sci* 2012;69:2765-2778.
45. Van Itallie CM, Rogan S, Yu A, Vidal LS, Holmes J, Anderson JM. Two splice variants of claudin-10 in the kidney create paracellular pores with different ion selectivities. *Am J Physiol Renal Physiol* 2006;291:F1288-F1299.
46. Mineta K, Yamamoto Y, Yamazaki Y, Tanaka H, Tada Y, Saito K, Tamura A, Igarashi M, Endo T, Takeuchi K, *et al.* Predicted expansion of the claudin multigene family. *FEBS Lett* 2011;585:606-612.
47. Fujita H, Chiba H, Yokozaki H, Sakai N, Sugimoto K, Wada T, Kojima T, Yamashita T, Sawada N. Differential expression and subcellular localization of claudin-7, -8, -12, -13, and -15 along the mouse intestine. *J Histochem Cytochem* 2006;54:933-944.
48. Tamura A, Kitano Y, Hata M, Katsuno T, Moriwaki K, Sasaki H, Hayashi H, Suzuki Y, Noda T, Furuse M, *et al.* Megaintestine in claudin-15-deficient mice. *Gastroenterology* 2008;134:523-534.
49. Rahner C, Mitic LL, Anderson JM. Heterogeneity in expression and subcellular localization of claudins 2, 3, 4, and 5 in the rat liver, pancreas, and gut. *Gastroenterology* 2001;120:411-422.
50. Lu Z, Ding L, Lu Q, Chen YH. Claudins in intestines: Distribution and functional significance in health and diseases. *Tissue Barriers* 2013;1:e24978.
51. Ding L, Lu Z, Foreman O, Tatum R, Lu Q, Renegar R, Cao J, Chen YH. Inflammation and disruption of the mucosal architecture in claudin-7-deficient mice. *Gastroenterology* 2012;142:305-315.
52. Singh AB, Sharma A, Dhawan P. Claudin family of proteins and cancer: an overview. *J Oncol* 2010;2010:541957.
53. Severson EA, Parkos CA. Structural determinants of Junctional Adhesion Molecule A (JAM-A) function and mechanisms of intracellular signaling. *Curr Opin Cell Biol* 2009;21:701-707.
54. Gunzel D, Fromm M. Claudins and other tight junction proteins. *Compr Physiol* 2012;2:1819-1852.
55. Stiffler MA, Chen JR, Grantcharova VP, Lei Y, Fuchs D, Allen JE, Zaslavskaya LA, MacBeath G. PDZ domain binding selectivity is optimized across the mouse proteome. *Science* 2007;317:364-369.
56. Tanaka H, Takechi M, Kiyonari H, Shioi G, Tamura A, Tsukita S. Intestinal deletion of Claudin-7 enhances paracellular organic solute flux and initiates colonic inflammation in mice. *Gut* 2015;64:1529-1538.
57. Prasad S, Mingrino R, Kaukinen K, Hayes KL, Powell RM, MacDonald TT, Collins JE. Inflammatory processes have differential effects on claudins 2, 3 and 4 in colonic epithelial cells. *Lab Invest* 2005;85:1139-1162.
58. Szakal DN, Györfy H, Arato A, Cseh A, Molnar K, Papp M, Dezsöfi A, Veres G. Mucosal expression of claudins 2, 3 and 4 in proximal and distal part of duodenum in children with coeliac disease. *Virchows Arch* 2010;456:245-250.
59. Ebnet K, Suzuki A, Ohno S, Vestweber D. Junctional adhesion molecules (JAMs): more molecules with dual functions? *J Cell Sci* 2004;117:19-29.
60. Bazzoni G, Martinez-Estrada OM, Orsenigo F, Cordenonsi M, Citi S, Dejana E. Interaction of junctional adhesion molecule with the tight junction components ZO-1, cingulin, and occludin. *J Biol Chem* 2000;275:20520-20526.
61. Guillemot L, Hammar E, Kaister C, Ritz J, Caille D, Jond L, Bauer C, Meda P, Citi S. Disruption of the cingulin gene does not prevent tight junction formation but alters gene expression. *J Cell Sci* 2004;117:5245-5256.
62. Monteiro AC, Sumagin R, Rankin CR, Leoni G, Mina MJ, Reiter DM, Stehle T, Dermody TS, Schaefer SA, Hall RA, *et al.* JAM-A associates with ZO-2, afadin, and PDZ-GEF1 to activate Rap2c and regulate epithelial barrier function. *Mol Biol Cell* 2013;24:2849-2860.
63. Shin K, Fogg VC, Margolis B. Tight junctions and cell polarity. *Annu Rev Cell Dev Biol* 2006;22:207-235.
64. Martin-Padura I, Lostaglio S, Schneemann

- M, Williams L, Romano M, Fruscella P, Panzeri C, Stoppacciaro A, Ruco L, Villa A, *et al.* Junctional adhesion molecule, a novel member of the immunoglobulin superfamily that distributes at intercellular junctions and modulates monocyte transmigration. *J Cell Biol* 1998;142:117-127.
65. Laukoetter MG, Nava P, Lee WY, Severson EA, Capaldo CT, Babbitt BA, Williams IR, Koval M, Peatman E, Campbell JA, *et al.* JAM-A regulates permeability and inflammation in the intestine *in vivo*. *J Exp Med* 2007;204:3067-3076.
66. Liu Y, Nusrat A, Schnell FJ, Reaves TA, Walsh S, Pochet M, Parkos CA. Human junction adhesion molecule regulates tight junction resealing in epithelia. *J Cell Sci* 2000;113:2363-2374.
67. Bazzoni G. The JAM family of junctional adhesion molecules. *Curr Opin Cell Biol* 2003;15:525-530.
68. Vetrano S, Rescigno M, Cera MR, Correale C, Rumio C, Doni A, Fantini M, Sturm A, Borroni E, Repici A, *et al.* Unique role of junctional adhesion molecule-a in maintaining mucosal homeostasis in inflammatory bowel disease. *Gastroenterology* 2008;135:173-184.
69. Mariano C, Sasaki H, Brites D, Brito MA. A look at tricellulin and its role in tight junction formation and maintenance. *Eur J Cell Biol* 2011;90:787-796.
70. Ikenouchi J, Furuse M, Furuse K, Sasaki H, Tsukita S, Tsukita S. Tricellulin constitutes a novel barrier at tricellular contacts of epithelial cells. *J Cell Biol* 2005;171:939-945.
71. Raleigh DR, Marchiando AM, Zhang Y, Shen L, Sasaki H, Wang Y, Long M, Turner JR. Tight junction-associated MARVEL proteins marvel3, tricellulin, and occludin have distinct but overlapping functions. *Mol Biol Cell* 2010;21:1200-1213.
72. Krug SM, Amasheh S, Richter JF, Milatz S, Gunzel D, Westphal JK, Huber O, Schulzke JD, Fromm M. Tricellulin forms a barrier to macromolecules in tricellular tight junctions without affecting ion permeability. *Mol Biol Cell* 2009;20:3713-3724.
73. Ikenouchi J, Sasaki H, Tsukita S, Furuse M, Tsukita S. Loss of occludin affects tricellular localization of tricellulin. *Mol Biol Cell* 2008;19:4687-4693.
74. Hering NA, Fromm M, Schulzke JD. Determinants of colonic barrier function in inflammatory bowel disease and potential therapeutics. *J Physiol* 2012;590:1035-1044.
75. Bauer H, Zweimüller-Mayer J, Steinbacher P, Lametschwandtner A, Bauer HC. The dual role of zonula occludens (ZO) proteins. *J Biomed Biotechnol* 2010;2010:402593.
76. Gonzalez-Mariscal L, Betanzos A, Avila-Flores A. MAGUK proteins: structure and role in the tight junction. *Semin Cell Dev Biol* 2000;11:315-324.
77. Zhu J, Shang Y, Xia C, Wang W, Wen W, Zhang M. Guanylate kinase domains of the MAGUK family scaffold proteins as specific phospho-protein-binding modules. *EMBO J* 2011;30:4986-4997.
78. Guan Y, Watson AJ, Marchiando AM, Bradford E, Shen L, Turner JR, Montrose MH. Redistribution of the tight junction protein ZO-1 during physiological shedding of mouse intestinal epithelial cells. *Am J Physiol Cell Physiol* 2011;300:C1404-C1414.
79. Fanning AS, Lye MF, Anderson JM, Lavie A. Domain swapping within PDZ2 is responsible for dimerization of ZO proteins. *J Biol Chem* 2007;282:37710-37716.
80. Nomme J, Fanning AS, Caffrey M, Lye MF, Anderson JM, Lavie A. The Src homology 3 domain is required for junctional adhesion molecule binding to the third PDZ domain of the scaffolding protein ZO-1. *J Biol Chem* 2011;286:43352-43360.
81. Chen J, Xiao L, Rao JN, Zou T, Liu L, Bellavance E, Gorospe M, Wang JY. JunD represses transcription and translation of the tight junction protein zona occludens-1 modulating intestinal epithelial barrier function. *Mol Biol Cell* 2008;19:3701-3712.
82. Hernandez S, Chavez Munguia B, Gonzalez-Mariscal L. ZO-2 silencing in epithelial cells perturbs the gate and fence function of tight junctions and leads to an atypical monolayer architecture. *Exp Cell Res* 2007;313:1533-1547.
83. Ikenouchi J, Umeda K, Tsukita S, Furuse M, Tsukita S. Requirement of ZO-1 for the formation of belt-like

adherens junctions during epithelial cell polarization. *J Cell Biol* 2007;176:779-786.

84. Katsuno T, Umeda K, Matsui T, Hata M, Tamura A, Itoh M, Takeuchi K, Fujimori T, Nabeshima Y, Noda T, *et al.* Deficiency of zonula occludens-1 causes embryonic lethal phenotype associated with defected yolk sac angiogenesis and apoptosis of embryonic cells. *Mol Biol Cell* 2008;19:2465-2475.

85. Umeda K, Ikenouchi J, Katahira-Tayama S, Furuse K, Sasaki H, Nakayama M, Matsui T, Tsukita S, Furuse M, Tsukita S. ZO-1 and ZO-2 independently determine where claudins are polymerized in tight-junction strand formation. *Cell* 2006;126:741-754.

86. Xu J, Kausalya PJ, Phua DC, Ali SM, Hossain Z, Hunziker W. Early embryonic lethality of mice lacking ZO-2, but Not ZO-3, reveals critical and nonredundant roles for individual zonula occludens proteins in mammalian development. *Mol Cell Biol* 2008;28:1669-1678.

87. Umeda K, Matsui T, Nakayama M, Furuse K, Sasaki H, Furuse M, Tsukita S. Establishment and characterization of cultured epithelial cells lacking expression of ZO-1. *J Biol Chem* 2004;279:44785-44794.

88. McNeil E, Capaldo CT, Macara IG. Zonula occludens-1 function in the assembly of tight junctions in Madin-Darby canine kidney epithelial cells. *Mol Biol Cell* 2006;17:1922-1932.

89. Adachi M, Inoko A, Hata M, Furuse K, Umeda K, Itoh M, Tsukita S. Normal establishment of epithelial tight junctions in mice and cultured cells lacking expression of ZO-3, a tight-junction MAGUK protein. *Mol Cell Biol* 2006;26:9003-9015.

90. Miyoshi J, Takai Y. Molecular perspective on tight-junction assembly and epithelial polarity. *Adv Drug Deliv Rev* 2005;57:815-855.

91. Ooshio T, Fujita N, Yamada A, Sato T, Kitagawa Y, Okamoto R, Nakata S, Miki A, Irie K, Takai Y. Cooperative roles of Par-3 and afadin in the formation of adherens and tight junctions. *J Cell Sci* 2007;120:2352-2365.

92. Yamamoto T, Harada N, Kano K, Taya S, Canaani E, Matsuura Y, Mizoguchi A, Ide C, Kaibuchi K. The

Ras target AF-6 interacts with ZO-1 and serves as a peripheral component of tight junctions in epithelial cells. *J Cell Biol* 1997;139:785-795.

93. Tanaka-Okamoto M, Hori K, Ishizaki H, Itoh Y, Onishi S, Yonemura S, Takai Y, Miyoshi J. Involvement of afadin in barrier function and homeostasis of mouse intestinal epithelia. *J Cell Sci* 2011;124:2231-2240.

94. Indra I, Troyanovsky R, Troyanovsky SM. Afadin controls cadherin cluster stability using clathrin-independent mechanism. *Tissue Barriers* 2014;2:e28687.

95. Ooshio T, Kobayashi R, Ikeda W, Miyata M, Fukumoto Y, Matsuzawa N, Ogita H, Takai Y. Involvement of the interaction of afadin with ZO-1 in the formation of tight junctions in Madin-Darby canine kidney cells. *J Biol Chem* 2010;285:5003-5012.

96. Severson EA, Lee WY, Capaldo CT, Nusrat A, Parkos CA. Junctional adhesion molecule A interacts with Afadin and PDZ-GEF2 to activate Rap1A, regulate beta1 integrin levels, and enhance cell migration. *Mol Biol Cell* 2009;20:1916-1925.

97. Takai Y, Nakanishi H. Nectin and afadin: novel organizers of intercellular junctions. *J Cell Sci* 2003;116:17-27.

98. Sato T, Fujita N, Yamada A, Ooshio T, Okamoto R, Irie K, Takai Y. Regulation of the assembly and adhesion activity of E-cadherin by nectin and afadin for the formation of adherens junctions in Madin-Darby canine kidney cells. *J Biol Chem* 2006;281:5288-5299.

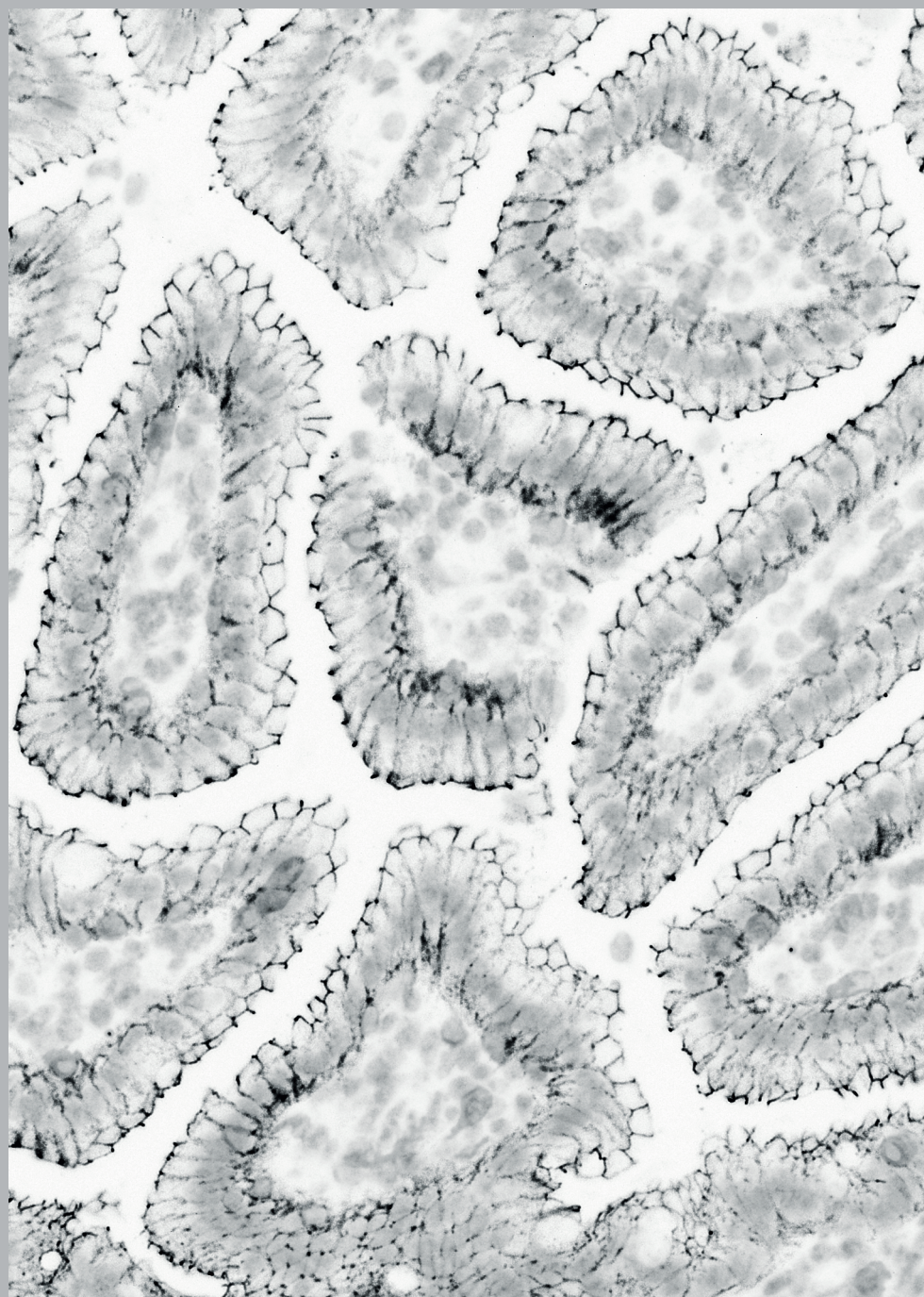
99. Yamada T, Kuramitsu K, Rikitsu E, Kurita S, Ikeda W, Takai Y. Nectin and junctional adhesion molecule are critical cell adhesion molecules for the apico-basal alignment of adherens and tight junctions in epithelial cells. *Genes Cells* 2013;18:985-998.

100. Cordenonsi M, D'Atri F, Hammar E, Parry DA, Kendrick-Jones J, Shore D, Citi S. Cingulin contains globular and coiled-coil domains and interacts with ZO-1, ZO-2, ZO-3, and myosin. *J Cell Biol* 1999;147:1569-1582.

101. Guillemot L, Schneider Y, Brun P, Castagliuolo I, Pizzuti D, Martinez D, Jond L, Bongiovanni M, Citi S.

- Cingulin is dispensable for epithelial barrier function and tight junction structure, and plays a role in the control of claudin-2 expression and response to duodenal mucosa injury. *J Cell Sci* 2012;125:5005-5014.
102. Ohnishi H, Nakahara T, Furuse K, Sasaki H, Tsukita S, Furuse M. JACOP, a novel plaque protein localizing at the apical junctional complex with sequence similarity to cingulin. *J Biol Chem* 2004;279:46014-46022.
103. Citi S, D'Atri F, Parry DA. Human and *Xenopus* cingulin share a modular organization of the coiled-coil rod domain: predictions for intra- and intermolecular assembly. *J Struct Biol* 2000;131:135-145.
104. D'Atri F, Citi S. Cingulin interacts with F-actin *in vitro*. *FEBS Lett* 2001;507:21-24.
105. Guillemot L, Citi S. Cingulin regulates claudin-2 expression and cell proliferation through the small GTPase RhoA. *Mol Biol Cell* 2006;17:3569-3577.
106. Paschoud S, Citi S. Inducible overexpression of cingulin in stably transfected MDCK cells does not affect tight junction organization and gene expression. *Mol Membr Biol* 2008;25:1-13.





# Chapter 3



## The intestinal barrier as an emerging target in the toxicological assessment of mycotoxins: a review

Peyman Akbari<sup>1,2</sup>, Saskia Braber<sup>1</sup>, Soheil Varasteh<sup>1,2</sup>, Arash Alizadeh<sup>1,2</sup>, Johan Garssen<sup>2,3</sup>, Johanna Fink-Gremmels<sup>1</sup>

<sup>1</sup> Division of Veterinary Pharmacology, Pharmacotherapy and Toxicology, Institute for Risk Assessment Sciences, Utrecht University, Utrecht, The Netherlands

<sup>2</sup> Division of Pharmacology, Utrecht Institute for Pharmaceutical Sciences, Faculty of Science, Utrecht University, Utrecht, The Netherlands

<sup>3</sup> Nutricia Research, Utrecht, The Netherlands

**This chapter is submitted for publication.**

## **Abstract**

Mycotoxins, the secondary metabolites of fungal species, are the most frequently occurring natural food contaminants in human and animal diets. Risk assessment of mycotoxins focused as yet on their mutagenic, genotoxic and potential carcinogenic effects. Recently, there is an increasing awareness of the adverse effects of various mycotoxins on vulnerable structures in the intestines. In particular an impairment of the barrier function of the epithelial lining cells and the sealing tight junction proteins has been noted, as this could result in an increased translocation of luminal antigens and pathogens and an excessive activation of the immune system. The current review aims to provide a summary of the available evidence regarding direct effects of various mycotoxins on the intestinal epithelial barrier. Available data, based on different cellular and animal studies, show that food-associated exposure to certain mycotoxins, especially trichothecenes and patulin, affect the intestinal barrier integrity and can even result in increased translocation of harmful stressors. It is therefore hypothesized that human exposure to certain mycotoxins, particularly deoxynivalenol, as the major trichothecene, may play an important role in etiology of various chronic intestinal inflammatory diseases, such as inflammatory bowel disease and in the prevalence of food allergies, particularly in children.

## Introduction

Since the early discovery of aflatoxins as food and feed contaminants, risk assessment of mycotoxin exposure has been initially focused on their mutagenic, genotoxic and potentially carcinogenic effects, as major human health risks (1-3). More recently, there is an increasing awareness of the adverse effects of various mycotoxins on vulnerable structures in the intestines and the impairment of intestinal integrity (4-7). A compromised barrier function is associated with an increased epithelial permeability and translocation of luminal allergens and pathogens, as well as a non-specific inflammatory response and an overstimulation of the gut-associated immune system (8-11). The most prominent example of a mycotoxin primarily associated with an impairment of the intestinal integrity is deoxynivalenol, a trichothecene, which first had been recognized for its pro-inflammatory and immunomodulatory activities (12-15). However, various other mycotoxins have been studied regarding their effects on the intestinal barrier, both *in vitro* as well as *in vivo*. The current review aims to provide a summary and discussion of the available evidence regarding direct effects of various mycotoxins on individual structures of the intestinal epithelial barrier. The mycotoxins addressed, include the aflatoxins, ochratoxin A, fumonisin B<sub>1</sub> and patulin, as well as T-2/HT-2 toxin, nivalenol and deoxynivalenol, as representatives of the class of the trichothecenes. The summary of the effects of individual mycotoxins on the intestinal barrier is preceded by a short introduction into common experimental models and test parameters to measure intestinal integrity.

## Experimental models used to assess intestinal permeability

### ***The Caco-2 cell model***

During the last few decades, the use of different intestinal epithelial cell lines from various animal species as well as from human origin has been used to assess the effects of drugs and toxins on the permeability of the intestinal epithelium. Among them, the Caco-2 cell line (ATCC® number: HTB-37), originally isolated from a human colon adenocarcinoma, is well-accepted as a reference model to conduct transport studies as well as to investigate the effects on barrier function. Caco-2 cells are routinely cultivated as monolayers on permeable filters. During culturing they undergo spontaneous differentiation resulting in polarization and formation of the tight junction (TJ) proteins between adjacent cells. Differentiated Caco-2 cells form polarized apical/mucosal and basolateral/serosal membranes that are impermeable and are structurally and functionally similar to epithelial cells of the small intestine (16-19). A major advantage of the common technique to grow Caco-2 cells on transwell inserts is the fact that transport of nutrients and drugs from the apical to the basolateral compartment can be measured. In turn the established cell monolayer can be challenged from the apical (luminal) side as well as the basolateral side with antigens and toxins and allow a wide range of functional parameters to be measured

(16, 20, 21). The Caco-2 cell model is also extensively used in pre-clinical pharmacological studies to assess the rate of absorption and the potential impact of soluble and efflux transporters on intestinal permeability (19, 22).

### ***Measurement of Transepithelial Electrical Resistance (TEER)***

TEER is the first parameter measured to evaluate the integrity of the epithelial barrier in the Caco-2 cell model. A simple voltmeter device equipped with a pair of chopstick-like electrodes, quantifies ion movement across a monolayer and is considered as an effective indicator for the developing barrier function. TEER is generally used to follow the cell differentiation process, and standard values for a completed non-permeable barrier are established based on individual devices and insert sizes. Even though TEER measurement is quick and easy and can be repeated as needed, it remains a non-specific endpoint. Routine TEER measurement is used to control the integrity of the epithelial layer in an experimental setting and as a first indicator of toxin-induced damages. However, no specific mechanisms and transport processes can be attributed to changes in TEER without further investigations. In comparison with the standard TEER assay, real-time cell electronic sensing was further developed. This technique is based on the continuous recording of cellular horizontal impedance, which enables a real-time monitoring of the integrity of the epithelial barrier and the potential effects of toxins and other agents that affect barrier integrity (23-26).

### ***Paracellular tracer flux assays***

In addition to TEER measurement, determination of the paracellular flux of marker substances across the cell monolayer can be monitored (27). These markers differ in size and need to be nontoxic, non-charged and water soluble, and they should neither be absorbed nor metabolized by the cells (28, 29). The most common paracellular markers used in *in vitro* models are fluorescent compounds (such as lucifer yellow, LY) or fluorescently labelled compounds (such as fluorescein isothiocyanate (FITC)-dextran and FITC-inulin) (30). In particular apical-to-basolateral flux of paracellular markers is used to identify a compromised intestinal barrier function (31).

Paracellular tracer transport can also be measured in *in vivo* models by testing the presence of macromolecular tracers in the blood (such as FITC-dextran) after oral gavage. In addition, site specific permeability alongside the gastrointestinal (GI) tract can be assessed by measuring the presence of a variety of small saccharide probes and/or chromium-labelled ethylene diamine tetra acetic acid (Cr-EDTA) in the urine of humans and experimental animals after oral administration. For example, sucrose and lactulose/mannitol are useful probes for determining permeability characteristics of the gastroduodenal region and the entire small intestine, while sucralose and Cr-EDTA are used to evaluate colonic permeability (28, 29, 32).



### **Assessment of the expression of TJ proteins**

The major functional elements of the epithelial barrier are the TJ proteins, sealing the intercellular space between adherent epithelial cells (8, 33). TJs form an anastomosing network near the luminal surface, thus preventing a paracellular transport of luminal antigens (Figure 1). TJs are composed of I) transmembrane proteins whose extracellular domains cross the plasma membrane and interact with their partners on the adjacent cells and II) cytoplasmic scaffolding proteins, which are entirely located on the intracellular side of the plasma membrane. Transmembrane TJs form a horizontal barrier at the apical-lateral membrane of epithelial cells and consist of occludin (OCLN), claudins (CLDNs), junctional adhesion molecules (JAMs) and tricellulin. The cytoplasmic scaffolding proteins, like zonula occludens (ZO)s proteins, provide a direct link between transmembrane TJ proteins and the actin cytoskeleton (34-36). Increased TJ mRNA expression can indicate ongoing repair mechanisms in an established epithelial cell monolayer (26). However, the assessment of TJs should not be limited to the gene level, since mRNA amount does not necessarily predict the protein level (37, 38). For example, our study showed that following deoxynivalenol exposure, a decrease in the protein level of CLDNs could be observed, associated with an up-regulation of the mRNA level of CLDNs (26). Therefore, for the interpretation of barrier damage, qPCR and Western blot analysis are generally performed in parallel to measure mRNA and protein levels of TJs, respectively. In addition, the visualization of the sub-cellular localization of TJs by immunostaining is an additional tool to identify intestinal barrier dysfunction. All these measurements can be performed in different *in vitro* cell culture models as well as in intestinal explants and *in vivo* models.

### **Intestinal explant model**

Next to cell culture models, intestinal explants have been introduced as a model to test intestinal integrity. The model is based on the long-term experience with intestinal specimen mounted in so-called Ussing chambers for the study of nutrient absorption. For these studies, sheets of intestinal segments are mounted in Ussing chambers and maintained in complete explant culture medium gassed with 95% O<sub>2</sub>, 5% CO<sub>2</sub> and kept at 37°C with or without shaking for the entire culture time (39). The major advantage of this model is that explants maintain the complex cellular community and intestinal architecture and therefore cell-cell interactions can be studied. Moreover, segment-specific responses can be monitored alongside the GI tract. The main limitation of intestinal explant is that the period of culture during which the morphology and function of cells is preserved, is very short, limiting the possibility to study delayed or long-term effects (39-41).

### **In vivo models**

In addition to the above-described *in vitro* (cell culture) or *ex vivo* (explant) assays, several markers of intestinal integrity can be directly measured *in vivo* in comparable models. This includes the paracellular flux assays and the assessment of the expression of TJ



proteins together with histological approaches that provide insight into changes of the intestinal architecture, but also into epithelial cell damage (31). Zonulin, as an example, is a physiological modulator of intercellular TJs and an increase in zonulin levels in serum is associated with an impaired intestinal permeability (42, 43). Moreover, to identify the intestinal epithelial damage, serum concentrations of intestinal fatty acid binding protein (IFABP) can be evaluated (44, 45), but both parameters have not been widely applied in the assessment of mycotoxins. In contrast, histological investigations describing the effects of mycotoxins on villus architecture, goblet cells and mucus production are among routine approaches to detect the presence and the extent of epithelial cell damage and intestinal integrity following the exposure to mycotoxins and other toxic agents in various animal species (31, 46-48).

## Effects of mycotoxins on intestinal permeability

Figure 1 provides a comprehensive overview of the available evidence regarding direct effects of various mycotoxins on the intestinal epithelial barrier. The direct effect of aflatoxins, ochratoxin A, patulin, fumonisin B<sub>1</sub>, T-2/HT-2 toxin, nivalenol and deoxynivalenol are extensively explained and discussed in the following section.

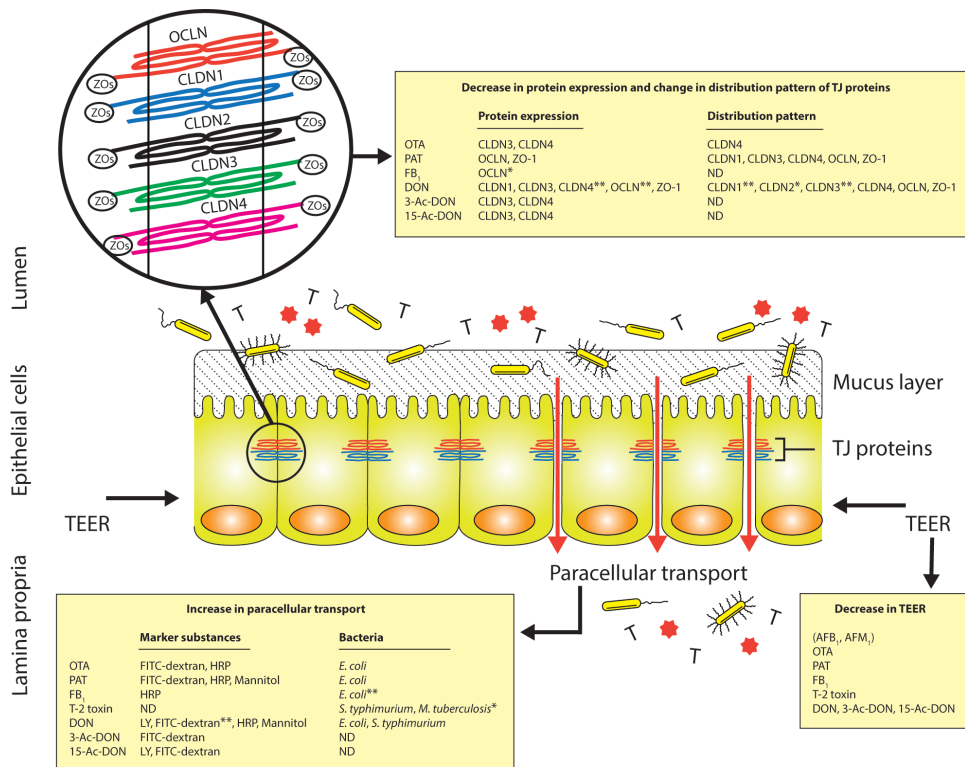


**Figure 1.** Schematic illustration of the mycotoxin-induced intestinal epithelial barrier breakdown. The gut mucosa is constantly challenged by a diverse microbial community (yellow rod-shaped bodies), food-borne toxins (T) and foreign antigens (red heptagrams). The most prominent example of food-borne toxins primarily associated with an impairment of the intestinal barrier are mycotoxins. Various mycotoxins have been shown to induce intestinal barrier breakdown demonstrated by a decrease in TEER, an increase in paracellular transport and changes in the expression as well as distribution pattern of different TJ proteins. The data shown in the figure have been demonstrated by *in vitro* studies unless otherwise stated (\**in vivo* studies, \*\**in vitro* as well as *in vivo* studies). Abbreviations used: 3-Ac-DON, 3-acetyl-deoxynivalenol; 15-Ac-DON, 15-acetyl-deoxynivalenol; AFB<sub>1</sub>, aflatoxin B<sub>1</sub>; AFM<sub>1</sub>, aflatoxin M<sub>1</sub>; CLDN, claudin; DON, deoxynivalenol; *E. coli*, *Escherichia coli*; FB<sub>1</sub>, fumonisin B<sub>1</sub>; FITC-dextran; fluorescein isothiocyanate-dextran; HRP, horseradish peroxidase; LY, lucifer yellow; *M. tuberculosis*, *Mycobacterium tuberculosis*; ND, not determined; OCLN, occludin; OTA, ochratoxin A; PAT, patulin; *S. typhimurium*, *Salmonella typhimurium*; TEER, transepithelial electrical resistance; TJ, tight junction; ZO, zonula occludens.

**Aflatoxins**

Aflatoxins are naturally occurring mycotoxins that are produced by various species of *Aspergillus*. The major aflatoxins commonly isolated from foods and feeds are aflatoxins B<sub>1</sub>, B<sub>2</sub>, G<sub>1</sub> and G<sub>2</sub> (49). Aflatoxin B<sub>1</sub> (AFB<sub>1</sub>), considered as the most toxic form, is metabolized by liver cytochrome P450 (CYP) enzymes (mainly by CYP3A4 and CYP1A2) to an AFB<sub>1</sub>-8,9-exo-epoxide and AFB<sub>1</sub>-8,9-endo-epoxide. The exo-epoxide rapidly binds to DNA and forms the 8,9-dihydro-8-(N7-guanyl)-9-hydroxy AFB<sub>1</sub> (AFB<sub>1</sub>-N7-Gua) adduct. If this DNA-damage is not repaired before DNA replication, it causes mutational effects in the 3<sup>rd</sup> base of codon 249 in the p53 tumor suppressor gene. P53 is the most frequently targeted gene in human carcinogenesis, with a mutation frequency of 50% in most major cancers (50-52), hence, this mutation is considered as a key event in aflatoxin-induced carcinogenesis. The endo-epoxide primarily binds to cellular proteins, and is associated with direct cytotoxicity and the impairment of liver function. AFB<sub>1</sub> is classified as a group 1 carcinogen (carcinogenic to humans) by the International Agency for Research on Cancer (IARC) (53). Epidemiological evidence suggests a synergistic effect of aflatoxin B<sub>1</sub> and chronic hepatitis B virus infections in the prevalence of liver cancer in humans (51, 54-56).

Another important hepatic metabolite of AFB<sub>1</sub> is aflatoxin M<sub>1</sub> (AFM<sub>1</sub>), which is excreted into milk both in animals as well as in humans. This results in an undesirable exposure of infants. AFM<sub>1</sub> is less biologically active than AFB<sub>1</sub>, but can also be converted into an AFM<sub>1</sub>-epoxide that can bind to DNA and form a AFM<sub>1</sub>-N7-Gua which leads to hepatotoxicity and hepato-carcinogenicity (49, 57, 58). IARC has classified AFM<sub>1</sub> as a group 2B carcinogen (possibly carcinogenic to humans) (53).

**Effects of aflatoxins on intestinal barrier function**

In consideration of the primary hepatotoxicity and hepato-carcinogenicity, only very few studies have been conducted showing that aflatoxins exposure might compromise also intestinal permeability (Table 1). Gratz *et al.* (59) showed that AFB<sub>1</sub> induces a time-dependent decrease in TEER values of Caco-2 cells. This effect was only observed at high concentrations and in the presence of activated CYP3A4, confirming the biotransformation-dependent toxicity of AFB<sub>1</sub>. Another study conducted by Caloni *et al.* (60) reported that exposure to much lower AFM<sub>1</sub> concentrations either to the apical or basolateral surface of the Caco-2 cell monolayer results in a slight, but significant TEER decrease. The sub-cellular localization of OCLN and ZO-1 remained unaffected as observed by immunostaining. Further studies would be necessary to unravel the potential clinical impact of aflatoxins, in particular AFM<sub>1</sub>, on epithelial barrier integrity in infants.

**Table 1.** Modulation of the intestinal barrier function by aflatoxins

Model	Concentration Exposure time	Effects on barrier function	References
<b>Aflatoxins</b>			
Caco-2 cells	150 $\mu$ M 72 h	AFB <sub>1</sub> ; Decrease in TEER values	(59)
Caco-2 cells	3.2-33 nM 24 h	AFM <sub>1</sub> ; Decrease in TEER values	(60)

**Ochratoxin A**

Ochratoxin A (OTA) is a mycotoxin produced by various species of *Aspergillus* and *Penicillium* (57). Exposure to OTA is a worldwide phenomenon, as evidenced by the presence of OTA in the majority of the tested human blood samples in many countries (61-63). The kidney is the major target organ for OTA and its derivatives, and some epidemiological studies in humans have associated the exposure to OTA with a chronic tubulointerstitial nephritis (also denoted Balkan endemic nephropathy (BEN)) and urothelial tract tumors (57, 64, 65). At higher concentrations OTA has been shown to be nephrotoxic, teratogenic and immunotoxic. IARC has classified OTA as a group 2B carcinogen (possibly carcinogenic to humans) on the basis of sufficient evidence for carcinogenicity in animal studies (53). A number of mechanisms are described to be involved in OTA toxicity, including I) inhibition of protein synthesis through inhibition of phenylalanyl-tRNA synthetase, II) mitochondrial dysfunctions and the production of reactive oxygen and nitrogen species (ROS and RNS) and lipid peroxidation, III) inhibition of histone acetyltransferase, which leads to disruption of mitosis and chromosomal instability as well as, IV) DNA adducts, particularly deoxyguanosine (dG) adducts (66-70). Although, the kidney is generally believed to be the main target organ for OTA toxicity, its well-known inhibition of cellular protein synthesis and the generation of reactive oxygen as well as nitrogen species suggest that the GI tract may be a possible target organ for OTA as well (5, 7).

**Effects of ochratoxin A on intestinal barrier function**

Modulation of the intestinal barrier by OTA has mainly been studied using the *in vitro* Caco-2 cell model (Table 2). For the first time, Maresca *et al.* (71) showed that the OTA exposure results in a concentration- and time-dependent decrease in TEER values of both Caco-2 and HT-29-D4 cells. They showed that the apical surface is more susceptible to OTA in comparison with exposure via the basolateral surface; in contrast, other studies reported that both apical and basolateral surfaces are equally affected by OTA (71, 72). Ranaldi *et al.* (73) found that the TEER decrease in OTA-exposed Caco-2 cells at concentrations up to 200  $\mu$ M for 48 h is reversible and a full recovery of TEER value is achieved within 24 h

after cessation of mycotoxin exposure. It has been reported that the OTA-induced TEER decrease is accompanied with an increase in the translocation of paracellular markers, such as 4, 10 kDa FITC-dextran and horseradish peroxidase (HRP, ~44 kDa) (Table 2). The OTA-induced permeability is shown to be size selective, since translocation of 20 and 40 kDa FITC-dextran remain unchanged after exposure of Caco-2 cells to OTA up to 100  $\mu$ M for 24 h (6, 72). Depletion of specific CLDN isoforms, in particular CLDN3 and CLDN4 as well as changes in their cellular distribution are well documented, but there are no data on the other components of the TJ complex such as OCLN and ZO<sub>s</sub> (72-74). Of clinical relevance is the finding that the OTA-induced intestinal barrier impairment in a concentrations equal or higher than 1  $\mu$ M OTA triggers a concentration- and time-dependent increase in the translocation of *Escherichia coli* across Caco-2 cell monolayers (6).

**Table 2.** Modulation of the intestinal barrier function by ochratoxin A

Model	Concentration Exposure time	Effects on barrier function	References
<b>Ochratoxin A</b>			
Caco-2 cells	100 $\mu$ M 24 h	Decrease in TEER values Increase in permeability of 4 and 10 kDa FITC-dextran Decrease in protein expression of CLDN3 and CLDN4	(72)
Caco-2 cells	1-100 $\mu$ M 12 h	Decrease in TEER values Increase in permeability of HRP and 4 kDa FITC-dextran Increase in translocation of commensal <i>Escherichia coli</i> (strain k12)	(6)
Caco-2 cells	100 $\mu$ M 24 h	Decrease in TEER values Decrease in protein expression of CLDN3 and CLDN4	(74)
Caco-2 cells	40-1000 $\mu$ M 48 h	Decrease in TEER values Affect the distribution pattern of CLDN4	(73)
Caco-2 cells	10 $\mu$ M 3 h	Neither a significant decrease in TEER values nor an increase in permeability of [ <sup>14</sup> C]-mannitol	(83)
Caco-2 cells HT-29-D4 cells	0.1-100 $\mu$ M 48 h	Decrease in TEER values	(71)

### Patulin

Patulin (PAT) is a mycotoxin produced by various species of *Penicillium*, *Aspergillus* and *Byssoschylamys*, known as fruit spoiling fungi (57, 75). Based on experimental models in mice, PAT was initially suspected to increase the prevalence of gastric cancers, but the IARC has classified PAT as a group 3 carcinogen (not carcinogenic to humans) due to

inadequate evidence for the carcinogenicity of PAT in both experimental animals and humans (76). Currently, the GI tract and the immune system are thought to be the most affected tissues following PAT exposure (75, 77). PAT is believed to induce cytotoxicity by forming covalent adducts with essential cellular thiols (organic compounds that contain a sulfhydryl group), by which it inhibits the activity of many enzymes. One of the most likely cellular targets of PAT is the sulfhydryl group of cysteine (Cys) and glutathione (GSH) leading to depletion of glutathione and subsequent increased generation of ROS (57, 78-81). A recent study conducted by Boussabbeh *et al.* (82) revealed that PAT induces apoptosis through the ROS-mediated endoplasmic reticulum stress pathway.

### **Effects of patulin on intestinal barrier function**

Impairment of intestinal barrier integrity induced by PAT has been clearly shown in different studies (Table 3). PAT is found to induce a rapid and dramatic decrease in TEER values of Caco-2 and HT-29-D4 monolayers (84-86). PAT exposure to either apical or basolateral surface resulted in a concentration- and time-dependent decrease of TEER levels. The apical surface seems to be slightly more sensitive than the basolateral surface (85, 86). Mohan *et al.* (87) showed that PAT at concentrations equal or higher than 1.6  $\mu\text{M}$  causes an increase in plasma membrane permeability, observed by increased TOTO-3 fluorescence intensity. In addition, it has been reported that PAT induces the permeability of different paracellular markers such as HRP and FITC-dextran of 4-40 kDa across the intestinal epithelium (Table 3) (6, 86, 88). Maresca *et al.* (6) showed that the impairment of intestinal integrity by PAT results in an increased translocation of *Escherichia coli* across Caco-2 cell monolayers. There are different studies demonstrating specific effects of PAT on TJs. For example, it is shown that 5 h exposure of Caco-2 cell monolayers to 100  $\mu\text{M}$  PAT leads to proteolytic cleavage of OCLN and a significant reduction in ZO-1 protein levels. However, the expression levels of CLDN1, CLDN3 and CLDN4 were not changed (86). Kawauchiya *et al.* (89) demonstrated that the exposure of Caco-2 cells to 50  $\mu\text{M}$  PAT, resulted in a gradual decrease in protein expression of ZO-1, while the expression levels of CLDN4 and OCLN remained unaffected up to 72 h. Interestingly, the decreased ZO-1 expression observed in latter study was correlated with an increased phosphorylation of this protein, while phosphorylation of CLDN4 and OCLN were not detected. This is in contrast to the finding of Katsuyama *et al.* (88) who reported an increase in phosphorylation of CLDN4 following a 24 h exposure of Caco-2 cells to PAT at a concentration of 50  $\mu\text{M}$ . PAT also affects the distribution pattern of different TJs including CLDN1, CLDN3, CLDN4, OCLN and ZO-1 (86, 88, 89). Moreover, PAT exposed to isolated rat colonic mucosa at a concentration of 500  $\mu\text{M}$  for 2 h has been shown to induce intestinal barrier breakdown demonstrated by a decrease in TEER values and an increase in [ $^{14}\text{C}$ ]-mannitol (182 Da) permeability (87). There are a few possible mechanisms underlying the PAT-induced impairment of TJs and intestinal barrier function. For example, Mahfoud *et al.* (85) showed that the PAT-induced TEER decrease involves in inhibition of protein tyrosine phosphatase (PTP) through inactivation of cysteine residues in the catalytic



domains of PTP. The high affinity of PAT for sulfhydryl groups of Cys and GSH (explained above) may account for the barrier impairment, since addition of 1.6 mM GSH was found to completely prevent PAT-induced TEER drop. Therefore, higher amount of GSH in Caco-2 cells compared to HT-29-D4 cells (8.0 vs 4.5 nmol/mg of protein) may explain the different sensitivity of these cells to PAT (85). It has been recently suggested that PAT decreases the expression of density-enhanced phosphatase-1 (DEP-1) through down-regulation of proliferator-activated receptor gamma (PPAR $\gamma$ ) (88). DEP-1 is a class III transmembrane phosphatidyl-inositol-phosphate, which has been proposed to regulate different signal transduction pathways, such as cell migration, proliferation, differentiation and adhesion (90, 91). Furthermore, it has been observed that a PAT-mediated decrease of DEP-1 results in hyper-phosphorylation of CLDN4 and subsequently hinders the interaction between ZO-1 and CLDN4, which leads to release of CLDN4 from the TJ network (88). In addition, McLaughlin *et al.* (86) speculated that matrix metalloproteinases (MMPs) may play a role, at least partly, in the observed intestinal barrier impairment induced by PAT, since inhibition of MMP partially protected OCLN from PAT-mediated cleavage. However, according to their findings, the reduction in ZO-1 levels is not prevented by MMP inhibitors.

### ***Fumonisin B<sub>1</sub>***

Fumonisin B<sub>1</sub> (FB<sub>1</sub>) is the major representative of structurally related fumonisins produced by various species of *Fusarium*, predominantly by *Fusarium verticillioides*. Initially, FB<sub>1</sub> has been associated with an increased prevalence of esophageal cancers in humans in the Transkei region of South Africa (92-94). IARC has classified FB<sub>1</sub> as a group 2B carcinogen (possibly carcinogenic to humans) (53). Maternal exposure to fumonisins increases the risk of neural tube defects (such as spina bifida and anencephaly) in offspring, mainly through interference with the function of folate-binding protein and utilization of folic acid (95-98). FB<sub>1</sub> has been shown to be hepatotoxic, nephrotoxic, carcinogenic and immunotoxic in various animal species (99). The main mechanism of action is inhibition of the enzyme ceramide synthase (CerS) (99-102). CerS is a key enzyme that catalyzes the formation of complex sphingolipids from the sphingoid bases (99, 103). FB<sub>1</sub> is observed to inhibit mainly CerS4 isomers (CerS1 and CerS2 isomers are also inhibited to a lesser extent) and leads to the accumulation of sphingoid bases (including sphinganine and sphingosine) and in turn to a depletion of ceramide and complex sphingolipids (57, 99-102). It is well known that sphingolipids participate in a variety of cellular signaling pathways, such as regulation of cell proliferation, differentiation and apoptosis (103, 104). Although liver and kidney are thought to be the most affected tissues by FB<sub>1</sub> in animal species, the GI tract has also been reported as a possible target organ for FB<sub>1</sub> (99, 105). It has been shown that a single subcutaneous injection of FB<sub>1</sub> (25 mg/kg body weight (bw)) causes a transient increase in sphinganine and sphingosine in the mouse small intestine over 24 h (102). Exposure of pigs to FB<sub>1</sub> (1.5 mg/kg bw) for 7 days results in a significant increase in the concentration of sphinganine and sphingosine, and a decrease in the total glycolipid content as well as alteration in the jejunal glycolipid composition, whereas no

changes are observed in the duodenum and ileum (100).

**Table 3.** Modulation of the intestinal barrier function by patulin

Model	Concentration Exposure time	Effects on barrier function	References
<b>Patulin</b>			
Caco-2 cells	100 $\mu$ M 5 h	Decrease in TEER values Increase in permeability of 4-40 kDa FITC-dextran Proteolysis of OCLN Decrease in protein expression of ZO-1 Affect the distribution pattern of CLDN1, CLDN3, CLDN4, OCLN and ZO-1	(86)
Caco-2 cells	50 $\mu$ M 72 h	Decrease in TEER values Decrease in protein expression of ZO-1 Increase in phosphorylation of ZO-1 Affect the distribution pattern of CLDN4, OCLN and ZO-1	(89)
Caco-2 cells	50 $\mu$ M 36 h	Decrease in TEER values Increase in permeability of 4 kDa FITC-dextran Increase in phosphorylation of CLDN4 Affect the distribution pattern of ZO-1	(88)
Caco-2 cells	1-100 $\mu$ M 12 h	Decrease in TEER values Increase in permeability of HRP and 4 kDa FITC-dextran Increase in translocation of commensal <i>Escherichia coli</i> (strain k12)	(6)
Caco-2 cells	0.2-100 $\mu$ M 72 h	Increase in plasma membrane permeability	(87)
Caco-2 cells	25 nM-95 $\mu$ M 24 h	Decrease in TEER values	(84)
Caco-2 cells HT-29-D4 cells	1-100 $\mu$ M 24 h	Decrease in TEER values	(85)
Rat colonic explants	100-500 $\mu$ M 2 h	Decrease in TEER values Increase in permeability of [ $^{14}$ C]-mannitol	(87)

**Effects of fumonisin B<sub>1</sub> on intestinal barrier function**

Impairment of the intestinal barrier integrity induced by FB<sub>1</sub> has been shown in different *in vitro*, *ex vivo* and *in vivo* studies (Table 4). A concentration- and time-dependent decrease in TEER values of IPEC-1 cells (intestinal porcine epithelial cells) has been observed after FB<sub>1</sub> exposure and this process was time required as significant effects occurred only after a long term exposure (at least 8 days after FB<sub>1</sub> exposure) (100, 106). Bouhet *et al.* (106) demonstrated that FB<sub>1</sub>-induced decrease in TEER values is independent from the differentiation stage of IPEC-1 cells and this TEER drop is partially reversible. Another study has shown that the impaired intestinal barrier results in an increase of permeability for FB<sub>1</sub> across the IPEC-1 cells, suggesting that after long-term exposure, the very low absorption rate (normally ~3%) may increase over time (100). Surprisingly, an increase in TEER values of porcine jejunal explants is reported after 2 h exposure to FB<sub>1</sub> at concentration of 10 µM. In contrast, a significant increase in HRP permeability is reported following treatment with 10 µM FB<sub>1</sub> over the same time period (107). *In vitro* and *in vivo* studies have showed that FB<sub>1</sub>-induced barrier function impairment causes an increase in the translocation of pathogenic *Escherichia coli* across intestinal epithelial cells (105, 108). Furthermore, *Escherichia coli* could be recovered from lung and mesenteric lymph nodes 7 days after oral exposure of pigs to FB<sub>1</sub> at a dose of 0.5 mg/kg bw (108). Bracarense *et al.* (109) observed that the exposure of piglets to a FB<sub>1</sub>-contaminated diet (3 mg/kg) for 5 weeks significantly decreases the protein expression of OCLN in ileum. Further studies would be needed to clarify the involvement of TJ impairment in FB<sub>1</sub>-induced impairment of the intestinal integrity.

**Trichothecenes**

The class of trichothecenes comprises a unique family of over 200 tetracyclic sesquiterpenoid fungal metabolites produced by various species of the genera *Fusarium*, *Stachybotrys*, *Cephalosporium*, *Myrothecium*, *Spicellum*, *Verticimonosporium*, *Trichoderma* and *Trichothecium* (110-112). Common structure elements of trichothecenes are a C-9, -10 double bond and C-12, -13 epoxide moiety contributing to the toxicity of trichothecenes (110, 113, 114). Trichothecenes are classified into four different types (type A-D) according to the characteristic functional group. Type A trichothecenes are characterized by a hydroxyl motif at C-8 (e.g. T-2/HT-2 toxins), whereas type B trichothecenes carry a keto (carbonyl) motif at this position (e.g. nivalenol, deoxynivalenol). Type C trichothecenes have an additional epoxide group at the C-7, -8 or C-9, -10 position (e.g. crotoxin), while type D trichothecenes possess a macrocyclic ring between the C-4, -15 positions (e.g. roridin) (110-113, 115). Among them, type A and type B are known to be the most prevalent trichothecenes (112, 116). At the cellular level, type A and type B trichothecenes not only interact with the peptidyl-transferase at the 60S ribosomal subunit to cause a translational arrest and protein synthesis inhibition, but also activate intracellular protein kinases, particularly mitogen-activated protein kinases (MAPKs) and their downstream effectors resulting in a process, known as ribotoxic stress response (111, 112, 115,

117). Rapidly dividing cells, particularly intestinal epithelial cells and immune cells, are generally believed to be the major target organs for type A and type B trichothecenes (118, 119). In consideration of the complex group of trichothecenes and the availability of detailed investigations, only major representatives of this class of mycotoxins such as T-2/HT-2 toxin, nivalenol (NIV) and deoxynivalenol (DON) will be discussed in more detail below. Their effects on intestinal barrier integrity are summarized in Table 5 at the end of this chapter.

**Table 4.** Modulation of the intestinal barrier function by fumonisin B<sub>1</sub>

Model	Concentration Exposure time	Effects on barrier function	References
<b>Fumonisin B<sub>1</sub></b>			
IPEC-1 cells	50-200 µM 16 d	Decrease in TEER values Increase in permeability of FB <sub>1</sub>	(100)
IPEC-1 cells	20-200 µM 4 h	Increase in translocation of pathogenic <i>Escherichia coli</i> (strain 28C)	(105)
IPEC-1 cells	50-500 µM 28 d	Decrease in TEER values	(106)
Porcine jejunal explants	10 µM 2 h	Increase in TEER values Increase in permeability of HRP	(107)
Piglet	3 mg/kg feed 5 w	Decrease in protein expression of OCLN in ileum	(109)
Piglet	0.5 mg/kg bw 7 d	Increase in translocation of pathogenic <i>Escherichia coli</i> (strain 28CNaI <sup>a</sup> )	(108)

### **T-2/HT-2 toxin**

Historically, prolonged exposure of humans to T-2 toxin has been associated with a disease known as Alimentary Toxic Aleukia (ATA); characterized by nausea, vomiting, diarrhea, gastroenteritis, leukopenia (aleukia), hemorrhages, skin inflammation and in severe cases a death due to asphyxia (120). Genotoxicity and mutagenicity of T-2 is still a matter of controversial debate and IARC has classified T-2 toxin as a group 3 carcinogen (not carcinogenic to humans) due to inadequate evidence for the carcinogenicity in both experimental animals and humans (121). The major mechanisms of toxicity of T-2 toxin are described as I) inhibition of protein synthesis (at the initiation step of protein translation) through interaction with the peptidyl-transferase at the 60S ribosomal subunit and II) generation of ROS and oxidative stress leading to caspase-mediated cellular apoptosis (111, 112, 117, 122). Rapidly after ingestion, T-2 toxin is mainly metabolized into HT-2

toxin, through a deacetylation reaction by intestinal microflora, and various hydroxylated metabolites in the liver. The toxicity of HT-2 is quite similar to that of the T-2 toxin and their effects cannot be differentiated. However, it has been speculated that HT-2 toxin is responsible for the observed *in vivo* toxicity following T-2 toxin ingestion (112, 114, 119).

#### **Effects of T2/HT-2 toxin on intestinal barrier function**

Despite the well-documented clinical and pathological intestinal lesions induced by T-2 toxin (118), the effects of T-2 toxin on intestinal integrity have hardly been studied (Table 5). However, a study conducted by Goossens *et al.* (123) clearly showed that T-2 toxin causes an impairment of the barrier function at a concentration of 21 nM as observed by a decrease in TEER values and an increase in the passage of the antibiotics doxycycline and paromomycin across IPEC-J2 cells (intestinal porcine epithelial cells). Another study reported that the exposure of mice to T-2 toxin (3.3 mg/kg bw) for 20 days results in an increased translocation of *Mycobacterium tuberculosis* (124). In addition, a significant increase in the translocation of *Salmonella typhimurium* across IPEC-J2 cell monolayer occurs already 30 minutes after T-2 toxin exposure with concentrations as low as 2.1 nM (125). Surprisingly in the same study, TEER values remained unaffected up to 24 h after exposure to concentrations of T-2 toxin ranging from 1.6 to 10.7 nM (125). The exact mechanisms underlying the gut barrier dysfunction induced by T-2/HT-2 toxin are unknown and would require further investigations.

#### **Nivalenol**

Nivalenol (NIV) is one of the less studied type B trichothecenes and little is known about the toxicity of NIV in humans (126). Some studies suggest that exposure to dietary NIV could be associated with an increased incidence of esophageal and gastric cancers in certain regions of China (114, 126, 127). However, IARC has classified NIV as a group 3 carcinogen (not carcinogenic to humans) due to inadequate evidence for the carcinogenicity in both experimental animals and humans (121). NIV is usually found together with DON and synergistic interactions between them are assumed (128). DON and NIV share highly similar chemical structures and the only difference between them is a single oxygen atom at the C-4 position in the trichothecene structure (hydrogen and hydroxyle group at the C-4 position in DON and NIV, respectively) (112, 114, 115). Although less prevalent in food commodities, NIV is generally believed to have a higher toxicity than DON (4, 46, 129). Unlike DON, NIV inhibits protein synthesis by inhibiting the initiation step of protein translation through interaction with peptidyl transferase at the 60S ribosomal subunit (111). Using different approaches, the effects of NIV on intestinal epithelial cells have been acknowledged. Recently, it has been reported that NIV induces oxidative stress in IEC-6 cells (non-tumorigenic rat intestinal epithelial cell line) by generation of ROS and inducible nitric oxide synthase (iNOS), which leads to activation of nuclear factor kappa B (NF- $\kappa$ B) and nuclear factor erythroid 2-related factor 2 (Nrf2) pathways (130). A study conducted by Bianco *et al.* (129) showed that NIV induces apoptosis in IEC-6 cells by

inhibition of the anti-apoptotic protein B cell lymphoma-2 (BCL-2) and the induction of the pro-apoptotic protein Bcl-2-associated X protein (BAX) as well as caspase-3 activation. Induction of apoptosis was further confirmed in *ex vivo* pig jejunal explant and *in vivo* pig intestinal loops (46). However, the effect of NIV on the intestinal barrier function has not been studied yet.

### ***Deoxynivalenol and its mono-acetylated derivatives***

Deoxynivalenol (DON) is believed to be the most widely distributed trichothecene (14, 114). The high incidence of human exposure is confirmed by the analysis of urine samples for DON and its glucuronides, demonstrating that the exposure incidence exceeds 90% of the tested population in many cases (131-135). Human exposure to DON can cover all age groups, even the developing fetus, since DON crosses the placental barrier (136, 137). Genotoxicity and mutagenicity of DON is widely studied and IARC has classified DON as a group 3 carcinogen (not carcinogenic to humans) (121). DON modulates the function of various organ systems. For example, DON is also known as vomitoxin, since it induces a strong emetic effect due to an interaction with the dopaminergic system in the central nervous system (14, 138, 139). Other neurological effects of DON in regulating overall activity and satiety have recently been discussed (138, 140, 141). Another important target of DON is the immune system and DON can induce both immunostimulatory as well as immunosuppressive responses depending on dose, frequency and duration of exposure. As an example, low dose exposure to DON triggers immune responses, whereas a high dose leads to leukocyte apoptosis and subsequent immunosuppression (14, 142). At the cellular level, DON inhibits protein synthesis (at the elongation-termination step of protein translation) through interaction with the peptidyl-transferase at the 60S ribosomal subunit (111). The binding of DON to the ribosome, rapidly activates MAPK signaling pathways and induces caspase-mediated apoptosis in a process, known as the “ribotoxic stress response” (2, 14, 111).

In addition to DON itself, two acetylated derivatives (3-acetyl-DON, 3-Ac-DON and 15-acetyl-DON, 15-Ac-DON) may be produced by *Fusarium* species simultaneously, but at much lower levels than DON. Due to similarity in the chemical structure, the mode of action of 3-Ac-DON and 15-Ac-DON is generally considered to be the same as DON (14, 15). Recently, the contribution of plant-derived conjugates, such as glucosides of DON, to overall DON exposure is considered as well (143).

### ***Effects of DON, 3-Ac-DON and 15-Ac-DON on intestinal barrier function***

The contribution of DON to the loss of intestinal barrier function has been extensively examined in different *in vitro*, *ex vivo* and *in vivo* studies (Table 5). Evidence in different human (Caco-2, T84 and HT-29) as well as porcine (IPEC-1 and IPEC-J2) intestinal epithelial cells have shown that DON induces a concentration- and time-dependent drop in TEER values (26, 118, 144-146). It could be concluded that IPEC-1 cells are more sensitive to DON compared to Caco-2 cells as indicated by the DON-induced TEER drop (147). This

difference may be associated with different origin and type of these cell lines, as Caco-2 cells are human colon adenocarcinoma cells, while IPEC-1 cells are non-transformed and non-carcinoma cells obtained from porcine small intestines (142, 148). Recently, we showed that the DON-induced TEER drop considerably depends on the side of application and this response is much more pronounced when DON is applied to the basolateral, rather than the apical surface of Caco-2 cells (26). The same surface-dependent effect is also observed in IPEC-J2 cells (146). Using horizontal impedance measurements, we and others could show that DON disintegrates a human Caco-2 cell monolayer within the first few hours of exposure in concentrations as low as 1.5  $\mu\text{M}$  (26, 149). The DON-induced TEER drop in established epithelial cell monolayers is accompanied with a concentration-dependent increase in the flux of paracellular markers such as mannitol, HRP, LY and 4 kDa FITC-dextran (Table 5) (6, 26, 27). Goossens *et al.* (123) observed that the decrease in TEER is accompanied with an increase in passage of smaller molecules such as the antibiotics doxycycline and paromomycin across IPEC-J2 cells. This is in line with the assumption that an increased flux of paracellular markers is size selective, since our study with two molecular sizes of FITC-dextran (4 and 40 kDa) revealed that DON exposure induces a significant increase in the flux of 4 kDa FITC-dextran in the Caco-2 cells, but not of 40 kDa FITC-dextran (26). A similar concentration-dependent increase in permeability was observed in pig jejunal explants exposed to 20 to 50  $\mu\text{M}$  DON for up to 2 h (147). Intestinal barrier breakdown was further confirmed *in vivo* by our previous study showing that a single oral application of DON (25 mg/kg bw) to mice results in significant increase in 4 kDa FITC-dextran permeability (26). Of clinical relevance is the fact that a DON-induced impairment of intestinal integrity may result in the increased transfer of luminal antigens and bacteria. Pinton *et al.* (147) described that DON treatment causes a concentration- and time-dependent increase in translocation of pathogenic *Escherichia coli* across IPEC-1 cell monolayers. Another study found that DON-induced loss of epithelial barrier function, observed by decrease in TEER and increase in paracellular flux, is correlated with increase in translocation of commensal *Escherichia coli* across Caco-2 cells (6). DON-enhanced translocation of *Salmonella typhimurium* is reported in both undifferentiated and differentiated IPEC-J2 cells, although undifferentiated cells are found to be more sensitive in comparison to differentiated cells (150). DON-induced permeability in various *in vitro* and *in vivo* models is accompanied with specific alterations in the expression (at transcriptional and protein levels) as well as distribution of different TJs. An up-regulation in mRNA levels of CLDN3, CLDN4, OCLN and ZO-1 were observed in DON-exposed Caco-2 cells (26, 27, 151). CLDNs have been reported to be the most susceptible TJs regarding DON exposure to human intestinal epithelial cells (26, 77, 118, 147). However, in addition to CLDNs, OCLN and ZO-1 have also been shown to be influenced by DON in porcine intestinal epithelial cells (146, 152, 153). Up-regulation of TJ mRNA is often reported as an effect of DON, whereas at the same time a significant reduction in the protein level of different TJs is observed (26, 27). Therefore, it is assumed that DON primarily targets the TJ proteins and that the RNA



upregulation needs to be considered as a compensatory mechanism (26, 27, 151, 154). Another explanation could be that in addition to protein synthesis inhibition (which could explain the decrease in protein level of TJs), DON augments and prolongs the usually transient expression of genes either by transcriptional enhancement or transcript stabilization (leading to increased transcriptional rates of TJs), a mechanism described as superinduction (155, 156).

*In vivo* exposure to DON-contaminated diet also significantly affects different TJs and segment-specific effects of DON are reported to occur throughout the intestine. Our previous study, as an example, indicated that up-regulation of the different CLDNs caused by a gavage with DON is most pronounced in the mouse distal small intestine compared to other segments of the intestine (26). Surprisingly, our group found that even after low-level exposure to DON, which has been generally considered as acceptable in animal feeds, substantial changes occur in markers of intestinal integrity. For example, up-regulation of different TJ proteins were observed alongside the intestine, whereas in the jejunum, the mRNA expression of certain TJs (CLDN4, OCLN, ZO-1 and ZO-2) was down-regulated (154). Furthermore, Lessard *et al.* (157) also observed the down-regulation of CLDN3, CLDN4 and OCLN mRNA levels in the ileum of pigs consuming a DON contaminated diet, whereas no effect was observed in the jejunum. A study conducted in broiler chickens showed an upregulation of CLDN1, CLDN5, ZO-1 and ZO-2 mRNA levels in the ileum after dietary DON, while only CLDN5 was affected in the jejunum (151).

Several studies demonstrated a decrease in protein expression of CLDN4 and OCLN in pig jejunum and ileum after a DON diet (109, 147). In contrast to other studies, Alizadeh *et al.* (154) showed that the protein expression of OCLN is significantly increased in duodenum, jejunum and colon of DON-treated pigs compared to control animals, which is probably related to the short-term, low-dose exposure to DON. In addition, DON is able to interrupt the distribution pattern of TJs (including CLDNs, OCLN and ZO-1) as demonstrated within different *in vitro* as well as *in vivo* models (26, 146, 153). Our recent murine study showed that already 6 h after an oral DON gavage (25 mg/kg bw) an irregular distribution of CLDN1, CLDN2, CLDN3 has been observed in the distal small intestine, whereas in the colon no differences in the TJ distribution pattern were detected (26).

Unlike well-documented effects of DON on gut barrier, knowledge about toxicity of its acetylated derivatives is still limited and only a few studies have addressed intestinal barrier impairment induced by 3-Ac-DON and 15-Ac-DON (Table 5). Kadota *et al.* (158) showed that 15-Ac-DON has a higher potency to affect the permeability of Caco-2 cells compared to DON and 3-Ac-DON. The potency of DON and its acetylated derivatives on the barrier function of IPEC-1 cells are ranked as 15-Ac-DON > DON > 3-Ac-DON based on the decrease in TEER values and the increase in the permeability of 4 kDa FITC-dextran. Measuring the protein expression of CLDNs clearly showed that 15-Ac-DON has a more pronounced effect on the expression of CLDN3 and CLDN4 in IPEC-1 cells compared to DON and 3-Ac-DON (118).

As mentioned above, interaction of DON with the peptidyl-transferase at the 60S

ribosomal subunit has been associated not only with translational arrest and protein synthesis inhibition, but also with an activation of the intracellular protein kinases (particularly MAPKs) and their downstream signaling partners in a process known as the ribotoxic stress response (15, 118, 134, 159). MAPKs play a crucial role in many physiological processes including cell growth, differentiation, apoptosis and immune responses (159). Further studies have shown that TJ structure and function can also be regulated by signaling molecules involved in MAPK pathways (86, 160). At the molecular level, MAPK extracellular signal-regulated kinase 1 and 2 (ERK1/2), c-Jun N-terminal kinase (JNK) and p38 are described to get rapidly activated by DON in human as well as porcine intestinal cell lines (118, 161) and this activation leads to a decrease in the expression of CLDNs (118, 162).

Different observations of DON-induced activation of MAPKs have been reported in *ex vivo* as well as *in vivo* models. Using IPEC-1 cells, Pinton *et al.* (162) showed that the DON-activated MAPK ERK1/2 correlates with a reduction in barrier function observed by decrease in TEER, increase in paracellular permeability and decrease in the expression of CLDN4. Interestingly, inhibition of ERK1/2 phosphorylation restored the barrier function of differentiated IPEC-1 cells (162). In addition, a study conducted by the same author showed that none of the MAPKs, such as ERK1/2, JNK and p38 are significantly activated neither in *ex vivo* (pig jejunal explants exposed to DON) nor in *in vivo* (jejunum of DON-fed pigs) models (118). However, another study using the same *ex vivo* and *in vivo* approaches, reported that DON significantly enhances the phosphorylation of ERK1/2 and p38, whereas the phosphorylation of JNK remains unaffected (163).

Only a few studies displayed differences between DON and its acetylated derivatives regarding their potency to activate MAPKs. 15-Ac-DON, as an example, has a greater capacity to activate MAPK ERK1/2, p38 and JNK, in the porcine intestinal epithelial cells and in pig jejunal explants compared to DON and 3-Ac-DON (118).

**Table 5.** Modulation of the intestinal barrier function by trichothecenes

Model	Concentration Exposure time	Effects on barrier function	References
<b>T-2 toxin</b>			
IPEC-J2 cells	0.21-210 nM 72 h	Decrease in TEER values Increase in permeability of doxycycline and paromomycin	(123)
IPEC-J2 cells	1.6-10.7 nM 1 h	Increase in translocation of <i>Salmonella typhimurium</i> (strain 112910a)	(125)
Mouse	3.3 mg/kg bw 20 d	Increase in translocation of <i>Mycobacterium tuberculosis</i> (strain H37RvR-KM)	(124)
<b>Deoxynivalenol</b>			
Caco-2 cells	1.39-12.5 $\mu$ M 24 h	Decrease in TEER values Decrease in horizontal impedance value Increase in permeability of LY and 4 kDa FITC-dextran Increase in transcript level of CLDN3, CLDN4, OCLN and ZO-1 Decrease in protein expression of CLDN1, CLDN3 and CLDN4 Affect the distribution pattern of CLDN1, CLDN3, CLDN4, OCLN and ZO-1	(26)
Caco-2 cells	0.16-16 $\mu$ M 24 h	Decrease in TEER values Increase in permeability of mannitol Increase in transcript level of CLDN4 and OCLN Decrease in protein expression of CLDN4	(27)
Caco-2 cells	5-100 $\mu$ M 48 h	Decrease in TEER values Increase in permeability of 4 kDa FITC-dextran Increase in translocation of pathogenic <i>Escherichia coli</i> (strain 28C) Decrease in protein expression of CLDN4	(147)
Caco-2 cells	1-100 $\mu$ M 12 h	Decrease in TEER values Increase in permeability of HRP and 4 kDa FITC-dextran Increase in translocation of commensal <i>Escherichia coli</i> (strain k12)	(6)
Caco-2 cells	0.37-1.5 $\mu$ M 6-120 h	Decrease in horizontal impedance value of undifferentiated cells	(149)

Caco-2 cells T84 cells	0.16-0.67 $\mu$ M 14 d	Decrease in TEER values Increase in permeability of LY	(144)
HT-29-D4 cells	0.001-100 $\mu$ M 48 h	Decrease in TEER values	(145)
IPEC-1 cells	30 $\mu$ M 48 h	Decrease in TEER values Increase in permeability of 4 kDa FITC-dextran Decrease in protein expression of CLDN4 Affect the distribution pattern of CLDN4	(162)
IPEC-1 cells	5-50 $\mu$ M 48 h	Decrease in TEER values Increase in permeability of 4 kDa FITC-dextran Decrease in protein expression of CLDN3 and CLDN4	(147)
IPEC-1 cells IPEC-J2 cells	0.67-6.7 $\mu$ M 48 h	Decrease in protein expression of ZO-1 Affect the distribution pattern of ZO-1	(153)
IPEC-J2 cells	6.74 $\mu$ M 48 h	Decrease in TEER values Decrease in protein expression of CLDN3, OCLN and ZO-1 Affect the distribution pattern of ZO-1	(152)
IPEC-J2 cells	0.67-13.4 $\mu$ M 24-72 h	Decrease in TEER values Decrease in protein expression of CLDN3 and ZO-1 Affect the distribution pattern of CLDN3	(146)
IPEC-J2 cells	1.68-33.7 $\mu$ M 72 h	Decrease in TEER values Increase in permeability of doxycycline and paromomycin	(123)
IPEC-J2 cells	0.33-3.3 $\mu$ M 24 h	Increase in translocation of pathogenic <i>Salmonella typhimurium</i> (strain 112910a)	(150)
Porcine jejunal explants	5-50 $\mu$ M 2 h	Increase in permeability of 4 kDa FITC-dextran	(147)
Piglet	3 mg/kg feed 5 w	Decrease in protein expression of OCLN in ileum	(109)
Pig	0.9 mg/kg feed 10 d	Increase in transcript level of CLDNs (caecum), OCLN (duodenum, ileum, caecum and colon) and ZO5 (duodenum and colon) Decrease in transcript level of CLDN4, OCLN, ZO-1 and ZO-2 in jejunum Increase in protein expression of OCLN in duodenum, jejunum and colon	(154)

Pig	2.85 mg/kg feed 5 w	Decrease in protein expression of CLDN4 in jejunum	(147)
Pig	3.5 mg/kg feed 6 w	Decrease in transcript level of CLDN3, CLDN4 and OCLN in ileum	(157)
Mouse	25 mg/kg bw 6 h	Increase in permeability of 4 kDa FITC-dextran Increase in transcript level of CLDN2, CLDN3 and CLDN4 in distal small intestine Affect the distribution pattern of CLDN1-3 in distal small intestine	(26)
Broiler chicken	7.5 mg/kg feed 3 w	Increase in transcript level of CLDN5 in jejunum and CLDN1, CLDN5, ZO-1 and ZO-2 in ileum	(151)

### 3- and 15-acetyl deoxynivalenol

Caco-2 cells	3.37 $\mu$ M 6 h	Decrease in TEER values 15-Ac-DON > DON > 3-Ac-DON  Increase in permeability of LY 15-Ac-DON	(158)
IPEC-1 cells	10-30 $\mu$ M 24-48 h	Decrease in TEER values Increase in permeability of 4 kDa FITC-dextran 15-Ac-DON > DON > 3-Ac-DON  Decrease in protein expression of CLDN3 and CLDN4 15-Ac-DON > DON = 3-Ac-DON	(118)

Clinically relevance and conclusions

A dynamic and well-regulated intestinal barrier is necessary to protect the body against dietary antigens and the residential intestinal microflora. This barrier is created by an impermeable layer of epithelial cells, sealed by specific TJ proteins prohibiting paracellular diffusion of luminal antigens and pathogens (Figure 1). An impaired intestinal barrier leads to mucosal inflammation and has been linked to the pathogenesis of various chronic intestinal inflammatory diseases, such as Crohn’s disease, ulcerative colitis, coeliac disease and irritable bowel syndrome (164-169). TJs sealing the epithelial monolayer are one of the most important functional elements of the intestinal barrier, and a decrease in the abundance and a re-distribution of different TJ proteins is observed in all major chronic intestinal inflammatory diseases as summarized in Table 6.

**Table 6.** Aspect of TJ-related barrier dysfunction in chronic intestinal inflammatory diseases

Inflammatory disease	TJ proteins	References
Crohn’s disease	OCN, CLDN3, CLDN5, CLDN8, JAM: ▼ CLDN2: ▲ Redistribution of OCLN, CLDN3, CLDN5, CLDN8	(168, 170, 171)
Ulcerative colitis	OCN, CLDN1, CLDN4, JAM, Tricellulin: ▼ CLDN2: ▲ Redistribution of OCLN, CLDN1, CLDN4	(167, 168, 170, 172)
Coeliac disease	OCN, ZO-1: ▼ CLDN2, CLDN3: ▲ Redistribution of OCLN	(165, 173)
Irritable bowel syndrome	OCN, CLDN1, ZO-1: ▼ Redistribution of OCLN, CLDN1, ZO-1	(164)

Expression: ▼ decrease, ▲ increase

Dietary exposure of humans and animals to mycotoxins is of growing concern due to the apparently still increasing prevalence of these fungal toxins in food and feed commodities (2, 57, 174, 175). Due to this increasing prevalence in food commodities, mycotoxins appear to be important, but often neglected substances that are able to affect TJ proteins and impair the integrity of the intestinal barrier. Even though mycotoxins have not been associated with a specific intestinal disease, the investigations summarized above demonstrate that mycotoxins affect the expression and function of TJ proteins in different ways. Among the various mycotoxins, particularly DON has been identified to modulate

the expression, intracellular localization and function of TJ proteins (Figure 1), while PAT seems to directly affect the epithelial cell monolayer. PAT is only found incidentally as a contaminant of fruit juices and other fruit products, whereas DON is found in major food supplies, such as wheat and other cereal products, which are consumed daily. This suggests a role of this frequently occurring mycotoxin in the etiology of chronic intestinal inflammatory diseases. The observation that even pathogenic bacteria are translocated from the intestinal lumen to the internal environment, when animals are challenged with mycotoxins, confirm their significance in inflammatory reactions. Considering the lactational transfer of various mycotoxins (transfer of various mycotoxins from maternal plasma into milk), exposure of infants deserve special attention. Even minor changes in the (developing) barrier function can lead to exposure to luminal antigens in early phases of life and may result in accelerated immunological responses and clinical manifestations, such as allergies. The prevalence of wheat allergy in children is increasing (176-178), and as DON is mainly found in wheat and wheat-derived products, it cannot be excluded that DON plays also a role in the onset of allergic reactions in children. Further studies should be devoted to the effects of frequently occurring mycotoxins in human food supplies on the TJ proteins and their effect on the intestinal barrier should be included in the overall risk assessment of mycotoxins in foods.



## References

1. Bennett JW, Klich M. Mycotoxins. *Clin Microbiol Rev* 2003;16:497-516.
2. Wu F, Groopman JD, Pestka JJ. Public health impacts of foodborne mycotoxins. *Annu Rev Food Sci Technol* 2014;5:351-372.
3. Liu Y, Wu F. Global burden of aflatoxin-induced hepatocellular carcinoma: a risk assessment. *Environ Health Perspect* 2010;118:818-824.
4. Pinton P, Oswald IP. Effect of deoxynivalenol and other Type B trichothecenes on the intestine: a review. *Toxins* 2014;6:1615-1643.
5. Grenier B, Applegate TJ. Modulation of intestinal functions following mycotoxin ingestion: meta-analysis of published experiments in animals. *Toxins* 2013;5:396-430.
6. Maresca M, Yahia N, Younes-Sakr L, Boyron M, Caporiccio B, Fantini J. Both direct and indirect effects account for the pro-inflammatory activity of enteropathogenic mycotoxins on the human intestinal epithelium: stimulation of interleukin-8 secretion, potentiation of interleukin-1 $\beta$  effect and increase in the transepithelial passage of commensal bacteria. *Toxicol Appl Pharmacol* 2008;228:84-92.
7. Bouhet S, Oswald IP. The effects of mycotoxins, fungal food contaminants, on the intestinal epithelial cell-derived innate immune response. *Vet Immunol Immunopathol* 2005;108:199-209.
8. Groschwitz KR, Hogan SP. Intestinal barrier function: molecular regulation and disease pathogenesis. *J Allergy Clin Immunol* 2009;124:3-20.
9. Odenwald MA, Turner JR. Intestinal permeability defects: is it time to treat? *Clin Gastroenterol Hepatol* 2013;11:1075-1083.
10. Pastorelli L, De Salvo C, Mercado JR, Vecchi M, Pizarro TT. Central role of the gut epithelial barrier in the pathogenesis of chronic intestinal inflammation: lessons learned from animal models and human genetics. *Front Immunol* 2013;4:280.
11. DeMeo MT, Mutlu EA, Keshavarzian A, Tobin MC. Intestinal permeation and gastrointestinal disease. *J Clin Gastroenterol* 2002;34:385-396.
12. Rotter BA, Prelusky DB, Pestka JJ. Toxicology of deoxynivalenol (vomitoxin). *J Toxicol Environ Health* 1996;48:1-34.
13. Pestka JJ, Moorman MA, Warner RL. Altered serum immunoglobulin response to model intestinal antigens during dietary exposure to vomitoxin (deoxynivalenol). *Toxicol Lett* 1990;50:75-84.
14. Pestka JJ. Deoxynivalenol: mechanisms of action, human exposure, and toxicological relevance. *Arch Toxicol* 2010;84:663-679.
15. Pestka JJ. Deoxynivalenol-induced proinflammatory gene expression: mechanisms and pathological sequelae. *Toxins* 2010;2:1300-1317.
16. Sun H, Pang KS. Permeability, Transport, and Metabolism of Solutes in Caco-2 Cell Monolayers: A Theoretical Study. *Drug Metab Dispos* 2007;36:102-123.
17. Sambuy Y, De Angelis I, Ranaldi G, Scarino ML, Stammati A, Zucco F. The Caco-2 cell line as a model of the intestinal barrier: influence of cell and culture-related factors on Caco-2 cell functional characteristics. *Cell Biol Toxicol* 2005;21:1-26.
18. Hidalgo IJ, Raub TJ, Borchardt RT. Characterization of the human colon carcinoma cell line (Caco-2) as a model system for intestinal epithelial permeability. *Gastroenterology* 1989;96:736-749.
19. Artursson P, Palm K, Luthman K. Caco-2 monolayers in experimental and theoretical predictions of drug transport. *Adv Drug Deliv Rev* 2012;64:280-289.
20. Sun H, Chow EC, Liu S, Du Y, Pang KS. The Caco-2 cell monolayer: usefulness and limitations. *Expert Opin Drug Metab Toxicol* 2008;4:395-411.
21. Shimizu M. Interaction between food substances and the intestinal epithelium. *Biosci Biotechnol Biochem* 2010;74:232-241.
22. Hubatsch I, Ragnarsson EG, Artursson P. Determination of drug permeability and prediction of drug absorption in Caco-2 monolayers. *Nat Protoc* 2007;2:2111-2119.

23. Benson K, Cramer S, Galla HJ. Impedance-based cell monitoring: barrier properties and beyond. *Fluids Barriers CNS* 2013;10:5.
24. Sun M, Fu H, Cheng H, Cao Q, Zhao Y, Mou X, Zhang X, Liu X, Ke Y. A dynamic real-time method for monitoring epithelial barrier function *in vitro*. *Anal Biochem* 2012;425:96-103.
25. Abassi YA, Xi B, Zhang W, Ye P, Kirstein SL, Gaylord MR, Feinstein SC, Wang X, Xu X. Kinetic cell-based morphological screening: prediction of mechanism of compound action and off-target effects. *Chem Biol* 2009;16:712-723.
26. Akbari P, Braber S, Gremmels H, Koelink PJ, Verheijden KA, Garssen J, Fink-Gremmels J. Deoxynivalenol: a trigger for intestinal integrity breakdown. *FASEB J* 2014;28:2414-2429.
27. De Walle JV, Sergent T, Piront N, Toussaint O, Schneider YJ, Larondelle Y. Deoxynivalenol affects *in vitro* intestinal epithelial cell barrier integrity through inhibition of protein synthesis. *Toxicol Appl Pharmacol* 2010;245:291-298.
28. Arrieta MC, Bistriz L, Meddings JB. Alterations in intestinal permeability. *Gut* 2006;55:1512-1520.
29. Bjarnason I, MacPherson A, Hollander D. Intestinal Permeability: An Overview. *Gastroenterology* 1995;108:1566-1581.
30. Jimison LH, Tria SA, Khodagholy D, Gurfinkel M, Lanzarini E, Hama A, Malliaras GG, Owens RM. Measurement of barrier tissue integrity with an organic electrochemical transistor. *Adv Mater* 2012;24:5919-5923.
31. Bischoff SC, Barbara G, Buurman W, Ockhuizen T, Schulzke JD, Serino M, Tilg H, Watson A, Wells JM. Intestinal permeability-a new target for disease prevention and therapy. *BMC Gastroenterol* 2014;14:189.
32. Meddings JB, Gibbons I. Discrimination of site-specific alterations in gastrointestinal permeability in the rat. *Gastroenterology* 1998;114:83-92.
33. Peterson LW, Artis D. Intestinal epithelial cells: regulators of barrier function and immune homeostasis. *Nat Rev Immunol* 2014;14:141-153.
34. Tsukita S, Furuse M, Itoh M. Multifunctional strands in tight junctions. *Nat Rev Mol Cell Biol* 2001;2:285-293.
35. Chiba H, Osanai M, Murata M, Kojima T, Sawada N. Transmembrane proteins of tight junctions. *Biochim Biophys Acta* 2008;1778:588-600.
36. Schneeberger EE, Lynch RD. The tight junction: a multifunctional complex. *Am J Physiol Cell Physiol* 2004;286:C1213-C1228.
37. Schwanhauser B, Busse D, Li N, Dittmar G, Schuchhardt J, Wolf J, Chen W, Selbach M. Global quantification of mammalian gene expression control. *Nature* 2011;473:337-342.
38. Vogel C, Abreu Rde S, Ko D, Le SY, Shapiro BA, Burns SC, Sandhu D, Boutz DR, Marcotte EM, Penalva LO. Sequence signatures and mRNA concentration can explain two-thirds of protein abundance variation in a human cell line. *Mol Syst Biol* 2010;6:400.
39. Kolf-Clauw M, Castellote J, Joly B, Bourges-Abella N, Raymond-Letron I, Pinton P, Oswald IP. Development of a pig jejunal explant culture for studying the gastrointestinal toxicity of the mycotoxin deoxynivalenol: histopathological analysis. *Toxicol In Vitro* 2009;23:1580-1584.
40. Randall KJ, Turton J, Foster JR. Explant culture of gastrointestinal tissue: a review of methods and applications. *Cell Biol Toxicol* 2011;27:267-284.
41. Kolf-Clauw M, Sassahara M, Lucioi J, Rubira-Gerez J, Alassane-Kpembi I, Lyazhri F, Borin C, Oswald IP. The emerging mycotoxin, enniatin B1, down-modulates the gastrointestinal toxicity of T-2 toxin *in vitro* on intestinal epithelial cells and *ex vivo* on intestinal explants. *Arch Toxicol* 2013;87:2233-2241.
42. Fasano A. Zonulin and its regulation of intestinal barrier function: the biological door to inflammation, autoimmunity, and cancer. *Physiol Rev* 2011;91:151-175.
43. Fasano A. Zonulin, regulation of tight junctions, and autoimmune diseases. *Ann N Y Acad Sci* 2012;1258:25-33.
44. Pelsers MM, Namiot Z, Kisielewski W, Namiot A,

- Januszkiewicz M, Hermens WT, Glatz JF. Intestinal-type and liver-type fatty acid-binding protein in the intestine. Tissue distribution and clinical utility. *Clin Biochem* 2003;36:529-535.
45. Furuhashi M, Hotamisligil GS. Fatty acid-binding proteins: role in metabolic diseases and potential as drug targets. *Nat Rev Drug Discov* 2008;7:489-503.
46. Cheat S, Gerez JR, Cogne J, Alassane-Kpembé I, Bracarense AP, Raymond-Letron I, Oswald IP, Kolf-Clauw M. Nivalenol has a greater impact than deoxynivalenol on pig jejunum mucosa *in vitro* on explants and *in vivo* on intestinal loops. *Toxins* 2015;7:1945-1961.
47. Pinton P, Graziani F, Pujol A, Nicoletti C, Paris O, Ernouf P, Di Pasquale E, Perrier J, Oswald IP, Maresca M. Deoxynivalenol inhibits the expression by goblet cells of intestinal mucins through a PKR and MAP kinase dependent repression of the resistin-like molecule beta. *Mol Nutr Food Res* 2015;59:1076-1087.
48. Blikslager AT, Moeser AJ, Gookin JL, Jones SL, Odle J. Restoration of barrier function in injured intestinal mucosa. *Physiol Rev* 2007;87:545-564.
49. Leong YH, Latiff AA, Ahmad NI, Rosma A. Exposure measurement of aflatoxins and aflatoxin metabolites in human body fluids. A short review. *Mycotoxin Res* 2012;28:79-87.
50. Hamid AS, Tesfamariam IG, Zhang Y, Zhang ZG. Aflatoxin B1-induced hepatocellular carcinoma in developing countries: Geographical distribution, mechanism of action and prevention. *Oncol Lett* 2013;5:1087-1092.
51. Wild CP, Turner PC. The toxicology of aflatoxins as a basis for public health decisions. *Mutagenesis* 2002;17:471-481.
52. Bedard LL, Massey TE. Aflatoxin B1-induced DNA damage and its repair. *Cancer Lett* 2006;241:174-183.
53. IARC. IARC Monographs on the Evaluation of Carcinogenic Risks to Humans: Some Traditional Herbal Medicines, Some Mycotoxins, Naphthalene and Styrene. International Agency for Research on Cancer Press LYON FRANCE 2002;82.
54. Wu HC, Santella R. The role of aflatoxins in hepatocellular carcinoma. *Hepat Mon* 2012;12:e7238.
55. Liu Y, Chang CC, Marsh GM, Wu F. Population attributable risk of aflatoxin-related liver cancer: systematic review and meta-analysis. *Eur J Cancer* 2012;48:2125-2136.
56. Nordenstedt H, White DL, El-Serag HB. The changing pattern of epidemiology in hepatocellular carcinoma. *Dig Liver Dis* 2010;42:S206-S214.
57. Marin S, Ramos AJ, Cano-Sancho G, Sanchis V. Mycotoxins: occurrence, toxicology, and exposure assessment. *Food Chem Toxicol* 2013;60:218-237.
58. Egner PA, Yu X, Johnson JK, Nathasingh CK, Groopman JD, Kensler TW, Roebuck BD. Identification of aflatoxin M1-N7-guanine in liver and urine of tree shrews and rats following administration of aflatoxin B1. *Chem Res Toxicol* 2003;16:1174-1180.
59. Gratz S, Wu QK, El-Nezami H, Juvonen RO, Mykkanen H, Turner PC. *Lactobacillus rhamnosus* strain GG reduces aflatoxin B1 transport, metabolism, and toxicity in Caco-2 Cells. *Appl Environ Microbiol* 2007;73:3958-3964.
60. Caloni F, Cortinovis C, Pizzo F, De Angelis I. Transport of Aflatoxin M(1) in Human Intestinal Caco-2/TC7 Cells. *Front Pharmacol* 2012;3:111.
61. Peraica M, Domijan AM, Matasin M, Lucic A, Radic B, Delas F, Horvat M, Bosanac I, Balija M, Grgicevic D. Variations of ochratoxin A concentration in the blood of healthy populations in some Croatian cities. *Arch Toxicol* 2001;75:410-414.
62. Studer-Rohr I, Schlatter J, Dietrich DR. Kinetic parameters and intraindividual fluctuations of ochratoxin A plasma levels in humans. *Arch Toxicol* 2000;74:499-510.
63. Pfohl-Leschkowicz A, Manderville RA. Ochratoxin A: An overview on toxicity and carcinogenicity in animals and humans. *Mol Nutr Food Res* 2007;51:61-99.
64. Grollman AP, Jelakovic B. Role of environmental toxins in endemic (Balkan) nephropathy. October 2006, Zagreb, Croatia. *J Am Soc Nephrol* 2007;18:2817-2823.
65. Fink-Gremmels J. Ochratoxin A in food: recent developments and significance. *Food Addit Contam*

2005;22:S1-S5.

66. Pfohl-Leszkowicz A, Manderville RA. An update on direct genotoxicity as a molecular mechanism of ochratoxin A carcinogenicity. *Chem Res Toxicol* 2012;25:252-262.
67. Sorrenti V, Di Giacomo C, Acquaviva R, Barbagallo I, Bognanno M, Galvano F. Toxicity of ochratoxin A and its modulation by antioxidants: a review. *Toxins* 2013;5:1742-1766.
68. Mally A. Ochratoxin A and mitotic disruption: mode of action analysis of renal tumor formation by ochratoxin A. *Toxicol Sci* 2012;127:315-330.
69. Omar RF, Hasinoff BB, Mejilla F, Rahimula AD. Mechanism of ochratoxin A stimulated lipid peroxidation. *Biochem Pharmacol* 1990;40:1183-1191.
70. Fink-Gremmels J, Jahn A, Blom MJ. Toxicity and metabolism of ochratoxin A. *Nat Toxins* 1995;3:214-220.
71. Maresca M, Mahfoud R, Pfohl-Leszkowicz A, Fantini J. The mycotoxin ochratoxin A alters intestinal barrier and absorption functions but has no effect on chloride secretion. *Toxicol Appl Pharmacol* 2001;176:54-63.
72. McLaughlin J, Padfield PJ, Burt JP, O'Neill CA. Ochratoxin A increases permeability through tight junctions by removal of specific claudin isoforms. *Am J Physiol Cell Physiol* 2004;287:C1412-C1417.
73. Ranaldi G, Mancini E, Ferruzza S, Sambuy Y, Perozzi G. Effects of red wine on ochratoxin A toxicity in intestinal Caco-2/TC7 cells. *Toxicol In Vitro* 2007;21:204-210.
74. Lambert D, Padfield PJ, McLaughlin J, Cannell S, O'Neill CA. Ochratoxin A displaces claudins from detergent resistant membrane microdomains. *Biochem Biophys Res Commun* 2007;358:632-636.
75. Moake MM, Padilla-Zakour OI, Worobo RW. Comprehensive Review of Patulin Control Methods in Foods. *Compr Rev Food Sci Food Saf* 2005;4:8-21.
76. IARC. IARC monographs on the evaluation of carcinogenic risks to humans. International Agency for Research on Cancer Press LYON FRANCE 1987;1-42.
77. Maresca M, Fantini J. Some food-associated mycotoxins as potential risk factors in humans predisposed to chronic intestinal inflammatory diseases. *Toxicon* 2010;56:282-294.
78. Fliege R, Metzler M. Electrophilic properties of patulin. N-acetylcysteine and glutathione adducts. *Chem Res Toxicol* 2000;13:373-381.
79. Puel O, Galtier P, Oswald IP. Biosynthesis and toxicological effects of patulin. *Toxins* 2010;2:613-631.
80. Schebb NH, Faber H, Maul R, Heus F, Kool J, Irth H, Karst U. Analysis of glutathione adducts of patulin by means of liquid chromatography (HPLC) with biochemical detection (BCD) and electrospray ionization tandem mass spectrometry (ESI-MS/MS). *Anal Bioanal Chem* 2009;394:1361-1373.
81. Pfenning C, Esch HL, Fliege R, Lehmann L. The mycotoxin patulin reacts with DNA bases with and without previous conjugation to GSH: implication for related alpha,beta-unsaturated carbonyl compounds? *Arch Toxicol* 2014.
82. Boussabbah M, Ben Salem I, Prola A, Guilbert A, Bacha H, Abid-Essefi S, Lemaire C. Patulin induces apoptosis through ROS-mediated endoplasmic reticulum stress pathway. *Toxicol Sci* 2015;144:328-337.
83. Sergeant T, Garsou S, Schaut A, De Saeger S, Pussemier L, Van Peteghem C, Larondelle Y, Schneider YJ. Differential modulation of ochratoxin A absorption across Caco-2 cells by dietary polyphenols, used at realistic intestinal concentrations. *Toxicol Lett* 2005;159:60-70.
84. Assuncao R, Ferreira M, Martins C, Diaz I, Padilla B, Dupont D, Braganca M, Alvito P. Applicability of *in vitro* methods to study patulin bioaccessibility and its effects on intestinal membrane integrity. *J Toxicol Environ Health A* 2014;77:983-992.
85. Mahfoud R, Maresca M, Garmy N, Fantini J. The mycotoxin patulin alters the barrier function of the intestinal epithelium: mechanism of action of the toxin and protective effects of glutathione. *Toxicol Appl Pharmacol* 2002;181:209-218.
86. McLaughlin J, Lambert D, Padfield PJ, Burt JP, O'Neill CA. The mycotoxin patulin, modulates tight junctions

in caco-2 cells. *Toxicol In Vitro* 2009;23:83-89.

87. Mohan HM, Collins D, Maher S, Walsh EG, Winter DC, O'Brien PJ, Brayden DJ, Baird AW. The mycotoxin patulin increases colonic epithelial permeability *in vitro*. *Food Chem Toxicol* 2012;50:4097-4102.

88. Katsuyama A, Konno T, Shimoyama S, Kikuchi H. The mycotoxin patulin decreases expression of density-enhanced phosphatase-1 by down-regulating PPARgamma in human colon cancer cells. *Tohoku J Exp Med* 2014;233:265-274.

89. Kawauchiya T, Takumi R, Kudo Y, Takamori A, Sasagawa T, Takahashi K, Kikuchi H. Correlation between the destruction of tight junction by patulin treatment and increase of phosphorylation of ZO-1 in Caco-2 human colon cancer cells. *Toxicol Lett* 2011;205:196-202.

90. Balavenkatraman KK, Jandt E, Friedrich K, Kautenburger T, Pool-Zobel BL, Ostman A, Bohmer FD. DEP-1 protein tyrosine phosphatase inhibits proliferation and migration of colon carcinoma cells and is upregulated by protective nutrients. *Oncogene* 2006;25:6319-6324.

91. Petermann A, Haase D, Wetzel A, Balavenkatraman KK, Tenev T, Guhrs KH, Friedrich S, Nakamura M, Mawrin C, Bohmer FD. Loss of the protein-tyrosine phosphatase DEP-1/PTPRJ drives meningioma cell motility. *Brain Pathol* 2011;21:405-418.

92. Sydenham EW, Thiel PG, Marasas WFO, Shephard GS, V. SDJ, Koch KR. Natural occurrence of some Fusarium mycotoxins in corn from low and high esophageal cancer prevalence areas of the Transkei, Southern Africa. *J Agric Food Chem* 1990;38:1900-1903.

93. Rheder JP, Marasas WFO, Thiel PG, Sydenham EW, Shephard GS, van Schalkwyk DJ. Fusarium moniliforme and Fumonisin in Corn in Relation to Human Esophageal Cancer in Transkei. *Phytopathology* 1992;82:353-357.

94. Chu FS, Li GY. Simultaneous occurrence of fumonisin B1 and other mycotoxins in moldy corn collected from the People's Republic of China in regions with high incidences of esophageal cancer. *Appl Environ*

*Microbiol* 1994;60:847-852.

95. Sadler TW, Merrill AH, Stevens VL, Sullards MC, Wang E, Wang P. Prevention of fumonisin B1-induced neural tube defects by folic acid. *Teratology* 2002;66:169-176.

96. Missmer SA, Suarez L, Felkner M, Wang E, Merrill AH Jr, Rothman KJ, Hendricks KA. Exposure to fumonisins and the occurrence of neural tube defects along the Texas-Mexico border. *Environ Health Perspect* 2006;114:237-241.

97. Marasas WF, Riley RT, Hendricks KA, Stevens VL, Sadler TW, Gelineau-van Waes J, Missmer SA, Cabrera J, Torres O, Gelderblom WC, *et al.* Fumonisin disrupt sphingolipid metabolism, folate transport, and neural tube development in embryo culture and *in vivo*: a potential risk factor for human neural tube defects among populations consuming fumonisin-contaminated maize. *J Nutr* 2004;134:711-716.

98. Gelineau-van Waes J, Starr L, Maddox J, Aleman F, Voss KA, Wilberding J, Riley RT. Maternal fumonisin exposure and risk for neural tube defects: mechanisms in an *in vivo* mouse model. *Birth Defects Res A Clin Mol Teratol* 2005;73:487-497.

99. Voss KA, Smith GW, Haschek WM. Fumonisin: Toxicokinetics, mechanism of action and toxicity. *Anim Feed Sci Tech* 2007;137:299-325.

100. Loiseau N, Debrauwer L, Sambou T, Bouhet S, Miller JD, Martin PG, Viadere JL, Pinton P, Puel O, Pineau T, *et al.* Fumonisin B1 exposure and its selective effect on porcine jejunal segment: sphingolipids, glycolipids and trans-epithelial passage disturbance. *Biochem Pharmacol* 2007;74:144-152.

101. Loiseau N, Polizzi A, Dupuy A, Therville N, Rakotonirainy M, Loy J, Viadere JL, Cossalter AM, Bailly JD, Puel O, *et al.* New insights into the organ-specific adverse effects of fumonisin B1: comparison between lung and liver. *Arch Toxicol* 2015;89:1619-1629.

102. Enongene EN, Sharma RP, Bhandari N, Voss KA, Riley RT. Disruption of sphingolipid metabolism in small intestines, liver and kidney of mice dosed subcutaneously with fumonisin B1. *Food Chem Toxicol* 2000;38:793-799.

103. Mullen TD, Hannun YA, Obeid LM. Ceramide synthases at the centre of sphingolipid metabolism and biology. *Biochem J* 2012;441:789-802.
104. Ribeiro DH, Ferreira FL, da Silva VN, Aquino S, Correa B. Effects of aflatoxin B1 and fumonisin B1 on the viability and induction of apoptosis in rat primary hepatocytes. *Int J Mol Sci* 2010;11:1944-1955.
105. Bouhet S, Oswald IP. The intestine as a possible target for fumonisin toxicity. *Mol Nutr Food Res* 2007;51:925-931.
106. Bouhet S, Hourcade E, Loiseau N, Fikry A, Martinez S, Roselli M, Galtier P, Mengheri E, Oswald IP. The mycotoxin fumonisin B1 alters the proliferation and the barrier function of porcine intestinal epithelial cells. *Toxicol Sci* 2004;77:165-171.
107. Lalles JP, Lessard M, Boudry G. Intestinal barrier function is modulated by short-term exposure to fumonisin B1 in Ussing chambers. *Vet Res Commun* 2009;33:1039-1043.
108. Oswald IP, Desautels C, Laffitte J, Fournout S, Peres SY, Odin M, Le Bars P, Le Bars J, Fairbrother JM. Mycotoxin fumonisin B1 increases intestinal colonization by pathogenic *Escherichia coli* in pigs. *Appl Environ Microbiol* 2003;69:5870-5874.
109. Bracarense AP, Lucoli J, Grenier B, Drociunas Pacheco G, Moll WD, Schatzmayr G, Oswald IP. Chronic ingestion of deoxynivalenol and fumonisin, alone or in interaction, induces morphological and immunological changes in the intestine of piglets. *Br J Nutr* 2012;107:1776-1786.
110. McCormick SP, Stanley AM, Stover NA, Alexander NJ. Trichothecenes: from simple to complex mycotoxins. *Toxins* 2011;3:802-814.
111. Rocha O, Ansari K, Doohan FM. Effects of trichothecene mycotoxins on eukaryotic cells: a review. *Food Addit Contam* 2005;22:369-378.
112. Wu Q, Dohnal V, Kuca K, Yuan Z. Trichothecenes: structure-toxic activity relationships. *Curr Drug Metab* 2013;14:641-660.
113. Sudakin DL. Trichothecenes in the environment: relevance to human health. *Toxicol Lett* 2003;143:97-107.
114. Escriva L, Font G, Manyes L. *In vivo* toxicity studies of fusarium mycotoxins in the last decade: a review. *Food Chem Toxicol* 2015;78:185-206.
115. Shank RA, Foroud NA, Hazendonk P, Eudes F, Blackwell BA. Current and future experimental strategies for structural analysis of trichothecene mycotoxins-a prospectus. *Toxins* 2011;3:1518-1553.
116. Nathanail AV, Syvahuoko J, Malachova A, Jestoi M, Varga E, Michlmayr H, Adam G, Sievilainen E, Berthiller F, Peltonen K. Simultaneous determination of major type A and B trichothecenes, zearalenone and certain modified metabolites in Finnish cereal grains with a novel liquid chromatography-tandem mass spectrometric method. *Anal Bioanal Chem* 2015;407:4745-4755.
117. Wu QH, Wang X, Yang W, Nussler AK, Xiong LY, Kuca K, Dohnal V, Zhang XJ, Yuan ZH. Oxidative stress-mediated cytotoxicity and metabolism of T-2 toxin and deoxynivalenol in animals and humans: an update. *Arch Toxicol* 2014;88:1309-1326.
118. Pinton P, Tsybulskyy D, Lucoli J, Laffitte J, Callu P, Lyazhri F, Grosjean F, Bracarense AP, Kolf-Clauw M, Oswald IP. Toxicity of deoxynivalenol and its acetylated derivatives on the intestine: differential effects on morphology, barrier function, tight junction proteins, and mitogen-activated protein kinases. *Toxicol Sci* 2012;130:180-190.
119. Li Y, Wang Z, Beier RC, Shen J, De Smet D, De Saeger S, Zhang S. T-2 toxin, a trichothecene mycotoxin: review of toxicity, metabolism, and analytical methods. *J Agric Food Chem* 2011;59:3441-3453.
120. Joffe AZ. Alimentary toxic aleukia. Alimentary toxic aleukia. In: Kadis, S. Ciegler, A. Ajl, S. J. (ed) *Microbial Toxins*. Academic Press, New York. 1971;7:139-189.
121. IARC. IARC Monographs on the Evaluation of Carcinogenic Risks to Humans: Some Naturally Occurring Substances: Food Items and Constituents, Heterocyclic Aromatic Amines and Mycotoxins. International Agency for Research on Cancer Press LYON FRANCE 1993;56.

122. Chaudhari M, Jayaraj R, Bhaskar AS, Lakshmana Rao PV. Oxidative stress induction by T-2 toxin causes DNA damage and triggers apoptosis via caspase pathway in human cervical cancer cells. *Toxicology* 2009;262:153-161.
123. Goossens J, Pasmans F, Verbrugghe E, Vandenbroucke V, De Baere S, Meyer E, Haesebrouck F, De Backer P, Croubels S. Porcine intestinal epithelial barrier disruption by the *Fusarium* mycotoxins deoxynivalenol and T-2 toxin promotes transepithelial passage of doxycycline and paromomycin. *BMC Vet Res* 2012;8:245.
124. Kanai K, Kondo E. Decreased resistance to mycobacterial infection in mice fed a trichothecene compound (T-2 toxin). *Jpn J Med Sci Biol* 1984;37:97-104.
125. Verbrugghe E, Vandenbroucke V, Dhaenens M, Shearer N, Goossens J, De Saeger S, Eeckhout M, D'Herde K, Thompson A, Deforce D, *et al.* T-2 toxin induced *Salmonella* Typhimurium intoxication results in decreased *Salmonella* numbers in the cecum contents of pigs, despite marked effects on *Salmonella*-host cell interactions. *Vet Res* 2012;43:22.
126. EFSA. Scientific Opinion on risks for animal and public health related to the presence of nivalenol in food and feed. *EFSA journal* 2013;11:3262.
127. Hsia CC, Wu ZY, Li YS, Zhang F, Sun ZT. Nivalenol, a main *Fusarium* toxin in dietary foods from high-risk areas of cancer of esophagus and gastric cardia in China, induced benign and malignant tumors in mice. *Oncol Rep* 2004;12:449-456.
128. Alassane-Kpembi I, Kolf-Clauw M, Gauthier T, Abrami R, Abiola FA, Oswald IP, Puel O. New insights into mycotoxin mixtures: the toxicity of low doses of Type B trichothecenes on intestinal epithelial cells is synergistic. *Toxicol Appl Pharmacol* 2013;272:191-198.
129. Bianco G, Fontanella B, Severino L, Quaroni A, Autore G, Marzocco S. Nivalenol and deoxynivalenol affect rat intestinal epithelial cells: a concentration related study. *PLoS One* 2012;7:e52051.
130. Del Regno M, Adesso S, Popolo A, Quaroni A, Autore G, Severino L, Marzocco S. Nivalenol induces oxidative stress and increases deoxynivalenol pro-oxidant effect in intestinal epithelial cells. *Toxicol Appl Pharmacol* 2015;285:118-127.
131. Hepworth SJ, Hardie LJ, Fraser LK, Burley VJ, Mijal RS, Wild CP, Azad R, McKinney PA, Turner PC. Deoxynivalenol exposure assessment in a cohort of pregnant women from Bradford, UK. *Food Addit Contam Part A Chem Anal Control Expo Risk Assess* 2012;29:269-276.
132. Sarkanj B, Warth B, Uhlig S, Abia WA, Sulyok M, Klapac T, Krška R, Banjari I. Urinary analysis reveals high deoxynivalenol exposure in pregnant women from Croatia. *Food Chem Toxicol* 2013;62:231-237.
133. Turner PC, Ji BT, Shu XO, Zheng W, Chow WH, Gao YT, Hardie LJ. A biomarker survey of urinary deoxynivalenol in China: the Shanghai Women's Health Study. *Food Addit Contam Part A Chem Anal Control Expo Risk Assess* 2011;28:1220-1223.
134. Wang Z, Wu Q, Kuca K, Dohnal V, Tian Z. Deoxynivalenol: signaling pathways and human exposure risk assessment-an update. *Arch Toxicol* 2014;88:1915-1928.
135. Warth B, Sulyok M, Fruhmman P, Berthiller F, Schuhmacher R, Hametner C, Adam G, Frohlich J, Krška R. Assessment of human deoxynivalenol exposure using an LC-MS/MS based biomarker method. *Toxicol Lett* 2012;211:85-90.
136. Danicke S, Brussow KP, Goyarts T, Valenta H, Ueberschar KH, Tiemann U. On the transfer of the *Fusarium* toxins deoxynivalenol (DON) and zearalenone (ZON) from the sow to the full-term piglet during the last third of gestation. *Food Chem Toxicol* 2007;45:1565-1574.
137. Nielsen JK, Vikstrom AC, Turner P, Knudsen LE. Deoxynivalenol transport across the human placental barrier. *Food Chem Toxicol* 2011;49:2046-2052.
138. Maresca M. From the gut to the brain: journey and pathophysiological effects of the food-associated trichothecene mycotoxin deoxynivalenol. *Toxins* 2013;5:784-820.



139. Sobrova P, Adam V, Vasatkova A, Beklova M, Zeman L, Kizek R. Deoxynivalenol and its toxicity. *Interdiscip Toxicol* 2010;3:94-99.
140. Bonnet MS, Roux J, Mounien L, Dallaporta M, Troadec JD. Advances in deoxynivalenol toxicity mechanisms: the brain as a target. *Toxins* 2012;4:1120-1138.
141. Yazar S, Omurtag GZ. Fumonisin, trichothecenes and zearalenone in cereals. *Int J Mol Sci* 2008;9:2062-2090.
142. Pestka JJ. Deoxynivalenol: Toxicity, mechanisms and animal health risks. *Anim Feed Sci Tech* 2007;137:283-298.
143. Berthiller F, Dall'Asta C, Schuhmacher R, Lemmens M, Adam G, Krska R. Masked mycotoxins: determination of a deoxynivalenol glucoside in artificially and naturally contaminated wheat by liquid chromatography-tandem mass spectrometry. *J Agric Food Chem* 2005;53:3421-3425.
144. Kasuga F, Hara-Kudo Y, Saito N, Kumagai S, Sugita-Konishi Y. *In vitro* effect of deoxynivalenol on the differentiation of human colonic cell lines Caco-2 and T84. *Mycopathologia* 1998;142:161-167.
145. Maresca M, Mahfoud R, Garmy N, Fantini J. The mycotoxin deoxynivalenol affects nutrient absorption in human intestinal epithelial cells. *J Nutr* 2002;132:2723-2731.
146. Diesing AK, Nossol C, Danicke S, Walk N, Post A, Kahlert S, Rothkotter HJ, Kluess J. Vulnerability of polarised intestinal porcine epithelial cells to mycotoxin deoxynivalenol depends on the route of application. *PLoS One* 2011;6:e17472.
147. Pinton P, Nougayrede JP, Del Rio JC, Moreno C, Marin DE, Ferrier L, Bracarense AP, Kolf-Clauw M, Oswald IP. The food contaminant deoxynivalenol, decreases intestinal barrier permeability and reduces claudin expression. *Toxicol Appl Pharmacol* 2009;237:41-48.
148. Alassane-Kpembi I, Puel O, Oswald IP. Toxicological interactions between the mycotoxins deoxynivalenol, nivalenol and their acetylated derivatives in intestinal epithelial cells. *Arch Toxicol* 2015;89:1337-1346.
149. Manda G, Mocanu MA, Marin DE, Taranu I. Dual effects exerted *in vitro* by micromolar concentrations of deoxynivalenol on undifferentiated caco-2 cells. *Toxins* 2015;7:593-603.
150. Vandenbroucke V, Croubels S, Martel A, Verbrugghe E, Goossens J, Van Deun K, Boyen F, Thompson A, Shearer N, De Backer P, *et al.* The mycotoxin deoxynivalenol potentiates intestinal inflammation by *Salmonella typhimurium* in porcine ileal loops. *PLoS One* 2011;6:e23871.
151. Osselaere A, Santos R, Hautekiet V, De Backer P, Chiers K, Ducatelle R, Croubels S. Deoxynivalenol impairs hepatic and intestinal gene expression of selected oxidative stress, tight junction and inflammation proteins in broiler chickens, but addition of an adsorbing agent shifts the effects to the distal parts of the small intestine. *PLoS One* 2013;8:e69014.
152. Gu MJ, Song SK, Park SM, Lee IK, Yun CH. *Bacillus subtilis* Protects Porcine Intestinal Barrier from Deoxynivalenol via Improved Zonula Occludens-1 Expression. *Asian-Australas J Anim Sci* 2014;27:580-586.
153. Diesing AK, Nossol C, Panther P, Walk N, Post A, Kluess J, Kreutzmann P, Danicke S, Rothkotter HJ, Kahlert S. Mycotoxin deoxynivalenol (DON) mediates biphasic cellular response in intestinal porcine epithelial cell lines IPEC-1 and IPEC-J2. *Toxicol Lett* 2011;200:8-18.
154. Alizadeh A, Braber S, Akbari P, Garssen J, Fink-Gremmels J. Deoxynivalenol Impairs Weight Gain and Affects Markers of Gut Health after Low-Dose, Short-Term Exposure of Growing Pigs. *Toxins* 2015;7:2071-2095.
155. Azcona-Olivera JI, Ouyang Y, Murtha J, Chu FS, Pestka JJ. Induction of cytokine mRNAs in mice after oral exposure to the trichothecene vomitoxin (deoxynivalenol): relationship to toxin distribution and protein synthesis inhibition. *Toxicol Appl Pharmacol* 1995;133:109-120.
156. Azcona-Olivera JI, Ouyang YL, Warner RL, Linz JE, Pestka JJ. Effects of vomitoxin (deoxynivalenol)

and cycloheximide on IL-2, 4, 5 and 6 secretion and mRNA levels in murine CD4<sup>+</sup> cells. *Food Chem Toxicol* 1995;33:433-441.

157. Lessard M, Savard C, Deschene K, Lauzon K, Pinilla VA, Gagnon CA, Lapointe J, Guay F, Chorfi Y. Impact of deoxynivalenol (DON) contaminated feed on intestinal integrity and immune response in swine. *Food Chem Toxicol* 2015;80:7-16.

158. Kadota T, Furusawa H, Hirano S, Tajima O, Kamata Y, Sugita-Konishi Y. Comparative study of deoxynivalenol, 3-acetyldeoxynivalenol, and 15-acetyldeoxynivalenol on intestinal transport and IL-8 secretion in the human cell line Caco-2. *Toxicol In Vitro* 2013;27:1888-1895.

159. Plotnikov A, Zehorai E, Procaccia S, Seger R. The MAPK cascades: signaling components, nuclear roles and mechanisms of nuclear translocation. *Biochim Biophys Acta* 2011;1813:1619-1633.

160. Matter K, Balda MS. Signalling to and from tight junctions. *Nat Rev Mol Cell Biol* 2003;4:225-236.

161. Sergent T, Parys M, Garsou S, Pussemier L, Schneider YJ, Larondelle Y. Deoxynivalenol transport across human intestinal Caco-2 cells and its effects on cellular metabolism at realistic intestinal concentrations. *Toxicol Lett* 2006;164:167-176.

162. Pinton P, Braicu C, Nougayrede JP, Laffitte J, Taranu I, Oswald IP. Deoxynivalenol impairs porcine intestinal barrier function and decreases the protein expression of claudin-4 through a mitogen-activated protein kinase-dependent mechanism. *J Nutr* 2010;140:1956-1962.

163. Luciola J, Pinton P, Callu P, Laffitte J, Grosjean F, Kolf-Clauw M, Oswald IP, Bracarense AP. The food contaminant deoxynivalenol activates the mitogen activated protein kinases in the intestine: interest of *ex vivo* models as an alternative to *in vivo* experiments. *Toxicon* 2013;66:31-36.

164. Bertiaux-Vandaele N, Youmba SB, Belmonte L, Leclaire S, Antonietti M, Gourcerol G, Leroi AM, Dechelotte P, Menard JF, Ducrotte P, *et al.* The expression and the cellular distribution of the tight junction proteins are altered in irritable bowel

syndrome patients with differences according to the disease subtype. *Am J Gastroenterol* 2011;106:2165-2173.

165. Drago S, El Asmar R, Di Pierro M, Grazia Clemente M, Tripathi A, Sapone A, Thakar M, Iacono G, Carroccio A, D'Agate C, *et al.* Gliadin, zonulin and gut permeability: Effects on celiac and non-celiac intestinal mucosa and intestinal cell lines. *Scand J Gastroenterol* 2006;41:408-419.

166. Gibson PR. Increased gut permeability in Crohn's disease: is TNF the link? *Gut* 2004;53:1724-1725.

167. Hering NA, Fromm M, Schulzke JD. Determinants of colonic barrier function in inflammatory bowel disease and potential therapeutics. *J Physiol* 2012;590:1035-1044.

168. Vetrano S, Rescigno M, Cera MR, Correale C, Rumio C, Doni A, Fantini M, Sturm A, Borroni E, Repici A, *et al.* Unique role of junctional adhesion molecule-a in maintaining mucosal homeostasis in inflammatory bowel disease. *Gastroenterology* 2008;135:173-184.

169. Suzuki T. Regulation of intestinal epithelial permeability by tight junctions. *Cell Mol Life Sci* 2013;70:631-659.

170. Prasad S, Mingrino R, Kaukinen K, Hayes KL, Powell RM, MacDonald TT, Collins JE. Inflammatory processes have differential effects on claudins 2, 3 and 4 in colonic epithelial cells. *Lab Invest* 2005;85:1139-1162.

171. Zeissig S, Burgel N, Gunzel D, Richter J, Mankertz J, Wahnschaffe U, Kroesen AJ, Zeitz M, Fromm M, Schulzke JD. Changes in expression and distribution of claudin 2, 5 and 8 lead to discontinuous tight junctions and barrier dysfunction in active Crohn's disease. *Gut* 2007;56:61-72.

172. Heller F, Florian P, Bojarski C, Richter J, Christ M, Hillenbrand B, Mankertz J, Gitter AH, Burgel N, Fromm M, *et al.* Interleukin-13 is the key effector Th2 cytokine in ulcerative colitis that affects epithelial tight junctions, apoptosis, and cell restitution. *Gastroenterology* 2005;129:550-564.

173. Szakal DN, Gyorffy H, Arato A, Cseh A, Molnar K, Papp M, Dezsöfi A, Veres G. Mucosal expression

of claudins 2, 3 and 4 in proximal and distal part of duodenum in children with coeliac disease. *Virchows Arch* 2010;456:245-250.

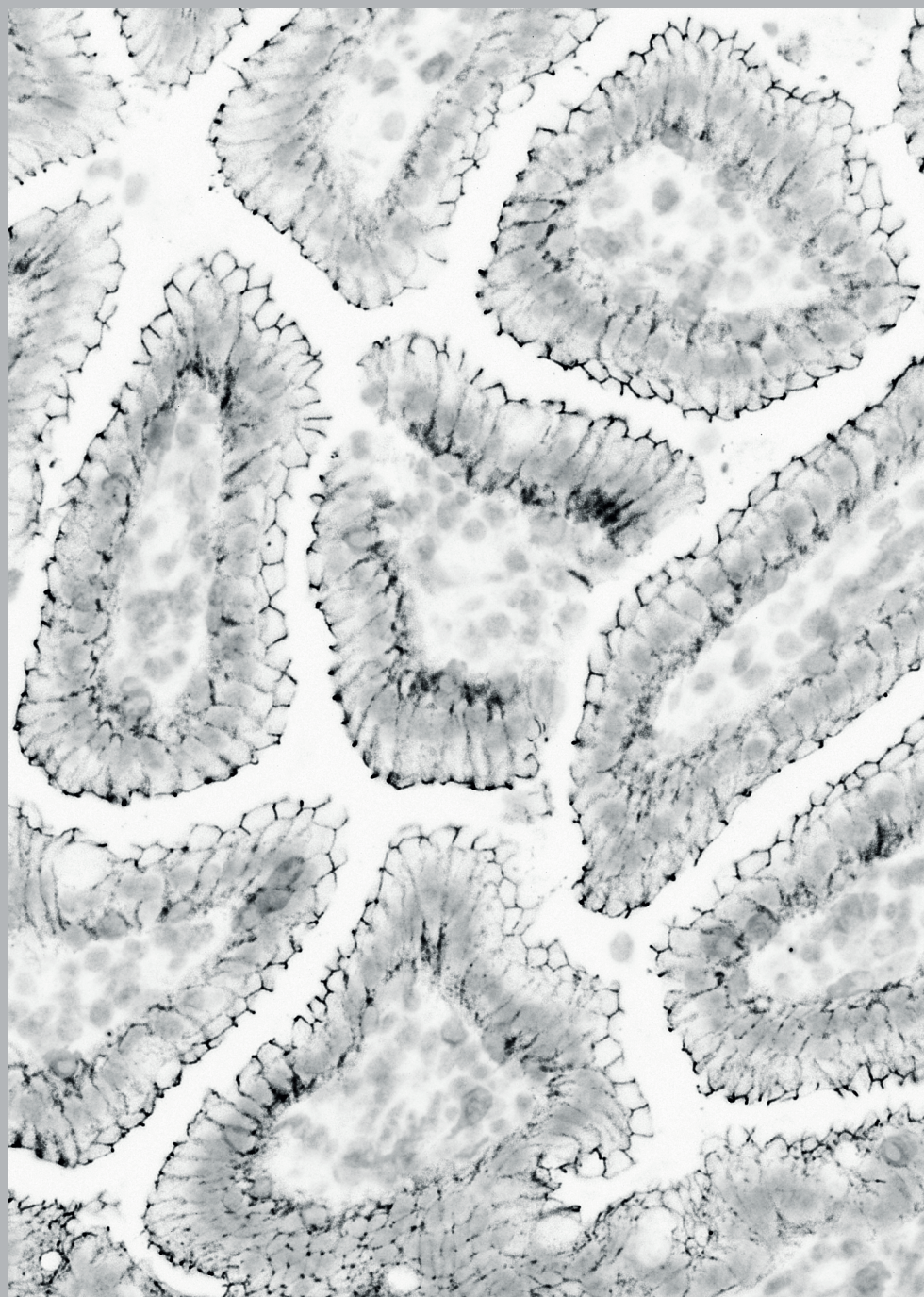
174. Bhat R, Rai RV, Karim AA. Mycotoxins in Food and Feed: Present Status and Future Concerns. *Compr Rev Food Sci Food Saf* 2010;9:57-81.

175. Rodrigues I, Naehrer K. A three-year survey on the worldwide occurrence of mycotoxins in feedstuffs and feed. *Toxins* 2012;4:663-675.

176. Cianferoni A, Khullar K, Saltzman R, Fiedler J, Garrett JP, Naimi DR, Spergel JM. Oral food challenge to wheat: a near-fatal anaphylaxis and review of 93 food challenges in children. *World Allergy Organ J* 2013;6:14.

177. Sievers S, Rawel HM, Ringel KP, Niggemann B, Beyer K. Wheat protein recognition pattern in tolerant and allergic children. *Pediatr Allergy Immunol* 2015.

178. Makela MJ, Eriksson C, Kotaniemi-Syrjanen A, Palosuo K, Marsh J, Borres M, Kuitunen M, Pelkonen AS. Wheat allergy in children - new tools for diagnostics. *Clin Exp Allergy* 2014;44:1420-1430.



# Chapter 4



## Deoxynivalenol: a trigger for intestinal integrity breakdown

Peyman Akbari<sup>1,2,\*</sup>, Saskia Braber<sup>1,\*</sup>, Hendrik Gremmels<sup>3</sup>, Pim J. Koelink<sup>2</sup>, Kim A.T. Verheijden<sup>2</sup>, Johan Garssen<sup>2,4</sup>, Johanna Fink-Gremmels<sup>1</sup>

<sup>1</sup> Division of Veterinary Pharmacology, Pharmacotherapy and Toxicology, Institute for Risk Assessment Sciences, Utrecht University, Utrecht, The Netherlands

<sup>2</sup> Division of Pharmacology, Utrecht Institute for Pharmaceutical Sciences, Faculty of Science, Utrecht University, Utrecht, The Netherlands

<sup>3</sup> Department of Nephrology and Hypertension, University Medical Center Utrecht, Utrecht, The Netherlands

<sup>4</sup> Nutricia Research, Utrecht, The Netherlands

\* Both authors have equally contributed to this manuscript

**This chapter is published in The FASEB Journal 2014; 28(6): 2414-2429.**

## Abstract

Disintegration of the colonic epithelial barrier is considered a key event in the initiation and progression of inflammatory bowel and coeliac disease. As the primary aetiology of these diseases remains unknown, we hypothesized that the trichothecene deoxynivalenol (DON), a fungal metabolite found in grain-based human diets, might be one of the triggers resulting in an impairment of the intestinal tight junction network preceding an inflammatory response. Using horizontal impedance measurements we demonstrate that DON disintegrates a human Caco-2 cell monolayer within less than 1 hour after exposure to concentrations as low as 1.39  $\mu\text{M}$ . This initial trigger is followed by a decrease in transepithelial resistance and an increased permeability of marker molecules such as lucifer yellow and FITC-labelled dextran. In parallel, the increase in paracellular transport of FITC-dextran is demonstrated *in vivo* in B6C3F<sub>1</sub> mice, challenged orally with DON. *In vitro* claudin protein levels are decreased and correlated with a displacement within the cells *in vitro* and *in vivo*, accompanied with a compensatory up-regulation of mRNA levels of claudins and their binding partner ZO-1. In treated mice alterations in villus architecture in the entire intestinal tract resemble the disintegration of the epithelial barrier, a characteristic of chronic inflammatory bowel disease.



## Introduction

The intestinal epithelial barrier is essential for the maintenance of physiological gut functions and serves as the first line of host defence against potentially harmful stressors from the environment, such as bacteria and viruses, as well as natural antigens and toxins occurring in food (1-3). The physical intestinal barrier is primarily formed by epithelial cells, connected by tight junction (TJ) proteins, which form an anastomosing network sealing adjacent epithelial cells near the luminal surface thus preventing a paracellular transport of luminal antigens (4, 5).

TJs are composed of I) transmembrane proteins, including occludin and claudins, which form a linear barrier at the apical-lateral membrane of the cell, II) peripheral membrane proteins (cytoplasmic scaffolding proteins), like zonula occludens (ZO) proteins, that serve as a link between the transmembrane TJ proteins; and cytosolic and nuclear proteins (6, 7). It is well accepted that a breakdown of the normally impeccable epithelial barrier of the intestine results in the development of a “leaky” gut. Disintegrated intestinal TJ proteins allow the paracellular infiltration of luminal antigens and is considered as a pivotal pathogenic factor in the onset and promotion of chronic intestinal inflammations such as inflammatory bowel disease (IBD) and coeliac disease (8-10).

Recent evidence has suggested that certain food contaminants, in particular the mycotoxin deoxynivalenol (DON) can impair intestinal barrier functions (11-14) and may be directly involved in intestinal inflammation (15-17). DON, a *Fusarium* metabolite, is among the most frequently detected contaminants of cereal-based foods including breakfast cereals (18-21). Considering this regular human exposure, the aim of the current study was to characterize the sequence of events induced by DON that lead to a compromised intestinal barrier function.

Using human Caco-2 cell monolayers as an *in vitro* model, we investigated the effect of DON on barrier integrity following apical and basolateral exposure, the paracellular transport of marker molecules and alterations in the expression and cellular distribution of TJ proteins. *In vivo* experiments in male B6C3F<sub>1</sub> mice, challenged orally with DON, were conducted to substantiate the *in vitro* findings and to demonstrate the impact of DON exposure on villus architecture.

The presented results challenge the hypothesis that nutritional DON exposure and the postulated high concentrations of the toxin in the intestinal lumen are the possible explanation for the observed translocation of luminal pathogens, while at the same time providing convincing evidence that DON acts as a trigger for intestinal integrity breakdown.



## Materials and Methods

### Deoxynivalenol solution

Purified DON (D0156; Sigma-Aldrich, St Luis, Mo, USA) was dissolved in absolute ethanol (99.9%, JT Baker, Deventer, the Netherlands) to prepare a 25 mM stock solution, stored at -20°C. Serial dilutions of this stock were prepared in cell culture medium. All other chemicals were of the highest purity available.

### *In vitro* experiments

#### Caco-2 cell cultures

Human epithelial colorectal adenocarcinoma (Caco-2) cells were obtained from the American Type Tissue Collection (Code HTB-37) (Manassas, VA, USA, passages 79-91) and were cultured in 75 cm<sup>2</sup> culture flasks (Greiner, Frickenhausen, Germany) in Dulbecco's modified Eagle's minimum essential medium (DMEM), containing 25 mM Hepes, 4.5 g/l glucose (Gibco, Invitrogen, Carlsbad, CA, USA) and supplemented with 10% heat-inactivated fetal calf serum (Gibco), Penicillin (100 U/ml)/Streptomycin (100 µg/ml) (Biocambrex, Verviers, Belgium), Glutamine (2 mM) (Biocambrex) and Non-essential Amino Acids (1%) (Gibco). The cells were maintained in a humidified atmosphere of 95% air and 5% CO<sub>2</sub> at 37°C. Medium was refreshed every 2-3 days and cells were passaged once a week. For subculture, the confluent cells were trypsinized using 0.05% trypsin and 0.54 mM ethylene diamine tetraacetic acid (EDTA) and were diluted in culture medium.

#### Caco-2 cell monolayers on transwell inserts

All *in vitro* experiments were conducted with Caco-2 cells grown on 0.3 cm<sup>2</sup> high pore density polyethylene terephthalate membrane transwell inserts with 0.4 µm pores (Falcon, BD Biosciences, Franklin Lakes, NJ, USA) placed in a 24-well plate, if not otherwise stated. The cells were seeded at a density of  $0.3 \times 10^5$  cells/insert. The cells were incubated at 37°C in a humidified atmosphere of 95% air and 5% CO<sub>2</sub>. After 17-19 days culturing a confluent monolayer was achieved, with a mean transepithelial electrical resistance (TEER) exceeding 400 Ω.cm<sup>2</sup> measured by a Millicell-ERS Volt-Ohm-meter (Millipore, Temecular, CA, USA). Each transwell experiment started when the TEER values reached this plateau.

#### Lactate dehydrogenase assay

Caco-2 cells grown on inserts as described above were exposed to DON (0-37.5 µM) for 24 h and the cytotoxic effect of DON on the Caco-2 cells was evaluated by measuring lactate dehydrogenase (LDH) leakage. LDH leakage was measured in the culture media of the apical and basolateral compartment using the CytoTox 96® Non-Radioactive CytoToxicity Assay Kit (Promega Corporation, Madison, WI, USA), according to manufacturer's instructions.

### Transepithelial Electrical Resistance (TEER) measurement

Caco-2 cells were grown on inserts as described above. The integrity of the cellular monolayer was evaluated by measuring TEER using a Millicell-ERS Volt-Ohm-meter (Millipore, Temecular, CA, USA). Mean TEER values for untreated cell monolayers were  $435 \pm 15 \Omega \cdot \text{cm}^2$ . The cells were challenged by adding increasing concentrations of DON (0, 0.05, 0.15, 0.46, 1.39, 4.17 and 12.5  $\mu\text{M}$ ) to the apical side, the basolateral side or both sides. TEER was measured at 0, 2, 4, 8, 12 and 24 h after DON exposure.

### Paracellular tracer flux assay

Caco-2 cell monolayers grown on inserts as described above were treated with increasing concentrations of DON in the apical and basolateral compartments for 24 h. Thereafter, membrane-impermeable molecules such as lucifer yellow (LY, molecular mass of 0.457 kDa, Sigma Chemical Co, St Luis, Mo, USA) and two different molecular sizes of fluorescein isothiocyanate-dextran (FITC-dextran, molecular mass of 4 and 40 kDa, Sigma Chemical Co, St Luis, Mo, USA) were added at a concentration of 16  $\mu\text{g}/\text{ml}$  to the apical compartment (350  $\mu\text{l}$ ) in the transwell plate for 4 h and paracellular flux was determined by measuring the fluorescence intensity in the basolateral compartment with a fluorimeter (FLUOstar Optima, BMG Labtech, Offenburg, Germany) set at excitation and emission wavelengths of 410 and 520 nm, respectively, for lucifer yellow, and 485 and 520 nm for FITC-dextran.

### Real-time horizontal impedance measurements

The cell xCELLigence system (Roche Applied Science, Mannheim, Germany) was used for dynamically monitoring of epithelial barrier integrity as described before (22, 23). Briefly, 50  $\mu\text{l}$  of the culture medium was added to 16-well E-plates (Roche Diagnostics, Mannheim, Germany) to obtain background readings of the individual wells. Caco-2 cells were seeded into these plates at a density of 5000 Caco-2 cells/well in 100  $\mu\text{l}$  medium and grown for approximately 2 days to reach confluence as indicated by a plateau in impedance signal. Since dome formation (24) may lead to detachment of the Caco-2 cells in this E-plate (not observed in transwell inserts) and decreased impedance measurements (from 60–72 h), the real-time horizontal impedance measurements started 2 days post-seeding to prevent effects of dome formation on these measurements. DON was added at increasing concentrations (0, 1.39, 4.17 and 12.5  $\mu\text{M}$ ) applied in temperature-equilibrated medium, followed immediately by real-time impedance measurements every 5 minutes over a period of 24 h. Impedance measurements were recorded at frequencies of 10, 25 and 50 kHz from which a compound signal, referred to cell index, was created (25). The relative change in impedance at a certain time point was calculated by dividing the cell index value by the reference time point (time zero) and corrected in relation to the control condition. Areas-Under-Curve (AUC) of each replicate were calculated for statistical analysis.

***In vitro* expression of TJ proteins: isolation of RNA and qRT-PCR analysis of Caco-2 cells**

Caco-2 cell monolayers grown on inserts and exposed to increasing concentrations of DON in the apical and basolateral compartments for 3, 6 and 24 h. Thereafter, cells were washed twice with ice-cold PBS and were harvested into 100  $\mu$ l RNA Lysis Buffer with  $\beta$ -mercaptoethanol. Total RNA was isolated using spin columns according to the manufacturer's instructions (Promega, Madison, WI, USA). The RNA amount was determined spectrophotometrically and purity of the RNA was measured by NanoDrop 2000 (Thermo Scientific, Waltham, WIL, USA) as A260/A280 ratio with expected values between 1.8 and 2. Subsequently, 1  $\mu$ g of extracted total RNA was reversely transcribed with the iScript<sup>TM</sup> cDNA Synthesis kit (Bio-Rad, Hercules, CA, USA). The cycling protocol for 20  $\mu$ l reaction mixes was 5 minutes at 25°C, followed by 30 minutes at 42°C, and 5 minutes at 85°C to terminate the reaction. After reverse transcription, cDNA was stored at -20°C. cDNA was diluted with nuclease-free water (1:9) directly before qRT-PCR analysis. The reaction mixture for the qRT-PCR, containing 10  $\mu$ l of the diluted cDNA mixed with 12.5  $\mu$ l iQSYBR Green Supermix (Bio-Rad, Hercules, CA, USA), forward and reverse primers (final concentration of 300 nM for each primer) and sterile deionized water, was prepared according to manufacturer's instructions. qRT-PCR was performed using the MyIQ single-colour real-time PCR detection system (Bio-Rad, Hercules, CA, USA) and MyIQ System Software Version 1.0.410 (Bio-Rad, Hercules, CA, USA). PCR cycle parameters: general denaturation at 95°C for 3 min, 1 cycle, followed by 40 cycles of 95°C for 20 s, annealing temperature (AT) for 30 s, and elongation at 72°C for 30 s. Gene specific primers for claudin1 (CLDN1), claudin3 (CLDN3), claudin4 (CLDN4), occludin (OCLN) and zonula occludens protein-1 (ZO-1) (Table 1) were designed by using the National Center for Biotechnology Information Primer-Basic Local Alignment Search Tool and were manufactured commercially (Eurogentec, Seraing, Belgium). Specificity and efficiency of selected primers (Table 1) were confirmed by qRT-PCR analysis of dilution series of pooled cDNA at a temperature gradient (55°C to 65°C) for primer-annealing and subsequent melting curve analysis. The geNorm software (version 3.5) was used to identify the most stable reference genes for this experiment. The mRNA quantity was calculated relative to the expression of two reference genes, Glyceraldehydes 3-phosphate dehydrogenase (GAPDH) and  $\beta$ -actin (ACTB). No significant effect of DON exposure on the Ct values of GAPDH and ACTB compared to the unstimulated cells (0  $\mu$ M DON) was observed (data not shown).

**Table 1.** Human primer sequences used for qRT-PCR analysis

Genes	Primer sequence (5'-3')		AT	References
	Forward	Reverse		
<b>CLDN1</b>	AGCTGGCTGAGACACTGAAGA	GAGAGGAAGGCACTGAACCA	63	NM_021101
<b>CLDN3</b>	CTGCTCTGCTGCTCGTGC	CGTAGTCCTTGCCTGCTAG	63	NM_001306
<b>CLDN4</b>	GTCTGCCTGCATCTCCTCTGT	CCTCTAAACCCGTCATCCA	62.5	NM_001305
<b>OCN</b>	TTGGATAAAGAATTGGATGACT	ACTGCTTGAATGATTCTTCT	57	NM_002538
<b>ZO-1</b>	GAATGATGGTTGGTATGGTGCG	TCAGAAGTGTGTCTACTGTCCG	55.8	NT_010194.17
<b>GAPDH</b>	ACCCACTCTCCACCTTTGAC	CCACCACCTGTTGCTGTAG	62.4	NM_002046
<b>ACTB</b>	CTGGAACGGTGAAGGTGACA	AAGGGACTTCTGTAACAATGCA	63	NM_001101

AT, annealing temperature (°C)

### Western blot analysis

Caco-2 cell monolayers were grown on inserts and incubated with increasing concentrations of DON in the apical and basolateral compartments for 24 h. Caco-2 monolayers were washed twice with cold PBS, and cells were lysed with 50 µl RIPA lysis buffer (50 mM Tris, 150 mM NaCl, 0.5% DOC, 1% NP-40, 0.1% SDS, pH 8.0) (Thermo scientific, Rockford, IL, USA) containing protease inhibitors (Roche Applied Science, Penzberg, Germany). After 5 minutes incubation with RIPA buffer, monolayers were harvested and centrifuged at 14.000 g for 15 minutes to yield a clear lysate. Total protein content was determined using the BCA protein assay following manufacturer's instructions (Thermo scientific, Rockford, IL, USA). Equal protein amounts of heat-denaturated non-reduced samples were separated electrophoretically (Criterion™ Gel, 4-20% Tris-HCL, Bio-Rad, Hercules, CA, USA) and electrotransferred onto polyvinylidene difluoride membranes (Bio-Rad, Veenendaal, The Netherlands). The membranes were blocked with PBS containing 0.05% Tween-20 (PBST) and 5% milk proteins for 1 h at room temperature. Subsequently, the primary antibodies CLDN1, CLDN3, CLDN4, OCLN and ZO-1 (Invitrogen) (detailed information is provided in Supplementary Table 1) were diluted according to manufacturer's instructions and incubated overnight at 4°C, followed by washing the blots in PBST. Secondary antibodies (Dako, Glostrup, Denmark) were applied for 2 h at room temperature. Blots were washed in PBST and incubated in commercial ECL reagents (Amersham Biosciences, Roosendaal, The Netherlands), and exposed to photographic film. Membranes were subsequently re-probed with rabbit monoclonal anti-human β-actin antibody (Cell Signaling, Danvers, MA, USA) (detailed information is provided in Supplementary Table 1) to assess homogeneity of loading. Films were scanned on a GS710 calibrated imagine densitometer (Bio-Rad Laboratories, Hercules, CA, USA) and the optical density (OD) for the immune-reactive bands was quantified.

### **Immunofluorescence staining Caco-2 cells**

Cellular localization of TJ proteins was assessed by immunofluorescence. Caco-2 cells were grown on inserts and exposed to 4.17  $\mu$ M DON in the apical and basolateral compartments for 24 h. Subsequently, the inserts with cells were fixed with 10% formalin for 10 minutes. After washing with PBS, the cells were permeabilized with PBS containing 0.1% Triton-X-100 for 5 min, and blocked with 5% serum for 30 minutes at room temperature. Thereafter the samples were incubated (2 h, room temperature) with different primary antibodies CLDN1, CLDN3, CLDN4, OCLN and ZO-1 (Invitrogen) (detailed information is provided in Supplementary Table 1) diluted in PBS containing 1% BSA according to manufacturer's instructions. The negative control lacking the primary antibodies were included (Supplementary Figure 3A). Samples were rinsed with PBS followed by incubation with Alexa-Fluor conjugated secondary antibody (Life Technologies) for 1 h at room temperature. A nuclear counterstaining was performed by incubating the samples for 1-3 minutes with Hoechst 33342 (Invitrogen) (1:2000). After washing, the inserts were mounted with ProLong Gold antifade reagent. Immunolocalization of TJ proteins was visualized and images were taken using the Nikon Eclipse TE2000-U microscope equipped with a Nikon Digital Sight DS-U1 camera.

### ***In vivo* experiments**

#### **Animals**

Male B6C3F<sub>1</sub> mice (n = 5-6 mice/experimental group), 6-7 weeks old (Charles River Laboratories, Maastricht, The Netherlands) were housed under controlled conditions in standard laboratory cages and were acclimated to the in house environment for two weeks. The room was maintained on a 12 h light/dark cycle at approximately ~20.5°C with a relative humidity of approximately ~61.5%. The AIN-93G-based diet (26), composed by Research Diet Services (Wijk bij Duurstede, the Netherlands), and water were provided *ad libitum*. The AIN-93G-based diet was checked for DON contamination by standard HPLC analyses with affinity column clean-up based on the method as described by Dombink-Kurtzman *et al.* (27) and no DON contamination exceeding the limit of 10  $\mu$ g/kg feed was detected. All *in vivo* experimental protocols were approved by the Ethics Committee for Animal Experiments (Reference number: DEC 2012.III.02.012) and were performed in compliance with governmental and international guidelines on animal experimentation.

#### **DON gavage and FITC-dextran permeability assay**

Feed was withdrawn from cages 2 h before toxin administration. DON, dissolved in 200  $\mu$ l PBS, was administered at a dose of 25 mg/kg body weight (bw) by oral gavage. Control animals received 200  $\mu$ l of vehicle. The 25 mg/kg dose represents approximately one-third to one-half of the LD50 for DON in mice (28). Two hours after DON administration, all animals received FITC-dextran (500 mg/kg bw; molecular mass 4 kDa; Sigma Chemical Co, St Luis, Mo, USA) by an oral gavage. The appearance of FITC-dextran in blood serum was

measured 4 h after the FITC-dextran gavage (6 h after DON administration). Directly after cervical dislocation, blood was obtained by heart puncture and collected in MiniCollect Z Serum Sep tubes (Greiner Bio-one). After 1 h the clotted blood samples were centrifuged for 10 minutes at 14.000 rpm and the sera were collected. Standard curves were obtained by a serial dilution of FITC-dextran in serum of mice that did not receive FITC-dextran and were not included in this experiment.

Serum samples from treated animals were diluted in an equal volume of PBS and the amount of FITC-dextran determined by measuring the fluorescence intensity using a spectrofluorimeter (FLUOstar Optima, BMG Labtech, Offenburg, Germany) set at excitation and emission wavelengths of 485 and 520 nm, respectively.

### ***In vivo* expression of TJ proteins: isolation of RNA and qRT-PCR of mice intestinal samples**

For mRNA studies, the mouse intestine was flushed with cold PBS and separated into different segments. These segments were defined as follows: proximal small intestine (first cm of the proximal part of the jejunum, approximately 2 cm after the stomach), middle small intestine (part of the intestine 7-8 cm after the first cm of the proximal part of the jejunum), distal small intestine (final cm before the ileum-caecum-colon junction), caecum and colon. These whole intestinal wall samples (approximately 1 cm) were snap frozen in liquid nitrogen and stored at -80°C for RNA isolation. Fifty mg of each sample was suspended into 350 µl RNA Lysis Buffer with β-mercaptoethanol and homogenized using a TissueLyser (Qiagen, Hilden, Germany) for 1 minute/25 Hz. RNA isolation, cDNA synthesis and qRT-PCR reactions were performed as described in materials and methods, *in vitro* experiments. Primer sequences with corresponding annealing temperatures are listed in Table 2.

### **Immunofluorescence staining of mice intestinal specimens**

The distal small intestine and colon (4-5 mice/experimental group) were fixed in 10% neutral buffered formalin and embedded in paraffin as a “Swiss roll” (29) to permit a complete microscopic examination. After paraffin embedding, 5 µm sections were cut (2-3 sections/antibody/animal). These Swiss-rolled paraffin sections were deparaffinized, endogenous peroxidase activity was blocked with 0.3% H<sub>2</sub>O<sub>2</sub> (Merck, Darmstadt, Germany) in methanol for 30 minutes at room temperature and rehydrated in a graded ethanol series to PBS. For antigen retrieval, the slides were boiled in 10 mM citrate buffer (PH 6.0) for 10 minutes in a microwave. The slides were cooled down to room temperature, rinsed with PBS (3x) and blocked with 5% serum for 30 minutes at room temperature. Thereafter, the immunofluorescence staining protocol with the primary antibodies CLDN1, CLDN2, CLDN3, CLDN4, OCLN (Invitrogen) and ZO-1 (Millipore) (detailed information in Supplementary Table 1) was performed as described above. The negative controls lacking the primary antibodies were included (Supplementary Figure 3B-D).

**Table 2.** Murine primer sequences used for qRT-PCR analysis

Genes	Primer sequence (5'-3')		AT	References
	Forward	Reverse		
<b>CLDN1</b>	TCTACGAGGGACTGTGGATG	TCAGATTCAGCTAGGAGTCG	57	NM_016674
<b>CLDN2</b>	GGCTGTTAGGCTCATCCAT	TGGCACCAACATAGGAACTC	55	NM_016675
<b>CLDN3</b>	AAGCCGAATGGACAAAGAA	CTGGCAAGTAGCTGCAGTG	58.7	NM_009902
<b>CLDN4</b>	CGCTACTCTTGCCATTACG	ACTCAGCACACCATGACTTG	55	NM_009903
<b>OCLN</b>	ATGTCCGGCCGATGCTCTC	TTTGGCTGCTCTTGGGTCTGTAT	61.2	NM_008756.2
<b>ZO-1</b>	CGAGGCATCATCCCAAATAAGAAC	TCCAGAAGTCTGCCCGATCAC	58.7	NM_009386
<b>GAPDH</b>	GAACATCATCCCTGCATCC	CACATTGGGGGTAGGAACAC	61	NM_008084.2
<b>ACTB</b>	ATGCTCCCCGGGCTGTAT	CATAGGAGTCCTTCTGACCCATTC	61	NM_007393.3

AT, annealing temperature (°C)

### Histomorphometric analysis of mouse intestines

The proximal small intestine and distal small intestine were fixed in 10% neutral buffered formalin and embedded as a “Swiss roll” (29). After paraffin embedding, 5 µm sections were cut and stained with haematoxylin/eosin (H&E) according to standard methods. Photomicrographs were taken with an Olympus BX50 microscope equipped with a Leica DFC 320 digital camera. The morphometric analysis of the sections was performed on 10 randomly selected, well-oriented villi and crypts per animal. A computerized microscope-based image analyser (Cell<sup>^</sup>D, Olympus, Europa GmbH, Germany) was used to determine histomorphometric parameters: villus height (measured from the tip of the villus to the villus-crypt junction), crypt depth (measured from the crypt-villus junction to the base of the crypt), villus width, villus surface area (total surface of the villus) and epithelial cell area (villus area minus villus area without epithelial cells). These regions of interest were manually defined for each villi separately and an example of the histomorphometric analysis of a villus is depicted in Supplementary Figure 1.

### Statistical analyses

Experimental results are expressed as mean ± SEM. Analyses were performed by using GraphPad Prism (version 5.0) (GraphPad, La Jolla, CA, USA). Differences between groups were statistically determined by using One-way ANOVA, with Bonferroni post hoc test for *in vitro* experiments and an unpaired two-tailed student's t-test for *in vivo* experiments. Results were considered statistically significant when  $P < 0.05$ .



## Results

### Cytotoxic effects of DON in Caco-2 cells

The direct cytotoxicity of DON was measured over a concentration range between 0 and 37.5  $\mu\text{M}$  by the LDH leakage assay. DON did not impair cell viability as indicated by LDH release in apical and basolateral compartments up to a concentration of 12.5  $\mu\text{M}$ . LDH release increased slightly but not significantly at this concentration (Figure 1). In all forthcoming experiments, DON concentrations equal to or below 12.5  $\mu\text{M}$  were used.

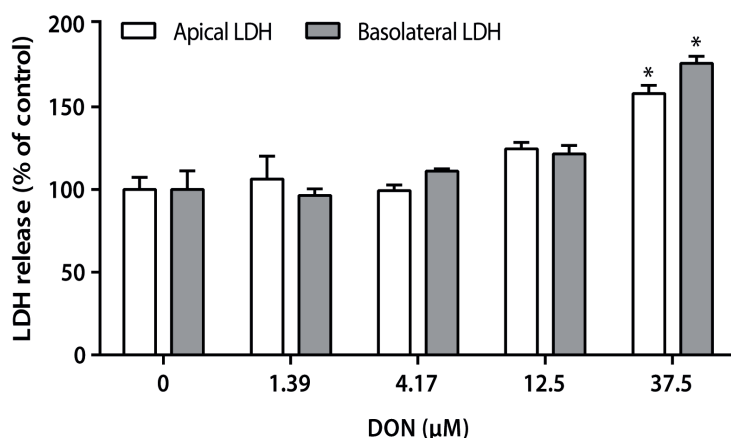


**Figure 1.** DON did not exert cytotoxic effects on Caco-2 cells. Caco-2 cells grown on inserts were incubated with increasing concentrations DON (0, 1.39, 4.17, 12.5 and 37.5  $\mu\text{M}$ ) for 24 h, followed by measurement of LDH release in the apical as well as the basolateral compartments of the transwell insert system. Results are expressed as percentage of LDH released by the non-treated cells  $\pm$  SEM of three independent experiments, each performed in triplicate (\* $P < 0.05$ ; significantly different from the non-stimulated cells).

### Effects of DON on TEER of a Caco-2 monolayer

Upon exposure to increasing concentrations of DON (0, 0.05, 0.15, 0.46, 1.39, 4.17 and 12.5  $\mu\text{M}$ ) added to the apical and basolateral compartments a clear dose-response curve was obtained. Concentrations up to 0.46  $\mu\text{M}$  DON remained without any effect, whereas the test concentration of 1.39  $\mu\text{M}$  resulted in a highly significant decrease of the TEER value (Figure 2A). To assess the differences in the routes of exposure, DON was added to either the apical or the basolateral side, or to both sides of the transwell chamber (Figure 2B). Results show that after basolateral exposure to DON the decrease of TEER values was more pronounced compared to the alterations observed after apical exposure to DON (Figure 2B), where only small effects were observed. The TEER decrease after dual exposure to DON from the apical and basolateral side was comparable with the decrease in

TEER values after basolateral exposure (Figure 2B). Since DON is quickly and expeditiously absorbed in the upper parts of the small intestine (30) and following absorption it is likely to be secreted into the gut lumen as DON is a substrate for ABC efflux transporters (31), exposure to both apical and basolateral side mimics the *in vivo* situation and will be used in the following experiments. The time dependency was established in experiments using increasing concentrations of DON (1.39, 4.17 and 12.5  $\mu\text{M}$ ), which were added to the apical as well as to the basolateral side. Different incubation time points (2, 4, 8, 12 and 24 h) were tested and a time dependent decrease in TEER was observed (Figure 2C). The first significant TEER decrease by DON was observed after 8 h.

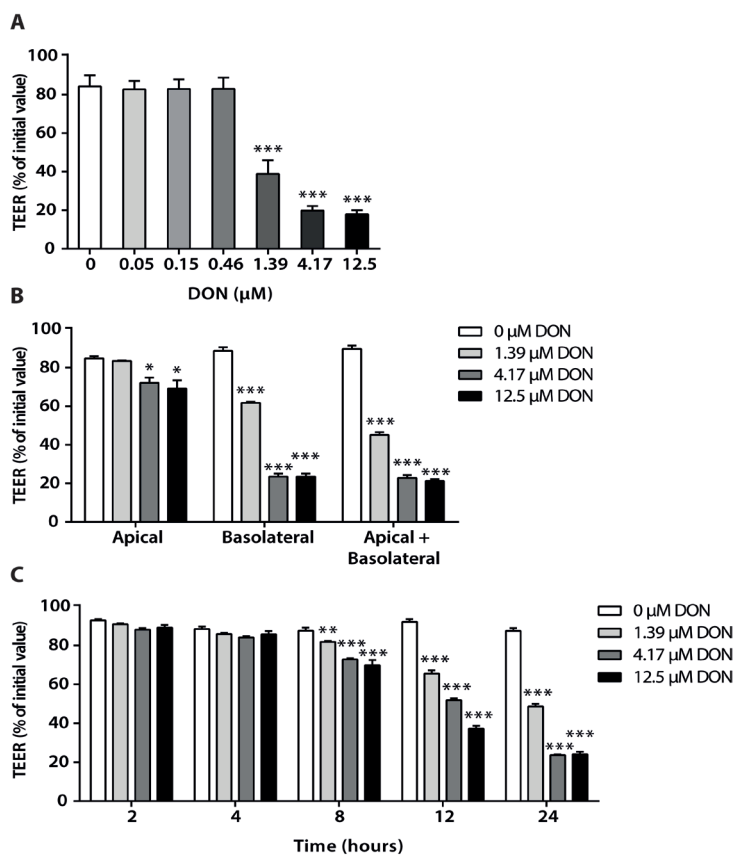


**Figure 2.** DON induced a decrease in TEER of the Caco-2 monolayer. Caco-2 cells were grown on inserts and the effect of the concentration of DON (A) (apical and basolateral DON exposure), the direction of DON exposure (B), and different incubation times (C) (apical and basolateral DON exposure) were examined. Subsequently, the TEER was measured as described in materials and methods. Results are expressed as a percentage of initial value as mean  $\pm$  SEM of three independent experiments, each performed in triplicate (\* $P < 0.05$ , \*\* $P < 0.01$ , \*\*\* $P < 0.001$ ; significantly different from the related non-stimulated cells).

### DON increases the permeability of the Caco-2 monolayer

Monitoring the permeability of the paracellular transport markers lucifer yellow (0.457 kDa) and two different molecular sizes of FITC-dextran (4 and 40 kDa, respectively) across the cell monolayer (Figure 3), indicated that DON (added to both apical and basolateral compartments) induced a significant increase in the translocation of lucifer yellow (0.457 kDa) and 4 kDa FITC-dextran from the apical to the basolateral chamber (Figure 3A, B). However, DON exposure (both apical and basolateral) did not affect the Caco-2 monolayer permeability of 40 kDa FITC-dextran, which remained unchanged (Figure 3B).

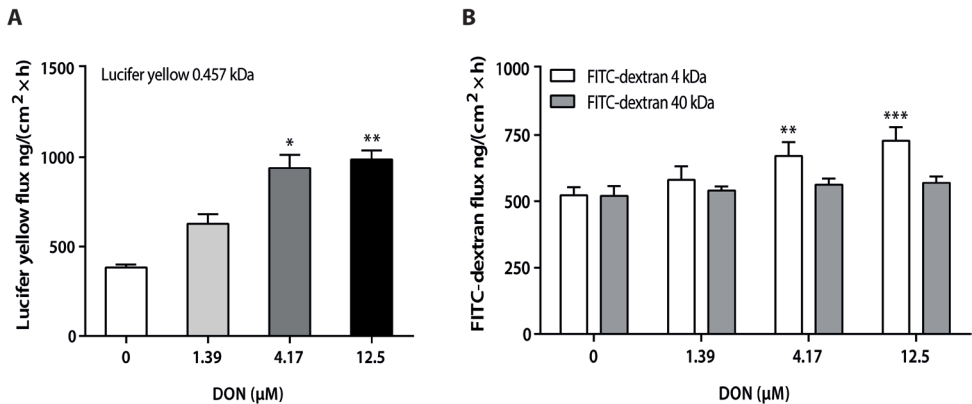


**Figure 3.** DON increased the permeability of the Caco-2 monolayer. Caco-2 cells were grown on inserts and stimulated with increasing concentrations of DON in the apical and basolateral compartments for 24 h. Subsequently, the translocation of lucifer yellow (0.457 kDa) (A) and two different molecular sizes FITC-dextran (4 and 40 kDa) (B) from the apical to the basolateral chamber was performed as described in materials and methods. Results are expressed in ng transport marker/(cm<sup>2</sup> × h) as mean  $\pm$  SEM of three independent experiments, each performed in triplicate (\* $P < 0.05$ , \*\* $P < 0.01$ , \*\*\* $P < 0.001$ ; significantly different from the non-stimulated cells).

### DON induces a decline in impedance values after real-time monitoring

Real-time recording of the horizontal impedance every 5 minutes over a period of 24 h following exposure of a Caco-2 monolayer to 3 different concentrations of DON (1.39, 4.17 and 12.5  $\mu$ M) showed an immediate and concentration-dependent decline in impedance values commencing within the first 15 minutes of DON exposure and lasting for almost the entire observation period (Figure 4A). Lines of individual experiments were summarized as Areas-Under-Curve (AUC) and this summary measure was used for statistics (in a separate panel, Figure 4B). P-values are One-way ANOVA tests to statistically determine the differences between groups.

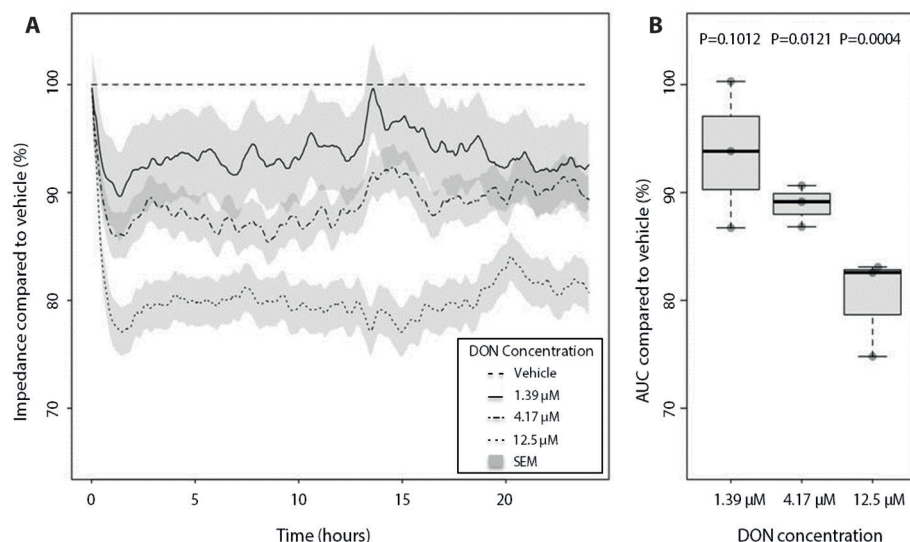


**Figure 4.** Real-time monitoring of DON-induced epithelial barrier dysfunction. Caco-2 cells were grown on E-plates to form a monolayer and were incubated with increasing concentrations of DON (0, 1.39, 4.17 and 12.5  $\mu$ M) for 24 h. The real-time resistance was monitored every 5 minutes as described in materials and methods. Results are expressed in relative change in impedance (in %) as mean  $\pm$  SEM of three independent experiments (A), each performed in quadruplicate. Areas-Under-Curve (AUC) of each replicate were calculated for statistical analysis (B). Results are expressed in AUCs compared to vehicle (0  $\mu$ M DON) (in %) as mean  $\pm$  SEM of three independent experiments, each performed in quadruplicate (P-values are given).

### DON up-regulates the mRNA expression of the TJ proteins in Caco-2 cells

In order to correlate the DON-induced impaired integrity with barrier dysfunctions, the mRNA expression levels of the different TJ proteins (CLDN1, CLDN3, CLDN4, OCLN and ZO-1) were measured. Caco-2 cell monolayers, grown on inserts, were exposed to increasing concentrations DON (1.39, 4.17 and 12.5  $\mu$ M) in apical and basolateral compartments for 3, 6 or 24 h. qRT-PCR analysis demonstrated that already after 3 h of DON exposure, the mRNA expression levels of CLDN3, CLDN4 and ZO-1 were up-regulated in a concentration-dependent manner (Figure 5A). After 6 h of DON exposure, the mRNA expression levels of all different TJ proteins were dose-dependently increased (Figure 5B). The mRNA expression of the TJ proteins in Caco-2 cells after 24 h of DON exposure, was comparable with the results after 6 h of DON exposure (Figure 5C).

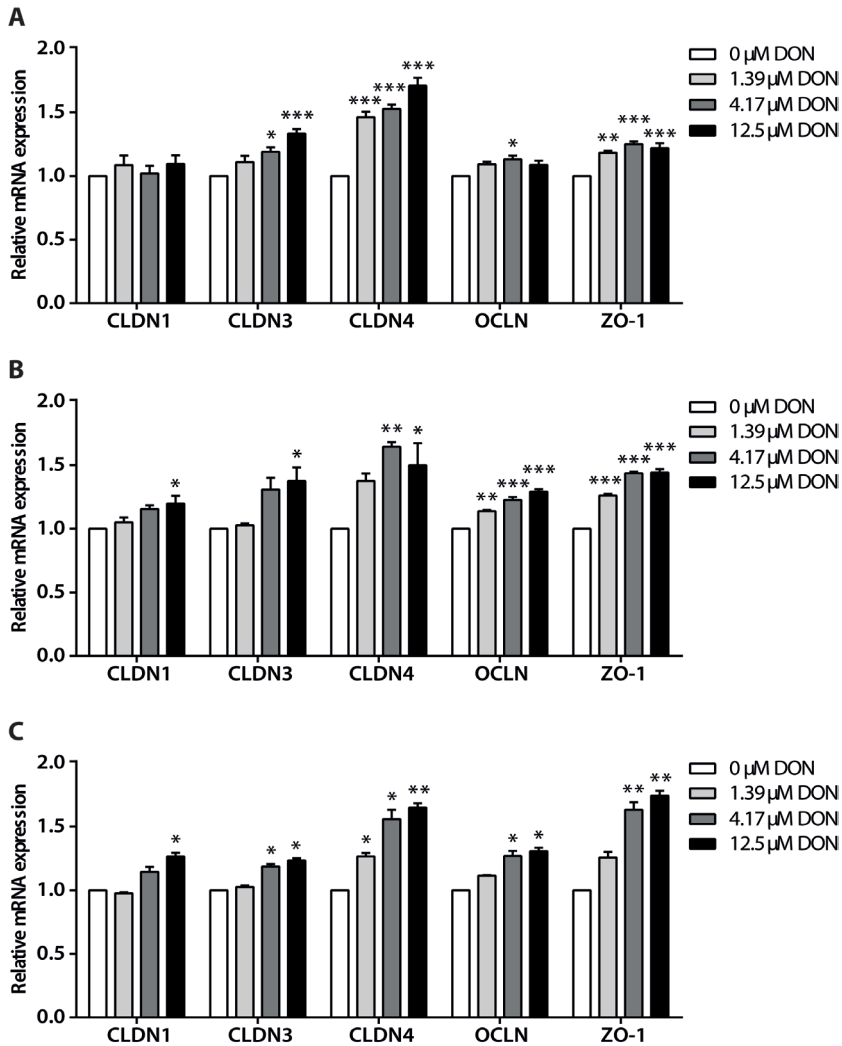


**Figure 5.** DON up-regulated the mRNA expression of the TJ proteins in Caco-2 cells. Caco-2 cells were grown on inserts and stimulated with increasing concentrations of DON (1.39, 4.17 and 12.5 μM) in apical and basolateral compartments for 3 h (A), 6 h (B) and 24 h (C). mRNA levels of TJ proteins (CLDN1, CLDN3, CLDN4, OCLN and ZO-1) were measured by qRT-PCR as described in materials and methods. Results are relative mRNA expression as mean  $\pm$  SEM of three independent experiments, each performed in triplicate. (\* $P < 0.05$ , \*\* $P < 0.01$ , \*\*\* $P < 0.001$ ; significantly different from the non-stimulated cells).

**DON selectively affects the TJ protein levels in Caco-2 cells**

Next to the assessment of mRNA expression of the TJ proteins, the effect of DON on the protein levels of several TJ proteins (CLDN1, CLDN3, CLDN4, OCLN and ZO-1) were quantified by Western blot analysis in Caco-2 cell lysates of cells that had been exposed to DON in apical and basolateral compartments for 24 h. A representative blot of each TJ proteins and the corresponding  $\beta$ -actin used as loading control are shown in Figure 6A, B (additional blots are available in Supplementary Figure 2). The optical density of the molecular weight bands of the different TJ proteins was measured and after normalization with  $\beta$ -actin also depicted in Figure 6A, B. A dose-dependent reduction of the CLDN1, CLDN3 and CLDN4 protein levels was observed in DON-exposed Caco-2 cells compared to untreated cells (Figure 6A). The OCLN and ZO-1 levels remained unchanged after DON challenge (Figure 6B).

**DON affects the distribution pattern of TJ proteins in Caco-2 cells**

To investigate the cellular localization of TJ proteins, Caco-2 cell monolayers grown on inserts were incubated with or without DON (4.17  $\mu$ M) at apical and basolateral compartments for 24 h, followed by an immunofluorescent staining. In the intact Caco-2 cells, CLDN1, CLDN3, CLDN4, OCLN and ZO-1 are localized at the cell membrane and appeared as continuous belt-like structures encircling the cells at the contact points with adjacent cells (Figure 6A, B). DON exposure disturbed the continuity of all tested TJ proteins, which appeared to be irregular distributed in the cells (Figure 6A, B).

***In vivo* exposure of B6C3F<sub>1</sub> mice to DON results in an increased intestinal permeability**

In order to confirm the DON-induced hyperpermeability observed in the Caco-2 monolayer, an *in vivo* intestinal permeability assay was performed in a mouse model using the paracellular tracer FITC-dextran (4 kDa). This tracer was significantly increased in serum of DON-treated mice when measured 4 h after a FITC-dextran oral gavage (Figure 7). This finding indicates that DON induced an increase in the *in vivo* intestinal permeability observed by the translocation of FITC-dextran across the intestinal interfaces in B6C3F<sub>1</sub> mice.

**DON selectively up-regulates the mRNA expression of the TJ proteins in different parts of the mouse intestines**

In order to extrapolate the DON-induced induction in mRNA expression of different TJ proteins observed in Caco-2 cells, the mRNA expression levels of the same TJ proteins (CLDN1, CLDN2, CLDN3, CLDN4, OCLN, and ZO-1) were measured in different segments of the mouse intestines (proximal, middle and distal small intestine, caecum and colon). CLDN4 mRNA expression levels were increased in all parts of the intestines of the DON-treated animals compared to the control animals (Figure 8A-E), whereas CLDN3 expression levels were increased after DON gavage in all parts of the intestines, except the proximal and middle small intestine (Figure 8C-E). The mRNA expression levels of CLDN2

were increased in the mouse middle and distal small intestine upon DON exposure as compared to the non-treated animals (Figure 8B, C). The ZO-1 mRNA expression levels were only increased in the proximal small intestine of the DON-treated animals (Figure 8A). The mRNA expression of OCLN and CLDN1 remained unaffected in all parts of the intestines of DON-exposed mice compared to control mice.

### **DON affects the distribution pattern of TJ proteins in the intestines of mice**

Considering that DON selectively up-regulated the mRNA levels of the TJ proteins in the mouse intestines, especially in the distal part of the small intestine, immunofluorescence staining of all TJ proteins (CLDN1, CLDN2, CLDN3, CLDN4, OCLN and ZO-1) were performed to show the cellular distribution and localization of TJ proteins. Results show that in the distal small intestine of control mice, CLDN1 and CLDN3 were expressed laterally between adjacent cells with neither a specific signal at the apical cell surface nor on the basal membrane. After DON gavage the CLDN1 and CLDN3 expression was more pronounced laterally and at the basal cytoplasm (Figure 9). CLDN2 distribution was mainly restricted to the crypts in the distal small intestine of control animals and was expressed laterally between adjacent cells. This CLDN2 expression pattern was disrupted after DON gavage. In contrast to the controls, CLDN2 expression was not restricted to the crypts anymore (Figure 9). CLDN4 was expressed in both, the tips and crypts of the villi in the distal small intestine. These findings clearly indicate that the expression of CLDN4 is restricted to selective sites and cannot be found on every tip or crypt of the villus epithelium. No pronounced effect on the CLDN4 distribution pattern in the distal small intestine was observed after the DON gavage (Figure 9). Unlike the distribution pattern of the claudins, expressed laterally between adjacent cells in the distal small intestine, OCLN and ZO-1 were localized in distinct dot-like structures at the apical region of the lateral plasma membrane of the epithelial cells of a villus, and no clear alterations were observed after DON exposure (Figure 9). Additionally, immunofluorescence staining of different TJ proteins (CLDN1, CLDN2, CLDN3, CLDN4, OCLN and ZO-1) were performed in the colon of control and DON-treated animals, to investigate whether the distribution pattern of TJ proteins in the colon is impacted by DON. No clear differences in the TJ distribution patterns of CLDN1, CLDN2, CLDN3, CLDN4, OCLN and ZO-1 were observed in the colon of DON-treated animals compared to control animals (Supplementary Figure 4).



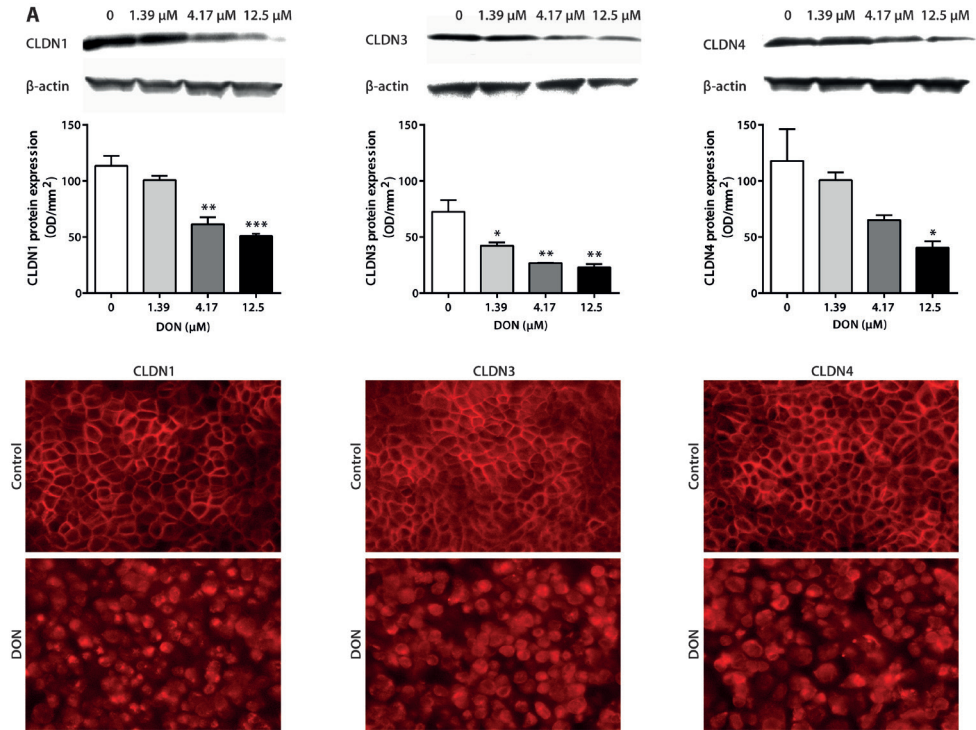


**Figure 6A.** DON selectively affected the TJ protein levels and localization. Caco-2 cells were grown on inserts and stimulated with increasing concentrations of DON (1.39, 4.17 and 12.5  $\mu$ M) in apical and basolateral compartments for 24 h. The Caco-2 monolayers were lysed and the protein extract was analyzed by Western blot analysis for CLDN1, CLDN3, CLDN4 and corresponding  $\beta$ -actin (representative blots are shown). Expression of the proteins was estimated by densitometry after normalization with  $\beta$ -actin. Values are expressed as mean ratio (TJ protein expression (OD/mm<sup>2</sup>) normalized to  $\beta$ -actin)  $\pm$  SEM of three independent experiments (\* $P$  < 0.05, \*\* $P$  < 0.01, \*\*\* $P$  < 0.001; significantly different from the unstimulated cells). For immunofluorescence, Caco-2 monolayers were incubated with DON (4.17  $\mu$ M) at apical and basolateral compartments and detected by antibodies for CLDN1, CLDN3 and CLDN4 as described in materials and methods. Magnification 400x.

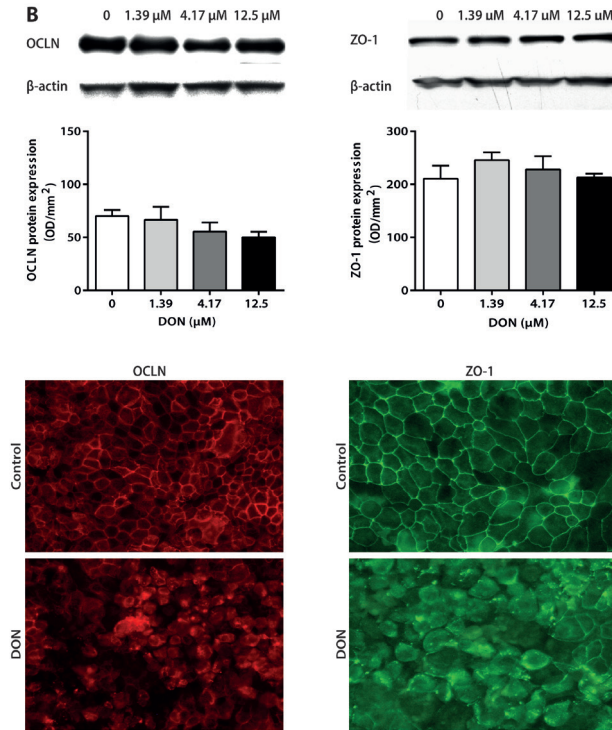


**Figure 6B.** DON selectively affected the TJ protein levels and localization. Caco-2 cells were grown on inserts and stimulated with increasing concentrations of DON (1.39, 4.17 and 12.5  $\mu\text{M}$ ) in apical and basolateral compartment for 24 h. The Caco-2 monolayers were lysed and the protein extract was analyzed by Western blot analysis for OCLN, ZO-1 and corresponding  $\beta$ -actin (representative blots are shown). Expression of the proteins was estimated by densitometry after normalization with  $\beta$ -actin. Values are expressed as mean ratio (TJ protein expression (OD/mm<sup>2</sup>) normalized to  $\beta$ -actin)  $\pm$  SEM of three independent experiments. For immunofluorescence, Caco-2 monolayers were incubated with DON (4.17  $\mu\text{M}$ ) at apical and basolateral compartments and detected by antibodies for OCLN and ZO-1 as described in materials and methods. Magnification 400x.

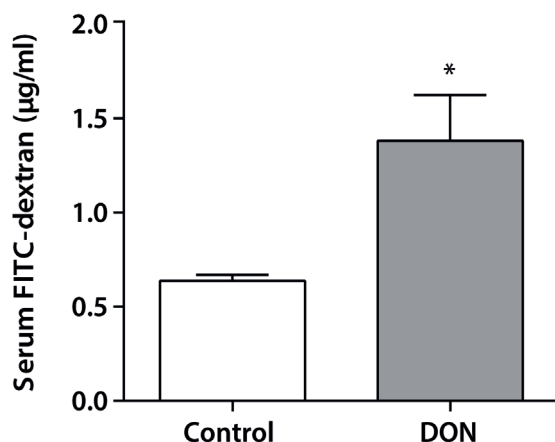


**Figure 7.** DON increased *in vivo* intestinal permeability in B6C3F<sub>1</sub> mice. Two hours after oral DON administration (25 mg/kg bw), mice were gavaged with 4 kDa FITC-dextran (500 mg/kg bw). Four hours after the FITC-dextran gavage the appearance of FITC-dextran was measured in blood as described in materials and methods.  $n = 5-6$  mice/experimental group. Values are expressed in  $\mu\text{g/ml}$  as mean  $\pm$  SEM (\* $P < 0.05$ ; significantly different from the control group).

### **DON induces histomorphological changes in the intestines of mice**

A quantitative histomorphometric analysis of the proximal and distal small intestine showed a significant decrease in villus height and villus area in the proximal (Figure 10A) as well as in the distal small intestine (Figure 10B) of DON-exposed mice in comparison to the non-treated animals. Furthermore, the epithelial cell area of the DON-treated mice was also significantly diminished in both proximal (Figure 10A) and distal small intestine (Figure 10B). The crypt depth was only increased in the proximal small intestine of the DON-treated mice compared to non-treated mice (crypt depth; control:  $131.71 \pm 5.20 \mu\text{m}$  versus DON:  $168.50 \pm 7.65 \mu\text{m}$ ,  $P < 0.01$ ), while no changes in villus width were observed in both parts of the small intestine followed by DON treatment.

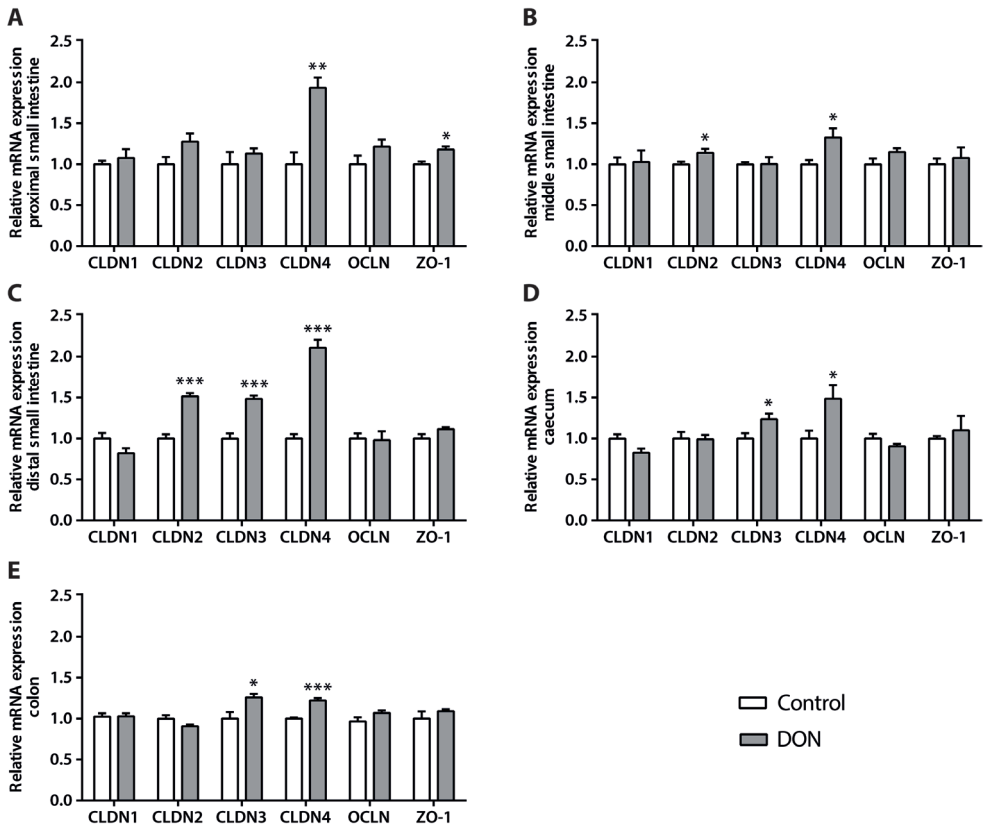


**Figure 8.** DON selectively affected the TJ mRNA expression levels and their localization in mouse intestine. Mice received DON by oral gavage (25 mg/kg bw). After 6 h, samples from different parts of the intestine (proximal (A), middle (B), distal small intestine (C), caecum (D) and colon (E)) were collected and mRNA levels of TJ proteins (CLDN1, CLDN2, CLDN3, CLDN4, OCLN, and ZO-1) were measured by qRT-PCR.  $n = 5-6$  mice/experimental group. Results are relative mRNA expression as mean  $\pm$  SEM (\* $P < 0.05$ , \*\* $P < 0.01$ , \*\*\* $P < 0.001$ ; significantly different from the control group).

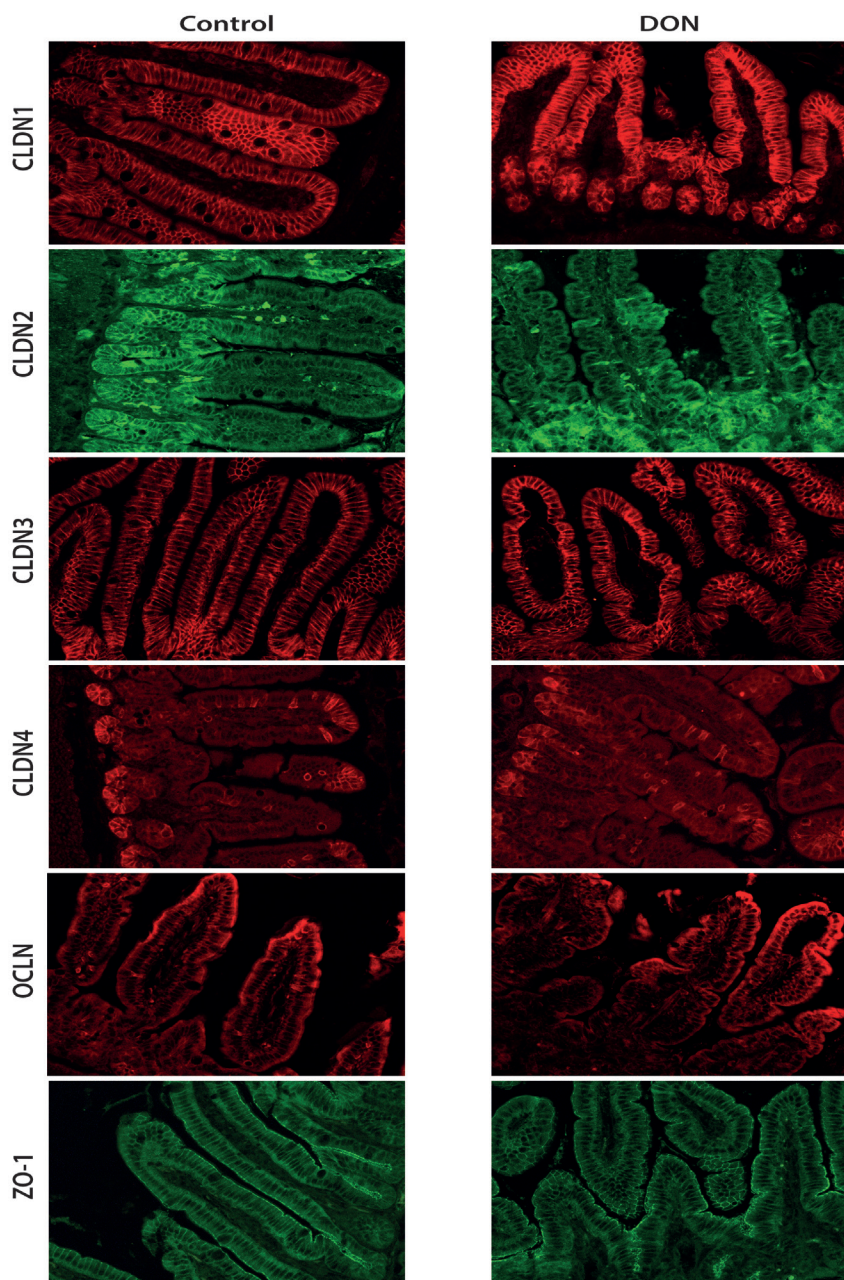


**Figure 9.** DON selectively affected the TJ localization in mouse intestine. Mice received DON by oral gavage (25 mg/kg bw). After 6 h, Swiss-rolled paraffin sections obtained from distal small intestine and were stained by immunofluorescence staining and detected by antibodies for CLDN1, CLDN2, CLDN3, CLDN4, OCLN and ZO-1 as described in materials and methods.  $n = 5-6$  mice/experimental group (2-3 sections/animal). Magnification 200x.

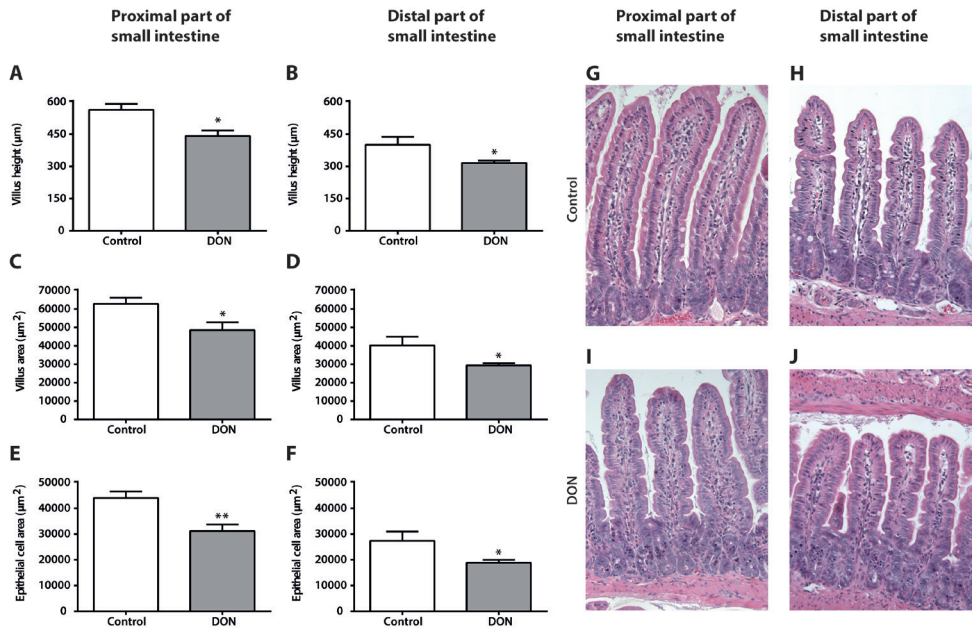


**Figure 10.** DON induced histomorphological changes in the intestine of mice. Mice received DON by oral gavage (25 mg/kg bw) and after 6 h, Swiss rolls obtained from the proximal (A, C, E, G and I) and distal (B, D, F, H and J) small intestine were stained with H&E for histomorphometric analysis (villus height (A, B), villus area (C, D), epithelial cell area (E, F) and related pictures from control (G, H) and DON-treated mice (I, J)). Magnification 200x.  $n = 5-6$  mice/experimental group. Results are expressed as mean  $\pm$  SEM (\* $P < 0.05$ , \*\* $P < 0.01$ ; significantly different from the control group).



## Discussion

A compromised intestinal barrier function has been associated with various diseases, including inflammatory bowel disease, coeliac disease and the irritable bowel syndrome. It is generally assumed that the primary cause leading to such a loss of intestinal integrity remains often unknown and is believed to be multifactorial. In this study we hypothesized that one of the factors that compromises the intestinal barrier function is the fungal toxin deoxynivalenol (DON). DON is a secondary metabolite and exotoxin of various fungal species of the genus *Fusarium*, which are soil-borne and invade living plants prior to harvest. As a small molecule (molecular weight: 296.3 g/mol), it resists technical processes of milling and food processing and can be detected in various food commodities. The high incidence of human exposure is confirmed by the analysis of urine samples for DON and its glucuronides, demonstrating that the exposure incidence exceeds in many cases 90% of the tested population (18-21). Experimental data showed that DON inhibits cellular protein synthesis and exerts a ribosomal stress syndrome associated with an inflammatory response, as recently reviewed by Pestka (32) and He *et al.* (33). Initially, incidental and human exposure to high concentrations of DON was associated with acute gastritis and intestinal distress (15). Recent experimental data with different *in vitro* systems, however, show that DON already at lower dietary concentrations is able to impair the integrity of epithelial cell monolayers. A dysfunctional epithelial cell barrier may be one of the predisposing factors leading to inflammatory diseases such as food allergy, inflammatory bowel disease and coeliac disease. Here we describe a series of experiments designed to identify the cascade of events exerted by DON that lead to the loss of epithelial barrier integrity *in vitro* and a compromised intestinal barrier function *in vivo* in mice exposed orally to DON, resembling human dietary exposure.

### *The impairment of TEER depends on the route of exposure*

A common early marker of an impairment of epithelial barrier integrity is a decrease in the TEER of an established Caco-2 cell monolayer at DON concentrations that do not affect cell viability. In an initial series of experiments we demonstrated that concentrations equal to or below 12.5  $\mu\text{M}$  DON did not impair Caco-2 cell viability (Figure 1), a finding that was in agreement with previous results (31). Considering the kinetics of DON, which is rapidly absorbed in the upper intestine (30), but is also secreted into the intestinal lumen as it is a substrate for ABC efflux transporters (31), we conducted TEER measurements following different routes of exposure. First, increasing concentrations of DON were added to the apical side mimicking the direct contact of the epithelial cells with contaminated food components. A dose-dependent decrease in TEER of the Caco-2 monolayer was observed after 24 h DON incubation. This is in agreement with previous studies (12, 13) and the data of De Walle *et al.* (11), who found a dose-dependent decrease in TEER of Caco-2 cells at concentrations between 0.17-17  $\mu\text{M}$  of DON after apical exposure of a cell monolayer. In turn, DON was added to the basolateral compartment to mimic the secretory pathway



of absorbed DON, which is mediated by the efflux transporters ABCB1 (Pg-p) and ABCC2 (MRP2) (31). Interestingly, the decrease in TEER values following basolateral exposure was more pronounced. This finding is in agreement with recent data by Diesing *et al.* (12), reporting that the basolateral surface of the intestinal barrier seems to be more susceptible to DON as compared to the apical exposure route in porcine IPEC-J2 cells. To further substantiate these findings, DON was added to both compartments of the transwell system. The measured decrease of TEER values was almost similar to the effects of a basolateral exposure to DON. Besides this dose-dependent effect of DON on the TEER of Caco-2 monolayers after 24 h, a time-dependent decrease in TEER was observed when comparing different incubation time points (2, 4, 8 and 12 h). Although, the gastrointestinal transit time of DON ingested with feed is expected to be less than one day, a 24 h DON incubation time is relevant for the *in vivo* situation, since DON is a daily food contaminant of wheat and grain products and intestinal epithelial cells are regularly exposed to DON during a day. Moreover, Azcona-Olivera *et al.* (28) observed that DON was still measurable in the mouse small (2.50 pmol/mg) and large intestine (7.80 pmol/mg) tissue 24 h after a DON gavage (25 mg/kg bw). In addition, following absorption in proximal intestine after oral ingestion, DON is likely to be secreted into the colon lumen due to the high expression of efflux transporters along the colon (31).

***The impairment of epithelial integrity facilitates a paracellular transport of macromolecules in vitro and in vivo***

The functional consequences of the readily measured impairment of the cell monolayer integrity was demonstrated by measuring the translocation of the paracellular transport markers lucifer yellow (0.457 kDa) and FITC-dextran (4 and 40 kDa). Upon 24 h exposure, DON induced a significant increase in the translocation of lucifer yellow and 4 kDa FITC-dextran from the apical compartment to the basolateral side. These findings are in agreement with the data of Pinton *et al.*, who demonstrated that upon 48 h DON exposure, the Caco-2 and IPEC-1 monolayers became more permeable for 4 kDa FITC-dextran (13, 16, 34). In contrast, we found no difference in the permeability of the 40 kDa FITC-dextran, indicating that larger molecules still cannot pass the epithelial barrier. DON-mediated changes in TJ proteins increase paracellular permeability to small molecules, but not transcellular flux of large molecules as this would require disruption of the cellular layer by cell death. The *in vivo* experiments with B6C3F<sub>1</sub> mice, orally exposed to DON confirmed the hyperpermeability as a significant increase in the translocation of FITC-dextran (4 kDa) from the gut lumen to blood circulation was observed in the DON-treated animals. Comparable findings were reported as yet only following exposure of animals to lipopolysaccharide (LPS) and even bacterial pathogens (35, 36).

***DON alters the function and expression of TJ proteins in vitro and in vivo***

The epithelial barrier function relies on TJ proteins eliminating the intercellular space, like ZO proteins that are peri-membrane proteins that link the apical membrane proteins

(such as occludin and claudins) with cytoskeleton proteins such as actin (37). Disruption of these actin filaments destroys the TJ protein network, thereby decreasing TEER values (38). The first evidence of a direct effect of DON on the TJ network was obtained by the horizontal impedance measurement. The real time analysis displayed that DON exposure induced an instant drop in impedance already in the first 1-2 h, followed by a marginal but not full recovery within the 24 h test period. These new findings demonstrate pronounced effects already at concentrations as low as 1.39  $\mu$ M DON, suggesting a direct effect of DON on TJ proteins, sealing the intercellular space. In this study the measured impedance is based on different frequencies (10, 25 and 50 kHz) merged to one signal, therefore we cannot discriminate between transcellular and paracellular impedance contributions. Although, there is a considerable overlap between the real-time impedance and TEER measurements (23), real-time impedance measurements clearly show the time-dependency of the events.

Since TEER and impedance measurements suggested alterations of TJ permeability and in order to describe the effect of DON on TJ proteins in more detail, the mRNA expression levels, protein levels, as well as cellular distribution of different TJ proteins (CLDN1, CLDN3, CLDN4, OCLN, and ZO-1) were measured in Caco-2 cells following DON exposure. qRT-PCR analyses pointed out that the mRNA expression of Caco-2 cells exposed to DON for 3 h showed a concentration-dependent up-regulation of the expression levels of CLDN3, CLDN4 and ZO-1, while the mRNA expression levels of all different TJ proteins, were increased upon 6 h DON exposure and these results were comparable with the results obtained after 24 h DON exposure. All individual time points of DON exposure show most probably a compensatory up-regulation of TJ mRNA levels. These results correlate to previous findings with IPEC cells (12) and complete the data of De Walle *et al.* (11), showing previously a raise in the mRNA expression levels of CLDN4 and OCLN in Caco-2 cells exposed to DON for 24 h. These findings were compared again with the *in vivo* mouse model by measuring the mRNA expression levels of TJ proteins after a DON gavage. Although a direct comparison between the *in vitro* findings in human Caco-2 cells with findings in mice needs to consider possible species differences and the fact that the samples taken in the *in vivo* study contained the entire intestinal wall and not only the epithelial cell layer. However, a number of interesting similarities in the response to DON were observed. For example, in line with the increase in mRNA expression of TJ proteins in DON-stimulated Caco-2 cells, in DON treated mice the mRNA expression levels of CLDN2, CLDN3 and CLDN4 were significantly increased in different parts of the intestines (small intestine, caecum and colon), whereas the ZO-1 mRNA expression levels were only increased in the proximal small intestine of the DON-treated animals. The CLDN1 and OCLN mRNA expression were not significantly affected in the treated mice as compared to the control animals. In the *in vivo* experiments CLDN2 was measured in addition to CLDN1, CLDN3 and CLDN4, whereas in Caco-2 cells CLDN2 is normally not expressed (39). The observed up-regulation of the different claudins was most pronounced in the distal part of small intestine. The epithelial cells along the distal part of the small intestine

are the most susceptible interface in the intestine, most probably because the distal small intestine is exposed to DON from both luminal and basolateral side (40). DON is quickly and expeditiously absorbed in the upper parts of the small intestine (30, 41) and following absorption it is likely secreted into the gut lumen as DON is a substrate for the efflux transporters ABCB1 (Pg-p) and ABCC2 (MRP2) (31).

When investigating the protein levels of the TJ proteins CLDN1, CLDN3, CLDN4, OCLN and ZO-1 in the Caco-2 cells of the *in vitro* DON model, a dose-dependent reduction of the CLDN1, CLDN3 and CLDN4 protein levels in DON-treated Caco-2 cells compared to untreated cells was demonstrated, while the OCLN and ZO-1 levels remained unchanged after DON stimulation. De Walle *et al.* (11) and Pinton *et al.* (13) also showed the absence of a decrease in ZO-1 expression in Caco-2 cells exposed to DON. While these findings reflect the results of the impedance measurements, they also indicate that the TJ network had not entirely lost its functions. This was also indicated by the observations that very large molecules such as 40 kDa FITC-dextran still could not pass the epithelial Caco-2 cell monolayer. These findings are also in agreement with results in different other cell lines (11, 12, 16). The decrease in claudin protein levels is associated with an increase in mRNA expression levels observed after 24 h DON exposure, which is most likely indicative of a repair mechanism. Whether or not such repair mechanisms are directly affected by DON at transcriptional level or are impaired by the previously described non-specific inhibition of the cellular protein synthesis as discussed by de Walle *et al.* (11), remains to be elucidated. The impact of the decrease in protein levels and the compensatory upregulation of mRNA levels of the measured TJ proteins are visualized by the analysis of the cellular localization of TJ proteins in Caco-2 cells. For the immunofluorescence staining the Caco-2 cells treated with 4.17  $\mu\text{M}$  DON were used, since concentrations from approximately 0.5-7  $\mu\text{M}$  DON represent plausible intestinal DON concentrations that may be found in the gastrointestinal tract after ingestion of moderately to highly DON-contaminated food as described in Sargent *et al.* (14). The samples of immunofluorescence analysis of Caco-2 cell monolayer show the membrane-associated localization of all TJ proteins, while DON-exposed cells exhibit irregular structures of the stained proteins, suggesting clumping and internalization of fragmented networks. These altered distribution patterns were not only observed for the claudin proteins, which were dose-dependently decreased, but also for OCLN and ZO-1, for which only marginal alteration in the total immunoreactive protein levels could be measured.

It is becoming increasingly apparent that a variety of pathological stimuli such as pro-inflammatory cytokines, microorganisms and toxins can induce endocytosis of several TJ proteins and as a consequent internalization of TJ proteins. The internalization of TJ proteins can be accompanied by their advanced degradation or a re-allocation to the plasma membrane. However, both mechanisms cause increased paracellular permeability due to the significant loss of TJ proteins at the plasma membrane of epithelial cells (42-46).

Comparable to the *in vitro* and *in vivo* findings, where the most pronounced effects on

TJ proteins were observed in the claudin family, immunofluorescence analysis of the distal small intestine of mice confirmed that DON exposure mainly affected the claudin distribution.

The lateral distribution pattern of CLDN1 and CLDN3 over the entire villi in the distal small intestine was observed in control mice and this typical pattern was even more pronounced after DON exposure resulting additionally in a visible expression at the basal cytoplasm. As already described by Rahner *et al.* (47) and Tamagawa *et al.* (48), CLDN2 is predominantly found in the crypts in mouse small intestine and this is confirmed in our study, where the CLDN2 was expressed laterally between adjacent cells in the crypts. However, after DON gavage this CLDN2 expression pattern is disrupted and not restricted to the crypts anymore, but is also distributed along the villus. Furthermore, our findings clearly indicate that the expression of CLDN4 is restricted to selective sites, and not found on every tip or crypt of the villus epithelium, which is in agreement with Tamagawa *et al.* (48). No pronounced effect on the CLDN4 distribution pattern in the distal small intestine was observed after the DON gavage. Unlike the distribution pattern of the claudins in the distal small intestine, OCLN and ZO-1 were localized in distinct dot-like structures at the apical region of the lateral plasma membrane in the epithelial cells of the villus, and no clear alterations were observed after DON exposure. Immunofluorescence staining of different TJ proteins were also performed in the colon of control and DON-treated animals to confirm the qRT-PCR analyses suggesting that the (distal) small intestine is most significantly affected by DON. As expected, no clear differences in the TJ distribution patterns of CLDN1, CLDN2, CLDN3, CLDN4, OCLN and ZO-1 were observed in the colon of DON-treated animals compared to control animals.

Taken together, it can be concluded that the most pronounced effects of DON on TJ proteins involve the claudin family as decreased claudin levels of the DON-treated Caco-2 cells as well as increased claudin levels in mouse intestine and an altered claudin distribution in the distal small intestine upon DON stimulation was observed. Claudins are known to be determinants of functional barrier properties, including size and charge selectivity of the paracellular permeability of the intestinal epithelium (49, 50). It also can be hypothesized that the claudins are more susceptible to DON exposure since these transmembrane proteins contain extracellular domains that may act as a binding site for DON as demonstrated for *Clostridium perfringens* enterotoxins interacting with CLDN3 (51). Claudins form a selective barrier between adjacent cells in contrast to the intracellular scaffold protein ZO-1, which interacts with intracellular domains of transmembrane proteins anchoring these proteins to the actin cytoskeleton (52).

A subsequently conducted histomorphometric analysis of the intestinal tissue of the DON exposed mice showed a significant decrease in villus height, villus area and also in the epithelial cell area in comparison to the non-treated animals. This result is in agreement with the data from Pinton *et al.* (17), reporting a significant reduction in the villus height along jejunum of pigs exposed to a DON-contaminated diet for 4 weeks. An *ex vivo* study by Kolf-Clauw *et al.* (53) shows alterations of pig jejunal explants including

shortened and coalescent villi following DON exposure for 4 h. One possible explanation for the shortened villi could be sloughing of epithelial lining from the surface of the villi and apoptosis and necrosis of the epithelial cells, since the epithelial cell area was also decreased in DON-treated animals. However, no prominent histological lesions were observed. Moreover, after acute mucosal injury by DON (at high dosage), villus contraction can take place, which is the initial phase of repair mechanisms aiming at the restoration of barrier function by reducing the total and denuded surface area of the villi. Villus contraction can be separated in an immediate contraction and second phase ongoing contraction which progresses in the first hours after injury and is mediated by endogenous prostaglandins (54).

In conclusion, the comparison of *in vitro* Caco-2 cell studies with the *in vivo* murine model suggests that the main molecular target of DON in the intestine is the TJ network. Disintegration of this network is accompanied by a loss of barrier function, which increases the risk of antigen transfer and an inflammatory response. Considering the high prevalence of dietary DON exposure in consumers of grains and grain-based products, the possible contribution of DON to the onset and propagation of inflammatory bowel disease warrant further investigation.

## Acknowledgements

This project is jointly financed by the European Union, European Regional Development Fund and The Ministry of Economic Affairs, Agriculture and Innovation, Peaks in the Delta, the Municipality of Groningen, the Provinces of Groningen, Fryslân and Drenthe, the Dutch Carbohydrate Competence Center (CCC WP25; [www.cccresearch.nl](http://www.cccresearch.nl)), Nutricia Research and FrieslandCampina. The authors would like to thank Rob Bleumink (The Center for Cell Imaging, Faculty of Veterinary Medicine, Utrecht University) for his help with the fluorescent imaging.

## References

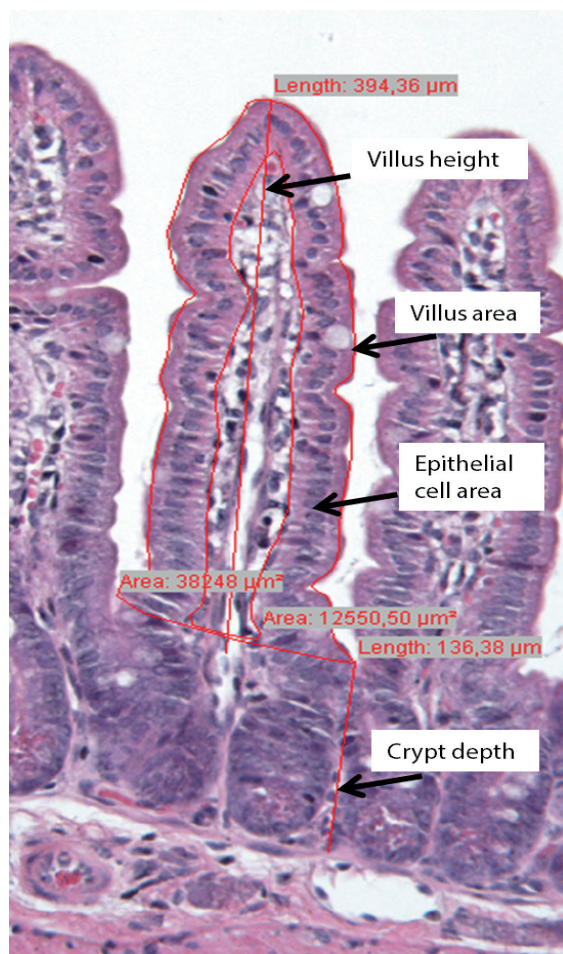
1. Groschwitz KR, Hogan SP. Intestinal barrier function: molecular regulation and disease pathogenesis. *J Allergy Clin Immunol* 2009;124:3-20.
2. Odenwald MA, Turner JR. Intestinal permeability defects: is it time to treat? *Clin Gastroenterol Hepatol* 2013;11:1075-1083.
3. Menard S, Cerf-Bensussan N, Heyman M. Multiple facets of intestinal permeability and epithelial handling of dietary antigens. *Mucosal Immunol* 2010;3:247-259.
4. Harhaj NS, Antonetti DA. Regulation of tight junctions and loss of barrier function in pathophysiology. *Int J Biochem Cell Biol* 2004;36:1206-1237.
5. Lutz KL, Siahhan TJ. Molecular structure of the apical junction complex and its contribution to the paracellular barrier. *J Pharm Sci* 1997;86:977-984.
6. Balda MS, Matter K. Tight junctions at a glance. *J Cell Sci* 2008;121:3677-3682.
7. Schneeberger EE, Lynch RD. Structure, function, and regulation of cellular tight junctions. *Am J Physiol* 1992;262:L647-L661.
8. Hollander D, Vadheim CM, Brettholz E, Petersen GM, Delahunty T, Rotter JL. Increased intestinal permeability in patients with Crohn's disease and their relatives. A possible etiologic factor. *Ann Intern Med* 1986;105:883-885.
9. DeMeo MT, Mutlu EA, Keshavarzian A, Tobin MC. Intestinal permeation and gastrointestinal disease. *J Clin Gastroenterol* 2002;34:385-396.
10. Heyman M, Abed J, Lebreton C, Cerf-Bensussan N. Intestinal permeability in coeliac disease: insight into mechanisms and relevance to pathogenesis. *Gut* 2012;61:1355-1364.
11. De Walle JV, Sergeant T, Piront N, Toussaint O, Schneider YJ, Larondelle Y. Deoxynivalenol affects *in vitro* intestinal epithelial cell barrier integrity through inhibition of protein synthesis. *Toxicol Appl Pharmacol* 2010;245:291-298.
12. Diesing AK, Nossol C, Danicke S, Walk N, Post A, Kahlert S, Rothkotter HJ, Kluess J. Vulnerability of polarised intestinal porcine epithelial cells to mycotoxin deoxynivalenol depends on the route of application. *PLoS One* 2011;6:e17472.
13. Pinton P, Nougayrede JP, Del Rio JC, Moreno C, Marin DE, Ferrier L, Bracarense AP, Kolf-Clauw M, Oswald IP. The food contaminant deoxynivalenol, decreases intestinal barrier permeability and reduces claudin expression. *Toxicol Appl Pharmacol* 2009;237:41-48.
14. Sergeant T, Parys M, Garsou S, Pussemier L, Schneider YJ, Larondelle Y. Deoxynivalenol transport across human intestinal Caco-2 cells and its effects on cellular metabolism at realistic intestinal concentrations. *Toxicol Lett* 2006;164:167-176.
15. Pestka JJ. Deoxynivalenol: mechanisms of action, human exposure, and toxicological relevance. *Arch Toxicol* 2010;84:663-679.
16. Pinton P, Braicu C, Nougayrede JP, Laffitte J, Taranu I, Oswald IP. Deoxynivalenol impairs porcine intestinal barrier function and decreases the protein expression of claudin-4 through a mitogen-activated protein kinase-dependent mechanism. *J Nutr* 2010;140:1956-1962.
17. Pinton P, Tsybulskyy D, Lucoli J, Laffitte J, Callu P, Lyazhri F, Grosjean F, Bracarense AP, Kolf-Clauw M, Oswald IP. Toxicity of deoxynivalenol and its acetylated derivatives on the intestine: differential effects on morphology, barrier function, tight junction proteins, and mitogen-activated protein kinases. *Toxicol Sci* 2012;130:180-190.
18. Sarkanj B, Warth B, Uhlig S, Abia WA, Sulyok M, Klapac T, Krška R, Banjari I. Urinary analysis reveals high deoxynivalenol exposure in pregnant women from Croatia. *Food Chem Toxicol* 2013;62:231-237.
19. Warth B, Sulyok M, Fruhmant P, Berthiller F, Schuhmacher R, Hametner C, Adam G, Frohlich J, Krška R. Assessment of human deoxynivalenol exposure using an LC-MS/MS based biomarker method. *Toxicol Lett* 2012;211:85-90.
20. Turner PC, Ji BT, Shu XO, Zheng W, Chow WH,

- Gao YT, Hardie LJ. A biomarker survey of urinary deoxynivalenol in China: the Shanghai Women's Health Study. *Food Addit Contam Part A Chem Anal Control Expo Risk Assess* 2011;28:1220-1223.
21. Hepworth SJ, Hardie LJ, Fraser LK, Burley VJ, Mijal RS, Wild CP, Azad R, McKinney PA, Turner PC. Deoxynivalenol exposure assessment in a cohort of pregnant women from Bradford, UK. *Food Addit Contam Part A Chem Anal Control Expo Risk Assess* 2012;29:269-276.
22. Abassi YA, Xi B, Zhang W, Ye P, Kirstein SL, Gaylord MR, Feinstein SC, Wang X, Xu X. Kinetic cell-based morphological screening: prediction of mechanism of compound action and off-target effects. *Chem Biol* 2009;16:712-723.
23. Sun M, Fu H, Cheng H, Cao Q, Zhao Y, Mou X, Zhang X, Liu X, Ke Y. A dynamic real-time method for monitoring epithelial barrier function *in vitro*. *Anal Biochem* 2012;425:96-103.
24. Kirkland SC. Dome formation by a human colonic adenocarcinoma cell line (HCA-7). *Cancer Res* 1985;45:3790-3795.
25. Urcan E, Haertel U, Styllou M, Hickel R, Scherthan H, Reichl FX. Real-time xCELLigence impedance analysis of the cytotoxicity of dental composite components on human gingival fibroblasts. *Dent Mater* 2010;26:51-58.
26. Reeves PG. Components of the AIN-93 diets as improvements in the AIN-76A diet. *J Nutr* 1997;127:S838-S841.
27. Dombrink-Kurtzman MA, Poling SM, Kendra DF. Determination of deoxynivalenol in infant cereal by immunoaffinity column cleanup and high-pressure liquid chromatography-UV detection. *J Food Prot* 2010;73:1073-1076.
28. Azcona-Olivera JI, Ouyang Y, Murtha J, Chu FS, Pestka JJ. Induction of cytokine mRNAs in mice after oral exposure to the trichothecene vomitoxin (deoxynivalenol): relationship to toxin distribution and protein synthesis inhibition. *Toxicol Appl Pharmacol* 1995;133:109-120.
29. Moolenbeek C, Ruitenberg EJ. The "Swiss roll": a simple technique for histological studies of the rodent intestine. *Lab Anim* 1981;15:57-59.
30. Danicke S, Valenta H, Doll S. On the toxicokinetics and the metabolism of deoxynivalenol (DON) in the pig. *Arch Anim Nutr* 2004;58:169-180.
31. Videmann B, Tep J, Cavret S, Lecoer S. Epithelial transport of deoxynivalenol: involvement of human P-glycoprotein (ABCB1) and multidrug resistance-associated protein 2 (ABCC2). *Food Chem Toxicol* 2007;45:1938-1947.
32. Pestka JJ. Deoxynivalenol-induced proinflammatory gene expression: mechanisms and pathological sequelae. *Toxins* 2010;2:1300-1317.
33. He K, Zhou HR, Pestka JJ. Mechanisms for ribotoxin-induced ribosomal RNA cleavage. *Toxicol Appl Pharmacol* 2012;265:10-18.
34. Kasuga F, Hara-Kudo Y, Saito N, Kumagai S, Sugita-Konishi Y. *In vitro* effect of deoxynivalenol on the differentiation of human colonic cell lines Caco-2 and T84. *Mycopathologia* 1998;142:161-167.
35. Yu P, Martin CM. Increased gut permeability and bacterial translocation in *Pseudomonas pneumonia*-induced sepsis. *Crit Care Med* 2000;28:2573-2577.
36. Wu X, Vallance BA, Boyer L, Bergstrom KS, Walker J, Madsen K, O'Kusky JR, Buchan AM, Jacobson K. *Saccharomyces boulardii* ameliorates *Citrobacter rodentium*-induced colitis through actions on bacterial virulence factors. *Am J Physiol Gastrointest Liver Physiol* 2008;294:G295-G306.
37. Hartsock A, Nelson WJ. Adherens and tight junctions: structure, function and connections to the actin cytoskeleton. *Biochim Biophys Acta* 2008;1778:660-669.
38. Canil C, Rosenshine I, Ruschkowski S, Sonnenberg MS, Kaper JB, Finlay BB. Enteropathogenic *Escherichia coli* decreases the transepithelial electrical resistance of polarized epithelial monolayers. *Infect Immun* 1993;61:2755-2762.
39. McLaughlin J, Padfield PJ, Burt JP, O'Neill CA. Ochratoxin A increases permeability through tight

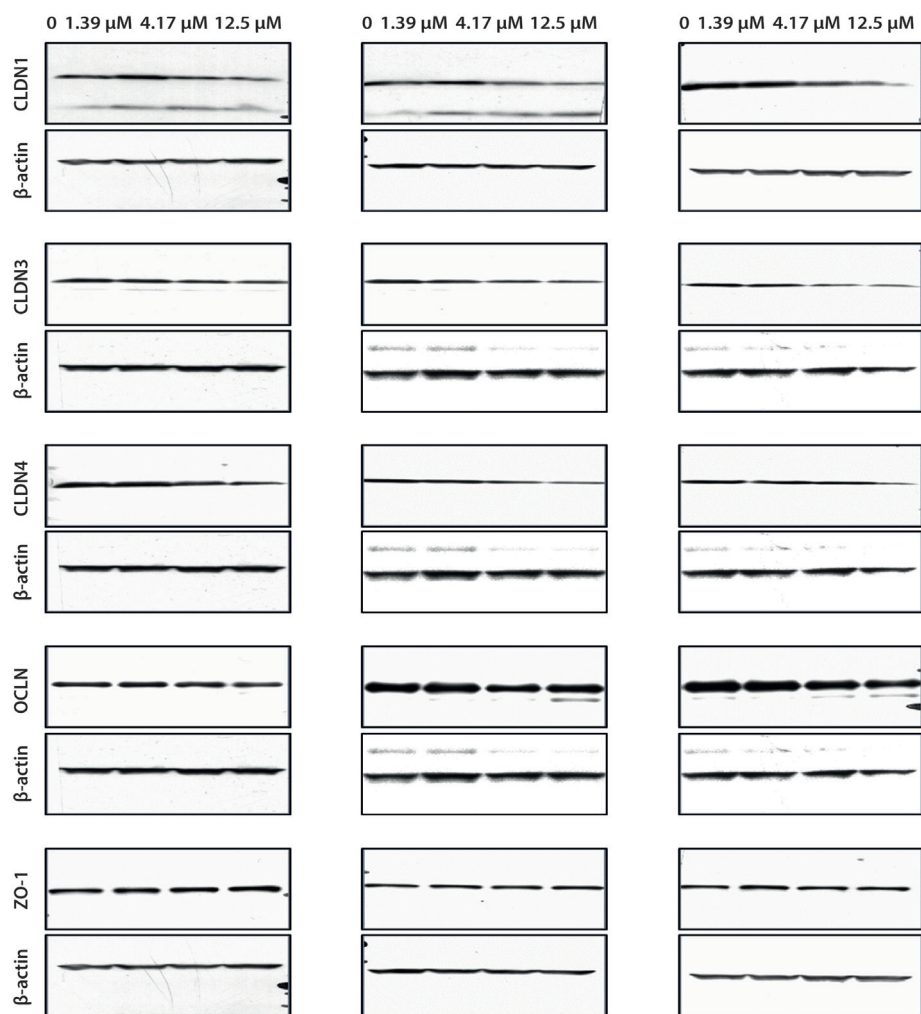


- junctions by removal of specific claudin isoforms. *Am J Physiol Cell Physiol* 2004;287:C1412-C1417.
40. Mutch DM, Anderle P, Fiaux M, Mansourian R, Vidal K, Wahli W, Williamson G, Roberts MA. Regional variations in ABC transporter expression along the mouse intestinal tract. *Physiol Genomics* 2004;17:11-20.
41. Prelusky DB, Hartin KE, Trenholm HL, Miller JD. Pharmacokinetic fate of <sup>14</sup>C-labeled deoxynivalenol in swine. *Fundam Appl Toxicol* 1988;10:276-286.
42. Matsuda M, Kubo A, Furuse M, Tsukita S. A peculiar internalization of claudins, tight junction-specific adhesion molecules, during the intercellular movement of epithelial cells. *J Cell Sci* 2004;117:1247-1257.
43. Zeissig S, Burgel N, Gunzel D, Richter J, Mankertz J, Wahnschaffe U, Kroesen AJ, Zeitz M, Fromm M, Schulzke JD. Changes in expression and distribution of claudin 2, 5 and 8 lead to discontinuous tight junctions and barrier dysfunction in active Crohn's disease. *Gut* 2007;56:61-72.
44. Bruewer M, Utech M, Ivanov AI, Hopkins AM, Parkos CA, Nusrat A. Interferon-gamma induces internalization of epithelial tight junction proteins via a macropinocytosis-like process. *FASEB J* 2005;19:923-933.
45. Ivanov AI, Nusrat A, Parkos CA. The epithelium in inflammatory bowel disease: potential role of endocytosis of junctional proteins in barrier disruption. *Novartis Found Symp* 2004;263:115-124.
46. Prasad S, Mingrino R, Kaukinen K, Hayes KL, Powell RM, MacDonald TT, Collins JE. Inflammatory processes have differential effects on claudins 2, 3 and 4 in colonic epithelial cells. *Lab Invest* 2005;85:1139-1162.
47. Rahner C, Mitic LL, Anderson JM. Heterogeneity in expression and subcellular localization of claudins 2, 3, 4, and 5 in the rat liver, pancreas, and gut. *Gastroenterology* 2001;120:411-422.
48. Tamagawa H, Takahashi I, Furuse M, Yoshitake-Kitano Y, Tsukita S, Ito T, Matsuda H, Kiyono H. Characteristics of claudin expression in follicle-associated epithelium of Peyer's patches: preferential localization of claudin-4 at the apex of the dome region. *Lab Invest* 2003;83:1045-1053.
49. Fujita H, Chiba H, Yokozaki H, Sakai N, Sugimoto K, Wada T, Kojima T, Yamashita T, Sawada N. Differential expression and subcellular localization of claudin-7, -8, -12, -13, and -15 along the mouse intestine. *J Histochem Cytochem* 2006;54:933-944.
50. Will C, Fromm M, Muller D. Claudin tight junction proteins: novel aspects in paracellular transport. *Perit Dial Int* 2008;28:577-584.
51. Fujita K, Katahira J, Horiguchi Y, Sonoda N, Furuse M, Tsukita S. Clostridium perfringens enterotoxin binds to the second extracellular loop of claudin-3, a tight junction integral membrane protein. *FEBS Lett* 2000;476:258-261.
52. Suzuki T. Regulation of intestinal epithelial permeability by tight junctions. *Cell Mol Life Sci* 2013;70:631-659.
53. Kolf-Clauw M, Castellote J, Joly B, Bourges-Abella N, Raymond-Letron I, Pinton P, Oswald IP. Development of a pig jejunal explant culture for studying the gastrointestinal toxicity of the mycotoxin deoxynivalenol: histopathological analysis. *Toxicol In Vitro* 2009;23:1580-1584.
54. Blikslager AT, Moeser AJ, Gookin JL, Jones SL, Odle J. Restoration of barrier function in injured intestinal mucosa. *Physiol Rev* 2007;87:545-564.

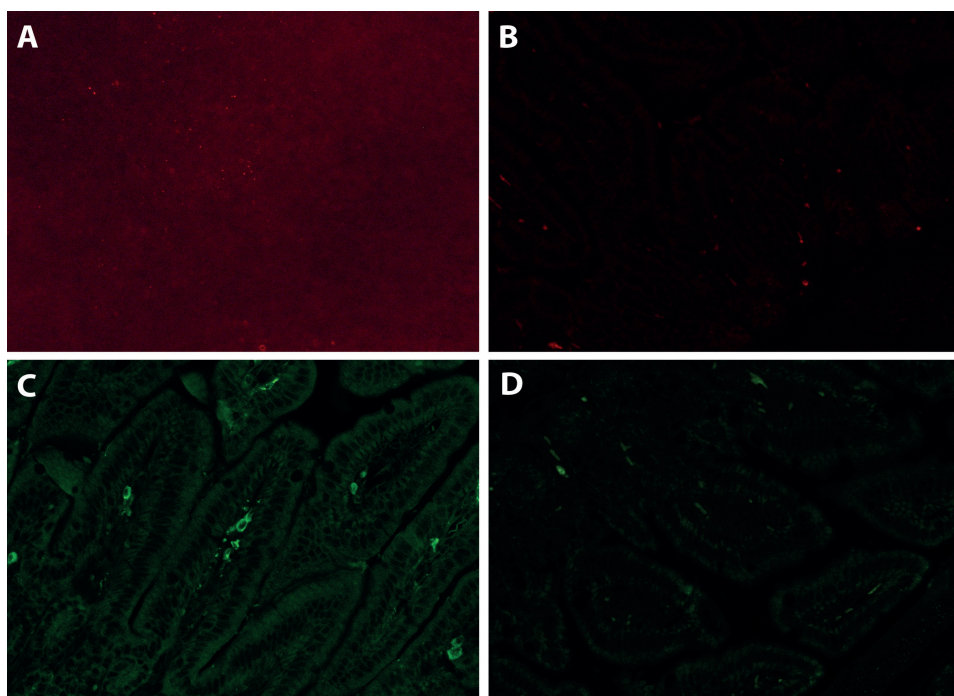
## Supplementary data



**Supplementary Figure 1.** An example of a villi picture measured via the computerized microscope-based image analyser (Cell<sup>^</sup>D). The measurement of the villus height, the crypt depth, the villus area (the total surface of the villi), and the epithelial cell area (villus area – villus area without epithelial cells) is indicated. Magnification 200x.

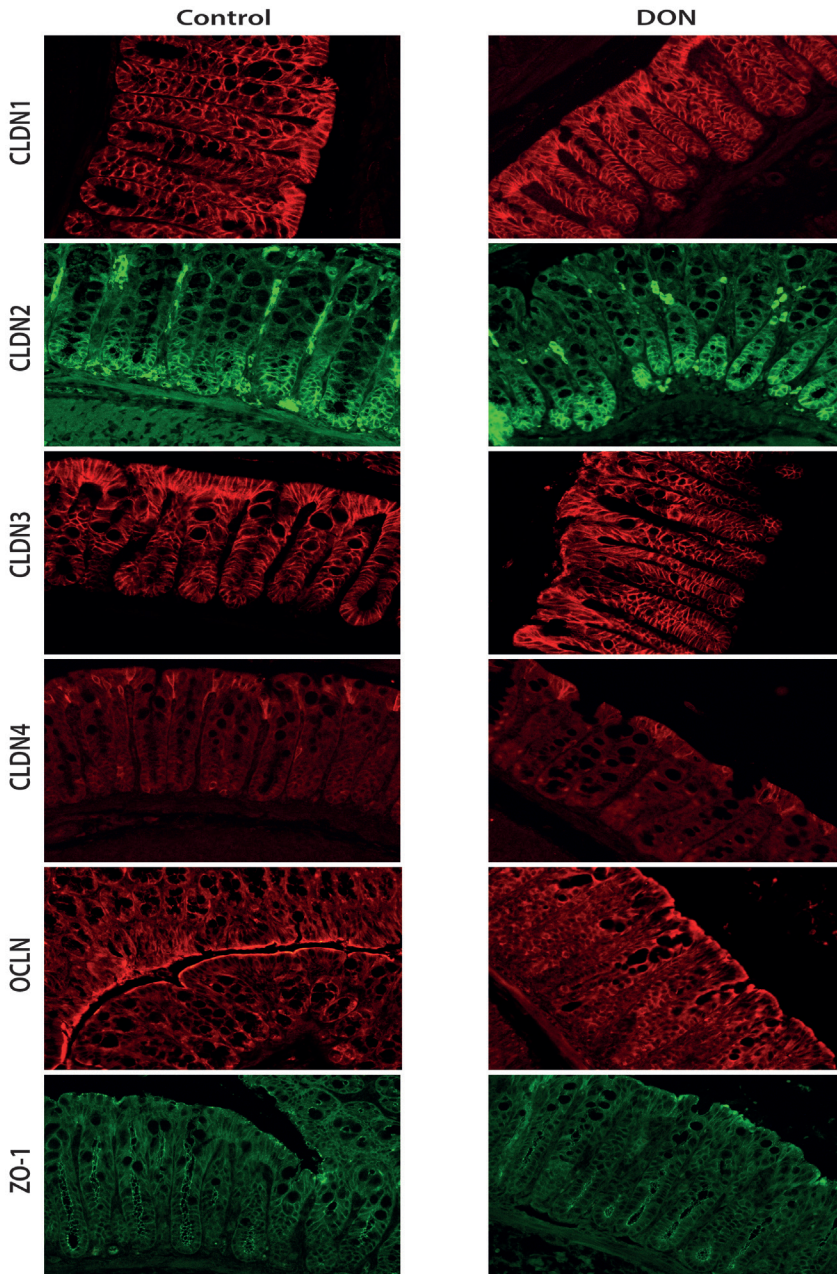


**Supplementary Figure 2.** DON selectively affected the TJ protein levels. Caco-2 cells were grown on inserts and stimulated with increasing concentrations of DON (1.39, 4.17 and 12.5  $\mu$ M) for 24 h. The Caco-2 monolayers were lysed and the protein extract was analyzed by Western blot analysis for CLDN1, CLDN3, CLDN4, OCLN, ZO-1 and related  $\beta$ -actin (blots of three independent experiments are depicted individually).



**Supplementary Figure 3.** For immunofluorescence staining, negative controls lacking the primary antibodies were included. For the immunofluorescence staining of Caco-2 monolayers incubated with DON (4.17  $\mu$ M), the second antibody goat anti-rabbit (A) was included. Magnification 400x. For the immunofluorescence staining of distal small intestine of the control and DON-treated mice, the second antibodies goat anti-rabbit (B), goat anti-mouse (C), goat anti-rat (D) were included. Magnification 200x.





**Supplementary Figure 4.** DON selectively affected the localization of TJ proteins in mouse colon. For immunofluorescence staining, Swiss-rolled paraffin sections obtained from colon were detected by antibodies for CLDN1, CLDN2, CLDN3, CLDN4, OCLN and ZO-1 as described in materials and methods.  $n = 5-6$  mice/experimental group (2-3 sections/animal). Magnification 200x.

**Supplementary Table 1.** Antibodies used for Western blot and immunofluorescence staining

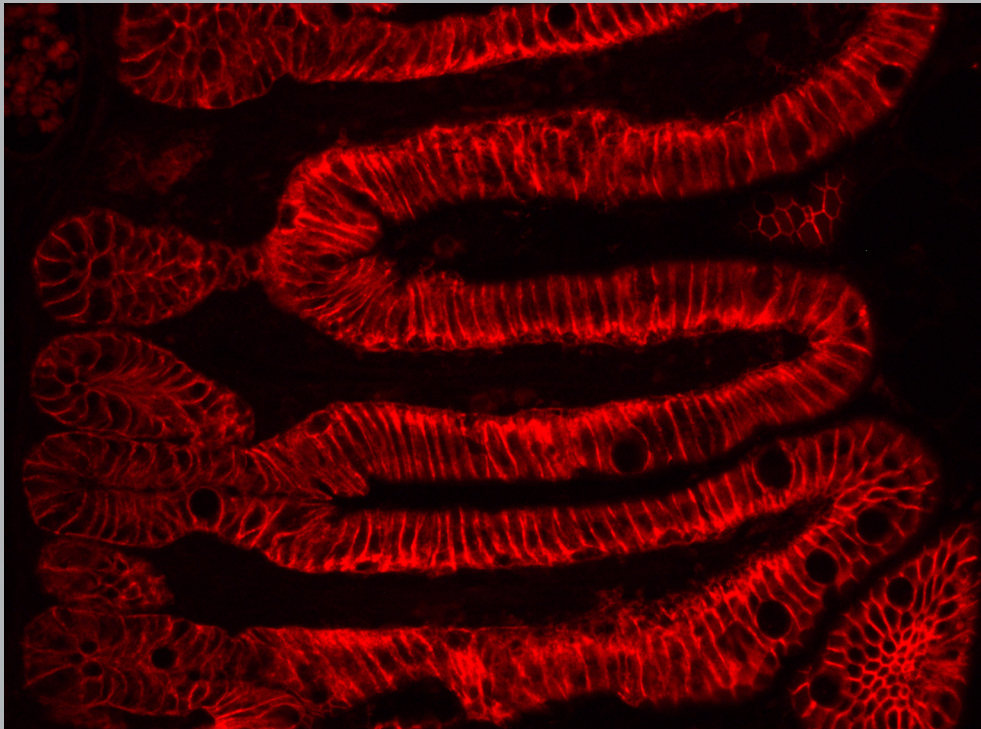
Antibody	Company	Isotype	Clonality	Con. WB	Con. IF
Rabbit anti-claudin1	Invitrogen 51-9000	Rabbit IgG	Polyclonal (JAY.8)	1:1000	1:50 ( <i>in vitro</i> + <i>in vivo</i> )
Mouse anti-claudin2	Invitrogen 32-5600	Mouse IgG2b	Monoclonal (12H12)		1:100 ( <i>in vivo</i> )
Rabbit anti-claudin3	Invitrogen 34-1700	Rabbit IgG	Polyclonal (Z23.JM)	1:500	1:50 ( <i>in vitro</i> + <i>in vivo</i> )
Mouse anti-claudin4	Invitrogen 32-9400	Mouse IgG1	Monoclonal (3E2C1)	1:1000	
Rabbit anti-claudin4	Invitrogen 36-4800	Rabbit IgG	Polyclonal (ZMD.306)		1:50 ( <i>in vitro</i> + <i>in vivo</i> )
Rabbit anti-occludin	Invitrogen 71-1500	Rabbit IgG	Polyclonal (Z-T22)	1:4000	1:50 ( <i>in vitro</i> + <i>in vivo</i> )
Rabbit anti-ZO-1	Invitrogen 40-2200	Rabbit IgG	Polyclonal (ZMD.436)	1:1000	1:50 ( <i>in vitro</i> )
Rat anti-ZO-1	Millipore (MABT11)	Rat IgG2ak	Monoclonal (R40.76)		1:50 ( <i>in vivo</i> )
Rabbit anti- $\beta$ -actin	Cell Signaling #4970	Rabbit IgG	Polyclonal (13E5)	1:4000	
Goat anti-rabbit	Dako E0432	IgG	Polyclonal	1:2000	
Rabbit anti-mouse	Dako P0260	IgG	Polyclonal	1:2000	
Alexa Fluor® goat anti-rabbit IgG	Life technologies A11011/A11008	IgG	Polyclonal		1:200
Alexa Fluor® goat anti-mouse IgG	Life technologies A11017	IgG	Polyclonal		1:200
Alexa Fluor® goat anti-rat IgG	Life technologies A11006	IgG	Polyclonal		1:200

July 2015 • Volume 145 • Number 7

**JN**

## THE JOURNAL OF NUTRITION

A Publication of the American Society for Nutrition • <http://jn.nutrition.org>



### **Galacto-oligosaccharides and intestinal barrier function**

Flavonoids and biomarkers of endothelial function and inflammation

Healthy lifestyle score and metabolic risk factors

Systematic review of palm oil and blood lipids

\* This page is a reproduction of the cover page from the Journal of Nutrition 2015; 145(7).



# Chapter 5



Galacto-oligosaccharides protect the intestinal barrier by maintaining the tight junction network and modulating the inflammatory responses after a challenge with the mycotoxin deoxynivalenol in human Caco-2 cell monolayers and B6C3F<sub>1</sub> mice

Peyman Akbari<sup>1,2</sup>, Saskia Braber<sup>1</sup>, Arash Alizadeh<sup>1,2</sup>, Kim A.T. Verheijden<sup>2</sup>, Margriet H.C. Schoterman<sup>3</sup>, Aletta D. Kraneveld<sup>2</sup>, Johan Garssen<sup>2,4</sup>, Johanna Fink-Gremmels<sup>1</sup>

<sup>1</sup> Division of Veterinary Pharmacology, Pharmacotherapy and Toxicology, Institute for Risk Assessment Sciences, Utrecht University, Utrecht, The Netherlands

<sup>2</sup> Division of Pharmacology, Utrecht Institute for Pharmaceutical Sciences, Faculty of Science, Utrecht University, Utrecht, The Netherlands

<sup>3</sup> FrieslandCampina, Amersfoort, The Netherlands

<sup>4</sup> Nutricia Research, Utrecht, The Netherlands

**This chapter is published in The Journal of Nutrition 2015; 145(7): 1604-1613.**

**A figure from this chapter has been selected as a cover illustration of The Journal of Nutrition as depicted on page 114.**

## Abstract

The integrity of the continuous layer of epithelial cells in the gastrointestinal tract protects organisms from exposure to luminal antigens, which are considered as the primary cause of chronic intestinal inflammation and allergic responses. The common wheat-associated fungal toxin deoxynivalenol (DON) acts as a specific disruptor of the intestinal tight junction network and might contribute to the pathogenesis of inflammatory bowel diseases (IBD). The aim of the current study was to assess whether defined galacto-oligosaccharides (GOS) can prevent the DON-induced epithelial dysfunction. In a parallel *in vitro/in vivo* approach, human epithelial intestinal Caco-2 cells, pretreated with different concentrations of GOS (0.5%, 1% and 2%) for 24 h, were stimulated with 4.2  $\mu$ M DON (24 h), while 6/7-week-old male B6C3F<sub>1</sub> mice were fed a diet supplemented with 1% GOS for 2 weeks before being orally exposed to DON (25 mg/kg bw, 6 h). Barrier integrity was determined by measuring transepithelial electrical resistance (TEER) and intestinal permeability to marker molecules lucifer yellow (LY) and fluorescein isothiocyanate-dextran (FITC-dextran). The calcium switch assay was conducted to study the reassembly of epithelial tight junction proteins. Alterations in tight junction and cytokine expression were assessed by qRT-PCR, Western blot analysis or ELISA, while their localization was visualized by immunofluorescence microscopy. Furthermore, sections of the proximal and distal small intestine were stained with hematoxylin/eosin for histomorphometric analysis. The *in vitro* data with Caco-2 cells grown in transwell inserts showed that medium supplemented with 2% GOS improved tight junction reassembly reaching an acceleration of 85% after 6 h ( $P < 0.05$ ). In turn, GOS pretreatment prevented the DON-induced loss of epithelial barrier function as measured by TEER (114% of control) and the DON-affected paracellular flux of the marker lucifer yellow was reduced (82.7% of pre-challenge values,  $P < 0.05$ ). Moreover, GOS pretreatment stabilized the expression and cellular distribution of claudin3 and suppressed by > 50% the DON-induced synthesis and release of interleukin-8 (IL-8/CXCL8), a typical marker for an inflammatory response ( $P < 0.05$ ). These findings were confirmed by *in vivo* experiments in mice where pretreatment with GOS prevented the DON-induced mRNA overexpression of claudin3 ( $P = 0.022$ ) and CXCL8 homologue CXCL1 ( $P = 0.06$ ) as well as the DON-induced morphological defects. The presented results demonstrate that GOS stimulate the tight junction reassembly and in turn mitigate the deleterious effects of DON on the intestinal barrier of Caco-2 cells and on villus architecture of B6C3F<sub>1</sub> mice.

## Introduction

The major function of the intestinal barrier is to protect the organism against invading bacterial and viral pathogens and food-borne toxins (1, 2). Defects in intestinal barrier function result in a paracellular influx of luminal antigens, which is considered as a pivotal pathogenic factor in the onset and promotion of intestinal inflammation and inflammatory bowel diseases (IBD) as well as allergies (3).

A dietary component that is known to affect the intestinal barrier function is the mycotoxin deoxynivalenol (DON) (4-8). DON is one of the most frequently occurring natural toxins in wheat and wheat-based products and can readily enter the food and feed chain, since DON is resistant to processing and heating (9). Consumption of foodstuffs contaminated by DON have been associated with human and animal intoxications and the pro-inflammatory and immunotoxic effects of DON are of increasing concern for farm animals, such as pigs, as well as for humans (10-14). Human exposure to DON can cover all age groups, even the developing fetus, as it also transfers across the placental barrier (15, 16). Therefore it is an important human safety issue and these epidemiological findings warrant the search for dietary supplements that can be used in infants as well as in adults for the mitigation of the adverse effects of DON on intestinal integrity.

Recently, the gut health promoting effects of non-digestible oligosaccharides are broadly acknowledged (17). In particular selected fractions of milk-derived galacto-oligosaccharides (GOS) are of interest due to their potential immunomodulatory and anti-inflammatory effects. GOS, which resemble oligosaccharides that occur naturally in human breast milk, are currently used in infant formulas (18). They are expected not only to modulate the composition and metabolism of the gut microbiota by increasing *Bifidobacterium* and *Lactobacillus* spp. numbers (19-21), but seem to prevent specific pathologies involving the gut immune system, such as food allergies and inflammatory bowel disease, as demonstrated in clinical trials already (19, 22, 23). However, the exact mechanisms involved in such immunomodulatory effects, remain to be elucidated.

The aim of the current experiments was to characterize the effects of GOS on the epithelial barrier using a standardized Caco-2 cell model and to investigate whether a potential barrier-stabilizing effect results also in an improved integrity of the intestinal barrier function and reduced inflammatory response during a DON challenge.

## Materials and Methods

### Galacto-oligosaccharides (GOS)

GOS are generally defined as a mixture of those substances produced from lactose by the enzyme  $\beta$ -galactosidase, comprising between 2 and 8 saccharide units (degree of polymerization, DP), with one of these units being a terminal glucose and the remaining saccharide units being galactose and disaccharides composing 2 units of galactose (24, 25). For the current experiments, the commercial product Vivinal® GOS syrup (FrieslandCampina Domo, Borculo, The Netherlands), containing approximately 45% galacto-oligosaccharides with a DP of 2-8, 16% free lactose, 14% glucose and 25% water, was used. Dilutions (0.5%, 1% and 2% GOS) were made in complete cell culture medium. Prior to the functional assays described below, the potential cytotoxicity of GOS at different concentrations for Caco-2 cells had been measured by the Alamar Blue assay (Invitrogen, Camarillo, CA, USA), a standard method to assess cell viability. These control experiments confirmed that GOS did not induce any cytotoxicity in Caco-2 cells at the selected test concentrations. In addition, close to equimolar concentrations of lactose (16%) and glucose (14%) present in the 2% GOS solution were included in the Caco-2 cell assays and had no effect on the DON-induced transepithelial electrical resistance (TEER) decrease and increase in paracellular flux of lucifer yellow (Supplementary Figure 1).

### Deoxynivalenol (DON)

Purified DON (D0156; Sigma, St Louis, MO, USA) was diluted in absolute ethanol (99.9%, JT Baker, Deventer, The Netherlands) to prepare a 25 mM stock solution and was stored at -20°C. For the cell culture experiments DON was diluted to a concentration of 4.2  $\mu$ M DON in complete cell culture medium and added for the challenge experiments to the apical side as well as to the basolateral side of the transwell plates for 24 h. This DON concentration was selected on the basis of our previous results and did not impair cell viability (8). Physico-chemical interactions between DON and GOS were excluded by co-incubation experiments with both compounds, since the free DON fraction remained unchanged as measured by standard HPLC analysis with affinity column clean up, based on the method described by Dombrink-Kurtzman *et al.* (26) (Supplementary Figure 2).

## *In vitro* experiments

### The Caco-2 cell model

Human epithelial colorectal adenocarcinoma (Caco-2) cells obtained from the American Type Tissue Collection (Code HTB-37) (Manassas, VA, USA, passages 102-114) were used according to established methods, also described by Akbari *et al.* (8). In brief, cells were cultured in Dulbecco's modified Eagle's minimum essential medium (DMEM) and seeded at a density of  $0.3 \times 10^5$  cells into 0.3 cm<sup>2</sup> high pore density (0.4  $\mu$ m) inserts with a polyethylene terephthalate membrane (BD Biosciences, San Diego, CA, USA) placed in a

24-well plate. The Caco-2 cells were maintained in a humidified atmosphere of 95% air and 5% CO<sub>2</sub> at 37°C. After 17-19 days of culturing, a confluent monolayer was obtained with a mean TEER exceeding 400 Ω.cm<sup>2</sup> measured by a Millicell-Electrical Resistance System Voltammeter (Millipore, Temecular, CA, USA). The Caco-2 cells were pre-incubated with different concentrations of GOS (0.5%, 1% and 2%) for 24 h before being exposed to DON in the presence of GOS for another 24 h. GOS and DON were added to both compartments (apical and basolateral) of the transwell insert unless otherwise stated.

Additional experiments with Caco-2 cells were conducted in which 1) GOS were only added to the apical compartment, 2) GOS (apical and basolateral) were removed after 24 h pretreatment and before the cells were challenged with DON in GOS-free DMEM medium and 3) GOS (apical and basolateral) were co-incubated with DON for 24 h (without pre-incubation with GOS). TEER measurements were conducted 24 h after DON incubation and thereafter the paracellular flux was measured using two different membrane-impermeable marker molecules, lucifer yellow (LY, 0.457 kDa) and fluorescein isothiocyanate-dextran (FITC-dextran, 4 kDa) (Sigma, St Luis, Mo, USA) added at a concentration of 16 µg/ml to the apical side (350 µl) in the transwell plate for 4 h (8). Medium without fluorescent marker molecules was used as a blank and the concentration of LY and FITC-dextran at the basolateral side was calculated on the basis of a standard curve in the concentration range of 0.19-12.5 µg marker molecule/ml.

### Calcium switch assay

Caco-2 cells grown on inserts were pretreated with different concentrations of GOS (0.5%, 1% and 2%) either on the apical side or on both sides of the transwell inserts for 24 h, as described above. Subsequently, Caco-2 cells were deprived from calcium by washing the cells twice with pre-warmed PBS and exposing the cells transiently for 20 minutes to 2 mM ethylene glycol-bis(2-aminoethyl ether)N,N,N',N'-tetraacetic acid (EGTA) (Sigma, St Luis, Mo, USA) in calcium- and magnesium-free Hanks' Balanced Salt Solution (HBSS) (Gibco, Invitrogen, Carlsbad, CA, USA). At the end of the incubation period, HBSS-EGTA was removed, the cells rinsed and allowed to recover in either complete cell culture DMEM (containing 2 mM CaCl<sub>2</sub>) or in DMEM supplemented with the addition of different concentrations GOS (0.5%, 1% and 2%). TEER was monitored at various time points (2, 4, 6, 8, 12, 24 h) during this recovery period as an index of tight junctions (TJs) reassembly and restoration of barrier function. The results are expressed as a percentage of initial value (27).

### TJ proteins: mRNA expression, Western blot analysis and cellular distribution

The levels of mRNA expression of the TJ target genes in Caco-2 cells pretreated with different concentrations GOS for 24 h before exposure to DON (in presence of GOS) for 6 h were measured by qRT-PCR. Cells were harvested and total RNA extraction, cDNA preparation and qRT-PCR analysis were performed as described previously (8). Forward and reverse primers for claudin1 (CLDN1), claudin3 (CLDN3), claudin4 (CLDN4), occludin

(OCLN), zonula occludens protein-1 (ZO-1) and zonula occludens protein-2 (ZO-2) (Table 1) were designed by using the National Center for Biotechnology Information Primer-Basic Local Alignment Search Tool and were manufactured commercially (Eurogentec, Seraing, Belgium). Specificity and efficiency of selected primers were confirmed by qRT-PCR analysis and dilution series of pooled cDNA at a temperature gradient (55°C to 65°C) for primer-annealing and subsequent melting curve analysis. Glyceraldehydes 3-phosphate dehydrogenase (GAPDH) and  $\beta$ -actin (ACTB) were used as reference genes and the GeNorm software (version 3.5) was used to identify the most stable reference genes.

For Western blots, GOS pretreated Caco-2 cells were exposed to DON for 24 h (in the presence of GOS) and total protein extracts were prepared as described previously (8). Equal protein amounts were separated by SDS-PAGE, blotted onto polyvinylidene difluoride membranes. Rabbit anti-CLDN3 (1:500, Invitrogen, Camarillo, CA, USA) or rabbit anti- $\beta$ -actin (1:4000, Cell Signaling, Beverly, MA, USA) served as primary antibodies for overnight incubations at 4°C and horseradish peroxidase-conjugated goat anti-rabbit (1:2000, Dako, Glostrup, Denmark) served as the secondary antibody applied for 2 h at room temperature. Blots were washed in PBS-tween, incubated in commercial enhanced chemiluminescence reagents (Amersham Biosciences, Roosendaal, The Netherlands) and exposed to photographic film and scanned on a GS710 calibrated imagine densitometer for quantification. The cellular localization of CLDN3 was assessed by immunofluorescence microscopy after staining with rabbit anti-CLDN3 (1:50, 34-1700, Invitrogen, Camarillo, CA, USA) (8), followed by incubation with Alexa-Fluor conjugated secondary antibody (Invitrogen, Carlsbad, CA, USA). Immunolocalization of CLDN3 was visualized, and images were taken with use of the confocal laser-scanning microscope Leica True Confocal Point Scanner with Spectral Detection-II (Leica Microsystems GmbH) with Leica Application Suite Advanced Fluorescence software.

### **Interleukin-8 (CXCL8): mRNA expression and secretion**

In parallel to the experimental steps as described for the TJ proteins above, the CXCL8 mRNA expression was analyzed by qRT-PCR (Primer sequences, Table 1) and release of CXCL8 from Caco-2 cells into the medium of the apical side as well as the basolateral side of the transwell insert was measured by ELISA using the Human IL-8 ELISA Set (BD Biosciences, San Diego, CA, USA) according to manufacturer's instructions.

**Table 1.** Human primer sequences used for qRT-PCR analysis

Genes	Primer sequence (5'-3')		AT	References
	Forward	Reverse		
<b>CLDN1</b>	AGCTGGCTGAGACACTGAAGA	GAGAGGAAGGCACTGAACCA	63	NM_021101
<b>CLDN3</b>	CTGCTCTGCTGCTCGTGTC	CGTAGTCCTTGCGGTCGTAG	63	NM_001306
<b>CLDN4</b>	GTCTGCCTGCATCTCCTCTGT	CCTCTAAACCCGTCCATCCA	62.5	NM_001305
<b>OCLN</b>	TTGGATAAAGAATTGGATGACT	ACTGCTTGCAATGATTCTTCT	57	NM_002538
<b>ZO-1</b>	GAATGATGGTTGGTATGGTGCG	TCAGAAGTGTGTCTACTGTCCG	55.8	NT_010194.17
<b>ZO-2</b>	GCCAAAACCCAGAACAAAGA	ACTGCTCTCTCCACCTCCT	65	NT_008470.19
<b>CXCL8</b>	ATGACTTCCAAGGTGGCCGTGGCT	TCTCAGCCCTTTCAAAAATTCTC	63	NM_000584
<b>GAPDH</b>	ACCCACTCTCCACCTTTGAC	CCACCACCTGTTGCTGTAG	62.4	NM_002046
<b>ACTB</b>	CTGGAACGGTGAAGGTGACA	AAGGGACTTCTGTAAACATGCA	63	NM_001101

AT, annealing temperature (°C)

### ***In vivo* experiments**

#### **Animals**

Male B6C3F<sub>1</sub> mice (n = 5/6 per group, 5/6 animals per cage), 6-7 weeks old with an average weight of 19.9 ± 0.32 gram (Charles River Laboratories, Maastricht, The Netherlands) were housed under controlled conditions in standard laboratory cages with sterilized woody-clean sawdust bedding (Technilab–BMI, Someren, The Netherlands) and were acclimated to the environment for two weeks. The room was maintained on a 12 h light-dark cycle at ~20.5°C with a relative humidity of ~61.5%. They were ad libitum provided with water and commercial rodent diet (AIN-93G) (28). Animals were randomly distributed into different experimental groups. All *in vivo* experimental protocols were approved by the local Ethics Committee for Animal Experiments (Reference number: DEC 2012.III.02.012) and were performed in compliance with national and international guidelines on animal experimentation.

#### **Diets and DON gavage**

The experimental AIN-93G-based diets were composed and mixed with 1% GOS (1 kg diet containing 22.22 g/kg Vivinal® GOS syrup) by Research Diet Services (Wijk bij Duurstede, The Netherlands). Carbohydrates in Vivinal GOS were compensated isocalorically in the control diet by means of cellulose (for GOS), lactose (for lactose), and dextrose (for glucose). The diet was checked for DON contamination by standard HPLC analyses with affinity column clean-up, based on the method as described by Dombrink-Kurtzman *et al.*



(26). None of experimental diets exceeded the detection limit of 10 µg DON per kg feed. The mice were fed the AIN-93G diet with or without 1% GOS for 2 weeks before being challenged with DON, given by oral gavage at a dose of 25 mg/kg body weight (bw) in 200 µl sterile PBS (29-31). Control mice received 200 µl sterile PBS. Six hours after the DON challenge, mice were sacrificed by cervical dislocation, blood was obtained by heart puncture and collected in MiniCollect Z Serum Sep tubes (Greiner Bio-one, Kremsmunster, Austria) and different parts of the intestine were collected and preserved for mRNA isolation and histology. Weight gain was monitored throughout the experiment and no significant differences were recorded between control- and GOS-fed animals, except at day 12, where a slight, but significant increase in weight gain was observed in the GOS-fed animals (Supplementary Figure 3). This slight increase in weight gain could possibly be related to the food intake, however this was not determined in this study.

#### **Intestinal specimen from mice used for isolation of mRNA and qRT-PCR analysis**

For mRNA isolation, the mouse intestine was flushed with cold PBS and separated into different segments. These segments were defined as follows: proximal small intestine (approximately 2 cm after the pylorus), middle small intestine (7-8 cm after the pylorus), distal small intestine (final 1 cm before the ileocecal-junction), caecum and colon (first 1 cm after caecum). These intestinal wall samples (approximately 1 cm) were snap frozen in liquid nitrogen and stored at -80°C until RNA isolation. Total RNA extraction, cDNA preparation and qRT-PCR analysis were performed as described previously (8). Primer sequences with corresponding annealing temperatures are listed in Table 2.

#### **Immunofluorescence staining of intestinal specimen of mice**

Swiss rolls (32) of the distal small intestine were fixed in 10% formalin and embedded in paraffin. For antigen retrieval, the 5 µm sections were boiled in 10 mM citrate buffer (pH 6.0) for 10 min in a microwave. Rabbit anti-CLDN3 (1:50, 34-1700, Invitrogen, Camarillo, CA, USA) was used as first antibody and after incubation, immunofluorescence staining was conducted as described above in Materials and Methods of the *in vitro* experiments.

#### **Histomorphometric analysis of intestinal specimen of mice**

Sections of the proximal and distal small intestine were stained with hematoxylin/eosin (H&E) according to standard procedures. Photomicrographs were taken with an Olympus BX50 microscope equipped with a Leica DFC 320 digital camera (magnification of 200x). The morphometric analysis of the sections was performed on 10 randomly selected, well-oriented villi and crypts per animal. A computerized microscope-based image analyzer (Cell<sup>^</sup>D, Olympus, Europa GmbH, Germany) was used to determine histomorphometric parameters: villus height (measured from the tip of the villus to the villus-crypt junction) and crypt depth (measured from the crypt-villus junction to the base of the crypt). These regions were manually defined for each villi (8).

**Table 2.** Murine primer sequences used for qRT-PCR analysis

Genes	Primer sequence (5'-3')		AT	References
	Forwad	Reverse		
<b>CLDN1</b>	TCTACGAGGGACTGTGGATG	TCAGATTCAGCTAGGAGTCG	57	NM_016674
<b>CLDN2</b>	GGCTGTTAGGCTCATCCAT	TGGCACCAACATAGGAATC	55	NM_016675
<b>CLDN3</b>	AAGCCGAATGGACAAAGAA	CTGGCAAGTAGCTGCAGTG	58.7	NM_009902
<b>CLDN4</b>	CGCTACTCTTGCCATTACG	ACTCAGCACACCATGACTTG	55	NM_009903
<b>OCLN</b>	ATGTCCGGCCGATGCTCTC	TTTGGCTGCTCTGGGTCTGTAT	61.2	NM_008756.2
<b>ZO-1</b>	CGAGGCATCATCCCAATAAGAAC	TCCAGAAGTCTGCCCGATCAC	58.7	NM_009386
<b>CXCL1</b>	GCGCCTATCGCCAATGAG	AGGGCAACACCTTCAAGCTCT	64.3	U20527
<b>CXCL2</b>	GGCTGTTGTGGCCAGTGAA	CTCAAGCTCTGGATGTTCTTGAAG	61.2	NM_009140.2
<b>IFN-<math>\gamma</math></b>	TCAAGTGGCATAGATGTGGAAGAA	TGGCTCTGCAGGATTTTCATG	61.4	NM_008337.3
<b>IL-1<math>\alpha</math></b>	ATGAAGCTCGTCAGGCAGAAG	GAGATAGTGTGTCACATCCTGAT	58.7	NM_010554.4
<b>IL-1<math>\beta</math></b>	ATCCCAAGCAATACCCAAGAA	GCTGATGTACCAAGTTGGGGAA	61	NM_008361.3
<b>IL-4</b>	GGTCTCAACCCCAGCTAGT	GCCGATGATCTCTCTCAAGTGAT	61.2	NM_021283.2
<b>IL-6</b>	TGGGACTGATGCTGGTGACA	TGGGAGTGGTATCCTCTGTGAA	63.1	NM_031168.1
<b>TNF-<math>\alpha</math></b>	AACGGCATGGATCTCAAAGA	TTTCTCCTGGTATGAGATAGCAAATC	64.3	NM_013693.3
<b>GAPDH</b>	GAACATCATCCCTGCATCC	CACATTGGGGGTAGGAACAC	61	NM_008084.2
<b>ACTB</b>	ATGCTCCCCGGGCTGTAT	CATAGGAGTCCTCTGACCCATTC	61	NM_007393.3

AT, annealing temperature (°C)

### Statistical analysis

Experimental results of *in vitro* experiments were expressed as mean  $\pm$  SEM of 3 independent experiments ( $n = 3$ ), each performed in triplicate (3 wells/condition). Differences between groups of *in vitro* experiments were statistically determined by using One-way ANOVA, with Bonferroni post hoc test. Additionally, Two-way ANOVA was used to compare the effects of 2% GOS treatment with or without DON exposure. Data of *in vivo* experiments were expressed as mean  $\pm$  SEM,  $n = 5$ -6 animals/experimental group (with the exception of Supplementary Figure 3, weight gain,  $n = 11$ -12 animals/experimental group) and were statistically analyzed by using a Two-way ANOVA followed by a Bonferroni post hoc test. Results were considered statistically significant when  $P < 0.05$ . Analyses were performed by using GraphPad Prism (version 6.0) (GraphPad, La Jolla, CA, USA). The required sample size to achieve the given power was calculated using the program PS-Power and Sample Size Calculation based on previous research.

## Results

### **GOS prevent the DON-induced impairment of the Caco-2 cell monolayer integrity**

As shown in Figure 1A, GOS modulated the DON-induced decrease in TEER in a concentration-dependent manner, and pretreatment with 2% GOS entirely prevented the loss of integrity ( $P < 0.001$ ). In line with these results, the DON-induced increase in tracer transport (LY and FITC-dextran) was decreased by GOS ( $P < 0.001$  and  $P < 0.01$ , respectively) (Figure 1B, C). As in all these experiments GOS were applied to the apical as well as basolateral sides, additional experiments were conducted in which GOS were given only to the apical side, or removed during the DON challenge, as indicated in Table 3. Under these conditions, 2% GOS induced a protective effect on the DON-induced impaired monolayer integrity, albeit less pronounced than in experiments where GOS were present at both sides and during the entire exposure period (Table 1). Neither 0.5% GOS, nor 1% GOS were effective ( $P > 0.99$  and  $P > 0.05$  for TEER and tracer transport, respectively) (Table 3). Co-incubation of GOS and DON (without pre-incubation with GOS) for 24 h did not counteract the DON-induced intestinal barrier disruption as observed in TEER values ( $P > 0.99$ ) and tracer transport ( $P > 0.99$ ) (Supplementary Figure 4).

### **GOS accelerate TJs reassembly after calcium deprivation in Caco-2 cells**

It was demonstrated that GOS caused a remarkable acceleration in TJs reassembly over a period of 24 h (2% GOS, 12 h,  $P < 0.001$ ) (Figure 2). This effect remained when GOS were removed during the recovery period (2% GOS, 12 h,  $P < 0.001$ ) and a significant acceleration in TJs reassembly was also observed when GOS were applied only at the apical side, albeit to a lesser degree (2% GOS, 12 h,  $P = 0.008$ ) (Supplementary Figure 5).

### **GOS prevent the DON-induced disturbance of CLDN3 expression and its cellular distribution in Caco-2 cell monolayers**

After a DON challenge of an established Caco-2 cell monolayer, mRNA expression levels of the TJ proteins CLDN3, CLDN4, OCLN, ZO-1 and ZO-2 were up-regulated compared to the untreated cells (Supplementary Figure 6A, B). Pretreatment with GOS resulted in a less pronounced induction of CLDN3 and this effect was statistically significant ( $P = 0.022$ ) (Figure 3A). GOS did not affect the DON-induced mRNA expression of CLDN4 ( $P = 0.38$ ), OCLN ( $P > 0.99$ ), ZO-1 ( $P > 0.99$ ) and ZO-2 ( $P > 0.99$ ) (Supplementary Figure 6A, B). Subsequent Western blot analyses showed that DON induced a significant decrease in CLDN3 protein levels ( $P = 0.006$ ) and this decrease was prevented by 2% GOS ( $P = 0.031$ ) (Figure 3B, C). Representative pictures of the CLDN3 cellular distribution of the Caco-2 monolayer are depicted in Figure 3D-F. DON exposure was associated with a disturbed and irregular cellular distribution of CLDN3 and a translocation of CLDN3 from the cellular membrane to the submembraneous space (Figure 3E) as compared to the control Caco-2 cells (Figure 3D). Control Caco-2 cells pretreated with GOS did not affect the CLDN3 cellular distribution (data not shown), while the DON-induced deranged distribution of

CLDN3 seemed to be prevented by GOS (Figure 3F).

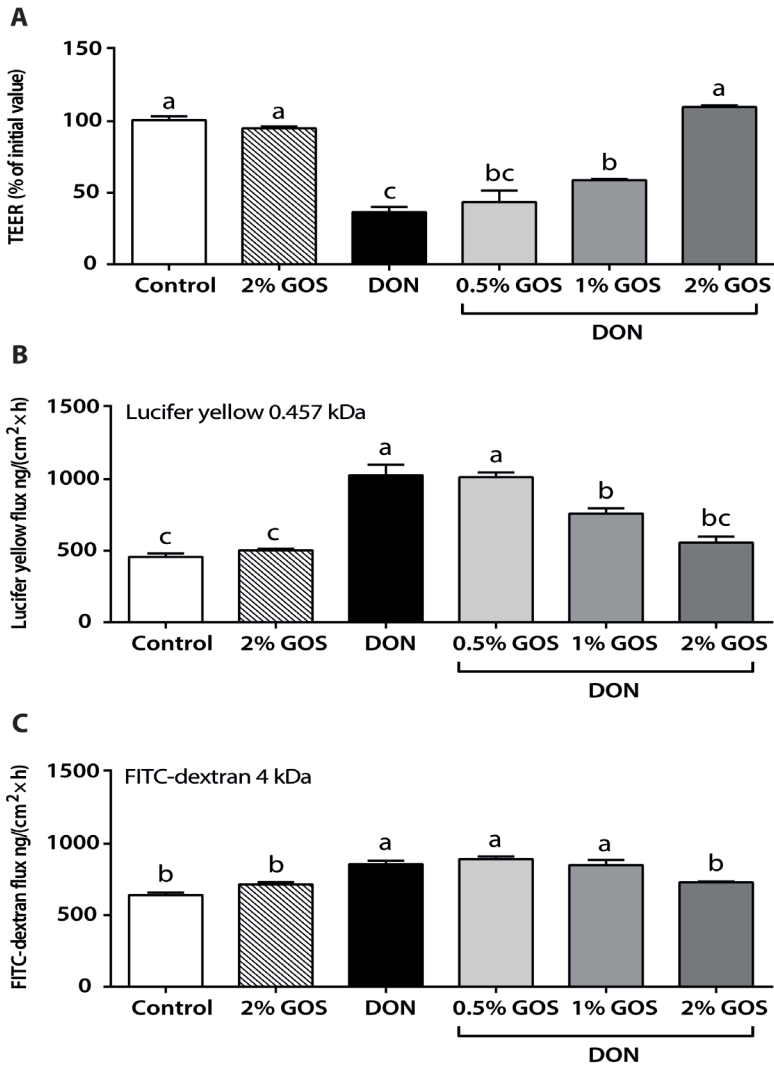


**Figure 1.** GOS prevent the DON-induced impairment of the Caco-2 cell monolayer integrity. Caco-2 cells were pretreated apically and basolaterally with GOS or DMEM medium prior to the addition of DON (apical and basolateral compartments). TEER (A) and the transport of lucifer yellow (B) as well as 4 kDa FITC-dextran (C) from the apical to the basolateral chamber were measured. Results are expressed as a percentage of initial value (TEER) or in the amount of tracer transported [ng/(cm<sup>2</sup>×h)] as mean ± SEM, n = 3. Labeled bars without a common letter differ, P < 0.05, Bonferroni post hoc test.

**Table 3.** Apical and/or basolateral GOS exposure differently protect from the DON-induced impairment of the Caco-2 cell monolayer integrity<sup>1</sup>

Group	Route of GOS application					
	Apical and basolateral <sup>2</sup>		Apical <sup>2</sup>		Apical and basolateral <sup>3</sup>	
	TEER	LY flux	TEER	LY flux	TEER	LY flux
<b>Control</b>	101 ± 2.7 <sup>a</sup>	458 ± 24 <sup>c</sup>	103 ± 4.1 <sup>a</sup>	261 ± 3.8 <sup>c</sup>	94.5 ± 1.2 <sup>a</sup>	305 ± 3.3 <sup>c</sup>
<b>2% GOS</b>	94.9 ± 1.5 <sup>a</sup>	503 ± 12 <sup>c</sup>	101 ± 3.3 <sup>a</sup>	271 ± 13 <sup>c</sup>	98.7 ± 1.7 <sup>a</sup>	292 ± 32 <sup>c</sup>
<b>DON</b>	36.4 ± 3.6 <sup>c</sup>	1027 ± 74 <sup>a</sup>	36.0 ± 1.0 <sup>c</sup>	761 ± 49 <sup>a</sup>	22.4 ± 1.8 <sup>c</sup>	1060 ± 65 <sup>a</sup>
<b>DON + 0.5% GOS</b>	43.4 ± 8.1 <sup>bc</sup>	1014 ± 34 <sup>a</sup>	40.9 ± 1.3 <sup>c</sup>	618 ± 22 <sup>ab</sup>	23.1 ± 0.8 <sup>c</sup>	1037 ± 86 <sup>a</sup>
<b>DON + 1% GOS</b>	58.6 ± 1.0 <sup>b</sup>	766 ± 38 <sup>b</sup>	45.7 ± 1.5 <sup>bc</sup>	624 ± 29 <sup>ab</sup>	24.6 ± 0.7 <sup>c</sup>	877 ± 35 <sup>ab</sup>
<b>DON + 2% GOS</b>	110 ± 1.2 <sup>a</sup>	556 ± 42 <sup>bc</sup>	55.4 ± 1.0 <sup>b</sup>	505 ± 49 <sup>b</sup>	32.6 ± 1.6 <sup>b</sup>	682 ± 28 <sup>b</sup>
<b>P value</b>	P < 0.001	P < 0.001	P < 0.001	P < 0.001	P < 0.001	P < 0.001

<sup>1</sup> Caco-2 cells were pretreated apically and basolaterally with GOS (24 h) and then with deoxynivalenol (apical and basolateral compartments) plus GOS (both apical and basolateral or only apical compartment) for another 24 h, or co-incubated apically and basolaterally with deoxynivalenol and GOS for 24 h. TEER and LY flux are measured and results are expressed as a percentage of initial value (TEER) or amount of LY transported [ng/(cm<sup>2</sup>×h)] as mean ± SEM, n = 3. Means in a column without a common letter differ, P < 0.05, Bonferroni post hoc test.

<sup>2</sup> Duration of GOS application: 24 h pre-incubation GOS, 24 h co-incubation GOS + deoxynivalenol.

<sup>3</sup> Duration of GOS application: 24 h pre-incubation GOS, 24 h incubation deoxynivalenol.

### ***In vivo* application of GOS prevent the DON-induced overexpression of CLDN3 mRNA and maintain its normal cellular distribution in mouse intestines**

The mRNA expression levels of CLDN2, CLDN3 and CLDN4 were increased in a different pattern along the intestine following a DON challenge. The most pronounced effect was observed in the distal part of the small intestine (Supplementary Figure 7). ZO-1, OCLN and CLDN1 remained unaffected in the different segments of the intestines of DON-exposed mice (P > 0.99) (Supplementary Figure 7). Interestingly, the DON-induced increase in CLDN3 mRNA expression (P = 0.004) was significantly suppressed in the distal small intestine of mice fed with 1% GOS diet compared to a normal diet (P = 0.024) (Figure 4A). Additionally, a significant decrease in the DON-induced CLDN2 mRNA expression was observed in the distal small intestine of mice fed a 1% GOS diet (P = 0.018). Dietary GOS did not affect the DON-induced mRNA expression of investigated TJ proteins in other segments than the distal small intestine (P > 0.99) (Supplementary Figure 7). To give an impression of the expression pattern of CLDN3 in the mouse distal small intestine,

representative pictures of an immunofluorescence staining are shown in Figure 4B-D. In the distal small intestine of control mice CLDN3 was located laterally between adjacent cells over the entire villus, with neither a specific signal at the apical surface nor on the basal membrane (Figure 4B) and this CLDN3 distribution pattern was also observed in the distal small intestine of control mice fed a GOS diet (data not shown). DON exposure seemed to alter this typical CLDN3 distribution pattern towards an accumulation in the basal cytoplasm (Figure 4C). It seemed that the distribution of CLDN3 in the distal small intestine of GOS-pretreated mice after DON exposure remained comparable to that of control animals (Figure 4D). Despite these effects of GOS against the DON-induced overexpression of CLDN3 mRNA and CLDN3 distribution, the DON-induced hyperpermeability of the intestines for FITC-dextran (4 kDa) ( $P = 0.08$ ) was not mitigated in mice fed with 1% GOS diet compared to normal diet ( $P > 0.99$ ) (Supplementary Figure 8).

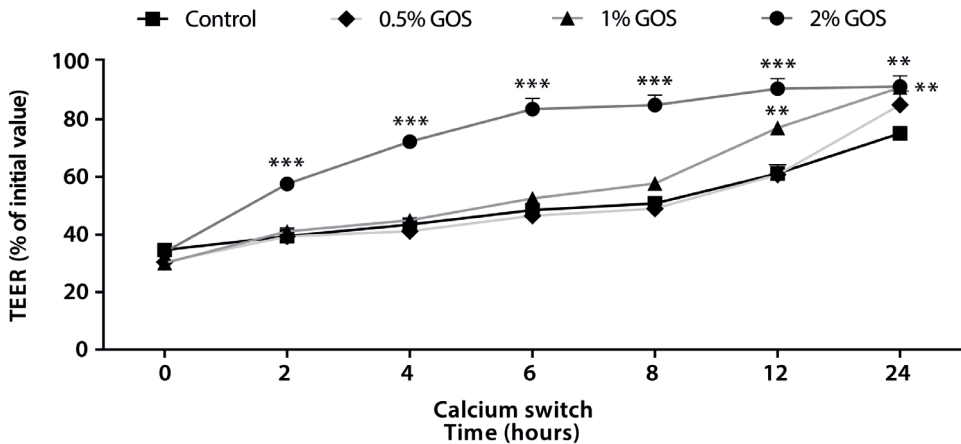


**Figure 2.** GOS accelerate TJs reassembly after calcium deprivation of Caco-2 cells. Caco-2 cells were pretreated apically and basolaterally with GOS before calcium deprivation and the TEER was measured during recovery (0, 2, 4, 6, 8, 12 and 24 h) in complete, calcium containing DMEM medium with GOS. Results are expressed as a percentage of initial value as mean  $\pm$  SEM,  $n = 3$ . \*\* $P < 0.01$ , \*\*\*  $P < 0.001$ ; significantly different from control at each independent time point, Bonferroni post hoc test.

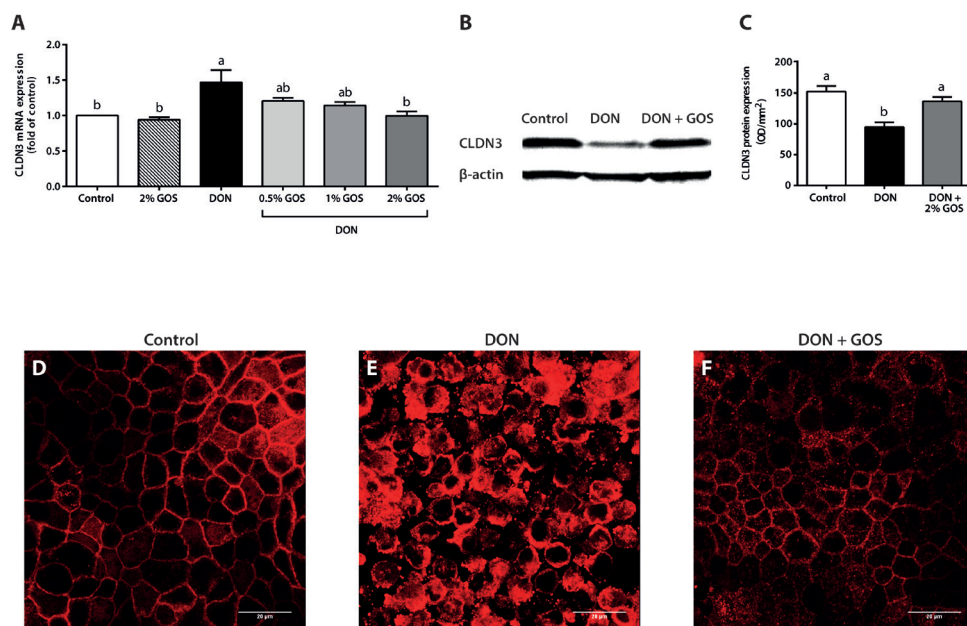


**Figure 3.** GOS prevent the DON-induced disturbance of CLDN3 expression and its cellular distribution in Caco-2 cell monolayers. CLDN3 mRNA (A) and protein levels (B and C) after a DON challenge (apical and basolateral compartments) in Caco-2 cells apically and basolaterally pretreated with GOS or DMEM medium. Results are expressed as CLDN3 mRNA expression (fold of control) (qRT-PCR, normalized to GAPDH and ACTB) or CLDN3 protein expression (OD/mm<sup>2</sup>) (Western blot, normalized to β-actin) as mean ± SEM, n = 3. Labeled bars without a common letter differ,  $P < 0.05$ , Bonferroni post hoc test. Immunofluorescence photomicrographs (D, E and F) of Caco-2 monolayers stained with CLDN3 in the presence and absence of GOS and DON. Representative results were reproduced in 3 separate experiments (400x magnification). The scale bar represents 20 μm.

### **GOS suppress the DON-induced increase in the mRNA expression as well as the synthesis and secretion of epithelial CXCL8 in Caco-2 cells**

DON induced an increase in mRNA expression levels of CXCL8 ( $P < 0.001$ ), and this effect could be prevented by 1% and 2% GOS pretreatment as shown by a decrease in CXCL8 mRNA levels ( $P = 0.023$  and  $P = 0.006$ , respectively) (Figure 5A). Subsequent quantification of the secreted CXCL8 in the cell culture medium, showed that 2% GOS-pretreatment prevented the DON-induced increase in CXCL8 levels in both apical and basolateral compartments ( $P < 0.001$  and  $P = 0.002$ , respectively) (Figure 5B, C).



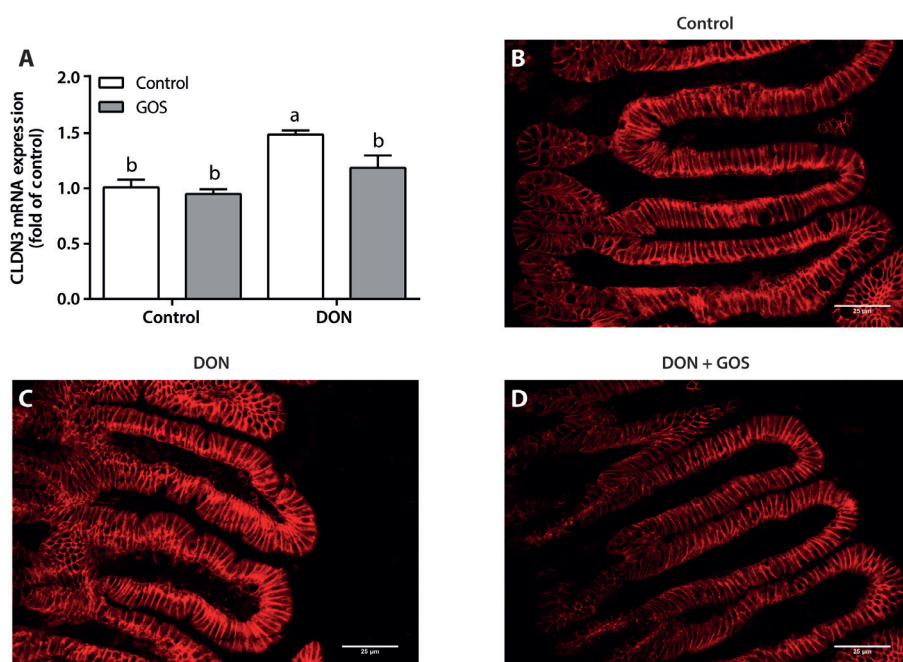


**Figure 4.** *In vivo* application of GOS prevent the DON-induced overexpression of CLDN3 mRNA and maintains its normal cellular distribution in mouse intestine. CLDN3 mRNA levels (A) after a DON challenge in the distal small intestine of mice supplemented with or without a GOS diet. qRT-PCR data are normalized to GAPDH and ACTB and expressed as CLDN3 mRNA expression (fold of control) as mean  $\pm$  SEM,  $n = 5-6$  animals/experimental group. Labeled bars without a common letter differ,  $P < 0.05$ , Bonferroni post hoc test. Representative immunofluorescence photomicrographs (B, C and D) of the mouse distal small intestine stained with CLDN3 (400x magnification). The scale bar represents 25  $\mu$ m.

#### **GOS suppress the DON-induced increase in the expression of the murine CXCL8 analogues CXCL1 and CXCL2 mRNA in the intestines**

The mRNA expression levels of different cytokines, such as IFN- $\gamma$ , IL-1 $\alpha$ , IL-1 $\beta$ , IL-4, IL-6, TNF- $\alpha$  and the murine CXCL8 homologues, CXCL1 (keratinocyte chemoattractant (KC)) and CXCL2 (macrophage inflammatory protein-2 $\alpha$  (MIP-2 $\alpha$ )) were measured in intestinal samples of DON-treated mice by qRT-PCR (Supplementary Figure 9). Only CXCL1 and CXCL2 mRNA expression was up-regulated in the DON-exposed mouse intestines, especially in the small intestine, compared to the non-treated mice (Supplementary Figure 10). In the animals pretreated with GOS, the DON-induced CXCL1 mRNA expression was partly suppressed in the distal small intestine ( $P = 0.06$ ) (Figure 5D, E).

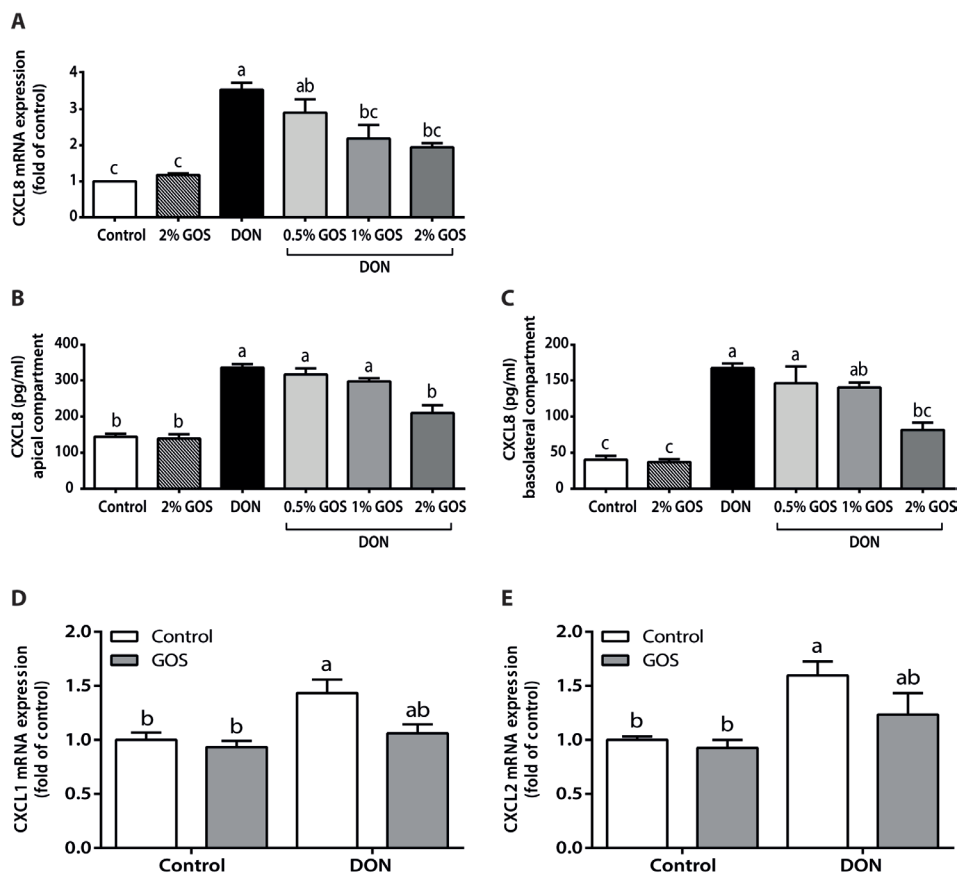


**Figure 5.** GOS suppress the DON-induced changes in the expression, synthesis and secretion of CXCL8 in Caco-2 cells, and the CXCL1 and CXCL2 mRNA expression in the mouse intestine. CXCL8 mRNA (A) and protein levels (B and C) after a DON challenge (apical and basolateral compartments) in Caco-2 cells apically and basolaterally pretreated with GOS or DMEM medium. CXCL1 and CXCL2 mRNA levels after a DON challenge in mice supplemented with or without GOS diet (D and E). ELISA results are expressed as pg/ml as mean  $\pm$  SEM and qRT-PCR data are normalized to GAPDH and ACTB and expressed as CXCL8 and CXCL1/CXCL2 mRNA expression (fold of control) as mean  $\pm$  SEM, *in vitro*  $n = 3$  and *in vivo*  $n = 5-6$  animals/experimental group. Labeled bars without a common letter differ,  $P < 0.05$ , Bonferroni post hoc test.

## GOS prevent the DON-induced histo-morphological alterations in the mouse intestine

DON-treated mice show a significant decrease in villus height (Figure 6A) in the proximal small intestine in comparison to the non-treated animals ( $P = 0.023$ ), while in the distal small intestine a slight decrease in villus height was observed after the DON gavage ( $P < 0.08$ ) (Figure 6C). Offering the mice a diet supplemented with 1% GOS prior to the DON challenge prevented these typical DON-induced histomorphological changes in the proximal small intestine ( $P = 0.032$ ) (Figure 6B, D). The crypt depth was significantly increased in the proximal small intestine in DON-treated mice compared to non-treated animals ( $P = 0.022$ ), but GOS did not have an effect on this parameter ( $P = 0.57$ ) (Supplementary Figure 11).

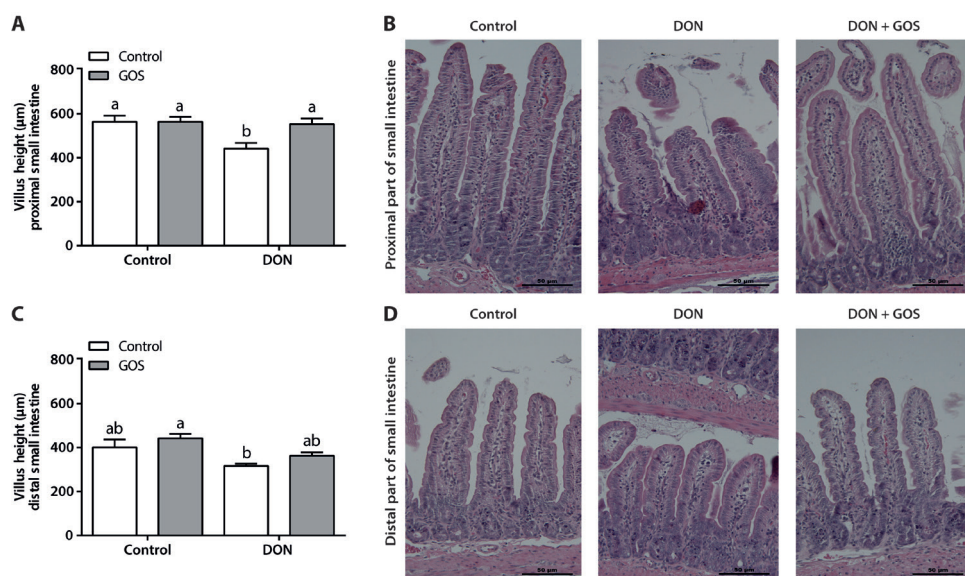


**Figure 6.** GOS prevent the DON-induced histomorphological alterations in the villi of the mouse intestine. Villus height in proximal (A) and distal (C) small intestine with representative photomicrographs of H&E-stained tissue (B, D) after a DON challenge in mice supplemented with or without a GOS diet (magnification of 200x). Results are expressed as mean  $\pm$  SEM,  $n = 5$ –6 animals/experimental group. Labeled bars without a common letter differ,  $P < 0.05$ , Bonferroni post hoc test. The scale bar represents 50  $\mu$ m.

## Discussion

Non-digestible oligosaccharides are known to exert a beneficial effect on the gut microbiota in infants and adults (19, 23) and are recommended as supportive therapy in patients with ulcerative colitis (22), and other chronic inflammatory conditions (17). While the risk factors and pathogenesis of chronic inflammatory bowel diseases are still not entirely elucidated (33), recent findings suggest a possible role for the wheat-associated mycotoxin deoxynivalenol (DON) in the induction and/or progression of human chronic intestinal inflammatory diseases (11, 34, 35). Given the global and frequent occurrence of DON, its stability during food processing and its known toxic effects, DON is considered to be of public health concern as food contaminant (9, 10, 36, 37). The aim of the current study was to assess the potential beneficial effects of defined GOS on the DON-induced intestinal damage in a series of *in vitro* models as well as in an *in vivo* study in mice. The presented *in vitro* results demonstrate the ability of GOS to prevent the DON-induced loss of barrier function measured as transepithelial resistance and paracellular transport of marker molecules. Comparing the results of the various experimental approaches in which GOS were added either to both, the apical and the basolateral sides, of the Caco-2 cell monolayer, or to the apical side only, or simultaneously with DON (without a pretreatment phase), showed that the most pronounced effect was achieved when a pretreatment of GOS added to both compartments was preceding the DON challenge. These findings suggest that GOS have predominantly a preventive effect, although a more rapid repair of existing DON lesions cannot be excluded. The latter mechanism is suggested by the calcium switch assay, showing an acceleration of the TJs reassembly by GOS and a decreased repair time of the transepithelial resistance after a calcium-deprivation period.

The difference between the results obtained with dual exposure of GOS to the apical and basolateral compartments, which were more pronounced than an application to the apical compartment only, were unexpected, as Gnoth *et al.* (38) and Eiwegger *et al.* (39) showed *in vitro* evidence for a transport of human milk oligosaccharides and prebiotic oligosaccharides, like GOS, across the intestinal epithelial layer. These findings suggest an absorption of orally applied GOS, which was recently supported by the presence of human milk oligosaccharides in the circulation (plasma and urine) of breastfed infants (40). A possible explanation for the different results in the current experiments regarding the route of GOS exposure could be the rather short pre-incubation time of 24 h, which might not be sufficient to allow an equilibrium between both compartments by means of transcellular transport of GOS.

The direct effect of GOS on TJs was further substantiated by the related gene expression profile of different TJ proteins (CLDN1, CLDN3, CLDN4, OCLN, ZO-1 and ZO-2) in DON-exposed cells with or without GOS pretreatment. Only the DON-induced CLDN3 mRNA expression could be almost entirely prevented by GOS. Western blot analyses pointed out that GOS pretreatment also prevented the DON-induced decrease in CLDN3 protein

expression. In addition, it seemed that the DON-induced derangement of the cellular distribution of CLDN3 was moderated by GOS visualized by immunofluorescence microscopy. This contradiction between increase in TJs mRNA expression and decrease in protein levels after DON exposure was earlier reported by De Walle *et al.* (41). DON seems to prolong the usually transient expression of genes related to activation of signaling cascades by transcriptional enhancement and/or transcript stabilization (42). Conflicting results are described related to mechanisms behind the DON-related effect on claudins, since Pinton *et al.* (43, 44) described that the DON-induced activation of the ERK signaling pathway inhibits CLDN4 protein expression, while others pointed out that extracellular signal-regulated kinase, c-Jun N-terminal kinase, and NF- $\kappa$ B pathways were not involved (41). These findings suggest that DON is not solely reducing the TJ protein expression by inhibition of protein synthesis, but by a complex de-regulation of gene expression and transcription pathways.

CLDN3 is already previously identified as one of the most affected TJ proteins after DON exposure in intestinal porcine epithelial cells derived from jejunum (IPEC-J2) (7) as well as in Caco-2 cells (8) and the effect of DON on members of the claudin-family has been also described in different *in vivo* studies (4, 8, 34, 41, 43, 44). Our *in vitro* results showing that GOS counteracted the DON-induced disturbance of CLDN3 expression was confirmed in the *in vivo* mouse model. CLDN3 is strongly expressed in the mouse small intestine (45) and plays an important role in the postnatal maturation of murine intestinal barrier functions (46). In the current study, the induction of CLDN3 mRNA expression in the distal small intestine after a DON challenge was shown to be prevented in mice pretreated with a GOS-supplemented diet. The mechanisms behind this effect await further clarification. However, CLDN3 is an important regulator of epithelial barrier permeability and seals the paracellular pathway against the passage of ions (47, 48), the DON-induced hyperpermeability of the intestines for FITC-dextran (4 kDa) was not mitigated by GOS. In a direct comparison between the *in vitro* findings and the findings in mice, it needs to be considered that in mice, more important determinants of intestinal permeability are present, such as the mucus layer, secretory IgA and distinct other cell types, including goblet cells, Paneth cells and immune cells, each of which contributes in a unique way to the maintenance of barrier integrity (49-52).

Previous investigations indicated that DON can induce both immunostimulatory or immunosuppressive responses depending on dose, frequency and duration of exposure (10, 53) and hence we studied some typical markers of intestinal inflammation. The chemokine CXCL8 is the most prominent cytokine expressed by Caco-2 cells and is secreted early in the inflammatory process by human enterocytes *in vivo*. It acts as a potent chemo-attractant for neutrophils, an effect which is also described following dietary DON exposure (35). The current study demonstrated that 1% and 2% GOS prevent the DON-induced epithelial mRNA expression of CXCL8 in Caco-2 cells. These findings are in line with previous results with oligosaccharides, in which it could be shown that  $\alpha$ 3-sialyllactose or fructo-oligosaccharides suppressed CXCL8 mRNA expression levels in

non-stimulated Caco-2 cells (54). The DON-induced CXCL8 release in both the apical and basolateral compartments was also counteracted by GOS. Basolateral secretion of CXCL8 plays a role in the recruitment of circulating neutrophils from the bloodstream to the site of tissue injury or infection, while it is speculated that apically secreted CXCL8 may initiate or augment the pathway responses in epithelial restitution prior to any potential loss of barrier integrity because of toxin production (55-58). Parallel to the *in vitro* experiments with human-derived Caco-2 cells, in the *in vivo* experiments with mice, the up-regulation of the murine CXCL8 homologues, CXCL1 and CXCL2, by DON was noted, especially in the small intestine. The effect on CXCL1 in the distal small intestine could be alleviated by GOS pretreatment as well. Previously it has been suggested GOS interact with peptidoglycan recognition protein 3 (PGLYRP3) and peroxisome proliferator-activated receptor  $\gamma$  (PPARG), carbohydrate receptors, such as C-type lectin and Toll-like receptor-4 that may contribute to the protective effects of GOS (17, 54, 59).

In addition, the control conditions with GOS did not affect the different parameters measured in the Caco-2 cell model as well as in the *in vivo* mouse model. Other *in vitro* and *in vivo* studies also described no effect in control conditions with GOS in combination with fructo-oligosaccharides (FOS) (60-63) and this could be related to the difficulty to positively affect the homeostatic environment.

In summary, the presented *in vitro* and *in vivo* studies demonstrated that GOS concentration-dependently are able to prevent typical adverse effects of the wheat-derived fungal toxin DON. Of particular interest is the effect of GOS on facilitating TJs reassembly and on the regulation of the CLDN3 expression. Moreover, a reduction of the inflammatory response (CXCL8 and CXCL1) following a DON challenge could be observed in line with a prevention of DON-induced alterations in villus architecture in the mouse intestine. Considering that the DON-induced alterations in the intestinal tract resemble those of human chronic inflammatory diseases (64-66) and the regular exposure of humans to DON due to its presence in wheat and wheat-derived products, further studies are warranted to assess in more detail the potential beneficial effects of GOS as supportive therapy in the prevention of toxin-induced inflammatory bowel diseases and related syndromes.

## Acknowledgements

This project is jointly financed by the European Union, European Regional Development Fund and The Ministry of Economic Affairs, Agriculture and Innovation, Peaks in the Delta, the Municipality of Groningen, the Provinces of Groningen, Fryslân and Drenthe, the Dutch Carbohydrate Competence Center (CCC WP25; [www.ccresearch.nl](http://www.ccresearch.nl)), Nutricia Research and FrieslandCampina.



## References

1. Camilleri M, Madsen K, Spiller R, Greenwood-Van Meerveld B, Verne GN. Intestinal barrier function in health and gastrointestinal disease. *Neurogastroenterol Motil* 2012;24:503-512.
2. Menard S, Cerf-Bensussan N, Heyman M. Multiple facets of intestinal permeability and epithelial handling of dietary antigens. *Mucosal Immunol* 2010;3:247-259.
3. Groschwitz KR, Hogan SP. Intestinal barrier function: molecular regulation and disease pathogenesis. *J Allergy Clin Immunol* 2009;124:3-20.
4. Pinton P, Tsybulskyy D, Lucioi J, Laffitte J, Callu P, Lyazhri F, Grosjean F, Bracarense AP, Kolf-Clauw M, Oswald IP. Toxicity of deoxynivalenol and its acetylated derivatives on the intestine: differential effects on morphology, barrier function, tight junction proteins, and mitogen-activated protein kinases. *Toxicol Sci* 2012;130:180-190.
5. Nossol C, Diesing AK, Kahlert S, Kersten S, Kluess J, Ponsuksili S, Hartig R, Wimmers K, Danicke S, Rothkotter HJ. Deoxynivalenol affects the composition of the basement membrane proteins and influences en route the migration of CD16(+) cells into the intestinal epithelium. *Mycotoxin Res* 2013;29:245-254.
6. Devreese M, Pasmans F, De Backer P, Croubels S. An *in vitro* model using the IPEC-J2 cell line for efficacy and drug interaction testing of mycotoxin detoxifying agents. *Toxicol In Vitro* 2013;27:157-163.
7. Diesing AK, Nossol C, Danicke S, Walk N, Post A, Kahlert S, Rothkotter HJ, Kluess J. Vulnerability of polarised intestinal porcine epithelial cells to mycotoxin deoxynivalenol depends on the route of application. *PLoS One* 2011;6:e17472.
8. Akbari P, Braber S, Gremmels H, Koelink PJ, Verheijden KA, Garssen J, Fink-Gremmels J. Deoxynivalenol: a trigger for intestinal integrity breakdown. *FASEB J* 2014;28:2414-2429.
9. Sugita-Konishi Y, Park BJ, Kobayashi-Hattori K, Tanaka T, Chonan T, Yoshikawa K, Kumagai S. Effect of cooking process on the deoxynivalenol content and its subsequent cytotoxicity in wheat products. *Biosci Biotechnol Biochem* 2006;70:1764-1768.
10. Pestka JJ. Deoxynivalenol: mechanisms of action, human exposure, and toxicological relevance. *Arch Toxicol* 2010;84:663-679.
11. Cano PM, Seebboth J, Meurens F, Cogne J, Abrami R, Oswald IP, Guzylack-Piriou L. Deoxynivalenol as a new factor in the persistence of intestinal inflammatory diseases: an emerging hypothesis through possible modulation of Th17-mediated response. *PLoS One* 2013;8:e53647.
12. Pestka JJ. Deoxynivalenol: Toxicity, mechanisms and animal health risks. *Anim Feed Sci Tech* 2007;137:283-298.
13. Pinton P, Oswald IP. Effect of deoxynivalenol and other Type B trichothecenes on the intestine: a review. *Toxins* 2014;6:1615-1643.
14. Larsen JC, Hunt J, Perrin I, Ruckebauer P. Workshop on trichothecenes with a focus on DON: summary report. *Toxicol Lett* 2004;153:1-22.
15. Danicke S, Brussow KP, Goyarts T, Valenta H, Ueberschar KH, Tiemann U. On the transfer of the Fusarium toxins deoxynivalenol (DON) and zearalenone (ZON) from the sow to the full-term piglet during the last third of gestation. *Food Chem Toxicol* 2007;45:1565-1574.
16. Nielsen JK, Vikstrom AC, Turner P, Knudsen LE. Deoxynivalenol transport across the human placental barrier. *Food Chem Toxicol* 2011;49:2046-2052.
17. Vos AP, M'Rabet L, Stahl B, Boehm G, Garssen J. Immune-modulatory effects and potential working mechanisms of orally applied nondigestible carbohydrates. *Crit Rev Immunol* 2007;27:97-140.
18. Sangwan V, Tomar SK, Singh RR, Singh AK, Ali B. Galactooligosaccharides: novel components of designer foods. *J Food Sci* 2011;76:R103-R111.
19. Vulevic J, Drakoularakou A, Yaqoob P, Tzortzis G, Gibson GR. Modulation of the fecal microflora profile and immune function by a novel trans-

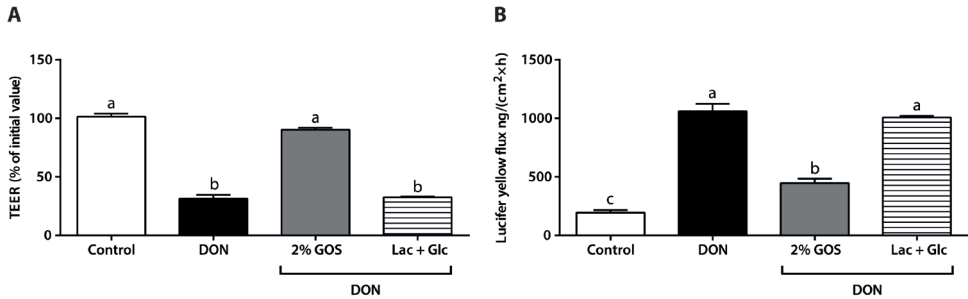


- galactooligosaccharide mixture (B-GOS) in healthy elderly volunteers. *Am J Clin Nutr* 2008;88:1438-1446.
20. Fanaro S, Marten B, Bagna R, Vigi V, Fabris C, Pena-Quintana L, Arguelles F, Scholz-Ahrens KE, Sawatzki G, Zelenka R, *et al.* Galacto-oligosaccharides are bifidogenic and safe at weaning: a double-blind randomized multicenter study. *J Pediatr Gastroenterol Nutr* 2009;48:82-88.
21. Ben XM, Zhou XY, Zhao WH, Yu WL, Pan W, Zhang WL, Wu SM, Van Beusekom CM, Schaafsma A. Supplementation of milk formula with galacto-oligosaccharides improves intestinal micro-flora and fermentation in term infants. *Chin Med J (Engl)* 2004;117:927-931.
22. Ishikawa H, Matsumoto S, Ohashi Y, Imaoka A, Setoyama H, Umesaki Y, Tanaka R, Otani T. Beneficial effects of probiotic bifidobacterium and galacto-oligosaccharide in patients with ulcerative colitis: a randomized controlled study. *Digestion* 2011;84:128-133.
23. Fanaro S, Boehm G, Garssen J, Knol J, Mosca F, Stahl B, Vigi V. Galacto-oligosaccharides and long-chain fructo-oligosaccharides as prebiotics in infant formulas: a review. *Acta Paediatr* 2005;94:22-26.
24. Torres DPM, Goncalves MP, Teixeira JA, Rodrigues LR. Galacto-Oligosaccharides: Production, Properties, Applications, and Significance as Prebiotics. *Compr Rev Food Sci Food Saf* 2010;9:438-454.
25. Coulter L, Timmermans J, Bas R, Van Den Dool R, Haaksman I, Klarenbeek B, Slaghek T, Van Dongen W. In-depth characterization of prebiotic galacto-oligosaccharides by a combination of analytical techniques. *J Agric Food Chem* 2009;57:8488-8495.
26. Dombink-Kurtzman MA, Poling SM, Kendra DF. Determination of deoxynivalenol in infant cereal by immunoaffinity column cleanup and high-pressure liquid chromatography-UV detection. *J Food Prot* 2010;73:1073-1076.
27. Artursson P, Magnusson C. Epithelial transport of drugs in cell culture. II: Effect of extracellular calcium concentration on the paracellular transport of drugs of different lipophilicities across monolayers of intestinal epithelial (Caco-2) cells. *J Pharm Sci* 1990;79:595-600.
28. Reeves PG, Nielsen FH, Fahey GC, Jr. AIN-93 purified diets for laboratory rodents: final report of the American Institute of Nutrition ad hoc writing committee on the reformulation of the AIN-76A rodent diet. *J Nutr* 1993;123:1939-1951.
29. Kinser S, Li M, Jia Q, Pestka JJ. Truncated deoxynivalenol-induced splenic immediate early gene response in mice consuming (n-3) polyunsaturated fatty acids. *J Nutr Biochem* 2005;16:88-95.
30. Moon Y, Pestka JJ. Cyclooxygenase-2 mediates interleukin-6 upregulation by vomitoxin (deoxynivalenol) *in vitro* and *in vivo*. *Toxicol Appl Pharmacol* 2003;187:80-88.
31. Azcona-Olivera JI, Ouyang Y, Murtha J, Chu FS, Pestka JJ. Induction of cytokine mRNAs in mice after oral exposure to the trichothecene vomitoxin (deoxynivalenol): relationship to toxin distribution and protein synthesis inhibition. *Toxicol Appl Pharmacol* 1995;133:109-120.
32. Moolenbeek C, Ruitenberg EJ. The "Swiss roll": a simple technique for histological studies of the rodent intestine. *Lab Anim* 1981;15:57-59.
33. Kostic AD, Xavier RJ, Gevers D. The microbiome in inflammatory bowel disease: current status and the future ahead. *Gastroenterology* 2014;146:1489-1499.
34. Maresca M, Fantini J. Some food-associated mycotoxins as potential risk factors in humans predisposed to chronic intestinal inflammatory diseases. *Toxicon* 2010;56:282-294.
35. Van De Walle J, Romier B, Larondelle Y, Schneider YJ. Influence of deoxynivalenol on NF-kappaB activation and IL-8 secretion in human intestinal Caco-2 cells. *Toxicol Lett* 2008;177:205-214.
36. Sobrova P, Adam V, Vasatkova A, Beklova M, Zeman L, Kizek R. Deoxynivalenol and its toxicity. *Interdiscip Toxicol* 2010;3:94-99.
37. Wang Z, Wu Q, Kuca K, Dohnal V, Tian Z. Deoxynivalenol: signaling pathways and human

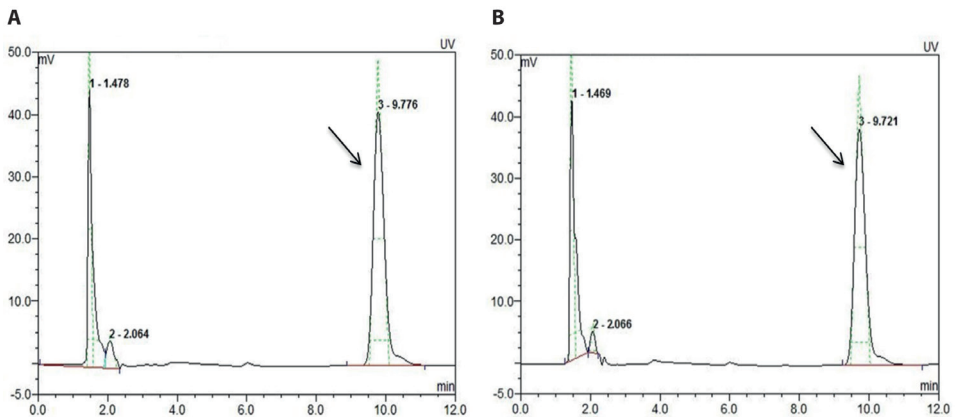
- exposure risk assessment-an update. *Arch Toxicol* 2014;88:1915-1928.
38. Gnoth MJ, Rudloff S, Kunz C, Kinne RK. Investigations of the *in vitro* transport of human milk oligosaccharides by a Caco-2 monolayer using a novel high performance liquid chromatography-mass spectrometry technique. *J Biol Chem* 2001;276:34363-34370.
  39. Eiwegger T, Stahl B, Haidl P, Schmitt J, Boehm G, Dehlink E, Urbanek R, Szeplfalus Z. Prebiotic oligosaccharides: *in vitro* evidence for gastrointestinal epithelial transfer and immunomodulatory properties. *Pediatr Allergy Immunol* 2010;21:1179-1188.
  40. Goehring KC, Kennedy AD, Prieto PA, Buck RH. Direct evidence for the presence of human milk oligosaccharides in the circulation of breastfed infants. *PLoS One* 2014;9:e101692.
  41. De Walle JV, Sergent T, Piront N, Toussaint O, Schneider YJ, Larondelle Y. Deoxynivalenol affects *in vitro* intestinal epithelial cell barrier integrity through inhibition of protein synthesis. *Toxicol Appl Pharmacol* 2010;245:291-298.
  42. Azcona-Olivera JI, Ouyang YL, Warner RL, Linz JE, Pestka JJ. Effects of vomitoxin (deoxynivalenol) and cycloheximide on IL-2, 4, 5 and 6 secretion and mRNA levels in murine CD4+ cells. *Food Chem Toxicol* 1995;33:433-441.
  43. Pinton P, Braicu C, Nougayrede JP, Laffitte J, Taranu I, Oswald IP. Deoxynivalenol impairs porcine intestinal barrier function and decreases the protein expression of claudin-4 through a mitogen-activated protein kinase-dependent mechanism. *J Nutr* 2010;140:1956-1962.
  44. Pinton P, Nougayrede JP, Del Rio JC, Moreno C, Marin DE, Ferrier L, Bracarense AP, Kolf-Clauw M, Oswald IP. The food contaminant deoxynivalenol, decreases intestinal barrier permeability and reduces claudin expression. *Toxicol Appl Pharmacol* 2009;237:41-48.
  45. Rahner C, Mitic LL, Anderson JM. Heterogeneity in expression and subcellular localization of claudins 2, 3, 4, and 5 in the rat liver, pancreas, and gut. *Gastroenterology* 2001;120:411-422.
  46. Patel RM, Myers LS, Kurundkar AR, Maheshwari A, Nusrat A, Lin PW. Probiotic bacteria induce maturation of intestinal claudin 3 expression and barrier function. *Am J Pathol* 2012;180:626-635.
  47. Milatz S, Krug SM, Rosenthal R, Gunzel D, Muller D, Schulzke JD, Amasheh S, Fromm M. Claudin-3 acts as a sealing component of the tight junction for ions of either charge and uncharged solutes. *Biochim Biophys Acta* 2010;1798:2048-2057.
  48. Gunzel D, Yu AS. Claudins and the modulation of tight junction permeability. *Physiol Rev* 2013;93:525-569.
  49. Pastorelli L, De Salvo C, Mercado JR, Vecchi M, Pizarro TT. Central role of the gut epithelial barrier in the pathogenesis of chronic intestinal inflammation: lessons learned from animal models and human genetics. *Front Immunol* 2013;4:280.
  50. Mantis NJ, Rol N, Cortes B. Secretory IgA's complex roles in immunity and mucosal homeostasis in the gut. *Mucosal Immunol* 2011;4:603-611.
  51. Johansson ME, Ambort D, Pelaseyed T, Schutte A, Gustafsson JK, Ermund A, Subramani DB, Holmen-Larsson JM, Thomsson KA, Bergstrom JH, *et al.* Composition and functional role of the mucus layers in the intestine. *Cell Mol Life Sci* 2011;68:3635-3641.
  52. Kim YS, Ho SB. Intestinal goblet cells and mucins in health and disease: recent insights and progress. *Curr Gastroenterol Rep* 2010;12:319-330.
  53. Bracarense AP, Lucioli J, Grenier B, Drociunas Pacheco G, Moll WD, Schatzmayr G, Oswald IP. Chronic ingestion of deoxynivalenol and fumonisin, alone or in interaction, induces morphological and immunological changes in the intestine of piglets. *Br J Nutr* 2012;107:1776-1786.
  54. Zenhom M, Hyder A, de Vrese M, Heller KJ, Roeder T, Schrezenmeier J. Prebiotic oligosaccharides reduce proinflammatory cytokines in intestinal Caco-2 cells via activation of PPARgamma and peptidoglycan

- recognition protein 3. *J Nutr* 2011;141:971-977.
55. Rossi O, Karczewski J, Stolte EH, Brummer RJ, van Nieuwenhoven MA, Meijerink M, van Neerven JR, van Ijzendoorn SC, van Baarlen P, Wells JM. Vectorial secretion of interleukin-8 mediates autocrine signalling in intestinal epithelial cells via apically located CXCR1. *BMC Res Notes* 2013;6:431.
56. Fusunyan RD, Quinn JJ, Ohno Y, MacDermott RP, Sanderson IR. Butyrate enhances interleukin (IL)-8 secretion by intestinal epithelial cells in response to IL-1 $\beta$  and lipopolysaccharide. *Pediatr Res* 1998;43:84-90.
57. Keshavarzian A, Fusunyan RD, Jacyno M, Winship D, MacDermott RP, Sanderson IR. Increased interleukin-8 (IL-8) in rectal dialysate from patients with ulcerative colitis: evidence for a biological role for IL-8 in inflammation of the colon. *Am J Gastroenterol* 1999;94:704-712.
58. Sturm A, Baumgart DC, d'Heureuse JH, Hotz A, Wiedenmann B, Dignass AU. CXCL8 modulates human intestinal epithelial cells through a CXCR1 dependent pathway. *Cytokine* 2005;29:42-48.
59. Ortega-Gonzalez M, Ocon B, Romero-Calvo I, Anzola A, Guadix E, Zarzuelo A, Suarez MD, Sanchez de Medina F, Martinez-Augustin O. Nondigestible oligosaccharides exert nonprebiotic effects on intestinal epithelial cells enhancing the immune response via activation of TLR4-NF $\kappa$ B. *Mol Nutr Food Res* 2014;58:384-393.
60. Vos AP, Haarman M, Buco A, Govers M, Knol J, Garssen J, Stahl B, Boehm G, M'Rabet L. A specific prebiotic oligosaccharide mixture stimulates delayed-type hypersensitivity in a murine influenza vaccination model. *Int Immunopharmacol* 2006;6:1277-1286.
61. de Kivit S, Saeland E, Kraneveld AD, van de Kant HJ, Schouten B, van Esch BC, Knol J, Sprickelman AB, van der Aa LB, Knippels LM, *et al.* Galectin-9 induced by dietary synbiotics is involved in suppression of allergic symptoms in mice and humans. *Allergy* 2012;67:343-352.
62. de Kivit S, Kraneveld AD, Knippels LM, van Kooyk Y, Garssen J, Willemsen LE. Intestinal epithelium-derived galectin-9 is involved in the immunomodulating effects of nondigestible oligosaccharides. *J Innate Immun* 2013;5:625-638.
63. Sagar S, Vos AP, Morgan ME, Garssen J, Georgiou NA, Boon L, Kraneveld AD, Folkerts G. The combination of *Bifidobacterium breve* with non-digestible oligosaccharides suppresses airway inflammation in a murine model for chronic asthma. *Biochim Biophys Acta* 2014;1842:573-583.
64. Villanacci V, Ceppa P, Tavani E, Vindigni C, Volta U, Gruppo Italiano Patologi Apparato D, Societa Italiana di Anatomia Patologica e Citopatologia Diagnostica/International Academy of Pathology Id. Coeliac disease: the histology report. *Dig Liver Dis* 2011;43:S385-S395.
65. Dickson BC, Streutker CJ, Chetty R. Coeliac disease: an update for pathologists. *J Clin Pathol* 2006;59:1008-1016.
66. Pironi L, Bonvicini F, Gionchetti P, D'Errico A, Rizzello F, Corsini C, Foroni L, Gallinella G. Parvovirus b19 infection localized in the intestinal mucosa and associated with severe inflammatory bowel disease. *J Clin Microbiol* 2009;47:1591-1595.

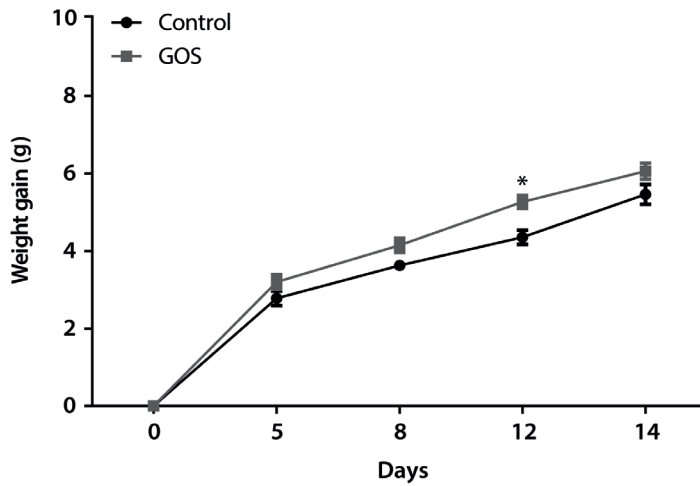
## Supplementary data



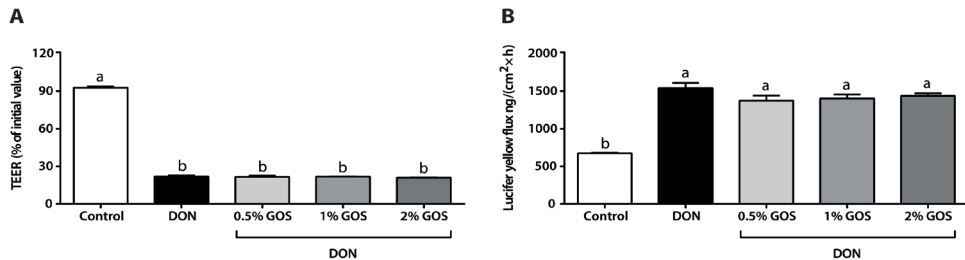
**Supplementary Figure 1.** Effects of lactose and glucose pretreatment on the DON-induced impairment of the Caco-2 cell monolayer integrity. Caco-2 cells grown on inserts were pretreated apically and basolaterally (24 h) either with GOS or equimolar concentrations of lactose (Lac, 16%) and glucose (Glc, 14%) as present in the 2% GOS solution before being challenged with DON (apical and basolateral compartments) for 24 h. The impairment of the barrier integrity was assessed by TEER measurement (A) and the transport of lucifer yellow (B) from the apical to the basolateral compartments. Results are expressed as a percentage of initial value (TEER) or in the amount of tracer transported [ng/(cm<sup>2</sup>×h)] as mean ± SEM, n = 1 (performed in triplicate). Labeled bars without a common letter differ, P < 0.05, Bonferroni post hoc test.



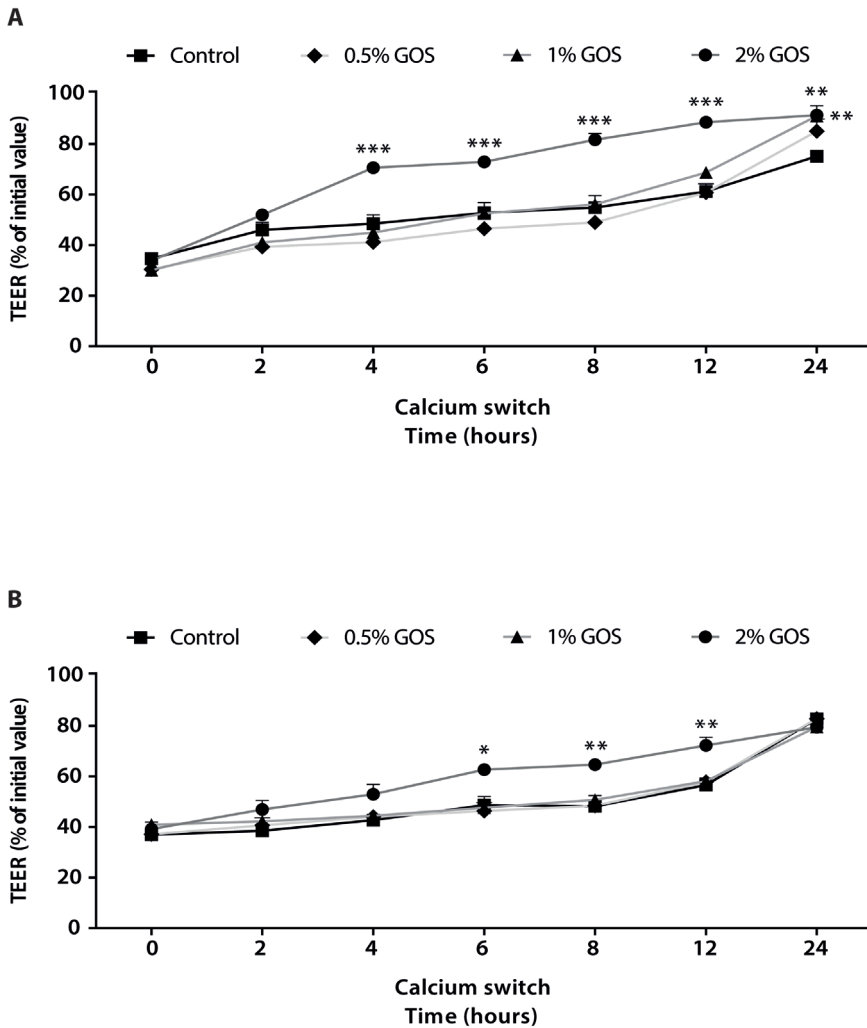
**Supplementary Figure 2.** Control incubations in cell free medium to identify possible physico-chemical interactions between DON and GOS. Chromatography of representative samples of the incubations with DON only (4.2 μM) (A) were compared with results from a co-incubation with the mixture of DON (4.2 μM) and GOS (2%) (B), as used in the *in vitro* experiments. After the incubation period (4 h), samples were filtered and directly subjected to HPLC analysis. No decline of the DON fraction (peak area at the retention time of 9.7 minutes, arrow) was observed, indicating that no unspecific binding reduced the free fraction of DON in the Caco-2 cell assays.



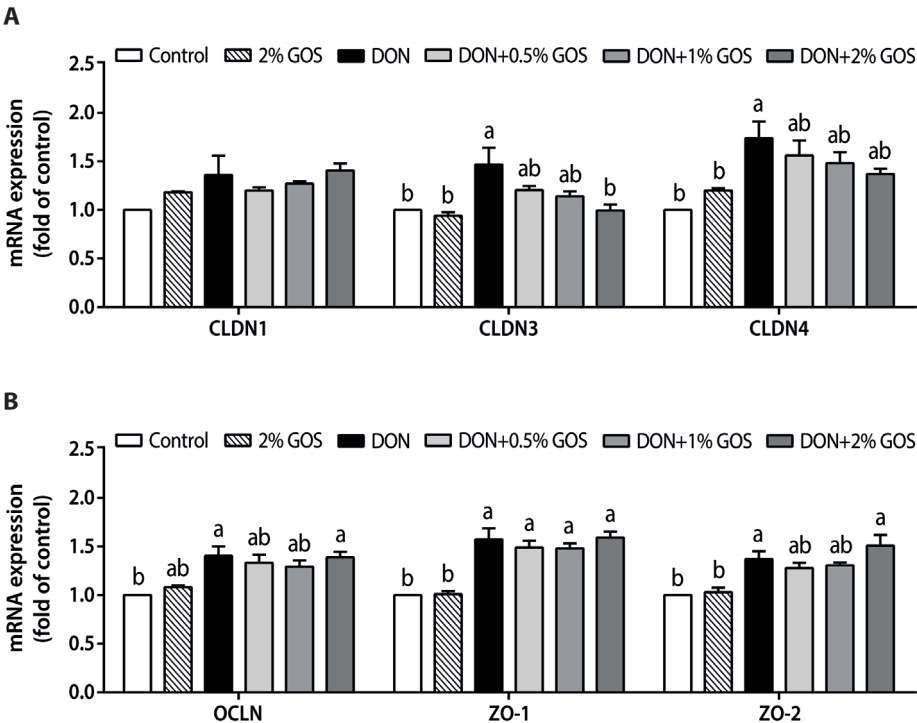
**Supplementary Figure 3.** Effect of GOS-supplemented diet for 2 weeks on the weight gain (day 0, 5, 8, 12, 14) in mice before being orally exposed to DON. Results are expressed as mean  $\pm$  SEM,  $n = 11$ –12 animals/experimental group. \*Different from control at that time,  $P < 0.05$ , Bonferroni post hoc test.



**Supplementary Figure 4.** Effects of GOS treatment on the DON-induced impairment of the Caco-2 cell monolayer integrity. Caco-2 cells grown on inserts were co-incubated (apical and basolateral compartments) with DON and GOS for 24 h (A, B). The impairment of the barrier integrity was assessed by TEER measurement (A), and the transport of lucifer yellow (B) from the apical to the basolateral compartments. Results are expressed as a percentage of initial value (TEER) or in the amount of tracer transported [ $\text{ng}/(\text{cm}^2 \times \text{h})$ ] as mean  $\pm$  SEM,  $n = 3$  (each performed in triplicate). Labeled bars without a common letter differ,  $P < 0.05$ , Bonferroni post hoc test.

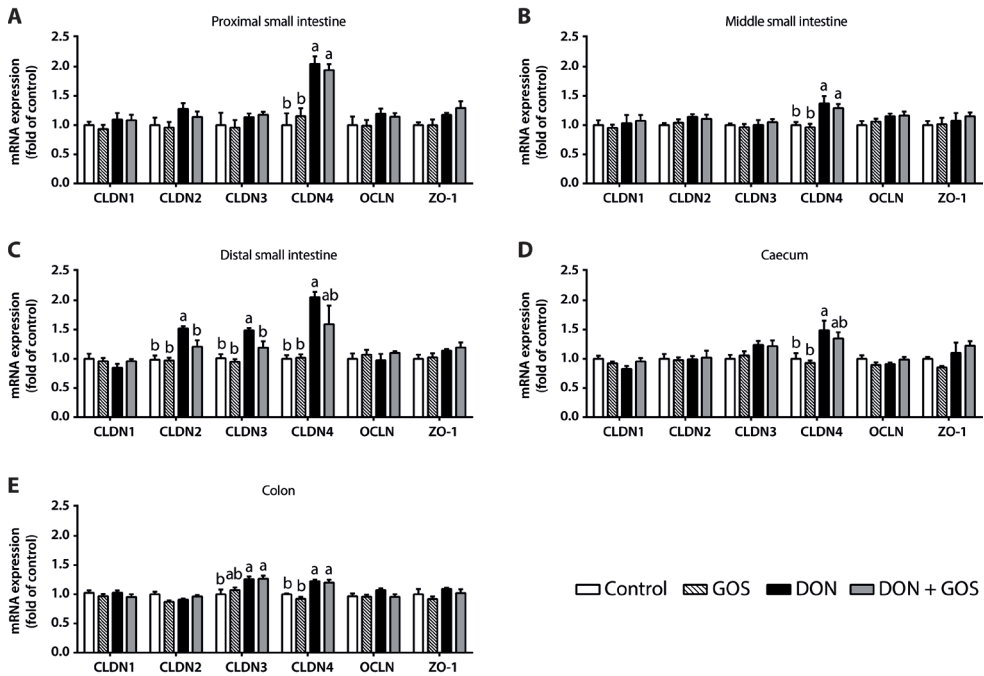


**Supplementary Figure 5.** Effects of GOS on the TJs reassembly of Caco-2 cells. Caco-2 cells were pretreated apically and basolaterally with GOS before calcium deprivation and TEER was measured during recovery (0, 2, 4, 6, 8, 12 and 24 h) in complete, calcium containing medium without GOS (A) or Caco-2 cells were incubated with GOS only at the apical side before and after calcium deprivation (B). Results are expressed as a percentage of initial value as mean  $\pm$  SEM,  $n = 3$  (each performed in triplicate) (\* $P < 0.05$ , \*\* $P < 0.01$ , \*\*\* $P < 0.001$ ; significantly different from control at each independent time point), Bonferroni post hoc test.

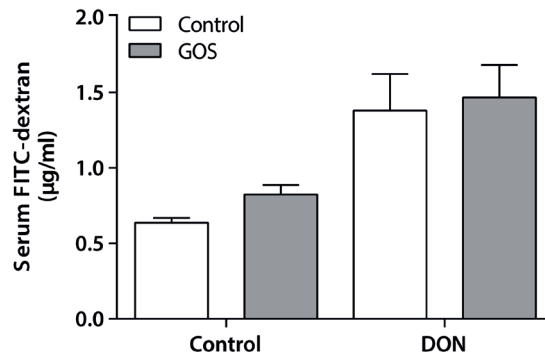


**Supplementary Figure 6.** Effects of GOS pretreatment on the mRNA expression of different TJ proteins after a DON challenge in Caco-2 cells. Caco-2 cells grown on inserts were pretreated apically and basolaterally with GOS (24 h) and then DON plus GOS (apical and basolateral compartments) for 6 h. mRNA levels of TJ proteins including CLDN1, CLDN3 and CLDN4 (A) as well as OCLN, ZO-1 and ZO-2 (B) were measured by qRT-PCR. qRT-PCR data are normalized to GAPDH and ACTB and expressed as mRNA expression (fold of control) as mean  $\pm$  SEM,  $n = 3$  (each performed in triplicate). Labeled bars without a common letter differ,  $P < 0.05$ , Bonferroni post hoc test.

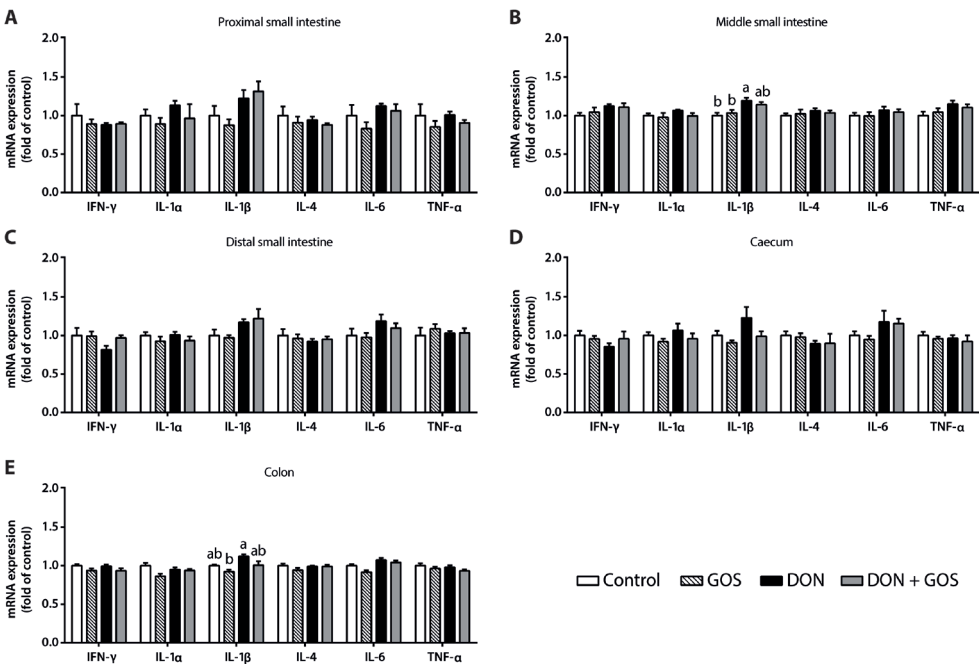




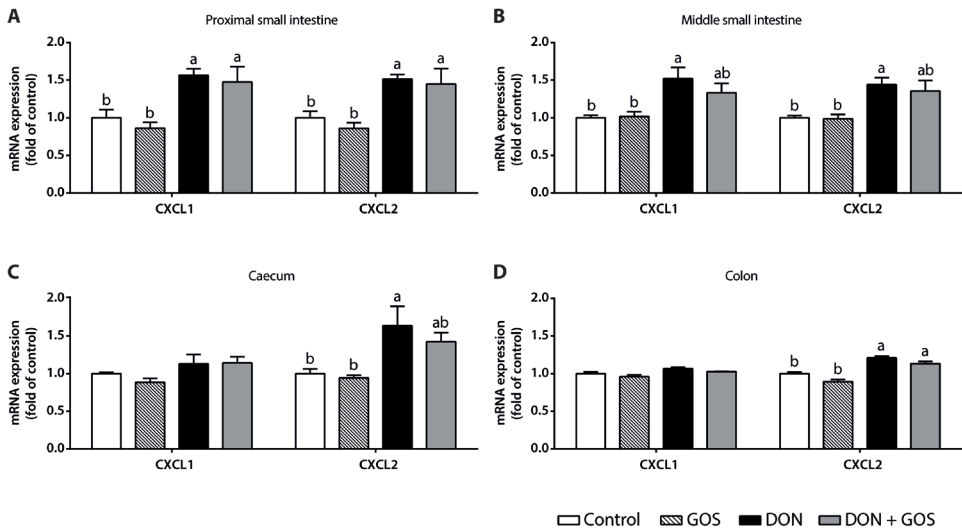
**Supplementary Figure 7.** Effects of GOS-supplemented diet for 2 weeks on the mRNA expression of murine TJ proteins in proximal small intestine (A), middle small intestine (B), distal small intestine (C), caecum (D), and colon (E) 6 h after a DON challenge. qRT-PCR data are normalized to GAPDH and ACTB and expressed as mRNA expression (fold of control) as mean  $\pm$  SEM,  $n = 5-6$  animals/experimental group. Labeled bars without a common letter differ,  $P < 0.05$ , Bonferroni post hoc test.



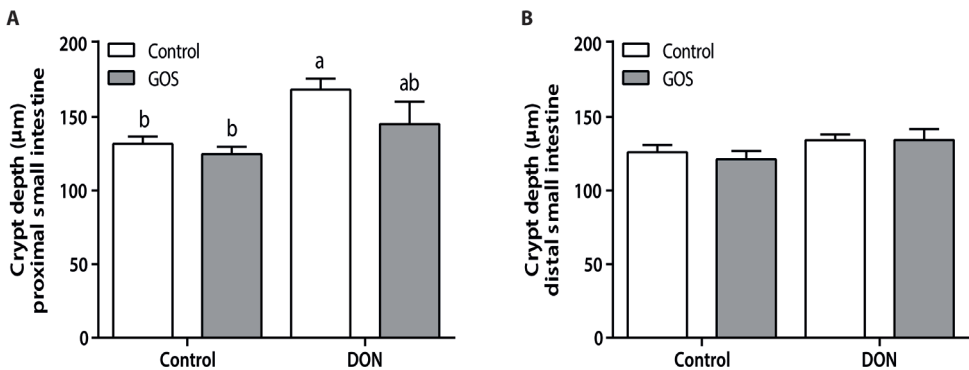
**Supplementary Figure 8.** Effect of GOS-supplemented diet for 2 weeks on the permeability of the mice intestine for FITC-dextran (4 kDa) 6 h after a DON challenge. Results are expressed as mean  $\pm$  SEM,  $n = 5-6$  animals/experimental group.



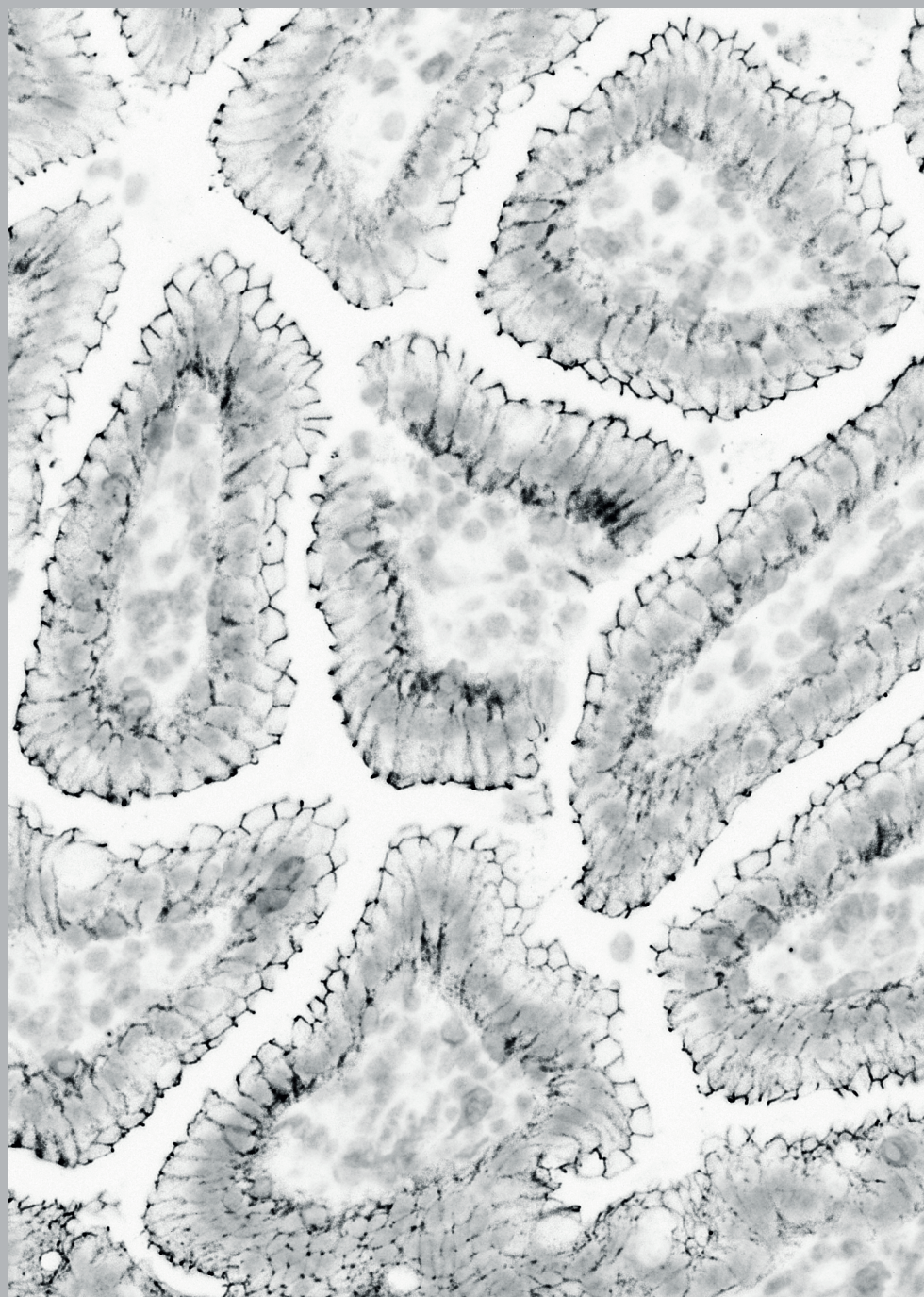
**Supplementary Figure 9.** Effects of GOS-supplemented diet for 2 weeks on the mRNA expression of murine cytokines in proximal small intestine (A), middle small intestine (B), distal small intestine (C), caecum (D), and colon (E) 6 h after a DON challenge. qRT-PCR data are normalized to GAPDH and ACTB and expressed as mRNA expression (fold of control) as mean  $\pm$  SEM,  $n = 5-6$  animals/experimental group. Labeled bars without a common letter differ,  $P < 0.05$ , Bonferroni post hoc test.



**Supplementary Figure 10.** Effects of GOS-supplemented diet for 2 weeks on the mRNA expression of murine CXCL8 homologues, CXCL1 and CXCL2, in proximal small intestine (A), middle small intestine (B), caecum (C), and colon (D) 6 h after a DON challenge. qRT-PCR data are normalized to GAPDH and ACTB and expressed as mRNA expression (fold of control) as mean  $\pm$  SEM,  $n = 5-6$  animals/experimental group. Labeled bars without a common letter differ,  $P < 0.05$ , Bonferroni post hoc test.



**Supplementary Figure 11.** Effects of GOS-supplemented diet for 2 weeks on the DON-increased crypt depth along mice proximal (A) and distal (B) small intestine. Results are expressed as mean  $\pm$  SEM,  $n = 5-6$  animals/experimental group. Labeled bars without a common letter differ,  $P < 0.05$ , Bonferroni post hoc test.



# Chapter 6



## Characterizing microbiota-independent effects of oligosaccharides in intestinal epithelial cells: insight into the role of structure and size

Peyman Akbari<sup>1,2</sup>, Johanna Fink-Gremmels<sup>1</sup>, Rianne H.A.M. Willems<sup>3</sup>, Elisabetta Difilippo<sup>3</sup>, Henk A. Schols<sup>3</sup>, Margriet H.C. Schoterman<sup>4</sup>, Johan Garssen<sup>2,5</sup>, Saskia Braber<sup>1</sup>

<sup>1</sup> Division of Veterinary Pharmacology, Pharmacotherapy and Toxicology, Institute for Risk Assessment Sciences, Utrecht University, Utrecht, The Netherlands

<sup>2</sup> Division of Pharmacology, Utrecht Institute for Pharmaceutical Sciences, Faculty of Science, Utrecht University, Utrecht, The Netherlands

<sup>3</sup> Laboratory of Food Chemistry, Wageningen University, Wageningen, The Netherlands

<sup>4</sup> FrieslandCampina, Amersfoort, The Netherlands

<sup>5</sup> Nutricia Research, Utrecht, The Netherlands

**This chapter is submitted for publication.**

## Abstract

The direct effect of galacto-oligosaccharides (GOS), including Vivinal® GOS syrup (VGOS) and purified Vivinal® GOS (PGOS), on the epithelial integrity and corresponding CXCL8 release was examined in a Caco-2 cell model for intestinal barrier dysfunction. To investigate structure-activity relationships, the effects of individual DP fractions of VGOS were evaluated. Moreover, the obtained results with GOS were compared with Caco-2 monolayers incubated with fructo-oligosaccharides (FOS) and Inulin. Caco-2 cell monolayers were pre-treated (24 h) with or without specific oligosaccharides or DP fractions of VGOS (DP2 to DP6) before being exposed for 12 h or 24 h to the fungal toxin deoxynivalenol (DON). Measurements of the transepithelial electrical resistance (TEER) and lucifer yellow (LY) permeability were conducted to investigate barrier integrity. The calcium switch assay was used to study the reassembly of epithelial tight junction proteins. Release of interleukin-8 (IL-8/CXCL8), a typical marker for inflammation, was measured by ELISA. In comparison to PGOS, FOS and Inulin, VGOS showed the most pronounced protective effect on the DON-induced impairment of the monolayer integrity, acceleration of the tight junction reassembly and the subsequent CXCL8 release. DP2 and DP3 in concentrations occurring in VGOS prevented the DON-induced epithelial barrier disruption, which could be related to their high prevalence in VGOS. However, no effects of the separate DP GOS fractions were observed on CXCL8 release. The current comparative study demonstrates the direct, microbiota-independent effects of oligosaccharides on the intestinal barrier function and shows the differences between individual galacto- and fructo-oligosaccharides. This microbiota-independent effect of oligosaccharides depends on the oligosaccharide structure, DP length and concentration.



## Introduction

Human milk oligosaccharides (HMOs) play an essential role in the postnatal growth and development of the intestinal and immune system (1). As the sufficient supply of the neonate with HMOs cannot always be guaranteed, various attempts were made to design alternative prebiotic oligosaccharides that mimic the gut health promoting effects of HMOs. At present, prebiotic oligosaccharides, for example the mixture of 90%GOS/10%lcFOS, aiming to mimic molecular size distribution of neutral HMOs, are widely used in infant formulas (2, 3). Although these neutral oligosaccharides are structurally different from HMOs, they have prebiotic activities and clinical investigations have confirmed that infants given such a formula containing GOS or GOS/lcFOS, achieve an intestinal microbiota composition comparable to that of breastfed infants (4, 5). Besides the effects of GOS and the mixture of GOS/lcFOS on the gut microbiota (6, 7), direct interactions of these oligosaccharides with intestinal epithelial cells have recently been described by our group and others (8-11). It has been shown that these oligosaccharides improve and protect the intestinal barrier integrity and modulate the immune responses of epithelial cells.

GOS and FOS differ in origin and structure and it has been suggested previously that the biological function of oligosaccharides is influenced by their structures, molecular weight and type of glycosidic linkages (12, 13). GOS are oligosaccharides based on the milk sugar lactose, and the oligomers (degree of polymerization (DP)2-8) are produced by glycosylation of lactose using the enzyme  $\beta$ -galactosidase (14). Inulin, also called long-chain FOS (lcFOS), corresponds to unprocessed chicory Inulin, mainly composed of fructans (DP2-60) ending with a terminal glucose monomer, whereas FOS are composed of partially hydrolysed Inulin (DP2-8) and more molecules end with a fructose rather than with a glucose monomer (15, 16).

In addition to origin and structure, the specific DP composition is believed to influence the prebiotic activity and the degree of fermentation of oligosaccharides, since distinct sensitivity of human gut bacteria to selected DP of oligosaccharides has been observed (13, 17, 18). However, the direct interactions of individual DP fractions with intestinal epithelial cells have not yet been investigated.

In the current study, we aimed to compare direct, microbiota-independent effects of different galacto-oligosaccharides, on dysregulated intestinal epithelial barrier function and the related inflammatory response. Monolayers of the human intestinal epithelial cell line, Caco-2, served as a model system for intestinal barrier function, while the fungal toxin deoxynivalenol (DON) was used as a model compound to impair the intestinal integrity as previously described by Akbari *et al.* (19). Considering the protective effects of GOS in this Caco-2 cell model, we compared these results to the effects of FOS and Inulin and further evaluated the effect of individual DP fractions of GOS (ranging from DP2 to DP6).



## Materials and Methods

### Deoxynivalenol (DON)

Purified DON (D0156; Sigma-Aldrich, St Luis, Mo, USA) was dissolved in pure ethanol (99.9%, JT Baker, Deventer, the Netherlands) and stored at -20°C. The mycotoxin DON was selected as model compound to impair intestinal barrier integrity in the cell culture experiments. DON was diluted to a concentration of 4.2  $\mu$ M in complete cell culture medium and added to the apical side as well as to the basolateral side of the transwell inserts for either 12 h or 24 h. This DON concentration was selected on the basis of our previous results and did not affect the viability of the Caco-2 cells (19).

### Oligosaccharides

Galacto-oligosaccharides (Vivinal® GOS syrup (VGOS, 59% GOS on dry matter) and purified Vivinal® GOS (PGOS, 97% GOS on dry matter) without the monomeric sugars glucose, galactose and lactose were provided by FrieslandCampina Domo (Borculo, The Netherlands). Fructo-oligosaccharides (FOS, Orafiti®P95) and Inulin (Orafiti®LGI) were obtained from Beneo Orafiti (Tienen, Belgium). The detailed composition of the applied oligosaccharides is summarized in Table 1 (related to Figure 1-5, 8 and 9) and Table 2 (related to Figure 6 and 7), and the oligosaccharide structures are schematically depicted in Supplementary Figure 1. The concentrations used in this study are calculated based on the pure oligosaccharide fractions.

### Purification of GOS

Purified GOS with < 3% (w/w dry matter) monomers and lactose (purified from the lactose-based prebiotic Vivinal® GOS syrup) were used. For the purification, Vivinal® GOS syrup was enzymatically treated with a lactase to hydrolyze the lactose into glucose and galactose, after which the monosaccharides were removed by nanofiltration on laboratory scale (18). By the purification process of Vivinal® GOS syrup, next to lactose, also a part of the DP2 GOS is removed as well (Figure 1).

### High-Performance Anion-Exchange Chromatography with Pulsed Amperometric Detection (HPAEC-PAD)

Specific chain length profiles were characterized by HPAEC using a Dionex ICS 3000 system (Dionex, Sunnyvale, CA, USA), equipped with a Dionex CarboPac PA-1 column (2  $\times$  250 mm) in combination with a CarboPac PA-1 guard column (2  $\times$  50 mm) and a ISC5000 ED detector (Dionex) in the PAD mode as previously described (20, 21). Characterization of individual peaks were concluded comparing the obtained HPAEC-PAD profiles with SEC GOS-DP fractions and mass spectrometry.

**Table 1.** Characteristics of the applied oligosaccharides

Products	Dry matter	Oligosaccharides (wt % on DM)	Mono- and Di-saccharides (w/w)	DP
<b>VGOS</b>	75%	59	glucose, galactose, lactose: 41%	2-8
<b>PGOS</b>	>98%	97	glucose, galactose, lactose: 3%	2-8
<b>FOS</b>	>98%	93.2	glucose, fructose, sucrose: 6.8%	2-8
<b>Inulin</b>	>98%	96	glucose, fructose, sucrose: 4%	2-60

**Table 2.** Percentages of DP composition in VGOS

Compound	wt % on DM
<b>Galacto-oligosaccharides</b>	61.9
<b>DP2 (including lactose)</b>	37.8
<b>DP3</b>	22.0
<b>DP4</b>	10.8
<b>DP5</b>	4.8
<b>DP6 and higher</b>	2.3
<b>Lactose in DP2</b>	15.8
<b>Glucose</b>	20.7
<b>Galactose</b>	1.1
<b>Total</b>	99.5%

### Size Exclusion Chromatography (SEC)

The oligosaccharides present in Vivinal® GOS syrup were separated by SEC. Vivinal® GOS syrup was fractionated using a XK50 column (length 60 cm, GE Healthcare, Pittsburgh, PA, USA) filled with Bio-Gel P-2 Gel Resin (Fine 45-90 µm, BioRad Laboratories, Hercules, CA, USA) connected to a AktaPrime Plus (GE Healthcare, Pittsburgh, PA, USA). The jacket of the column was connected to a water bath in order to maintain the temperature at 50°C. Diluted Vivinal® GOS syrup (approx. 30% on DM) was injected onto the column (flowrate:

1.0 ml/min) using a 2 ml sample loop and eluted with demineralized water. Sampling was based on refractive index and samples corresponding to the same DP were pooled and subsequently freeze dried.

### **The Caco-2 cell model**

Human epithelial colorectal adenocarcinoma (Caco-2) cells obtained from American Type Tissue Collection (Code HTB-37) (Manassas, VA, USA, passages 90-102) were used according to established methods, also described by Akbari *et al.* (19). In brief, cells were cultured in Dulbecco's Modified Eagle Medium (DMEM) and seeded at a density of  $0.3 \times 10^5$  cells into 0.3 cm<sup>2</sup> high pore density (0.4 mm) inserts with a polyethylene terephthalate membrane (BD Biosciences, Franklin Lakes, NJ, USA) placed in a 24-well plate. Caco-2 cells were maintained in a humidified atmosphere of 95% air and 5% CO<sub>2</sub> at 37°C. After 17–19 days of culturing, a confluent monolayer was obtained with a mean TEER exceeding 400  $\Omega \cdot \text{cm}^2$  measured by a Millicell-Electrical Resistance System voltohmmeter (Millipore, Temecular, CA, USA).

Dilutions of the oligosaccharides VGOS, PGOS, FOS and Inulin (0.5%, 1% and 2%) and different DP fractions of VGOS (either in equimolar concentrations as present in VGOS or in a concentration of 0.75%) were prepared by dissolving in complete cell culture DMEM. Subsequently, cells were pre-incubated with different oligosaccharides or DP fractions of VGOS from apical side as well as basolateral side of the transwell inserts for 24 h before being challenged with DON in the presence of the different oligosaccharides or DP fractions of VGOS for another 24 h or 12 h, respectively. Prior to the functional assays described below, the potential cytotoxicity of the different oligosaccharides or DP fractions of VGOS in Caco-2 cells had been evaluated by measuring lactate dehydrogenase (LDH) leakage (Promega Corp., Madison, WI, USA). These control experiments confirmed that none of the above oligosaccharides induced any cytotoxicity in Caco-2 cells at the concentrations used in the assays (data not shown).

### **Transepithelial Electrical Resistance (TEER) measurement**

The integrity of the Caco-2 cell monolayer grown on inserts was investigated by monitoring the TEER across the monolayer. A Millicell-ERS Volttohmmeter connected to a pair of chopstick electrodes was used to measure TEER values either 12 h or 24 h after DON stimulation with or without pretreatment with the different oligosaccharides or DP fractions of VGOS for 24 h. Results are expressed as a percentage of the initial value.

### **Paracellular tracer flux assay**

Transport studies from the apical side to the basolateral side of a Caco-2 cell monolayer were performed using a membrane-impermeable molecule, lucifer yellow (LY, molecular mass: 0.457 kDa, Sigma, St Luis, Mo, USA). LY was added at a concentration of 16  $\mu\text{g/ml}$  to the apical compartment (350  $\mu\text{l}$ ) in the transwell plate for 4 h and the paracellular flux was determined by measuring the fluorescence intensity in the basolateral compartment

with a spectrofluorimeter (FLUOstar Optima, BMG Labtech, Offenburg, Germany) set at excitation and emission wavelengths of 410 and 520 nm, respectively.

### Calcium switch assay

Caco-2 cells grown on inserts were pretreated with various concentrations (0.5%, 1% and 2%) of different oligosaccharides (VGOS, PGOS, FOS and Inulin) on both sides of the transwell inserts for 24 h. Subsequently, Caco-2 cells were exposed transiently for 20 minutes to 2 mM ethylene glycol-bis(2-aminoethyl ether)N,N,N',N'-tetraacetic acid (EGTA) (Sigma, St Luis, Mo, USA) in calcium and magnesium free Hanks' Balanced Salt Solution (HBSS) (Gibco, Invitrogen, Carlsbad, CA, USA) to disrupt tight junction (TJ) proteins as previously described (8). At the end of the incubation period, cells were rinsed and allowed to recover in either complete cell culture DMEM (containing 2 mM  $\text{CaCl}_2$ ) or in DMEM supplemented with the addition of various concentrations (0.5%, 1% and 2%) of different oligosaccharides. During this recovery period, reassembly of TJs and restoration of barrier function were determined by measuring TEER at various time points (2, 4, 6, 12 and 24 h). The results are expressed as a percentage of initial value.

### CXCL8 secretion

The inflammatory marker, CXCL8, was quantified in the medium of the apical as well as the basolateral sides of the Caco-2 transwell inserts in response to the treatments. CXCL8 concentrations were measured by using the human IL-8 ELISA (BD Biosciences, Pharmingen, San Diego, CA, USA) according to manufacturer's instructions.

### Statistical analysis

Experimental results are expressed as mean  $\pm$  SEM. Analyses were performed by using GraphPad Prism (version 6.05) (GraphPad, La Jolla, CA, USA). Differences between groups were statistically determined by using One-way ANOVA, with Bonferroni post hoc test. Results were considered statistically significant when  $P < 0.05$ .

## Results

### VGOS and PGOS characteristics

Figure 1 shows the HPAEC-PAD chromatograms of VGOS and PGOS and clearly demonstrates that both GOS samples are complex mixtures of oligosaccharides with a DP of mainly 2-6 and various isomers per DP (Supplementary Figure 1). PGOS, derived from VGOS, is lacking predominantly the monosaccharides and lactose, although also some other components of GOS-DP2 were (partly) removed.

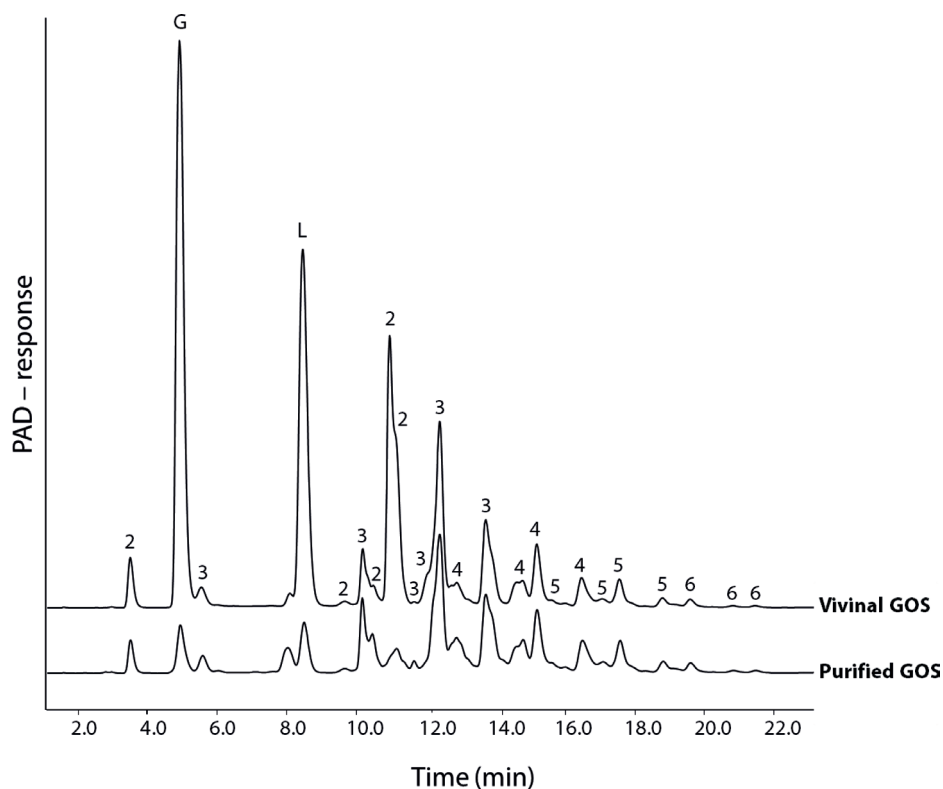


**Figure 1.** VGOS and PGOS characteristics. HPAEC-PAD elution patterns of Vivinal® GOS syrup and purified GOS. Numbers 2-6 correspond to galacto-oligosaccharides having a degree of polymerization from 2 to 6. G and L represent galactose/glucose and lactose, respectively.

### Different effects of VGOS and PGOS on the DON-induced impairment of the Caco-2 cell monolayer integrity

Pretreatment with VGOS prevented the DON-induced decrease in TEER values in a concentration-dependent manner as depicted in Figure 2A, while only the highest concentration of PGOS significantly attenuated the DON-induced TEER decrease.

However, this effect was significantly lower compared to 2% VGOS (Figure 2A). In line with the effects on the observed TEER values, the DON-induced increase in tracer transport (LY) was significantly decreased by 1% VGOS, 2% VGOS and 2% PGOS (Figure 2B).

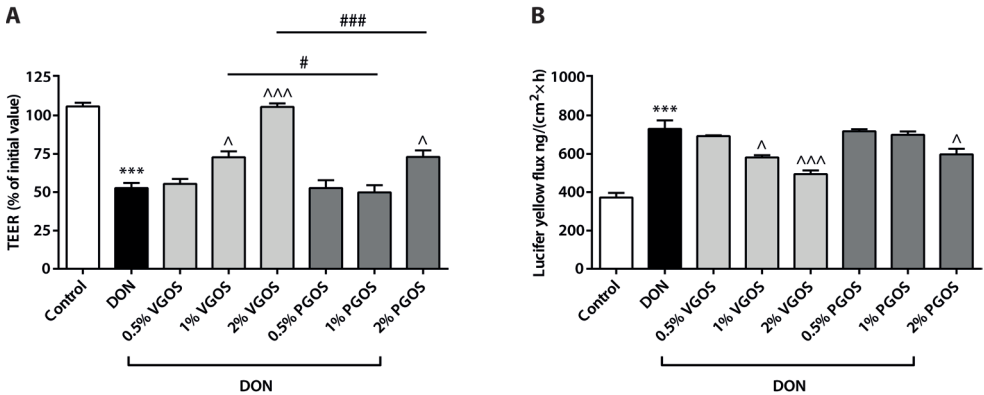


**Figure 2.** Different effects of VGOS and PGOS on the DON-induced impairment of the Caco-2 cell monolayer integrity. Caco-2 cells were pretreated apically and basolaterally with increasing concentrations (0.5%, 1% and 2%) of VGOS or PGOS (24 h) prior to the addition of DON (4.2  $\mu$ M) (apical and basolateral compartments) for another 24 h. Subsequently, TEER (A) and translocation of lucifer yellow from the apical to the basolateral compartment (B) were measured. Results are expressed as a percentage of initial value (TEER) or the amount of tracer transported [ng/(cm<sup>2</sup>×h)] as mean  $\pm$  SEM of three independent experiments, each performed in triplicate. (\*\*\*P < 0.001; significantly different from the unstimulated cells. ^P < 0.05, ^^^P < 0.001; significantly different from the DON-stimulated cells. #P < 0.05, ###P < 0.001; significantly different from each other).

### VGOS time-dependently accelerates TJs reassembly after calcium deprivation in Caco-2 cells

It was demonstrated that 2% VGOS caused a time-dependent acceleration in TJs reassembly over a period of 24 h (Figure 3A) and the first significant effect on TEER restoration was already observed 4 h after calcium recovery. In addition, 1% VGOS also showed a significant improvement in TEER values after 24 h recovery. Caco-2 cells incubated with 2% PGOS showed only improved restoration in TEER after 24 h recovery, whereas the other tested PGOS concentrations (0.5% and 1%) did not accelerate the TJs reassembly (Figure 3B).

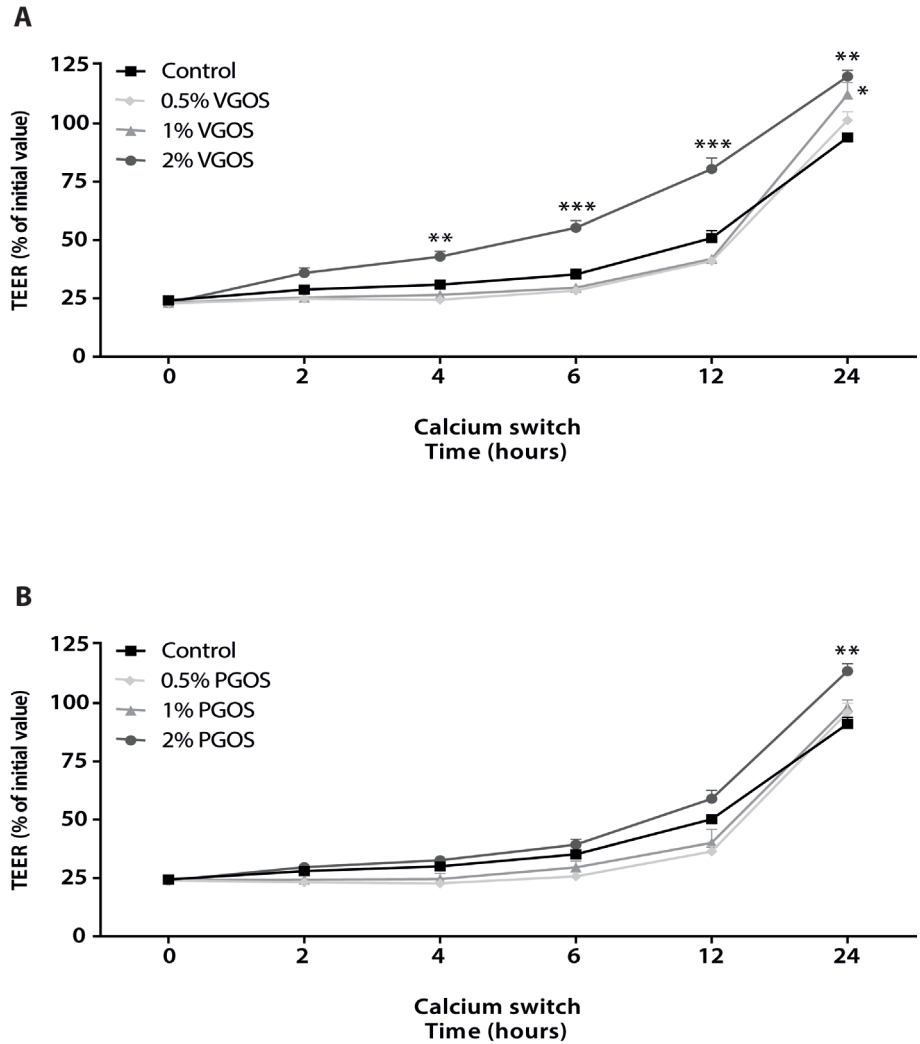


**Figure 3.** VGOS time-dependently accelerated TJs reassembly after calcium deprivation in Caco-2 cells. Caco-2 cells were pretreated apically and basolaterally with increasing concentrations (0.5%, 1% and 2%) of VGOS (A) or PGOS (B) (24 h) prior to transient calcium deprivation with HBSS-EGTA to disrupt TJ proteins. TEER was measured at the indicated time points (0, 2, 4, 6, 12 and 24 h) during recovery in complete, calcium containing DMEM medium either with VGOS (A) or PGOS (B). Results are expressed as a percentage of initial value as mean  $\pm$  SEM of three independent experiments, each performed in triplicate (\* $P < 0.05$ , \*\* $P < 0.01$ , \*\*\* $P < 0.001$ ; significantly different from the untreated cells).



### VGOS and not PGOS is able to suppress the DON-induced increase in CXCL8 release by Caco-2 cells

The DON-induced increased levels of secreted CXCL8 could be only prevented by incubation with 1% and 2% VGOS as observed by a concentration-dependent decrease in CXCL8 release on both sides (Figure 4A, B). PGOS exposure to Caco-2 cells did not affect CXCL8 secretion neither into the apical nor the basolateral compartment of the transwell system (Figure 4A, B).

### Supplementation of glucose, galactose and lactose to PGOS does not mimic the effect of VGOS against DON-induced barrier disruption and CXCL8 release

Supplementation of glucose, galactose and lactose (in equimolar concentrations as present in 2% VGOS, Table 2) to 2% PGOS did not improve the effect of PGOS on the DON-induced gut barrier impairment as observed by TEER (Figure 5A) and paracellular flux of LY (Figure 5B). In addition, this supplementation to PGOS did not mimic the protective effect of VGOS against the DON-induced increase in CXCL8 release (Figure 5C, D).

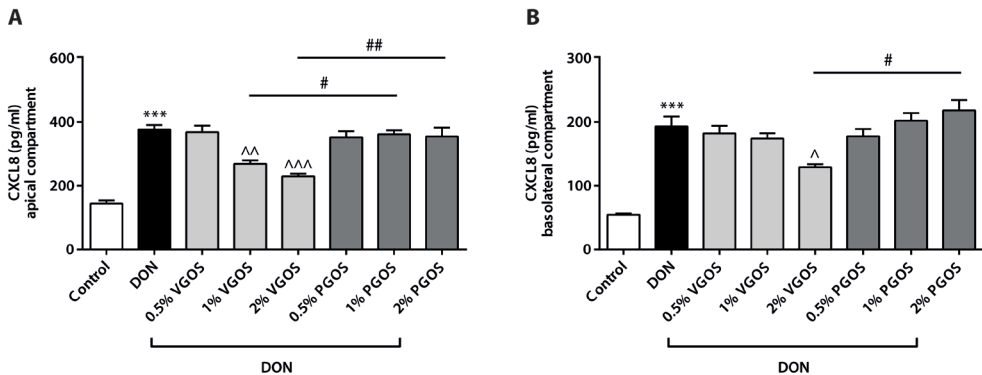


**Figure 4.** VGOS was able to suppress the DON-induced increase in CXCL8 release by Caco-2 cells. Caco-2 cells were pretreated apically and basolaterally with increasing concentrations (0.5%, 1% and 2%) of VGOS or PGOS (24 h) prior to the addition of DON (4.2  $\mu$ M) (apical and basolateral compartments) for another 24 h. CXCL8 secretion into medium of apical (A) and basolateral (B) compartments were measured by ELISA. Results are expressed as pg/ml as mean  $\pm$  SEM of three independent experiments, each performed in triplicate (\*\*\*P < 0.001; significantly different from the unstimulated cells. ^P < 0.05, ^^P < 0.01, ^^P < 0.001; significantly different from the DON-stimulated cells. #P < 0.05, ##P < 0.01; significantly different from each other).

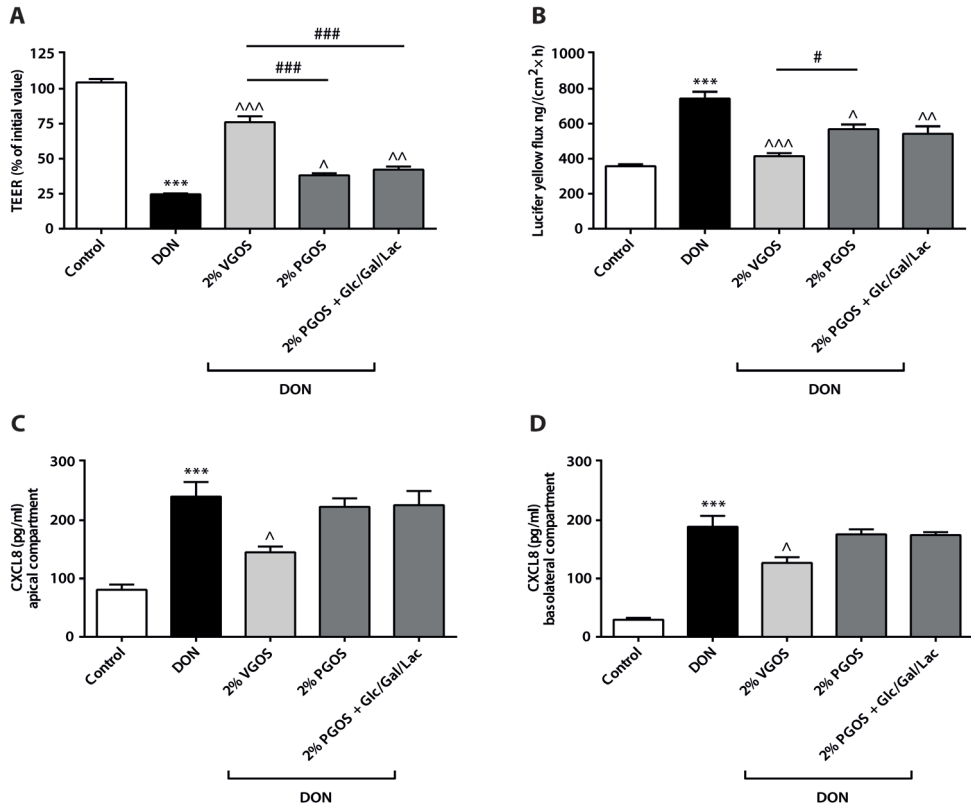


**Figure 5.** Supplementation of glucose, galactose and lactose to PGOS did not mimic the effect of VGOS against DON-induced barrier disruption and CXCL8 release. Caco-2 cells were pretreated apically and basolaterally with VGOS and PGOS with or without supplementation with glucose (Glc), galactose (Gal) and lactose (Lac) (24 h) prior to the addition of DON (4.2  $\mu$ M) (apical and basolateral compartments) for another 24 h. Subsequently, TEER (A), transport of lucifer yellow (B) and CXCL8 release into the apical (C) and basolateral (D) compartments were measured. Results are expressed as a percentage of initial value (TEER), the amount of tracer transported [ng/(cm<sup>2</sup>×h)] or pg/ml CXCL8 as mean  $\pm$  SEM of three independent experiments, each performed in triplicate (\*\*\*P < 0.001; significantly different from the unstimulated cells. ^P < 0.05, ^^P < 0.01, ^^^P < 0.001; significantly different from the DON-stimulated cells. #P < 0.05, ###P < 0.001; significantly different from each other).

### **Combined DP fractions of VGOS mimic VGOS in preventing DON-induced barrier disruption and CXCL8 release, whereas only individual DP2 and DP3 prevent the DON-induced barrier disruption**

Pretreatment with DP2 or DP3 (in equimolar concentrations as present in VGOS) prevented the DON-induced decrease in TEER values (Figure 6A). The DON-induced increase in tracer transport was significantly decreased by DP2, whereas the effect of DP3 was not significantly different ( $P = 0.076$ ) (Figure 6C). None of the individual DP4, DP5 or DP6 induced a preventive effect on the DON-induced intestinal epithelial barrier impairment as observed by TEER (Figure 6A) and paracellular flux of LY (Figure 6C) and none of the individual DP fractions (ranging from DP2 to DP6) was able to prevent the DON-induced increase in secreted CXCL8 (Figure 6E, G). The combination of different DP fractions of GOS (ranging from DP2 to DP6 in equimolar concentrations as present in VGOS) with or without glucose and galactose supplementation did show a protective effect against DON-induced gut barrier impairment and CXCL8 release comparable to the effect of VGOS (Figure 6B, D, F, H). In addition, the effects of individual DP fractions and the combined DP fractions were also determined in non-treated Caco-2 cells. These results indicated that neither individual DP fractions nor the combination of different DP fractions with or without glucose and galactose supplementation affect gut barrier function and CXCL8 release (Supplementary Figure 2A-H).

### **Different effects on the Caco-2 cell monolayer induced by individual DP fractions of VGOS with equal concentrations**

Next to investigating the effect of DPs in equimolar concentrations as present in VGOS, we studied the effects of the individual DP fractions in equal concentrations of 0.75% to clarify concentration-dependent effects of DP fractions. Pretreatment with 0.75% of individual DP2, DP3 or DP5 significantly prevented the DON-induced decrease in TEER values and DON-induced increase in tracer transport (Figure 7A, B) and these effects were similar to that of 0.75% VGOS (Figure 7A, B). DP4 (0.75%) did not significantly affect the DON-induced gut barrier impairment as measured by TEER (Figure 7A) and paracellular flux of LY (Figure 7B). Additionally, neither 0.75% VGOS nor the individual DP fractions (0.75%, ranging from DP2 to DP5) attenuated the DON-induced increase in CXCL8 release (Figure 7C, D).

### **FOS and Inulin characteristics**

Figure 8 shows the HPAEC-PAD chromatograms of FOS (A) and Inulin (B) and demonstrates that FOS clearly contain oligosaccharides up to DP7-8, either built up by fructose residues only ( $F_n$  series) as well as fructose residues with a terminally linked glucose moiety ( $GF_n$  series). Inulin mainly consists of fructose chains terminated with a glucose molecule representing a wide range of DPs (Supplementary Figure 1).

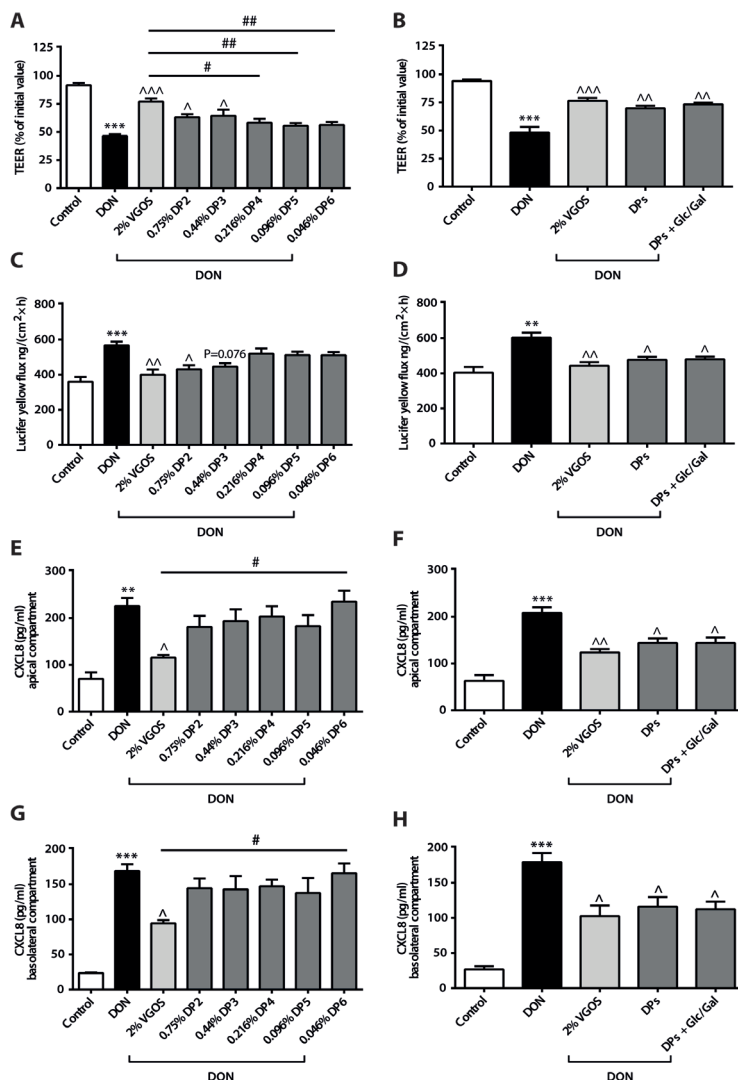


**Figure 6.** Combined DP fractions of VGOS mimicked VGOS effects in preventing DON-induced barrier disruption and CXCL8 release, whereas only individual DP2 and DP3 can prevent DON-induced barrier disruption. Caco-2 cells were pretreated apically and basolaterally with VGOS, individual DP fractions of GOS (ranging from DP2 to DP6) and combination of different DP fractions (DP2 to DP6) with or without supplementation with glucose (Glc) and galactose (Gal) (24 h) prior to the addition of DON (4.2  $\mu$ M) (apical and basolateral compartments) for 12 h. Subsequently, TEER (A, B), transport of lucifer yellow (C, D) and CXCL8 release into the apical (E, F) and basolateral (G, H) compartments were measured. Results are expressed as a percentage of initial value (TEER), the amount of tracer transported [ng/(cm<sup>2</sup>×h)] or pg/ml CXCL8 as mean  $\pm$  SEM of three independent experiments, each performed in triplicate (\*\* $P$  < 0.01, \*\*\* $P$  < 0.001; significantly different from the unstimulated cells.  $\wedge P$  < 0.05,  $\wedge\wedge P$  < 0.01,  $\wedge\wedge\wedge P$  < 0.001; significantly different from the DON-stimulated cells.  $\#P$  < 0.05,  $\#\#P$  < 0.01; significantly different from each other).

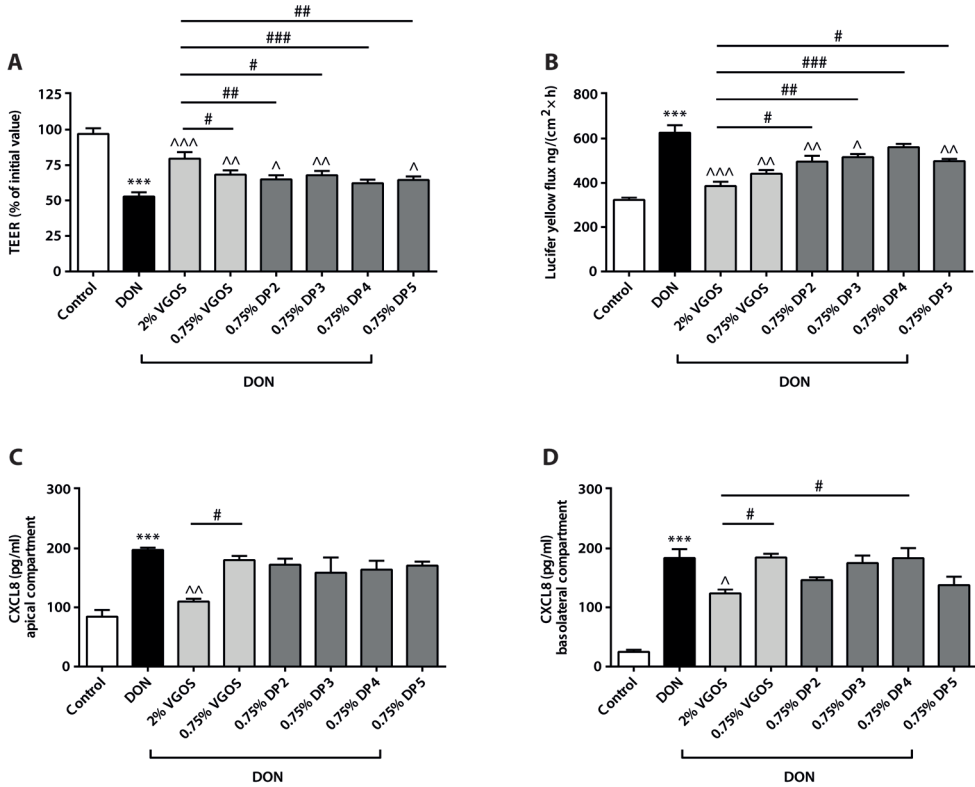


**Figure 7.** Different effects on the Caco-2 cell monolayer induced by individual DP fractions of VGOS with equal concentrations. Caco-2 cells were pretreated apically and basolaterally with VGOS (0.75% and 2%) or individual DP fractions of VGOS (0.75%, ranging from DP2 to DP5) (24 h) prior to the addition of DON (4.2  $\mu$ M) (apical and basolateral compartments) for 12 h. Subsequently, TEER (A), transport of lucifer yellow (B) and CXCL8 secretion into the medium of apical (C) and basolateral (D) compartments were measured. Results are expressed as a percentage of initial value (TEER), the amount of tracer transported [ng/(cm<sup>2</sup>×h)] or pg/ml CXCL8 as mean  $\pm$  SEM and are representative of two independent experiments, each performed in triplicate (\*\*\* $P$  < 0.001; significantly different from the unstimulated cells.  $\wedge P$  < 0.05,  $\wedge\wedge P$  < 0.01,  $\wedge\wedge\wedge P$  < 0.001; significantly different from the DON-stimulated cells. # $P$  < 0.05, ## $P$  < 0.01, ### $P$  < 0.001; significantly different from each other).

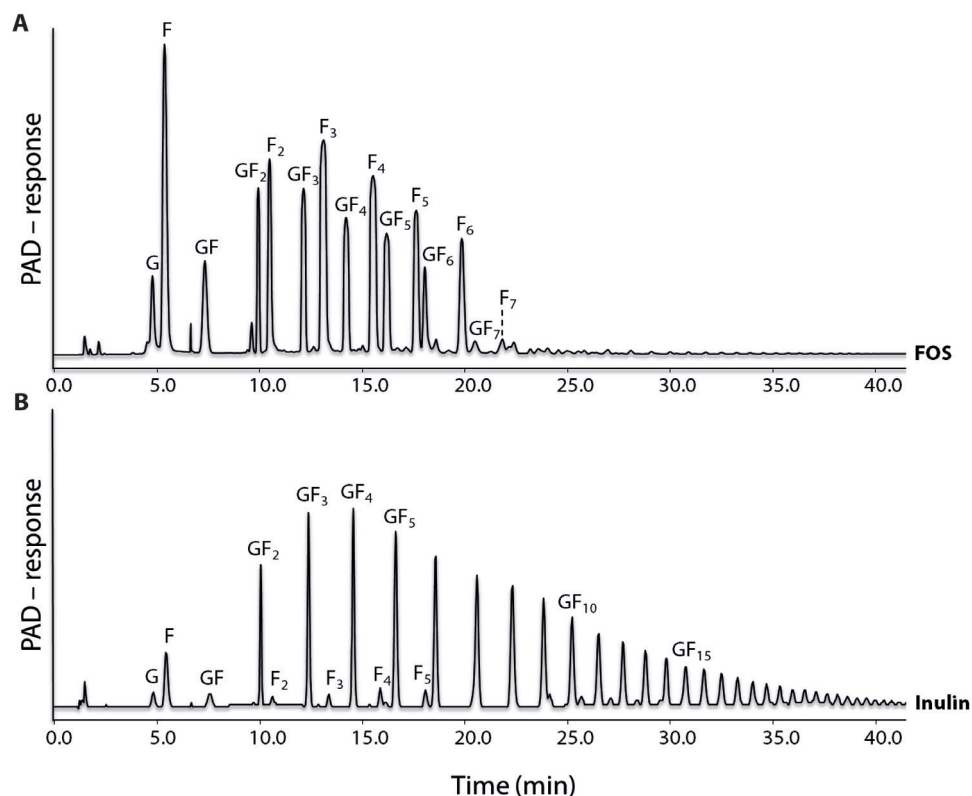


**Figure 8.** FOS and Inulin characteristics. HPAEC-PAD elution patterns of FOS (A) and Inulin (B). The  $F_n$  series represent oligomers consisting of fructose only, whereas the  $GF_n$  series represent fructose oligomers terminated with a terminal glucose molecule. The number of fructose units within an oligomer is indicated by  $n$ .

### Different effects of FOS and Inulin on the DON-induced barrier disruption, TJs reassembly and CXCL8 release

Furthermore, the microbiota-independent effects of GOS were compared to oligosaccharides with a different structure and DP, including Inulin and FOS. The highest concentration of FOS (2%) significantly modulated the DON-induced epithelial barrier disruption as measured by TEER values and paracellular flux of LY, whereas, none of the tested Inulin concentrations induced a preventive effect on the barrier integrity of the Caco-2 monolayer (Figure 9A, B). Caco-2 cells incubated with 2% FOS or 2% Inulin showed both improved restoration in TEER 24 h after calcium recovery, whereas the other tested concentrations (0.5% and 1%) did not accelerate the TJs reassembly after calcium deprivation (Figure 9C, D). DON-induced increase in CXCL8 secretion was affected neither by FOS nor by Inulin (Figure 9E, F).

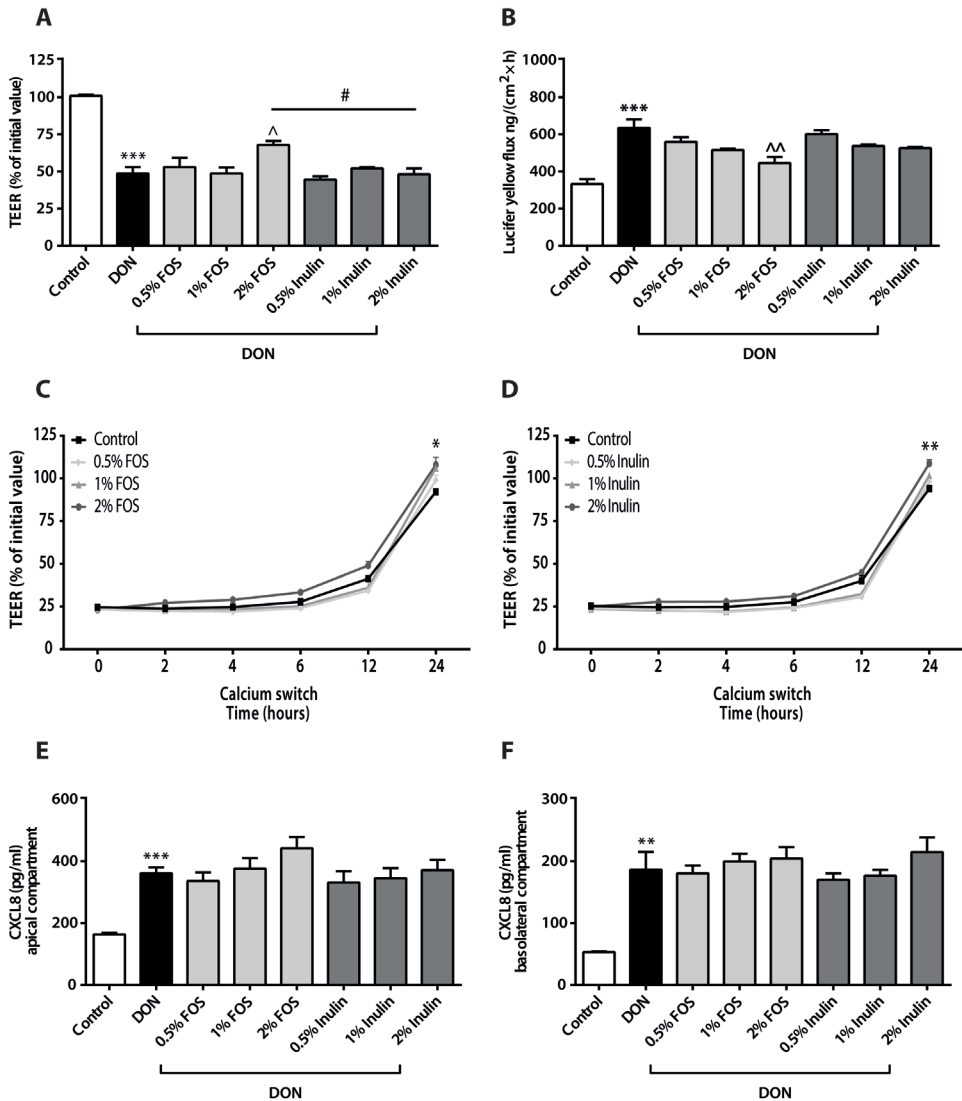


**Figure 9.** Different effects of FOS and Inulin on the DON-induced barrier disruption, TJs reassembly and CXCL8 release. Caco-2 cells were pretreated apically and basolaterally with increasing concentrations (0.5%, 1% and 2%) of FOS or Inulin (24 h) prior to the addition of DON (4.2 μM) (apical and basolateral compartments) for another 24 h (A, B, E, F) or transient calcium deprivation with HBSS-EGTA to disrupt TJ proteins (C, D). Subsequently, TEER values at the indicated time points (A, C, D), transport of lucifer yellow (B) and CXCL8 secretion into medium of apical (E) and basolateral (F) compartments were measured. Results are expressed as a percentage of initial value (TEER), the amount of tracer transported [ng/(cm<sup>2</sup>×h)] or pg/ml CXCL8 as mean ± SEM of three independent experiments, each performed in triplicate (\*P < 0.05, \*\*P < 0.01, \*\*\*P < 0.001; significantly different from the unstimulated cells. ΔP < 0.05, ΔΔP < 0.01; significantly different from the DON-stimulated cells. #P < 0.05; significantly different from each other).



## Discussion

Non-digestible oligosaccharides, including GOS and mixtures of GOS/lcFOS, are commonly used in infant formula as an alternative for HMOs, which are not commercially available (12, 22). Gut health promoting effects of GOS and GOS/lcFOS are not limited to the modulation of the intestinal microbiota, since also direct interaction between intestinal epithelial cells (IEC) and these oligosaccharides has recently been described (8-11). The prebiotic activity of GOS and FOS are believed to be determined by their unique structure and specific DP composition (12, 13, 17, 18). However, the effect of structure and DP composition of GOS or FOS on direct interaction with IEC has never been studied. Hence, in the current study the direct effects of Vivinal® GOS syrup, purified Vivinal® GOS and their DP fractions were compared in a DON-stimulated Caco-2 cell model for intestinal barrier dysfunction as previously described (19). We aimed to understand which DP fractions of VGOS are responsible for the observed protective effects. Furthermore, the effect of oligosaccharides with a different structure and DP than GOS, such as Inulin and FOS, were examined in this Caco-2 cell model.

The mycotoxin DON was used as a model compound to impair the intestinal integrity. DON is a 12,13-epoxytrichothecene and is known to directly impair TJ integrity and to induce an inflammatory response (19, 23, 24). Our group recently found that GOS stimulate the TJs reassembly and in turn mitigate the deleterious effects of DON on the intestinal barrier of Caco-2 cells and these effects are not related to a direct interaction between DON and GOS (8).

GOS are derived from lactose and consist of a chain of galactose units with a terminal glucose monomer, different glycosidic linkages (e.g.  $\beta(1-4)$  and  $\beta(1-6)$ ), and the DP varies between 2-8 (14, 25). GOS structures have the lactose building block in common with HMOs, although the latter is more complex, since HMO oligomers may also have galactose and N-acetylglucosamine (GlcNAc) in their backbone, which are further substituted with fructose and neuraminic acid (2, 26). Holscher *et al.* (27) found differential roles for specific HMOs in the differentiation and barrier function of Caco-2 cells.

In the current study, VGOS was most effective and purified GOS (PGOS) was significantly less effective with respect to the improvement of the impairment of the Caco-2 cell monolayer integrity as well as the modulation of immune responses, including CXCL8 release. The monosaccharides (glucose and galactose) and disaccharide (lactose) present in Vivinal® GOS syrup were not responsible for this superior effect of VGOS over PGOS, since combined supplementation of glucose, galactose and lactose to PGOS did not mimic the effect of VGOS against the DON-induced effects, as shown by the current experiments. We previously confirmed that similar concentrations of these saccharides present in the 2% GOS solution did not affect the DON-induced impairment of Caco-2 monolayer integrity (8). Comparing the HPAEC elution patterns (Figure 1), another difference between VGOS and PGOS is the amount of DP2, which is partly lost during the purification process. It could therefore be hypothesized that DP2 is driving the

higher potency of VGOS. In our experiments we demonstrated that isolated DP2 and DP3 fractions (in equimolar concentrations as present in VGOS) significantly prevented the DON-induced barrier disruption, whereas no effect of the larger DPs (equal or above DP4) was observed. The prominent effect of DP2 and DP3 seems to be related to their high prevalence in the VGOS mixture. When we tested equal concentrations (0.75%) of all available DPs, only DP4 was not effective in preventing the Caco-2 monolayer integrity disruption by DON.

Related to our results, the DP concentration and to a lesser extent the DP length may be crucial for the observed protective effects of galacto-oligosaccharides. Previous studies have already indicated that effect of individual oligosaccharides on the intestinal microbiota can be related to their DP composition. Ladirat *et al.* (18) described that addition of GOS or a DP3 fraction to a human faecal inoculum resulted in the highest *Bifidobacterium* spp. increase, whereas the DP4 and DP5 fractions displayed the lowest increase. In line with our results, they did not find significant differences between the DP GOS fractions and VGOS at similar concentrations. In a study with maltose-based oligosaccharides, DP3 oligomers showed the highest selectivity towards bifidobacteria, and oligosaccharides above DP7 did not promote the growth of beneficial bacteria, including bifidobacteria (13). In contrast, the presence of the larger DP fractions within GOS were effective in restoring the microbiota following an antibiotic-induced dysbacteriosis (18), whereas Sinclair *et al.* (28) showed that in particular higher DP GOS fractions were capable of inhibiting the *in vitro* binding of *Vibrio cholerae* toxin to its GM1 receptor. We therefore speculate that the DP length of oligosaccharides is related to different physiological effects.

In contrast to galacto-oligosaccharides, Inulin (or IcFOS), consists of a mixture of fructose residues linked by  $\beta(2-1)$  fructosyl-fructose glycosidic bonds with a glucose monomer at the end of almost each fructose chain within a DP range of 2-60. FOS has been produced from Inulin by partial enzymatic hydrolysis and differs from Inulin to its degree of polymerization (DP2-8) and fructose oligomers occur with or without the presence of a terminal glucose moiety (Figure 8) (16, 20). Schematic structures of GOS, FOS and Inulin are depicted in Supplementary Figure 1. Only 2% FOS showed moderate, but significant, protective effects against intestinal barrier dysfunction as observed by TEER recovery and decreased LY paracellular flux, whereas none of the mentioned parameters were affected by Inulin. Since the DP of both GOS and FOS varies from 2 to 8, we can speculate that these smaller DP fractions (DP2-8) are important for inducing the protective effects on barrier integrity compared to higher DP fractions (DP9-60). Also in a different experimental setting, Shoaf *et al.* (29) described that GOS were most effective in preventing bacterial colonization and pathogen invasion by their anti-adhesive capacity compared to the other oligosaccharides, including FOS, Inulin, lactulose and raffinose.

With regard to the potential anti-inflammatory properties of oligosaccharides, our results demonstrated that only VGOS was able to prevent the DON-induced CXCL8 release, whereas PGOS, the separate GOS DP fractions, FOS and Inulin did not prevent CXCL8

secretion. The anti-inflammatory activity of VGOS was also observed by Vendrig *et al.* (30) since peripheral blood mononuclear cells (PBMCs) derived from VGOS-treated foals were less responsive to a lipopolysaccharide challenge and did show lower IFN- $\gamma$  and IL-6 mRNA expression levels. Differences in chain length between different FOS-products could be responsible for differential effects in skewing the cytokine balance, since Vogt *et al.* (20) found a positive correlation between chain length of FOS and IL-10/IL-12 ratios in human PBMCs. Different *in vitro* and *ex vivo* studies displayed that short chain FOS and long chain FOS are able to induce a more anti-inflammatory or pro-inflammatory condition, respectively (20, 31, 32). In addition, higher concentrations of Inulin or short chain-FOS (10%) did significantly decrease the CXCL8 gene expression induced by *Citrobacter rodentium* (33) and in unstimulated Caco-2 cells, FOS reduced the CXCL8, IL-12 and TNF- $\alpha$  gene expression via activation of peptidoglycan recognition protein 3 (PGlyRP3) and peroxisome proliferator-activated receptor  $\gamma$  (PPAR $\gamma$ ) (11). In the presence of a GOS/lcFOS mixture, a potential role for Toll-like receptor 9 (TLR9) and galectin-9 in modulating cytokine production has been demonstrated (34, 35). In contrast, Ortega-González *et al.* (36) hypothesized that GOS and FOS are TLR4 ligands in intestinal epithelial cells, which may be a relevant mechanism for the immunomodulatory effects of prebiotics. However, this latter mechanism cannot explain our results in the Caco-2 cell model, since these cells do not express TLR4 (37). The direct effect of VGOS on cytokine expression and release is possibly mediated by other pattern recognition receptor(s) and this signaling pathway seems to be galacto-oligosaccharide-specific.

In summary, this study for the first time compared direct, microbiota-independent effects, of defined oligosaccharides, including GOS (Vivinal® GOS syrup (VGOS) and purified Vivinal® GOS (PGOS)), and their related DPs, as well the plant-derived oligosaccharides FOS and Inulin on intestinal epithelial cells. It can be concluded that the tested oligosaccharides have different capacities to regulate the DON-disrupted epithelial monolayer and the related immune response. VGOS showed the most significant protective effect on all tested parameters in a concentration-dependent manner. Overall, differences in oligosaccharide structure and size result in significant changes in the direct, microbiota-independent effects.

## Acknowledgements

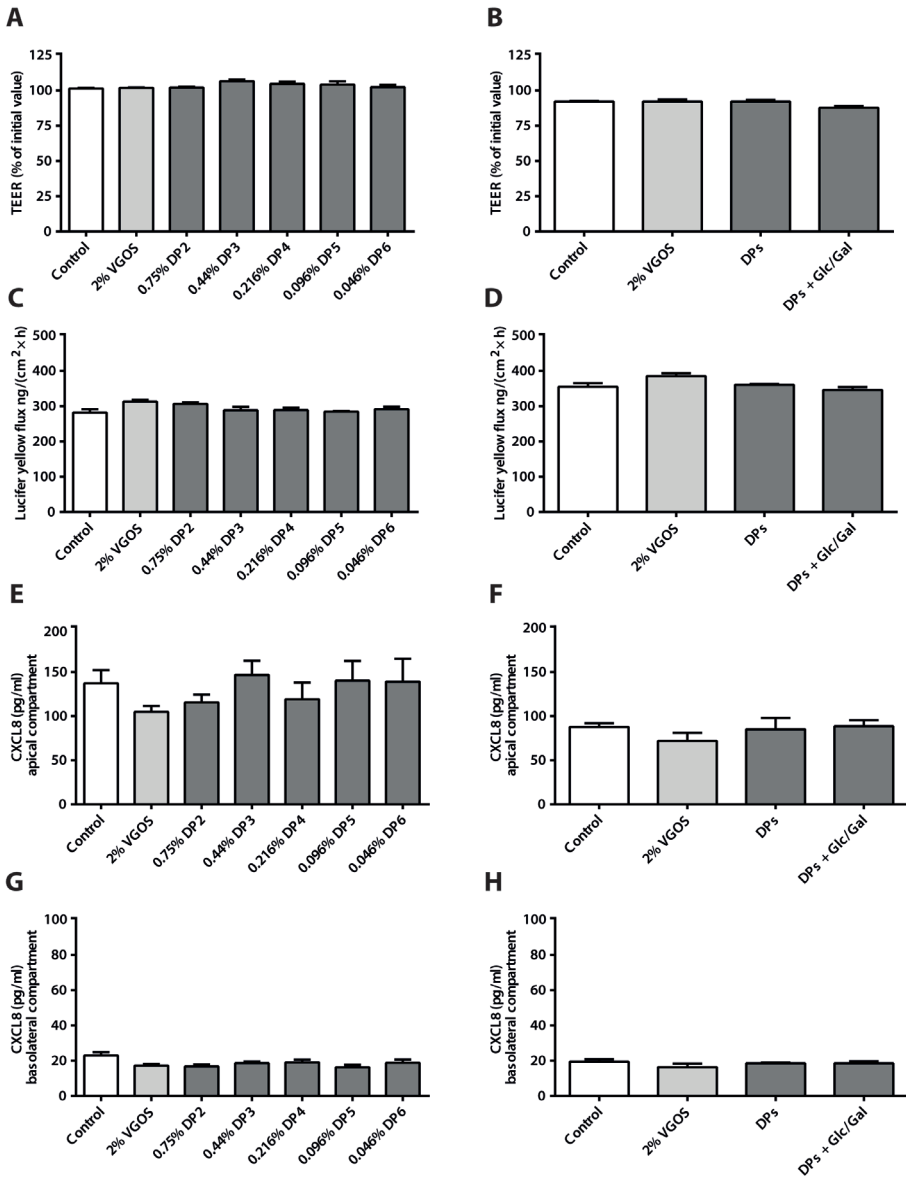
The authors would like to thank Eric Benjamins and Miranda Janssen of FrieslandCampina for the separation of the DP GOS fractions. The project is jointly funded by the European Union, European Regional Development Fund and The Ministry of Economic Affairs, Agriculture and Innovation, Peaks in the Delta, the Municipality of Groningen, the Provinces of Groningen, Fryslân and Drenthe, the Dutch Carbohydrate Competence Center (CCC WP25; [www.cccresearch.nl](http://www.cccresearch.nl)), Nutricia Research and FrieslandCampina.

## References

1. Bode L. The functional biology of human milk oligosaccharides. *Early Hum Dev* 2015;91:619-622.
2. Boehm G, Stahl B. Oligosaccharides from milk. *J Nutr* 2007;137:S847-S849.
3. Boehm G, Fanaro S, Jelinek J, Stahl B, Marini A. Prebiotic concept for infant nutrition. *Acta Paediatr* 2003;91:64-67.
4. Fanaro S, Boehm G, Garssen J, Knol J, Mosca F, Stahl B, Vigi V. Galacto-oligosaccharides and long-chain fructo-oligosaccharides as prebiotics in infant formulas: a review. *Acta Paediatr* 2005;94:22-26.
5. Ben XM, Zhou XY, Zhao WH, Yu WL, Pan W, Zhang WL, Wu SM, Van Beusekom CM, Schaafsma A. Supplementation of milk formula with galacto-oligosaccharides improves intestinal micro-flora and fermentation in term infants. *Chin Med J (Engl)* 2004;117:927-931.
6. Moro G, Minoli I, Mosca M, Fanaro S, Jelinek J, Stahl B, Boehm G. Dosage-related bifidogenic effects of galacto- and fructooligosaccharides in formula-fed term infants. *J Pediatr Gastroenterol Nutr* 2002;34:291-295.
7. Fanaro S, Marten B, Bagna R, Vigi V, Fabris C, Pena-Quintana L, Arguelles F, Scholz-Ahrens KE, Sawatzki G, Zelenka R, et al. Galacto-oligosaccharides are bifidogenic and safe at weaning: a double-blind randomized multicenter study. *J Pediatr Gastroenterol Nutr* 2009;48:82-88.
8. Akbari P, Braber S, Alizadeh A, Verheijden KA, Schoterman MH, Kraneveld AD, Garssen J, Fink-Gremmels J. Galacto-oligosaccharides Protect the Intestinal Barrier by Maintaining the Tight Junction Network and Modulating the Inflammatory Responses after a Challenge with the Mycotoxin Deoxynivalenol in Human Caco-2 Cell Monolayers and B6C3F1 Mice. *J Nutr* 2015;145:1604-1613.
9. Bhatia S, Prabhu PN, Benefiel AC, Miller MJ, Chow J, Davis SR, Gaskins HR. Galacto-oligosaccharides may directly enhance intestinal barrier function through the modulation of goblet cells. *Mol Nutr Food Res* 2015;59:566-573.
10. Varasteh S, Braber S, Garssen J, Fink-Gremmels J. Galacto-oligosaccharides exert a protective effect against heat stress in a Caco-2 cell model. *J Funct Foods* 2015;16:265-277.
11. Zenhom M, Hyder A, de Vrese M, Heller KJ, Roeder T, Schrezenmeier J. Prebiotic oligosaccharides reduce proinflammatory cytokines in intestinal Caco-2 cells via activation of PPARgamma and peptidoglycan recognition protein 3. *J Nutr* 2011;141:971-977.
12. Boehm G, Moro G. Structural and functional aspects of prebiotics used in infant nutrition. *J Nutr* 2008;138:S1818-S1828.
13. Sanz ML, Cote GL, Gibson GR, Rastall RA. Influence of glycosidic linkages and molecular weight on the fermentation of maltose-based oligosaccharides by human gut bacteria. *J Agric Food Chem* 2006;54:9779-9784.
14. Torres DPM, Goncalves MP, Teixeira JA, Rodrigues LR. Galacto-Oligosaccharides: Production, Properties, Applications, and Significance as Prebiotics. *Compr Rev Food Sci Food Saf* 2010;9:438-454.
15. Roberfroid MB. Inulin-type fructans: Functional food ingredients. *J Nutr* 2007;137:S2493-S2502.
16. Watzl B, Gierbach S, Roller M. Inulin, oligofructose and immunomodulation. *Br J Nutr* 2005;93:S49-S55.
17. Pompei A, Cordisco L, Raimondi S, Amaretti A, Pagnoni UM, Matteuzzi D, Rossi M. *In vitro* comparison of the prebiotic effects of two inulin-type fructans. *Anaerobe* 2008;14:280-286.
18. Ladirat SE, Schols HA, Nauta A, Schoterman MHC, Schuren FHJ, Gruppen H. *In vitro* fermentation of galacto-oligosaccharides and its specific size-fractions using non-treated and amoxicillin-treated human inoculum. *Bioact Carbohydr Dietary Fibre* 2014;3:59-70.
19. Akbari P, Braber S, Gremmels H, Koelink PJ, Verheijden KA, Garssen J, Fink-Gremmels J. Deoxynivalenol: a trigger for intestinal integrity breakdown. *FASEB J* 2014;28:2414-2429.

20. Vogt L, Ramasamy U, Meyer D, Pullens G, Venema K, Faas MM, Schols HA, de Vos P. Immune modulation by different types of beta 2-1 fructans is toll-like receptor dependent. *PLoS One* 2013;8:e68367.
21. Ladirat SE, Schuren FH, Schoterman MH, Nauta A, Gruppen H, Schols HA. Impact of galacto-oligosaccharides on the gut microbiota composition and metabolic activity upon antibiotic treatment during *in vitro* fermentation. *FEMS Microbiol Ecol* 2014;87:41-51.
22. Mussatto SI, Mancilha IM. Non-digestible oligosaccharides: A review. *Carbohydr Polym* 2007;68:587-597.
23. Pestka JJ. Deoxynivalenol: mechanisms of action, human exposure, and toxicological relevance. *Arch Toxicol* 2010;84:663-679.
24. Maresca M, Fantini J. Some food-associated mycotoxins as potential risk factors in humans predisposed to chronic intestinal inflammatory diseases. *Toxicon* 2010;56:282-294.
25. Coulier L, Timmermans J, Bas R, Van Den Dool R, Haaksman I, Klarenbeek B, Slaghek T, Van Dongen W. In-depth characterization of prebiotic galacto-oligosaccharides by a combination of analytical techniques. *J Agric Food Chem* 2009;57:8488-8495.
26. Bode L, Jantscher-Krenn E. Structure-function relationships of human milk oligosaccharides. *Adv Nutr* 2012;3:S383-S391.
27. Holscher HD, Davis SR, Tappenden KA. Human milk oligosaccharides influence maturation of human intestinal Caco-2Bbe and HT-29 cell lines. *J Nutr* 2014;144:586-591.
28. Sinclair HR, de Slegte J, Gibson GR, Rastall RA. Galactooligosaccharides (GOS) inhibit *Vibrio cholerae* toxin binding to its GM1 receptor. *J Agric Food Chem* 2009;57:3113-3119.
29. Shoaf K, Mulvey GL, Armstrong GD, Hutkins RW. Prebiotic galactooligosaccharides reduce adherence of enteropathogenic *Escherichia coli* to tissue culture cells. *Infect Immun* 2006;74:6920-6928.
30. Vendrig JC, Coffeng LE, Fink-Gremmels J. Effects of orally administered galacto-oligosaccharides on immunological parameters in foals: a pilot study. *BMC Vet Res* 2014;10:278.
31. Vogt L, Meyer D, Pullens G, Faas M, Smelt M, Venema K, Ramasamy U, Schols HA, De Vos P. Immunological properties of inulin-type fructans. *Crit Rev Food Sci Nutr* 2015;55:414-436.
32. Hosono A, Ozawa A, Kato R, Ohnishi Y, Nakanishi Y, Kimura T, Nakamura R. Dietary fructooligosaccharides induce immunoregulation of intestinal IgA secretion by murine Peyer's patch cells. *Biosci Biotechnol Biochem* 2003;67:758-764.
33. Johnson-Henry KC, Pinnell LJ, Waskow AM, Irrazabal T, Martin A, Hausner M, Sherman PM. Short-chain fructo-oligosaccharide and inulin modulate inflammatory responses and microbial communities in Caco2-bbe cells and in a mouse model of intestinal injury. *J Nutr* 2014;144:1725-1733.
34. de Kivit S, Kraneveld AD, Knippels LM, van Kooyk Y, Garssen J, Willemsen LE. Intestinal epithelium-derived galectin-9 is involved in the immunomodulating effects of nondigestible oligosaccharides. *J Innate Immun* 2013;5:625-638.
35. de Kivit S, Saeland E, Kraneveld AD, van de Kant HJ, Schouten B, van Esch BC, Knol J, Sprickelman AB, van der Aa LB, Knippels LM, *et al.* Galectin-9 induced by dietary synbiotics is involved in suppression of allergic symptoms in mice and humans. *Allergy* 2012;67:343-352.
36. Ortega-Gonzalez M, Ocon B, Romero-Calvo I, Anzola A, Guadix E, Zarzuelo A, Suarez MD, Sanchez de Medina F, Martinez-Augustin O. Nondigestible oligosaccharides exert nonprebiotic effects on intestinal epithelial cells enhancing the immune response via activation of TLR4-NFkappaB. *Mol Nutr Food Res* 2014;58:384-393.
37. Hsu RY, Chan CH, Spicer JD, Rousseau MC, Giannias B, Rousseau S, Ferri LE. LPS-induced TLR4 signaling in human colorectal cancer cells increases beta1 integrin-mediated cell adhesion and liver metastasis. *Cancer Res* 2011;71:1989-1998.

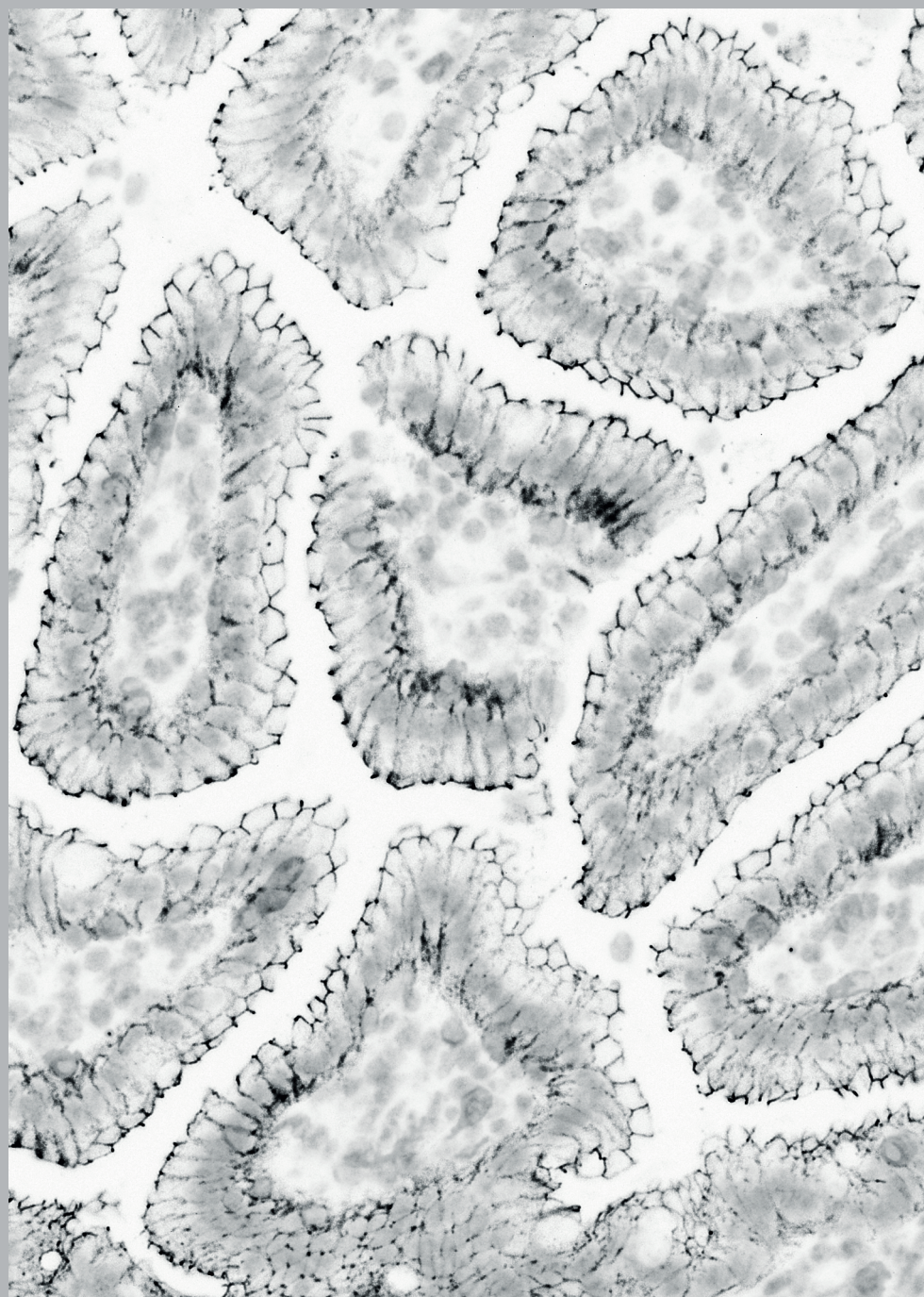




**Supplementary Figure 2.** The effects of individual and combined DP fractions of VGOS on the gut barrier function and CXCL8 release by Caco-2 cells. Caco-2 cells were incubated apically and basolaterally with VGOS, individual DP fractions of GOS (ranging from DP2 to DP6) and combination of different DP fractions (DP2 to DP6) with or without supplementation with glucose (Glc) and galactose (Gal) (36 h). Subsequently, TEER (A, B), transport of lucifer yellow (C, D) and CXCL8 release into the apical (E, F) and basolateral (G, H) compartments were measured. Results are expressed as a percentage of initial value (TEER), the amount of tracer transported [ng/(cm<sup>2</sup> × h)] or pg/ml (ELISA) as mean ± SEM, n = 1 (performed in triplicate).







# Chapter 7



## Inflammation-induced expression of the alarmin interleukin-33 can be suppressed by galactooligosaccharides

Peyman Akbari<sup>1,2,\*</sup>, Kim A.T. Verheijden<sup>2,\*</sup>, Linette E.M. Willemsen<sup>2</sup>, Aletta D. Kraneveld<sup>2</sup>, Gert Folkerts<sup>2</sup>, Johan Garssen<sup>2,3</sup>, Johanna Fink-Gremmels<sup>1</sup>, Saskia Braber<sup>1</sup>

<sup>1</sup> Division of Veterinary Pharmacology, Pharmacotherapy and Toxicology, Institute for Risk Assessment Sciences, Utrecht University, Utrecht, The Netherlands

<sup>2</sup> Division of Pharmacology, Utrecht Institute for Pharmaceutical Sciences, Faculty of Science, Utrecht University, Utrecht, The Netherlands

<sup>3</sup> Nutricia Research, Utrecht, The Netherlands

\* Both authors have equally contributed to this manuscript

This chapter is published in *International Archives of Allergy and Immunology* 2015; 167(2): 127-136.

## Abstract

The alarmin interleukin-33 (IL-33) and its receptor ST2 play an important role at mucosal barrier tissues, and seem to be crucial for Th2 cell mediated host defense. Galacto-oligosaccharides (GOS), used in infant formulas, exhibit gut and immune modulatory effects. To enhance our understanding of the immunomodulatory capacity of GOS, this study investigated the impact of dietary GOS intervention on IL-33 and ST2 expression related to intestinal barrier dysfunction or asthma. B6C3F<sub>1</sub> and BALB/c mice were fed a control diet with or without 1% GOS. To simulate intestinal barrier dysfunction, B6C3F<sub>1</sub> mice received a gavage with the mycotoxin deoxynivalenol (DON). To mimic asthma-like inflammatory airway responses, BALB/c mice were sensitized on day 0 and challenged on days 7-11 with house dust mite (HDM). Samples from the intestines and lungs were collected for IL-33 and ST2 analysis by qRT-PCR, immunoblotting and immunohistochemistry. Dietary GOS counteracted the DON-induced IL-33 mRNA expression and changed the IL-33 distribution pattern in the mouse small intestine. The IL-33 mRNA expression was positively correlated to the intestinal permeability. A strong positive correlation was also observed between IL-33 mRNA expression in the lung and the number of bronchoalveolar fluid cells. Reduced levels of IL-33 protein, altered IL-33 distribution and reduced ST2 mRNA expression were observed in the lungs of HDM-allergic mice after GOS intervention. Dietary GOS mitigated IL-33 at the mucosal surfaces in a murine model for intestinal barrier dysfunction and HDM-induced asthma. This promising effect may open up new avenues to use GOS not only as a prebiotic in infant nutrition, but also as a functional ingredient that targets inflammatory processes and allergies associated with IL-33 expression.

## Introduction

Non-digestible oligosaccharides, such as galacto-oligosaccharides (GOS) and fructo-oligosaccharides (FOS), are currently added to infant milk formulas to achieve an intestinal microbiota composition more similar to that of breastfed infants (1). Experimental evidence clearly indicates that infants given infant formula enriched with oligosaccharides, particularly GOS, showed a significant increase in *Bifidobacterium* and *Lactobacillus* spp. in the microbiota, resembling that of breastfed infants. From other studies, we know that growth of pathogens is reduced (2). Besides their effects on the intestinal flora, oligosaccharides can also modulate the activity of the immune system and regulate natural immune mechanisms (3). Interestingly, a reduction in the incidence of allergic manifestations and infections was observed after nutritional application with prebiotic oligosaccharides (90%GOS/10%lcfOS) (4, 5). Recent work by our group demonstrated that GOS also have microbiota-independent properties on intestinal epithelial cells (6, 7). The homeostasis of the epithelial inflammatory response within the intestinal epithelium can be regulated by the axis of interleukin-33 (IL-33) and its receptor ST2, which belongs to the IL-1/TLRs receptor superfamily (8). In recent years, scientific interest in IL-33 has grown, since this cytokine seems to be an indicator of Th2-mediated host defense and plays an important role in mucosal barrier tissues like the intestine and the surface of the airways, where it functions as an endogenous danger signal in response to tissue damage (9). Moreover, increased expression of IL-33 and its receptor ST2 has been reported in asthma and ulcerative colitis (UC) patients in association with pro-inflammatory effects (8, 10, 11).

Since there are indications that GOS can modulate barrier and immune functions and directly interact with epithelial cells, this study aimed to investigate whether the cytokine IL-33 and its receptor ST2 can be affected by the prebiotic GOS. An acute model for intestinal barrier dysfunction and a house dust mite (HDM)-induced allergic asthma model with an inflammation-induced expression of IL-33 were used to test our hypothesis. Dietary intervention with GOS mitigated the inflammation-induced expression of the alarmin IL-33 in these two murine models, while decreased ST2 mRNA expression was observed in lungs of HDM-allergic mice fed a GOS diet.

## Materials and Methods

### Animal studies

All *in vivo* experiments were conducted in compliance with the guidelines of Ethical Committee on the use of Laboratory Animals of the Utrecht University (DEC 2012.III.02.012 and 2013.II.01.003). Male B6C3F<sub>1</sub> and male BALB/c mice (6-8 weeks old) obtained from Charles River (Maastricht, The Netherlands) were housed under controlled conditions in standard laboratory cages or under bio-contained sterile conditions using HEPA® filtered isocages® (Tecniplast, Buguggiate, Italy), respectively. The present data were obtained from further analyses of samples from recently published studies (6, 12).

Animals were fed a control diet (AIN-93G) with or without 1% v/w GOS (Vivinal® GOS syrup with approximately 59% galacto-oligosaccharides, 21% lactose, 19% glucose, and 1% galactose on dry matter (dry matter of 75%); FrieslandCampina Domo, Borculo, The Netherlands) from day -14 to 0 (deoxynivalenol (DON) gavage study) and from day -14 to 14 (asthma study). Carbohydrates in Vivinal® GOS were compensated isocalorically in the control diet by means of cellulose (for GOS), lactose (for lactose), and dextrose (for glucose). Food and water were provided *ad libitum*. For the DON gavage study (Supplementary Figure 1), DON (D0156; Sigma, St. Louis, MO, USA) was administered at a dose of 25 mg/kg body weight (bw) by a single oral gavage to B6C3F<sub>1</sub> mice at day 0; control mice received sterile PBS. Six hours after the gavage, mice were sacrificed by cervical dislocation and the distal small intestine was collected for mRNA isolation and immunohistochemistry. For the asthma study (Supplementary Figure 1), BALB/c mice were intranasally (i.n.) sensitized with 1 µg house dust mite (HDM)/40 µL PBS (Greer Laboratories, Lenoir, NC, USA) under isoflurane anaesthesia on day 0 and i.n. challenged daily on days 7 to 11 with PBS (control) or 10 µg HDM/40 µL PBS. At day 14, mice were sacrificed by an intraperitoneal overdose of pentobarbital (600 mg/kg, Nembutal™, Ceva Santé Animale, Naaldwijk, The Netherlands) and the lungs were collected for mRNA isolation, Western blot analysis and immunohistochemistry.

### Fluorescein isothiocyanate-dextran permeability assay

To assess intestinal permeability changes, the intestinal permeability to 4 kDa fluorescein isothiocyanate (FITC)-dextran (Sigma-Aldrich, St. Louis, MO, USA) was measured as described previously (13). Briefly, 2 h after DON administration, all mice received FITC-dextran (500 mg/kg bw) by an oral gavage. Four hours after the FITC-dextran gavage, blood was obtained by heart puncture directly after cervical dislocation, and the appearance of FITC-dextran in blood serum was measured with a spectrofluorometer (FLUOstar Optima; BMG Labtech, Offenburg, Germany).

### Bronchoalveolar lavage

The trachea of the mice (asthma model) were cannulated and lungs were lavaged four times with 1 ml saline solution (0.9% NaCl, 37°C). The bronchoalveolar lavage fluid (BALF)



cells were centrifuged (400g, 5 min) and total number of BALF cells were counted using a Bürker-Türk chamber. Differential cell counts were performed on cytospin preparations stained by DiffQuick (Dade, Düdingen, Switzerland).

### qRT-PCR

Gene expression was determined by quantitative RT-PCR, as described previously (13). In brief, distal small intestine and lung tissue samples were homogenized in RNA lysis buffer with  $\beta$ -mercaptoethanol and RNA was extracted using spin columns according to manufacturer's instructions (Promega, Madison, WI, USA). cDNA was prepared from 1  $\mu$ g RNA using the iScript<sup>TM</sup> cDNA Synthesis kit (Bio-Rad, Hercules, CA, USA). qRT-PCR was performed using the MyIQ single-colour real-time PCR detection system (Bio-Rad, Hercules, CA, USA) with iQSYBR Green Supermix (Bio-Rad, Hercules, CA, USA) and IL-33 and ST2 primers were derived from the NCBI GenBank and manufactured commercially (Eurogentec, Seraing, Belgium). IL-33: forward: 5'-GGTGTGGATGGGAAGAAGCTG-3'; reverse: 5'-GAGGACTTTTGTGAAGGACG-3' and ST2 forward: 5'-CAAGTAGGACCTGTGCCCC-3'; reverse: 5'-CGTGCCAACAATTGACCTG-3'. The relative amounts of gene expression were standardized and calculated by the expression of house-keeping control gene ( $\beta$ -actin) as an internal standard, using the  $2^{-\Delta\Delta C_t}$  method.

### Immunoblotting

Total protein extracts were prepared as described previously (12). Equal protein amounts were separated by SDS-PAGE, blotted onto PVDF membranes and analyzed with goat anti-mouse IL-33 (R&D systems, Minneapolis, MN, USA, mouse monoclonal, AF3626, 1:500), rabbit anti-ST2 (Abcam, Cambridge, England, rabbit polyclonal, ab25877, 1:1000) or rabbit anti- $\beta$ -actin (Cell Signaling, Danvers, MA, USA, rabbit monoclonal, #4970, 1:4000). Appropriate horseradish peroxidase-conjugated secondary antibodies (Dako, Glostrup, Denmark) were used for detection by enhanced chemiluminescence (Amersham Biosciences, Roosendaal, The Netherlands). The band intensity was acquired by a GS710 calibrated image densitometer (Bio-Rad, Hercules, CA, USA).

### Immunohistochemistry

Immunohistochemistry was performed on formalin-fixed, paraffin-embedded distal small intestine (Swiss roll) and lung tissue using the IL-33 antibody (R&D systems, Minneapolis, MN, USA, mouse monoclonal, AF3626, 1:500) or ST2 antibody (Abcam, Cambridge, England, rabbit polyclonal, ab25877, 1:1200). For antigen retrieval, the slides were boiled in 10 mM citrate buffer (pH 6.0) for 10 min in a microwave (14). Digital images were acquired using an Olympus BX50 microscope (Olympus Europa GmbH, Hamburg, Germany) equipped with a Leica 320 digital camera (Leica Microsystems, Wetzlar, Germany). No staining was detected in negative controls, in which the primary antibody was omitted (Supplementary Figure 2).



**ELISA**

IL-33 and ST2 levels in BALF were measured by ELISA using the Mouse IL-33 ELISA set (R&D Systems, Minneapolis, MN, USA, DY3626) and Mouse ST2 ELISA set (R&D Systems, Minneapolis, MN, USA, DY1004) according to manufacturer's instructions.

**Statistical analysis**

Statistical analyses were performed by using GraphPad Prism 6.0 (Graphpad, LaJolla, CA, USA). Differences between groups were statistically determined by using One-way ANOVA followed by a Bonferroni multiple comparison test. Spearman's rank tests were conducted for analyses of correlation. Results were considered to be statistically significant when  $P < 0.05$ .

**Results****IL-33 mRNA expression is correlated to the intestinal permeability changes and to the number of BALF cells**

In the murine model for intestinal barrier dysfunction, a strong positive correlation was observed between the IL-33 mRNA expression levels in the mouse distal small intestine and intestinal permeability to 4 kDa FITC-dextran ( $r_s = 0.6634$ ,  $P = 0.002$ ; Figure 1A). In the HDM-induced asthma model, IL-33 mRNA expression levels in the lung positively correlated with the number of total BALF cells ( $r_s = 0.5424$ ,  $P = 0.0008$ ; Figure 1B). Differential analysis of the BALF cells showed an increase in eosinophils. The number of lymphocytes and neutrophils was significantly higher in HDM-allergic mice than in control mice (Supplementary Table 1).

**Dietary intervention with GOS counteracts the DON-induced IL-33 mRNA expression and distribution pattern in distal part of the mouse small intestine**

The prominent increase in IL-33 mRNA expression in the distal small intestine observed after DON gavage was prevented by GOS, since the IL-33 mRNA levels in DON-treated animals fed with a GOS diet were significantly lower than in the DON-treated animals given a control diet (Figure 2A).

Immunohistochemical staining confirmed that the IL-33 production was increased in the distal small intestine after DON gavage (Figure 2C) compared to the control mice fed a control or GOS diet (Figure 2B, D). The most pronounced differences were observed in the epithelial layer around the villi. The GOS diet prevented this DON-induced IL-33 production in the distal small intestine and a lower amount of IL-33-expressing epithelial cells was observed (Figure 2E). Related to the IL-33 mRNA expression, the increased ST2 mRNA expression in the distal small intestine of DON-treated animals was reduced in DON-treated animals fed a GOS diet, however this decrease was not significantly different

(Figure 2F). The ST2 immunohistochemical staining depicted in Figure 2G-J showed a strong expression pattern in the cytoplasm of the intestinal epithelial cells and ST2 was also detected in scattered lamina propria mononuclear cells. Similar patterns of ST2 expression for all experimental groups were observed (Figure 2G-J).

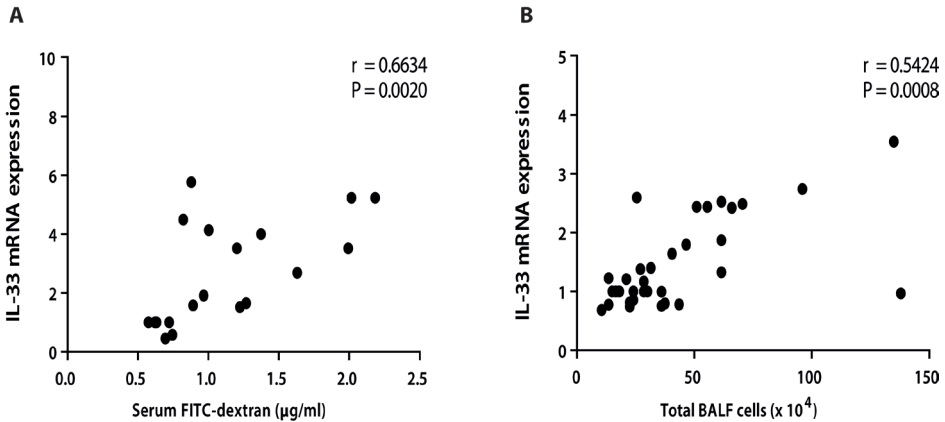


**Figure 1.** IL-33 mRNA expression correlated with the intestinal permeability and the number of BALF cells. Correlation of IL-33 mRNA expression in the distal small intestine and the intestinal permeability to 4 kDa FITC-dextran in the murine model for DON-induced intestinal barrier dysfunction (A). Correlation of IL-33 mRNA expression in the lungs and the total amount of BALF cells in the HDM-induced asthma model (B). Correlation was analyzed using the Spearman correlation test.

### Dietary intervention with GOS reduces IL-33 and ST2 mRNA expression and IL-33 protein levels in the lungs of HDM-allergic mice

The increase in IL-33 mRNA expression in the lungs of HDM-allergic mice was partly reduced by dietary intervention with GOS (Figure 3A), however this decrease was not statistically significant. The same trend has been observed for the IL-33 concentration in BALF (Figure 3B). Moreover, the IL-33 protein levels in lung tissue homogenates of GOS-treated HDM-allergic mice were significantly decreased compared with non-treated HDM-allergic mice (Figure 3C). Comparable with the Western blot data, immunohistochemical staining indicated that more IL-33 expressing cells were present in the lungs of the HDM-allergic mice (Figure 3E) than in the control mice (fed a control or GOS diet; Figure 3D, F). Dietary intervention with GOS caused a decrease in IL-33 expression in the lungs of HDM-allergic mice compared to the nontreated HDM-allergic mice (Figure 3G). Furthermore, a clear increase in ST2 mRNA expression was observed in the lungs of HDM-allergic mice, which was significantly reduced in HDM-allergic mice fed a GOS diet (Figure 4A). The ST2 levels in BALF (Figure 4B) and the ST2 protein levels in the lung (Figure 4C) did not significantly differ between the experimental groups; this was confirmed by immunohistochemical staining showing the airway epithelium as primary source for ST2 (Figure 4D-G).

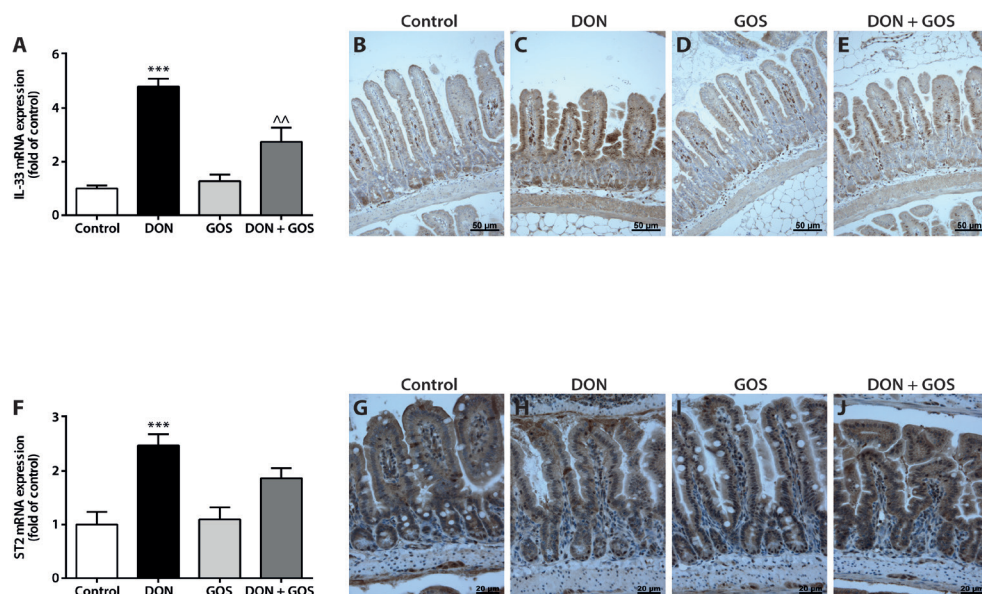


**Figure 2.** Dietary intervention with GOS counteracts the DON-induced IL-33 mRNA expression and distribution pattern in distal part of the mouse small intestine. Mice were fed a control diet or a diet supplemented with GOS for 2 weeks followed by an oral gavage with DON (25 mg/kg bw). Six hours after the DON challenge, the mRNA levels of IL-33 and ST2 were measured by qRT-PCR (A, F). Results are expressed as IL-33 or ST2 mRNA expression (fold of control) (qRT-PCR, normalized to  $\beta$ -actin) as mean  $\pm$  SEM (\*\*\* $P$  < 0.001; significantly different from the control group ^^ $P$  < 0.01; significantly different from the DON-treated animals).  $n$  = 5-6 animals/experimental group. For immunohistochemistry, Swiss-rolled paraffin sections obtained from distal small intestine were stained with anti-IL-33 (B, C, D, E) and anti-ST2 (G, H, I, J) antibodies as described in Materials and Methods. Magnification IL-33 staining: 200x and ST2 staining: 400x. The scale bar B-E and G-J represent 50  $\mu$ m and 20  $\mu$ m, respectively.

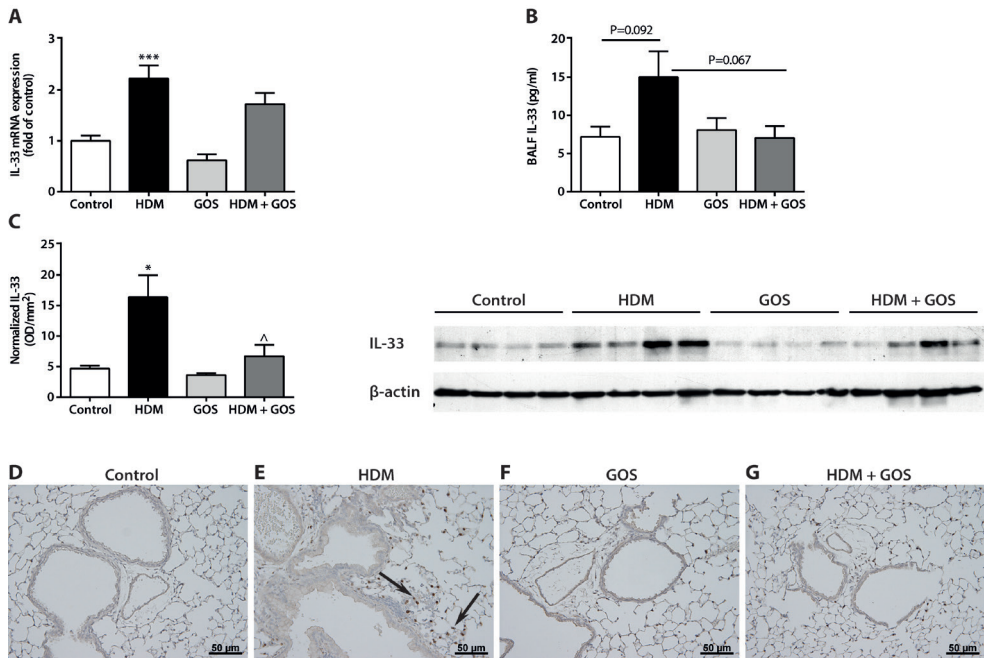


**Figure 3.** Dietary intervention with GOS reduces IL-33 protein levels and expression in the lungs of HDM-allergic mice. Mice fed a control diet or a diet supplemented with GOS from day -14 to 14, were sensitized with HDM on day 0 and were challenged on days 7 to 11 with HDM or PBS (control). IL-33 mRNA expression in lungs (A), IL-33 concentration in BALF (B) and IL-33 protein levels in lungs (C) were measured and results are expressed as IL-33 mRNA expression (fold of control) (qRT-PCR, normalized to  $\beta$ -actin), pg/ml BALF (ELISA) or OD/mm<sup>2</sup> (Western blot, normalized to  $\beta$ -actin) as mean  $\pm$  SEM (\* $P$  < 0.05; \*\*\* $P$  < 0.001; significantly different from the control group, ^ $P$  < 0.05; significantly different from the HDM-allergic animals).  $n$  = 7-9 animals/experimental group (qRT-PCR and ELISA). For immunohistochemistry, lung sections were stained with anti-IL-33 antibody (D, E, F, G) as described in Materials and Methods (Magnification 200x). The scale bar represents 50  $\mu$ m.

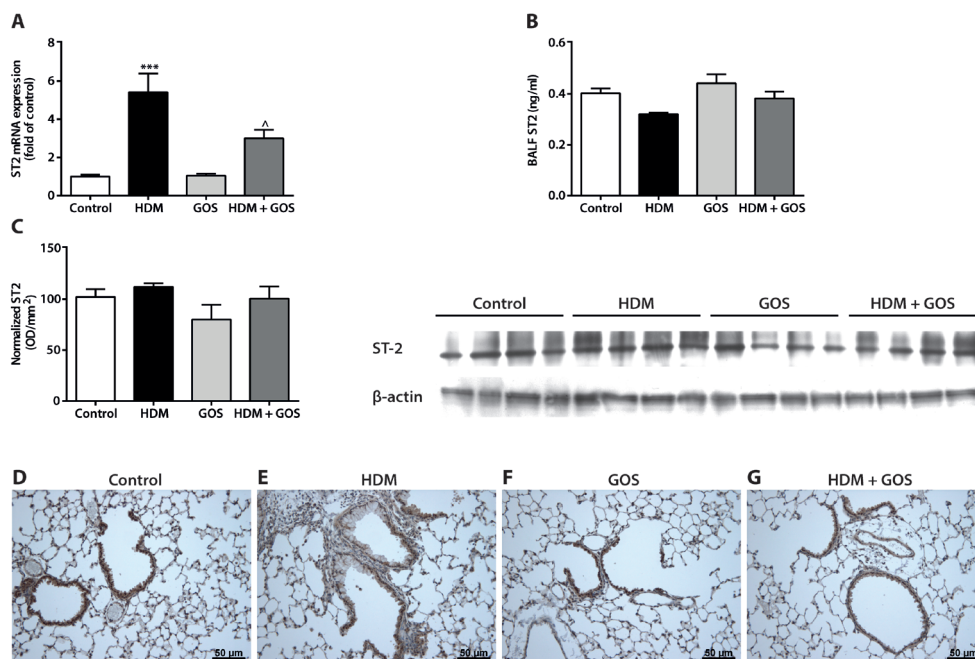


**Figure 4.** Dietary intervention with GOS reduces ST2 mRNA expression in the lungs of HDM-allergic mice. Mice fed a control diet or a diet supplemented with GOS from day -14 to 14, were sensitized with HDM on day 0 and were challenged on days 7 to 11 with HDM or PBS (control). ST2 mRNA expression in lungs (A), ST2 concentration in BALF (B) and ST2 protein levels in lungs (C) were measured and results are expressed as ST2 mRNA expression (fold of control) (qRT-PCR, normalized to  $\beta$ -actin), pg/ml BALF (ELISA) or OD/mm<sup>2</sup> (Western blot, normalized to  $\beta$ -actin) as mean  $\pm$  SEM (\*\*P < 0.01; \*\*\*P < 0.001; significantly different from the control group, ΔP < 0.05; significantly different from the HDM-allergic animals). n = 7-9 animals/experimental group (qRT-PCR and ELISA). For immunohistochemistry, lung sections were stained with anti-ST2 antibody (D, E, F, G) as described in Materials and Methods (Magnification 200x). The scale bar represents 50  $\mu$ m.

## Discussion

IL-33 is a member of the IL-1 cytokine family. It has a dual function: it activates various immune cells through the IL-33 receptor ST2 and acts as an intracellular factor with transcriptional properties (15). It also delivers an important danger signal in the cellular response to tissue damage, and epithelial cells at mucosal barrier sites constitutively express IL-33 (16). Specific effects in the gut can be exerted by IL-33, since mice injected intraperitoneally (i.p.) with recombinant IL-33 demonstrated an increase in permeability of the mucosal barrier, intestinal inflammation and hypertrophy and hyperplasia of goblet cells (17, 18).

In our study, the mycotoxin DON serves as a reliable and reproducible model of intestinal barrier dysfunction (13, 19) and a strong positive correlation was observed between IL-33 mRNA expression in the mouse distal small intestine and the intestinal permeability induced by the mycotoxin DON. Besides IL-33, the tight and adherens junctions are critical for the maintenance of intestinal barrier integrity (20–22). IL-33 impairs the epithelial barrier function; this was observed in a human colonic epithelial Caco-2 monolayer and in mice treated with exogenous IL-33. IL-33 injected intraperitoneally exacerbated sodium (DSS)-induced colitis in mice (23, 24). Observations in IL-33<sup>-/-</sup> mice suggested that IL-33 deficiency leads to delayed local inflammation and tissue damage during experimental colitis (25). On the other hand, it has been published recently that IL-33 promoted regulatory T cell function in the intestine. IL-23, an important pro-inflammatory cytokine in the pathogenesis of inflammatory bowel disease (IBD), inhibits this regulatory T cell responsiveness to IL-33 (26, 27). Furthermore, IL-33 is found to be prominently present in inflamed colon tissue, mainly localized to the surface epithelium and in the crypt cells, in patients with Crohn's disease and UC (8, 28, 29). In this study, a similar distribution pattern of IL-33 was observed in the mouse small intestine after disrupting the intestinal barrier with DON. Besides the increase in IL-33 expression observed by an immunohistochemical staining, a 5-fold increase was observed in IL-33 mRNA levels in the mouse distal small intestine after DON gavage, but the levels of other cytokines and chemokines, such as IFN- $\gamma$ , IL-1 $\alpha$ , IL-1 $\beta$ , IL-4, IL-6 and TNF- $\alpha$  remained unchanged (described by Akbari *et al.* (6)). The IL-33/ST2 system plays apparently an important role in IBD (29–31). Pastorelli *et al.* (28) described that a specific imbalance between IL-33 and ST2 may play a pathogenic role in UC, since ST2 is decreased in UC colonic epithelium and IL-33 is markedly increased in active UC. In the current study, no effect of the DON gavage on the ST2 distribution in the distal small intestine was observed; however, the ST2 mRNA expression was significantly increased in the distal small intestine of DON-treated animals.

The DON-induced increase in IL-33 was mitigated by dietary intervention with GOS, observed in IL-33 mRNA levels as well as by IL-33 distribution in the intestine, but GOS did not affect the DON-induced ST2 expression. Recently, we observed that GOS directly protected the intestinal barrier function by maintaining tight junction (TJ) proteins and modulating CXCL8 responses in a human Caco-2 cell monolayer and in a mouse model

for intestinal barrier dysfunction. However, the DON-induced hyperpermeability of the intestines for FITC-dextran (4 kDa) was not altered by GOS (6).

As IL-33 is implicated in Th2 type responses required for the development of allergic inflammation, the effect of dietary GOS on IL-33 expression was also investigated in a murine HDM-induced asthma model. In this model, the IL-33 mRNA expression levels in the lung positively correlated with the number of total BALF cells. Previous studies suggested that IL-33 and ST2 are both associated with the development and maintenance of allergic asthma and are correlated with disease severity (32, 33). It has been suggested that the IL-33-induced production of proinflammatory cytokines is a critical event that aggravates asthma (34). Treatments with anti-IL-33 monoclonal antibody have been reported to inhibit allergen-induced airway inflammation, Th2 cytokine production and mucus hypersecretion in mice (35).

Intranasally challenged IL-33-deficient mice showed impaired IL-5 and IL-13 production from group 2 innate lymphoid cells as well as lung inflammation and Th2 cell differentiation (36, 37). Administration of blocking anti-ST2 antibodies or ST2-Ig fusion protein to allergic mice abrogated the Th2-mediated inflammatory response (38). Contradictory results are described for T1/ST2-deficient mice, since Hoshino *et al.* (39) observed normal Th2 responses in these animals, while Townsend *et al.* (40) showed reduced levels of IL-4 and IL-5.

In line with the data of the intestinal barrier dysfunction model, dietary intervention with GOS resulted in lower IL-33 and ST2 levels and an altered IL-33 distribution in the lungs of HDM-allergic mice. In addition, the increased concentration of the Th2 cytokine IL-13 in the lung of HDM-allergic mice was significantly decreased by dietary intervention with GOS and the same trend was observed for the IL-5 concentration in the BALF, however this was not significantly different (Supplementary Table 2) (12).

The mode of action of GOS is complex and still not entirely understood. The reduced IL-33 expression exerted by GOS might result from alterations in the composition of the microbiota, since initially, GOS were considered as typical prebiotic supporting the growth of *Lactobacillus* and *Bifidobacterium* spp. in the large intestine (1, 41). GOS not only stimulate these bacteria, but affect the whole intestinal flora by production of short chain fatty acids, like butyrate and by decreasing the pH (1, 42). It is known that butyrate exerts anti-inflammatory properties explaining the desirable effects of various oligosaccharides (43). In turn, different immune-related, anti-allergic and anti-inflammatory effects were observed *in vivo* after GOS/lcFOS supplementation, suggesting a positive effect on mucosal immunity via suppression of the Th2 type responses, a down-regulation of total immunoglobulin levels and an induction of Th1- and T<sub>reg</sub>-cell polarization (4, 5, 44, 45).

Moreover, GOS seem to exert direct, microbiota-independent effects on the immune system by directly interacting with epithelial and immune cells as indicated by *in vitro* experiments (3, 6, 7, 46). Although direct interaction with Toll-like receptor 4 (TLR4) has been hypothesized (46), the direct effect of GOS on TJs reassembly in Caco-2 cells (6) indicates the involvement of other mechanisms as well, since Caco-2 do not express



TLR4. Furthermore, different galectins have distinct binding specificities for binding oligosaccharides (47). Indeed, previous investigations could show that dietary GOS enhanced the serum galectin-9 levels, which are involved in the regulation of immune responses and tolerance induction, which leads to a suppression of allergic symptoms in mice and humans (48).

These findings can be considered as first indication of a systemic modulatory effect of GOS, and they are now supported by our findings that GOS suppress IL-33, an alarmin that is produced at different mucosal surfaces. The parallel response of intestinal repair mechanisms and anti-allergic properties of GOS, may therefore be attributable to the systemic effects of signaling molecules like galectins and specific cytokines like IL-33. Further research is needed to investigate whether GOS directly interact with the IL-33/ST2 system or whether it prevents intestinal barrier disruption and allergic asthma by altering the microbiota composition which, indirectly, leads to a decreased IL-33 production.

In conclusion, dietary intervention with GOS mitigated the important immunomodulator IL-33 in mouse intestines, observed in a model for intestinal barrier dysfunction and in murine lungs in a house dust mite-induced asthma model, which is not necessarily associated with the ST2 expression. These preclinical experiments warrant studies on its clinical relevance and to unravel the mechanism behind this effect.

## Acknowledgements

The project is jointly funded by the European Union, European Regional Development Fund and The Ministry of Economic Affairs, Agriculture and Innovation, Peaks in the Delta, the Municipality of Groningen, the Provinces of Groningen, Fryslân and Drenthe, the Dutch Carbohydrate Competence Center (CCC WP25; [www.cccresearch.nl](http://www.cccresearch.nl)), Nutricia Research and FrieslandCampina.

## References

1. Fanaro S, Boehm G, Garssen J, Knol J, Mosca F, Stahl B, Vigi V. Galacto-oligosaccharides and long-chain fructo-oligosaccharides as prebiotics in infant formulas: a review. *Acta Paediatr* 2005;94:22-26.
2. Ben XM, Zhou XY, Zhao WH, Yu WL, Pan W, Zhang WL, Wu SM, Van Beusekom CM, Schaafsma A. Supplementation of milk formula with galacto-oligosaccharides improves intestinal micro-flora and fermentation in term infants. *Chin Med J (Engl)* 2004;117:927-931.
3. Jeurink PV, van Esch BC, Rijnierse A, Garssen J, Knippels LM. Mechanisms underlying immune effects of dietary oligosaccharides. *Am J Clin Nutr* 2013;98:S572-S577.
4. Arslanoglu S, Moro GE, Boehm G. Early supplementation of prebiotic oligosaccharides protects formula-fed infants against infections during the first 6 months of life. *J Nutr* 2007;137:2420-2424.
5. van Hoffen E, Ruiter B, Faber J, M'Rabet L, Knol EF, Stahl B, Arslanoglu S, Moro G, Boehm G, Garssen J. A specific mixture of short-chain galacto-oligosaccharides and long-chain fructo-oligosaccharides induces a beneficial immunoglobulin profile in infants at high risk for allergy. *Allergy* 2009;64:484-487.
6. Akbari P, Braber S, Alizadeh A, Verheijden KA, Schoterman MH, Kraneveld AD, Garssen J, Fink-Gremmels J. Galacto-oligosaccharides Protect the Intestinal Barrier by Maintaining the Tight Junction Network and Modulating the Inflammatory Responses after a Challenge with the Mycotoxin Deoxynivalenol in Human Caco-2 Cell Monolayers and B6C3F<sub>1</sub> Mice. *J Nutr* 2015;145:1604-1613.
7. Varasteh S, Braber S, Garssen J, Fink-Gremmels J. Galacto-oligosaccharides exert a protective effect against heat stress in a Caco-2 cell model. *J Funct Foods* 2015;16:265-277.
8. Garcia-Miguel M, Gonzalez MJ, Quera R, Hermoso MA. Innate immunity modulation by the IL-33/ST2 system in intestinal mucosa. *Biomed Res Int* 2013;2013:142492.
9. Cayrol C, Girard JP. IL-33: an alarmin cytokine with crucial roles in innate immunity, inflammation and allergy. *Curr Opin Immunol* 2014;31:31-37.
10. Miller AM. Role of IL-33 in inflammation and disease. *J Inflamm (Lond)* 2011;8:22.
11. Hamzaoui A, Berraies A, Kaabachi W, Haifa M, Ammar J, Kamel H. Induced sputum levels of IL-33 and soluble ST2 in young asthmatic children. *J Asthma* 2013;50:803-809.
12. Verheijden KA, Willemsen LE, Braber S, Leusink-Muis T, Delsing DJ, Garssen J, Kraneveld AD, Folkerts G. Dietary galacto-oligosaccharides prevent airway eosinophilia and hyperresponsiveness in a murine house dust mite-induced asthma model. *Respir Res* 2015;16:17.
13. Akbari P, Braber S, Gremmels H, Koelink PJ, Verheijden KA, Garssen J, Fink-Gremmels J. Deoxynivalenol: a trigger for intestinal integrity breakdown. *FASEB J* 2014;28:2414-2429.
14. Paulissen G, El Hour M, Rocks N, Gueders MM, Bureau F, Foidart JM, Lopez-Otin C, Noel A, Cataldo DD. Control of allergen-induced inflammation and hyperresponsiveness by the metalloproteinase ADAMTS-12. *J Immunol* 2012;189:4135-4143.
15. Ali S, Mohs A, Thomas M, Klare J, Ross R, Schmitz ML, Martin MU. The dual function cytokine IL-33 interacts with the transcription factor NF-kappaB to dampen NF-kappaB-stimulated gene transcription. *J Immunol* 2011;187:1609-1616.
16. Pichery M, Mirey E, Mercier P, Lefrancais E, Dujardin A, Ortega N, Girard JP. Endogenous IL-33 is highly expressed in mouse epithelial barrier tissues, lymphoid organs, brain, embryos, and inflamed tissues: in situ analysis using a novel IL-33-LacZ gene trap reporter strain. *J Immunol* 2012;188:3488-3495.
17. Schmitz J, Owyang A, Oldham E, Song Y, Murphy E, McClanahan TK, Zurawski G, Moshrefi M, Qin J, Li X, et al. IL-33, an interleukin-1-like cytokine that signals via the IL-1 receptor-related protein ST2 and induces T helper type 2-associated cytokines. *Immunity*

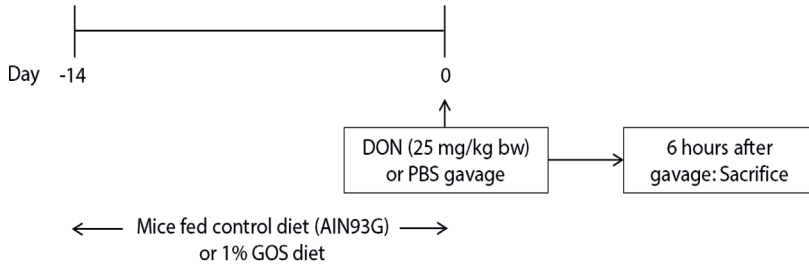
2005;23:479-490.

18. Yang Z, Grinchuk V, Urban JF Jr, Bohl J, Sun R, Notari L, Yan S, Ramalingam T, Keegan AD, Wynn TA, *et al.* Macrophages as IL-25/IL-33-responsive cells play an important role in the induction of type 2 immunity. *PLoS One* 2013;8:e59441.
19. Pinton P, Nougayrede JP, Del Rio JC, Moreno C, Marin DE, Ferrier L, Bracarense AP, Kolf-Clauw M, Oswald IP. The food contaminant deoxynivalenol, decreases intestinal barrier permeability and reduces claudin expression. *Toxicol Appl Pharmacol* 2009;237:41-48.
20. Groschwitz KR, Hogan SP. Intestinal barrier function: molecular regulation and disease pathogenesis. *J Allergy Clin Immunol* 2009;124:3-20.
21. Van Itallie CM, Anderson JM. Architecture of tight junctions and principles of molecular composition. *Semin Cell Dev Biol* 2014;36:157-165.
22. Niessen CM. Tight junctions/adherens junctions: basic structure and function. *J Invest Dermatol* 2007;127:2525-2532.
23. Sedhom MA, Pichery M, Murdoch JR, Foligne B, Ortega N, Normand S, Mertz K, Sanmugalingam D, Brault L, Grandjean T, *et al.* Neutralisation of the interleukin-33/ST2 pathway ameliorates experimental colitis through enhancement of mucosal healing in mice. *Gut* 2013;62:1714-1723.
24. Imaeda H, Andoh A, Aomatsu T, Uchiyama K, Bamba S, Tsujikawa T, Naito Y, Fujiyama Y. Interleukin-33 suppresses Notch ligand expression and prevents goblet cell depletion in dextran sulfate sodium-induced colitis. *Int J Mol Med* 2011;28:573-578.
25. Oboki K, Ohno T, Kajiwara N, Arae K, Morita H, Ishii A, Nambu A, Abe T, Kiyonari H, Matsumoto K, *et al.* IL-33 is a crucial amplifier of innate rather than acquired immunity. *Proc Natl Acad Sci U S A* 2010;107:18581-18586.
26. Schiering C, Krausgruber T, Chomka A, Frohlich A, Adelmann K, Wohlfert EA, Pott J, Griseri T, Bollrath J, Hegazy AN, *et al.* The alarmin IL-33 promotes regulatory T-cell function in the intestine. *Nature* 2014;513:564-568.
27. Matta BM, Lott JM, Mathews LR, Liu Q, Rosborough BR, Blazar BR, Turnquist HR. IL-33 Is an Unconventional Alarmin That Stimulates IL-2 Secretion by Dendritic Cells To Selectively Expand IL-33R/ST2+ Regulatory T Cells. *J Immunol* 2014;193:4010-4020.
28. Pastorelli L, Garg RR, Hoang SB, Spina L, Mattioli B, Scarpa M, Fiocchi C, Vecchi M, Pizarro TT. Epithelial-derived IL-33 and its receptor ST2 are dysregulated in ulcerative colitis and in experimental Th1/Th2 driven enteritis. *Proc Natl Acad Sci U S A* 2010;107:8017-8022.
29. Seidelin JB, Bjerrum JT, Coskun M, Widjaya B, Vainer B, Nielsen OH. IL-33 is upregulated in colonocytes of ulcerative colitis. *Immunol Lett* 2010;128:80-85.
30. Beltran CJ, Nunez LE, Diaz-Jimenez D, Farfan N, Candia E, Heine C, Lopez F, Gonzalez MJ, Quera R, Hermoso MA. Characterization of the novel ST2/IL-33 system in patients with inflammatory bowel disease. *Inflamm Bowel Dis* 2010;16:1097-1107.
31. Kobori A, Yagi Y, Imaeda H, Ban H, Bamba S, Tsujikawa T, Saito Y, Fujiyama Y, Andoh A. Interleukin-33 expression is specifically enhanced in inflamed mucosa of ulcerative colitis. *J Gastroenterol* 2010;45:999-1007.
32. Lloyd CM. IL-33 family members and asthma bridging innate and adaptive immune responses. *Curr Opin Immunol* 2010;22:800-806.
33. Oshikawa K, Kuroiwa K, Tago K, Iwahana H, Yanagisawa K, Ohno S, Tominaga SI, Sugiyama Y. Elevated soluble ST2 protein levels in sera of patients with asthma with an acute exacerbation. *Am J Respir Crit Care Med* 2001;164:277-281.
34. Nabe T. Interleukin (IL)-33: New Therapeutic Target for Atopic Diseases. *J Pharmacol Sci* 2014; 126:85-91.
35. Mizutani N, Nabe T, Yoshino S. Interleukin-33 and alveolar macrophages contribute to the mechanisms underlying the exacerbation of IgE-mediated airway inflammation and remodelling in mice. *Immunology* 2013;139:205-218.
36. Kamijo S, Takeda H, Tokura T, Suzuki M, Inui K, Hara

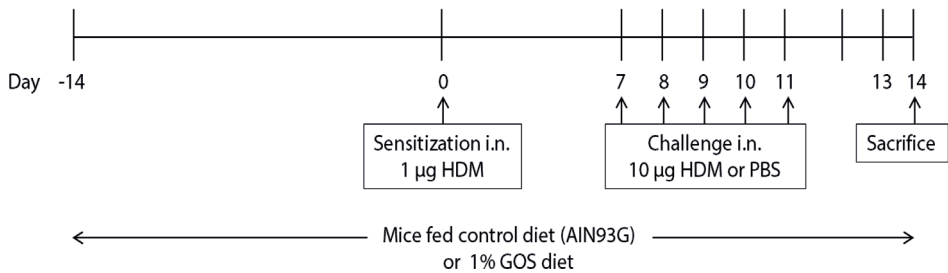
- M, Matsuda H, Matsuda A, Oboki K, Ohno T, *et al.* IL-33-mediated innate response and adaptive immune cells contribute to maximum responses of protease allergen-induced allergic airway inflammation. *J Immunol* 2013;190:4489-4499.
37. Halim TY, Steer CA, Matha L, Gold MJ, Martinez-Gonzalez I, McNagny KM, McKenzie AN, Takei F. Group 2 innate lymphoid cells are critical for the initiation of adaptive T helper 2 cell-mediated allergic lung inflammation. *Immunity* 2014;40:425-435.
38. Coyle AJ, Lloyd C, Tian J, Nguyen T, Eriksson C, Wang L, Ottoson P, Persson P, Delaney T, Lehar S, *et al.* Crucial role of the interleukin 1 receptor family member T1/ST2 in T helper cell type 2-mediated lung mucosal immune responses. *J Exp Med* 1999;190:895-902.
39. Hoshino K, Kashiwamura S, Kuribayashi K, Kodama T, Tsujimura T, Nakanishi K, Matsuyama T, Takeda K, Akira S. The absence of interleukin 1 receptor-related T1/ST2 does not affect T helper cell type 2 development and its effector function. *J Exp Med* 1999;190:1541-1548.
40. Townsend MJ, Fallon PG, Matthews DJ, Jolin HE, McKenzie AN. T1/ST2-deficient mice demonstrate the importance of T1/ST2 in developing primary T helper cell type 2 responses. *J Exp Med* 2000;191:1069-1076.
41. Giovannini M, Verduci E, Gregori D, Ballali S, Soldi S, Ghisleni D, Riva E, for the PTSG. Prebiotic Effect of an Infant Formula Supplemented with Galacto-Oligosaccharides: Randomized Multicenter Trial. *J Am Coll Nutr* 2014;33:385-393.
42. Holscher HD, Faust KL, Czerkies LA, Litov R, Ziegler EE, Lessin H, Hatch T, Sun S, Tappenden KA. Effects of prebiotic-containing infant formula on gastrointestinal tolerance and fecal microbiota in a randomized controlled trial. *JPEN J Parenter Enteral Nutr* 2012;36:S95-S105.
43. Oozeer R, van Limpt K, Ludwig T, Ben Amor K, Martin R, Wind RD, Boehm G, Knol J. Intestinal microbiology in early life: specific prebiotics can have similar functionalities as human-milk oligosaccharides. *Am J Clin Nutr* 2013;98:S561-S571.
44. Vos AP, M'Rabet L, Stahl B, Boehm G, Garssen J. Immune-modulatory effects and potential working mechanisms of orally applied nondigestible carbohydrates. *Crit Rev Immunol* 2007;27:97-140.
45. Schijf MA, Kruijsen D, Bastiaans J, Coenjaerts FE, Garssen J, van Bleek GM, van't Land B. Specific dietary oligosaccharides increase Th1 responses in a mouse respiratory syncytial virus infection model. *J Virol* 2012;86:11472-11482.
46. Ortega-Gonzalez M, Ocon B, Romero-Calvo I, Anzola A, Guadix E, Zarzuelo A, Suarez MD, Sanchez de Medina F, Martinez-Augustin O. Nondigestible oligosaccharides exert nonprebiotic effects on intestinal epithelial cells enhancing the immune response via activation of TLR4-NFkappaB. *Mol Nutr Food Res* 2014;58:384-393.
47. de Kivit S, Kraneveld AD, Garssen J, Willemsen LE. Glycan recognition at the interface of the intestinal immune system: target for immune modulation via dietary components. *Eur J Pharmacol* 2011;668:S124-S132.
48. de Kivit S, Saeland E, Kraneveld AD, van de Kant HJ, Schouten B, van Esch BC, Knol J, Sprickelman AB, van der Aa LB, Knippels LM, *et al.* Galectin-9 induced by dietary synbiotics is involved in suppression of allergic symptoms in mice and humans. *Allergy* 2012;67:343-352.

## Supplementary data

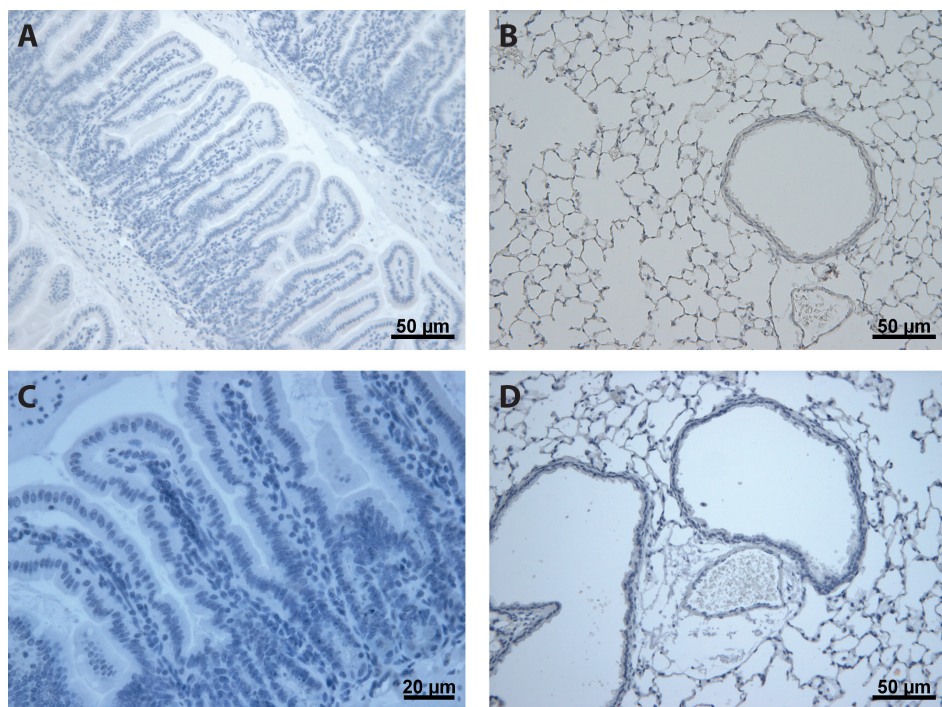
Mouse model for intestinal barrier dysfunction:



Mouse model for house dust mite-induced allergic asthma:



**Supplementary Figure 1.** Mouse model for intestinal barrier dysfunction and mouse model for HDM-induced allergic asthma.



**Supplementary Figure 2.** Negative controls immunohistochemistry. No staining was detected in negative controls, in which the primary antibody was omitted. A) negative control of IL-33 staining in distal small intestine, B) negative control of IL-33 staining in lungs, C) negative control of ST2 staining in distal small intestine, D) negative control of ST2 staining in lungs. The scale bar A, B as well as E represent 50  $\mu\text{m}$  and the scale bar C represents 20  $\mu\text{m}$ .

**Supplementary Table 1.** BALF cell count and differentiation in the HDM-allergic model

	Mean (*10 <sup>4</sup> ) ± SEM			
	Control	HDM	GOS	HDM + GOS
<b>Macrophages</b>	17.95 ± 2.15	33.19 ± 7.46	22.38 ± 2.35	19.36 ± 3.44
<b>Lymphocytes</b>	0.90 ± 0.25	4.54 ± 0.95***	0.57 ± 0.14	2.71 ± 0.60
<b>Neutrophils</b>	0.25 ± 0.08	3.97 ± 1.28*	0.26 ± 0.10	3.16 ± 1.41
<b>Eosinophils</b>	0.03 ± 0.03	20.92 ± 4.53***	0.05 ± 0.03	9.06 ± 4.53 (P=0.09)
<b>Total</b>	<b>19.13 ± 2.37</b>	<b>62.63 ± 11.48***</b>	<b>23.25 ± 2.32</b>	<b>34.29 ± 6.78<sup>^</sup></b>

\*P < 0.05; \*\*\*P < 0.001 significantly different from the control animals, <sup>^</sup>P < 0.05 significantly different from the HDM-allergic animals.

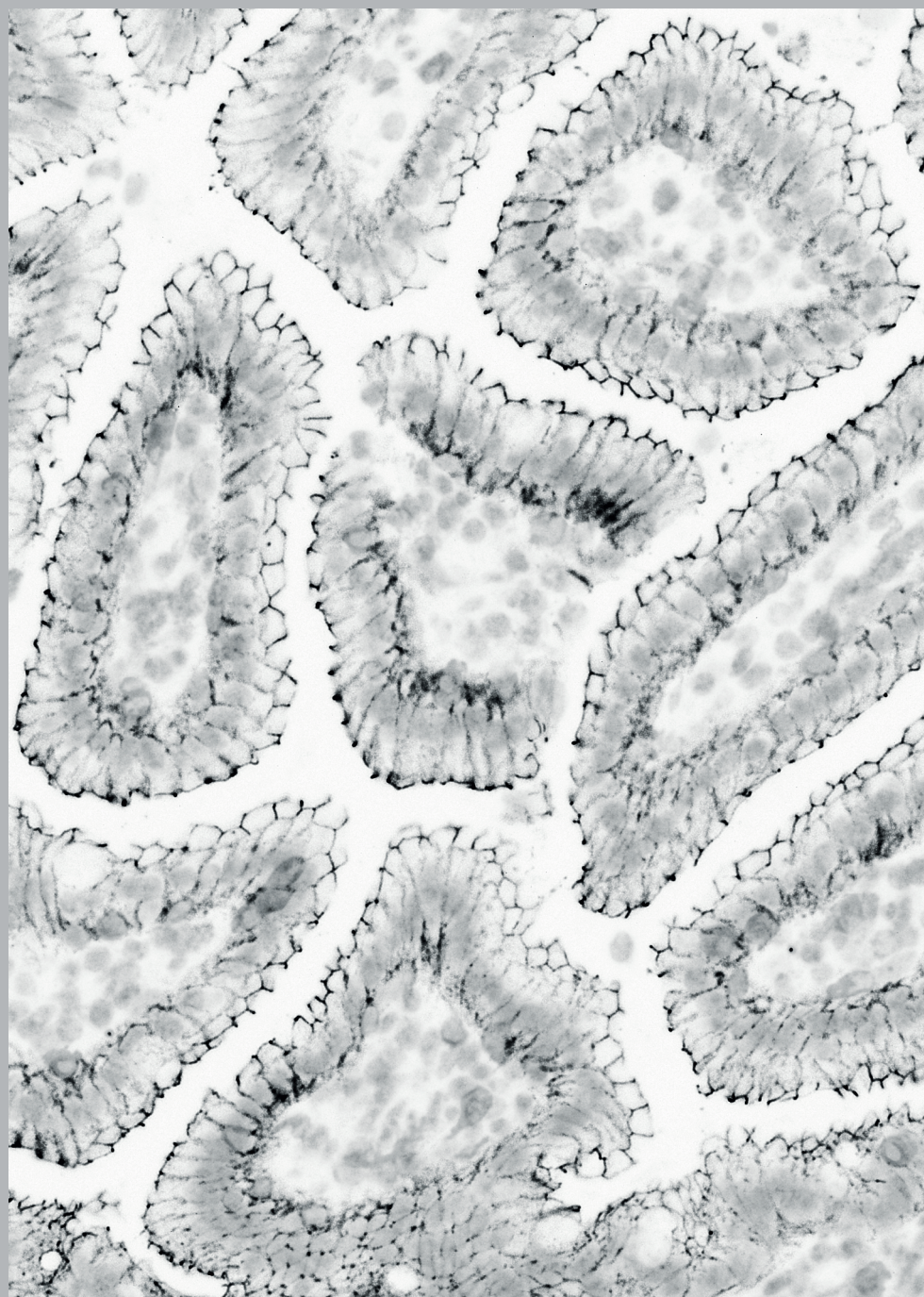
**Supplementary Table 2.** Cytokine concentrations in the HDM-allergic model

	Mean ± SEM			
	Control	HDM	GOS	HDM + GOS
<b>IL-13 (pg/mg protein)</b>	65.57 ± 3.02	99.07 ± 8.01***	46.91 ± 2.41	65.25 ± 2.82 <sup>^^</sup>
<b>IL-5 (pg/ml)</b>	7.07 ± 0.99	17.92 ± 5.91	3.53 ± 0.39	10.75 ± 3.13

IL-13 (pg/mg protein) measured in lung homogenates and IL-5 (pg/ml) measured in BALF.

\*\*\*P < 0.001 significantly different from the control animals, <sup>^^</sup>P < 0.01 significantly different from the HDM-allergic animals.





# *Chapter 8*



General summary

The experiments described in this thesis were performed to gain more insight into the effectiveness of non-digestible oligosaccharides, including GOS, FOS and Inulin, on the dysregulated intestinal epithelial barrier function and related immune responses. Here, we summarize the most important findings of this thesis and describe the potential effect of GOS in the prevention of a deoxynivalenol (DON)-induced intestinal barrier breakdown and related immune responses.

For a better understanding of the importance of tight junction (TJ) proteins related to intestinal barrier function, a review is presented in **Chapter 2** summarizing the current knowledge on molecular structure, expression alongside the GI tract and clinical implications of different intestinal TJs. **Chapter 2** further emphasizes the importance of interaction among different TJs in preserved gut barrier integrity. A dynamic and well-regulated barrier is crucial for gut immune homeostasis (1, 2) and maintenance of a functional intestinal barrier is acquired by a variety of specific and non-specific mechanisms, among which the expression and function of TJs is of particular interest (3, 4). As depicted in **Figure 1**, TJs form an anastomosing network sealing adjacent epithelial cells near the luminal surface to prevent a paracellular transport of luminal antigens, pathogens and toxins. They are composed of I) transmembrane proteins which their extracellular domains cross the plasma membrane and interact with their partners on the neighboring adjacent cells and II) cytoplasmic scaffolding proteins, which are entirely located on the intracellular side of the plasma membrane. Transmembrane TJs form a horizontal barrier at the apical-lateral membrane of epithelial cells and mainly consist of occludin (OCLN) and claudins (CLDNs). The cytoplasmic scaffolding proteins, like zonula occludens (ZOs), provide a direct link between transmembrane TJ proteins and the cytosolic and nuclear proteins (5-7). **Chapter 2** also aims to explain that any individual component of the TJ network is structurally and functionally different, but that all components interact with each other to form a network that ultimately results in an efficient intestinal barrier. The impairment of this biological barrier may be one of the predisposing factors leading to various chronic (intestinal) inflammatory diseases, including inflammatory bowel disease (Crohn's disease and ulcerative disease) and coeliac disease as well as allergic responses to food-derived antigens.

Dietary exposure of humans and animals to mycotoxins is of growing concern due to the apparently still increasing prevalence of these fungal toxins in food and feed commodities (8-10). Risk assessment of mycotoxin exposure initially focused on their potential mutagenic, genotoxic and carcinogenic effects, as major human health risks (10-12). More recently, there is an increasing awareness of the adverse effects of various mycotoxins on vulnerable structures in the intestines, targeting intestinal barrier function. Even though mycotoxins have only incidentally been associated with a specific intestinal disease, for example in acute gastroenteritis induced by trichothecenes and fumonisin in humans (10, 13, 14), the intestinal epithelium is the first biological barrier encountered by mycotoxins.

The most prominent example of a mycotoxin primarily associated with an impairment of the intestinal barrier is DON, which first had been recognized for its pro-inflammatory and immunomodulatory activities (15, 16). Therefore, **Chapter 3** aims to provide a summary of the available evidences regarding direct effects of various mycotoxins on the intestinal epithelial barrier. Available data, based on different cellular and animal studies, show that food-associated exposure to DON, T-2 toxin, patulin, ochratoxin A, fumonisin B<sub>1</sub> and aflatoxins disrupt the gut barrier function, albeit with different intensity. Because of lactational transfer (transfer from maternal plasma into breast milk) and the immaturity of intestinal barrier function at birth, infants are considered to be particularly susceptible for such an impairment of barrier functions, potentially resulting in increased translocation of pathogens as well as antigens (17-19). **Chapter 3** therefore also aims to improve the understanding of non-conventional endpoints, including intestinal integrity, in the risk assessment of mycotoxins taking into account also the vulnerability of certain age-groups of the human population and the risk for patients suffering from other chronic (infectious) diseases.

As outlined in **Chapter 2**, disintegration of the intestinal epithelial barrier is considered as a key event in the initiation and progression of intestinal inflammatory diseases and allergic responses. Since the primary aetiology of these diseases remains unknown, **Chapter 4** hypothesizes that the mycotoxin DON is one of the triggers resulting in an impairment of the intestinal TJ network and subsequently leading to a disturbed mucosal immune homeostasis. Therefore, we designed a series of experiments described in **Chapter 4** to identify the cascade of events exerted by DON that eventually lead to the loss of epithelial barrier integrity. Both, *in vitro* experiments with DON-exposed Caco-2 cell monolayers and *in vivo* experiments in mice orally exposed to DON, are presented. Caco-2 cell monolayers cultivated on permeable filters are commonly recognized as the most reliable *in vitro* model to assess the intestinal barrier function (20-22). Using horizontal impedance measurements, we demonstrate that exposure to low concentration of DON disintegrates the human Caco-2 cell monolayer already within the first 1-2 h. This initial trigger is followed by a concentration- and time-dependent decrease in transepithelial resistance (TEER). **Chapter 4** further shows that DON-induced impairment of the TEER values markedly depends on the route of exposure, which can be ranked as follows: apical and basolateral exposure ≥ basolateral exposure > apical exposure. The functional consequences of the readily measured impairment of the cell monolayer integrity is confirmed by an increased paracellular transport of macromolecules (LY, 0.457 kDa and FITC-dextran, 4 kDa) across Caco-2 cell monolayers. Paracellular transport can also be measured in *in vivo* models by detecting the presence of macromolecular tracers, given by oral gavage, in the blood of mice. In **Chapter 4**, it is clearly demonstrated in mice that the DON-induced impairment of epithelial integrity facilitates the translocation of FITC-dextran (4 kDa) from the gut lumen to the blood circulation. Decrease in TEER values and increase in permeability of marker molecules suggest a direct effect of DON on the

TJ network. When investigating the protein levels of the different TJs, a dose-dependent reduction of the CLDN1, CLDN3, and CLDN4 protein levels in DON-treated Caco-2 cells has been demonstrated, accompanied with a displacement of these proteins within the cells. These altered distribution patterns are not only observed for the CLDN proteins, but also for OCLN and ZO-1, for which only marginal alteration in the total immunoreactive protein levels could be measured. In turn, exposure of Caco-2 cell monolayers to DON induced an up-regulation of mRNA levels of different TJs (CLDN1, CLDN3, CLDN4, OCLN, and ZO-1) in a concentration-dependent manner, which might be regarded as a compensatory response to alterations of TJ protein levels. Segment-specific effects of DON along the mouse intestine are presented in **Chapter 4**. It is shown that the DON-induced up-regulation of the mRNA levels of different CLDNs is most pronounced in the mouse distal small intestine compared to other segments of the intestine. In addition, an altered distribution of CLDN1-3 is observed in the distal small intestine of DON-treated animals. Furthermore, histomorphometric analysis of the proximal and distal small intestine of the control and DON-exposed mice displays a significant decrease in villus height, villus area as well as in the epithelial cell area compared to control animals. We speculate that the changes in villus architecture, discussed in **Chapter 4**, are neither due to sloughing of epithelial lining from the surface of the villi, nor related to apoptosis or necrosis of the epithelial cells, since no prominent histological lesions have been observed. However, after acute mucosal injury by DON (at high dosage), villus contraction may take place, which might be a direct pharmacologic effect (DON is known to modulate dopaminergic and serotonergic receptor responses) or a non-specific defense mechanism aiming at the protection of the barrier function by reducing the total and denuded surface area of the villi (23, 24). **Figure 1** illustrates the effects of DON on intestinal epithelial barrier function as presented in **Chapter 4**.

To prevent the intestinal barrier disruption induced by DON or other exogenous stimuli, gut health promoting substances that protect the intestinal epithelial barrier need to be identified. Nowadays, the health promoting effects of non-digestible oligosaccharides have been broadly acknowledged (25). In particular, lactose-derived galacto-oligosaccharides (GOS) are of interest because of their potential immunomodulatory and anti-inflammatory effects. GOS, which resemble oligosaccharides that occur naturally in human breast milk, are expected not only to modulate the composition and metabolism of the gut microbiota (26-28), but seem to prevent specific pathologies in diseases associated with the intestinal immune system, such as food allergies and inflammatory bowel disease (26, 29, 30). Given the global and frequent occurrence of DON in food and feed (as discussed in **Chapter 3**) we again used in **Chapter 5** this challenge to assess whether GOS can prevent the DON-induced intestinal (epithelial) barrier disruption and the related immune responses. First, we demonstrated that GOS accelerate the TJs reassembly as demonstrated by a calcium switch assay, in which a decreased repair time of the transepithelial resistance after a calcium-deprivation



period has been observed after GOS incubation. In turn, GOS pretreatment prevented the DON-induced impairment of Caco-2 cell monolayer integrity as measured by TEER values and paracellular flux of the markers LY and 4 kDa FITC-dextran. **Chapter 5** further focuses on the direct effect of GOS on TJs and displays that only the DON-induced CLDN3 mRNA expression is almost entirely prevented by GOS. Western blot analyses pointed out that GOS pretreatment also prevent the DON-induced decrease in CLDN3 protein expression. In addition, the DON-induced derangement of the cellular distribution of CLDN3 was visualized by immunofluorescence microscopy and again, a preventive effect of GOS could be demonstrated. Previous investigations indicated that DON can induce both immunostimulatory or immunosuppressive responses depending on dose, frequency and duration of exposure (15, 31). Hence, in **Chapter 5** further investigations are presented on some typical markers of intestinal inflammation, including IFN- $\gamma$ , IL-1 $\alpha$ , IL-1 $\beta$ , IL-4, IL-6, TNF- $\alpha$  and CXCL8. The chemokine interleukin-8 (IL-8/CXCL8) is the most prominent cytokine expressed by Caco-2 cells and is secreted early in the inflammatory process by human enterocytes (32-34). We show, for the first time, that GOS pretreatment suppress the DON-induced synthesis and release of CXCL8 in Caco-2 cells. These *in vitro* findings are confirmed by *in vivo* experiments in mice where pretreatment with GOS partly prevented the DON-induced mRNA overexpression of CLDN3 and CXCL1 (the murine CXCL8 homologue). Furthermore, DON-induced changes in villus architecture (discussed in **Chapter 4** and **Chapter 5**) are mitigated in mice pretreated with a GOS-supplemented diet. The protective effects of GOS on DON-induced intestinal integrity breakdown and CXCL-8 release are depicted in **Figure 1**. As discussed in **Chapter 5**, the gut health promoting effects of GOS are generally ascribed to the modulation of intestinal microbiota and the direct interaction of these oligosaccharides with intestinal epithelial cells (IEC) has only recently been identified by us and others (35-38).

The prebiotic activity of GOS, FOS and Inulin are believed to be associated by their unique structure and specific degree of polymerization (DP) (39-42). However, the direct effect of structure and DP composition of GOS, FOS and Inulin on interaction with IEC awaited further clarification. Therefore, **Chapter 6** aims to compare the direct effects of four oligosaccharides (different in structure and DP), including Vivinal® galacto-oligosaccharides syrup (VGOS), purified galacto-oligosaccharides (PGOS), plant-derived oligosaccharides Inulin and fructo-oligosaccharides (FOS, a fermented product of Inulin with low DPs) in the previously described DON-stimulated Caco-2 cell model. Results show that the DON-induced impairment of the Caco-2 cell monolayer integrity is differently affected by the individual oligosaccharides. VGOS exhibited the most pronounced protective effect on the disrupted epithelial barrier as measured by TEER and paracellular flux of LY. The outstanding improvement of the barrier integrity by VGOS is, at least partly, related to acceleration in TJs reassembly as demonstrated by the calcium switch assay. Compared to VGOS, PGOS and isolated fractions of VGOS with different degrees of polymerization were less potent. A comparison of the obtained results pointed towards

a high potency of DP2 as well as DP3 (equimolar concentrations as present in VGOS), whereas higher DPs (equal or above DP4) showed only minimal and non-significant effects. In addition, PGOS is partly lacking GOS-DP2 due to the purification procedure. The comparison of GOS with FOS and Inulin, also demonstrated the higher potency of GOS, which more closely resemble the structure of human milk oligosaccharides (43, 44). Again, lower DPs as in the FOS product, show more pronounced effects than Inulin as such, in which a broad variety of long-chain oligosaccharides is present. On the other hand, the DP concentration present in VGOS can also play a role in the protective effect, since after incubation with equal DP concentrations (0.75%), also DP5 is effective in preventing the Caco-2 monolayer disruption.

In addition to the effects on intestinal barrier integrity, our comparative study demonstrates that the tested oligosaccharides have different capacities to inhibit the inflammatory response in Caco-2 cells, since only VGOS is able to prevent the DON-induced CXCL8 release, whereas none of the other oligosaccharides (PGOS, FOS, Inulin and DP fractions of VGOS) affect this DON-induced CXCL8 secretion. **Chapter 6** concludes that the most optimal protective effect (not only on the intestinal integrity, but also on the CXCL8 release) is achieved when combinations of all DP fractions are present, which emphasizes a possible synergistic effect of separate DPs. Therefore, the potential protective effect of VGOS is dependent on the combination of the different DP fractions, the DP length and DP concentration. The comparison of different classes of oligosaccharides presented in **Chapter 6** refers to the direct, microbiota-independent, effects of different oligosaccharides on IECs. However, it cannot be excluded that different results will be obtained when the microbiota has taken into account, although there is also some evidence that the bifidogenic effect of oligosaccharides is also more pronounced for lower DPs.

Besides the effect of DON on the epithelium-derived pro-inflammatory cytokines, we further aimed to test the contribution of epithelial damage on the epithelial derived Th2 cell inducing cytokine interleukin-33 (IL-33) (**Chapter 7**). The alarmin IL-33 and its receptor ST2 have been shown to play an important role in mucosal barrier tissues, like the intestine and the surface of the airways, where it functions as an endogenous danger signal in response to tissue damage (45, 46). The IL-33/ST2 system seems to be crucial for Th2 immune responses in various inflammatory diseases including auto-immune diseases (rheumatoid arthritis) and inflammatory bowel disease (46, 47). In addition to the observed protective effects of GOS on the intestinal barrier dysfunction (discussed in **Chapter 5** and **Chapter 6**), a reduction in the incidence of allergic manifestations and infections has also been reported after nutritional application with GOS and FOS early in life (48, 49). Hence, **Chapter 7** aims to investigate the impact of dietary GOS intervention on IL-33 and ST2 expression in a murine model for intestinal barrier dysfunction induced by DON (explained in **Chapter 4**) and in a murine model for house dust mite (HDM)-induced allergic asthma. A strong positive correlation between the IL-33 mRNA expression levels



in the mouse distal small intestine and the DON-induced intestinal barrier breakdown has been displayed in our study. DON increases the IL-33 expression in the distal part of the mouse small intestine, whereas the DON-induced IL-33 mRNA expression is accompanied with an increase in ST2 mRNA expression in the mouse distal small intestine. **Chapter 7** shows also for the first time that dietary intervention with GOS counteracts the DON-induced IL-33 mRNA expression and distribution pattern in the distal part of the mouse small intestine. In the HDM-induced allergic asthma model, the dietary intervention with GOS reduces the IL-33 protein levels and ST2 mRNA expression in the lungs of HDM-allergic mice. This promising effect may open up new avenues to use GOS not only as a prebiotic in infant nutrition, but also as a functional ingredient that targets inflammatory processes and allergic responses.

**In conclusion, this overall summary of the different chapters combined in this thesis pointed towards the major results obtained, including:**

- The direct, non-microbiota dependent, effects of galacto-oligosaccharides (GOS) on intestinal barrier integrity, particularly on the tight junctions.
- These direct, microbiota independent effects not only depend on the oligosaccharide structure, but also on the DP length and concentration.
- The protective effect of GOS, particularly Vivinal® GOS, against the detrimental effects of the 12,13-epoxytrichothecene deoxynivalenol, a mycotoxin that is found with increasing frequency in various food commodities, including breast milk.
- The anti-inflammatory effect of GOS on challenged epithelial cells, demonstrated by the prevention of the induction and release of CXCL8.
- The protective effect of dietary GOS intervention on the Th2-mediated immune responses induced by epithelial damage as observed by the suppression of the IL-33 expression.

***The above mentioned protective effects of GOS are summarized in the following figure:***

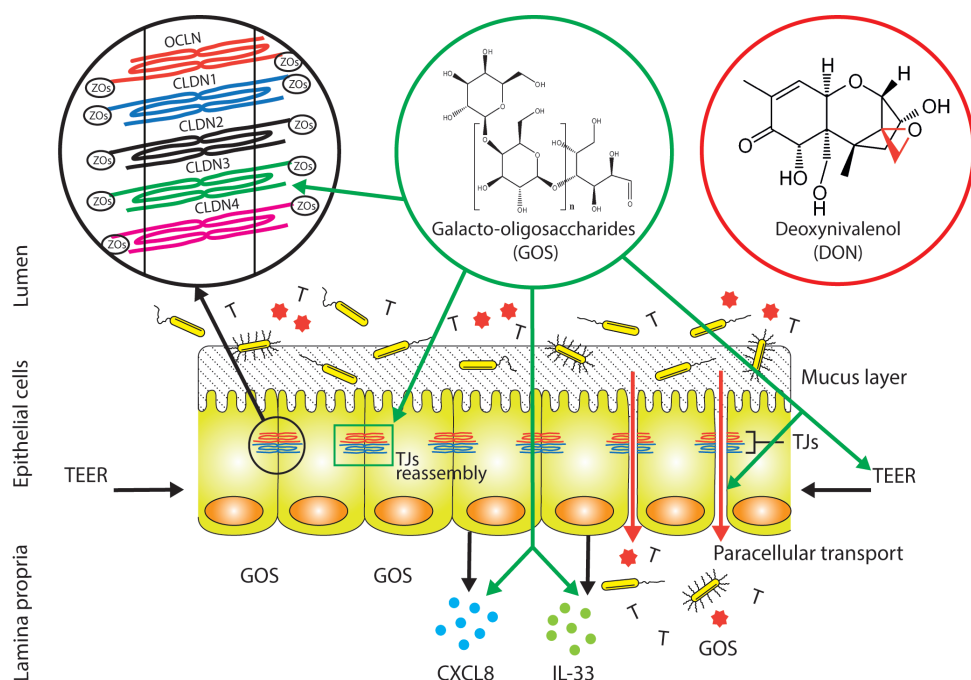


**Figure 1. Schematic illustration of the protective effects of GOS on the DON-induced intestinal epithelial barrier breakdown and epithelial-derived immune responses.**

The gut mucosa is constantly challenged by a diverse **microbial community** (yellow rod-shaped bodies), **food-borne toxins** (T) and **foreign antigens** (red heptagrams). Therefore, the precise regulation of the intestinal barrier, mainly formed by **TJs**, appears to be crucial for gut immune homeostasis (**Chapter 2**). The most prominent example of a food-borne toxin primarily associated with an impairment of the intestinal barrier is the mycotoxin **DON** (**Chapter 3**). DON disintegrates the intestinal epithelial barrier function as observed by a decrease in **TEER** values and an increase in **paracellular tracer transport** (**Chapter 4**). The DON-induced impairment of the epithelial integrity is related to changes in the expression level and/or cellular distribution of different TJs (**CLDNs**, **OCLN**, and **ZOs**) (**Chapter 3** and **Chapter 4**). **GOS** prevent the DON-induced intestinal epithelial barrier disruption as measured by **TEER** values and **paracellular transport**, whereas only the DON-induced **CLDN3** expression and distribution have been almost entirely prevented by GOS. Furthermore, GOS accelerate the **TJs reassembly**. In addition to the protection of the intestinal barrier function, GOS positively modify the gut-related immune responses, since the DON-induced epithelial derived **CXCL8** and alarmin **IL-33** are mitigated by GOS (**Chapter 5** and **Chapter 7**). Abbreviations used: CLDNs, claudins; CXCL8, chemokine CXC motif ligand 8; DON, deoxynivalenol; GOS, galacto-oligosaccharides; IL-33, interleukin-33; OCLN, occludin; TEER, transepithelial electrical resistance; TJs, tight junctions; ZOs, zonula occludens. The structure of a  $\beta(1-4)$  linked GOS molecule is adapted from Jeong *et al.* (50).

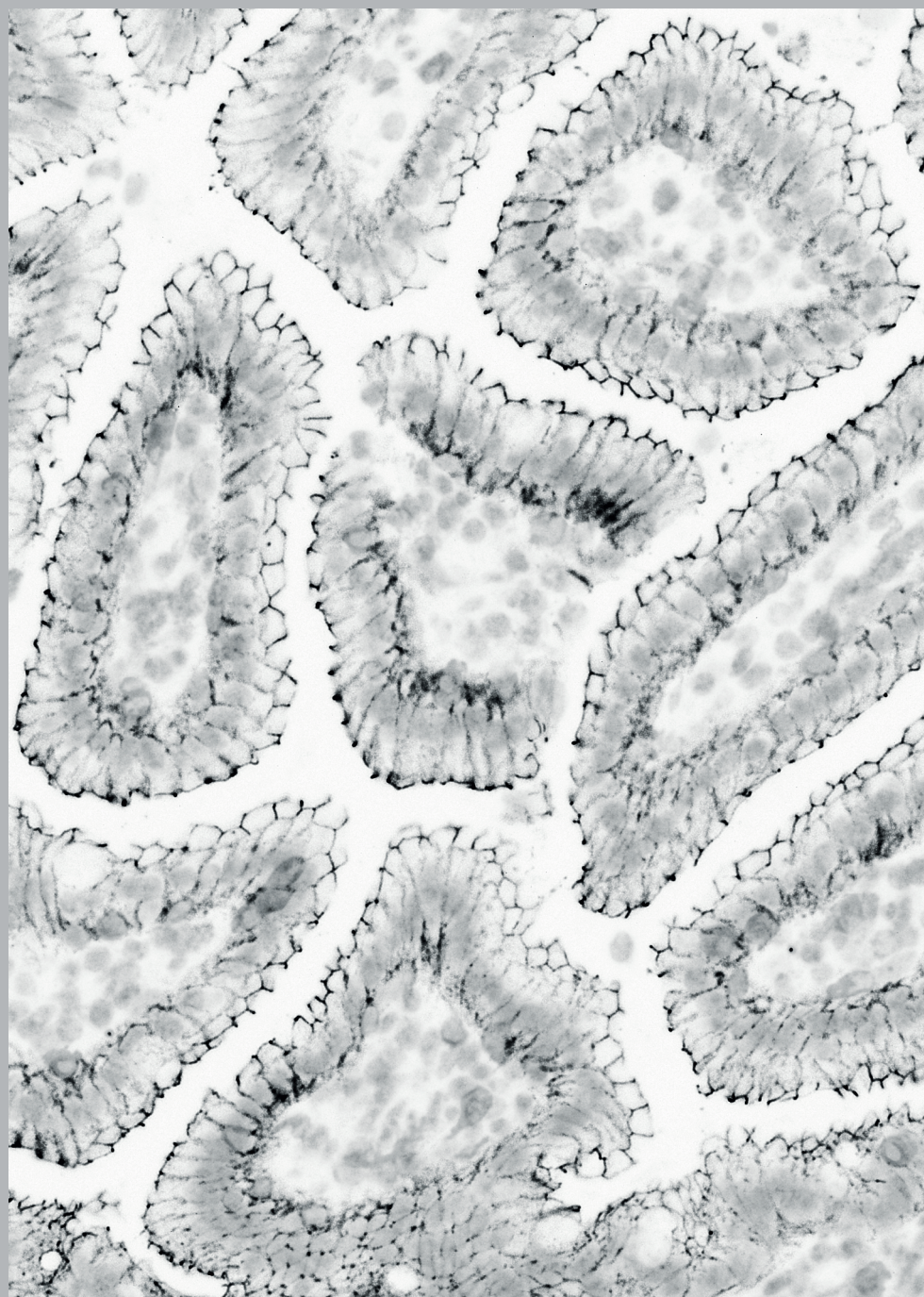
## References

1. Bischoff SC, Barbara G, Buurman W, Ockhuizen T, Schulzke JD, Serino M, Tilg H, Watson A, Wells JM. Intestinal permeability-a new target for disease prevention and therapy. *BMC Gastroenterol* 2014;14:189.
2. Menard S, Cerf-Bensussan N, Heyman M. Multiple facets of intestinal permeability and epithelial handling of dietary antigens. *Mucosal Immunol* 2010;3:247-259.
3. Groschwitz KR, Hogan SP. Intestinal barrier function: molecular regulation and disease pathogenesis. *J Allergy Clin Immunol* 2009;124:3-20.
4. Peterson LW, Artis D. Intestinal epithelial cells: regulators of barrier function and immune homeostasis. *Nat Rev Immunol* 2014;14:141-153.
5. Chiba H, Osanai M, Murata M, Kojima T, Sawada N. Transmembrane proteins of tight junctions. *Biochim Biophys Acta* 2008;1778:588-600.
6. Schneeberger EE, Lynch RD. The tight junction: a multifunctional complex. *Am J Physiol Cell Physiol* 2004;286:C1213-C1228.
7. Tsukita S, Furuse M, Itoh M. Multifunctional strands in tight junctions. *Nat Rev Mol Cell Biol* 2001;2:285-293.
8. Bhat R, Rai RV, Karim AA. Mycotoxins in Food and Feed: Present Status and Future Concerns. *Compr Rev Food Sci Food Saf* 2010;9:57-81.
9. Rodrigues I, Naehrer K. A three-year survey on the worldwide occurrence of mycotoxins in feedstuffs and feed. *Toxins* 2012;4:663-675.
10. Wu F, Groopman JD, Pestka JJ. Public health impacts of foodborne mycotoxins. *Annu Rev Food Sci Technol* 2014;5:351-372.
11. Bennett JW, Klich M. Mycotoxins. *Clin Microbiol Rev* 2003;16:497-516.
12. Liu Y, Wu F. Global burden of aflatoxin-induced hepatocellular carcinoma: a risk assessment. *Environ Health Perspect* 2010;118:818-824.
13. Bhat RV, Shetty PH, Amruth RP, Sudershan RV. A foodborne disease outbreak due to the consumption of moldy sorghum and maize containing fumonisin mycotoxins. *J Toxicol Clin Toxicol* 1997;35:249-255.
14. Bouhet S, Oswald IP. The intestine as a possible target for fumonisin toxicity. *Mol Nutr Food Res* 2007;51:925-931.
15. Pestka JJ. Deoxynivalenol: mechanisms of action, human exposure, and toxicological relevance. *Arch Toxicol* 2010;84:663-679.
16. Pestka JJ, Moorman MA, Warner RL. Altered serum immunoglobulin response to model intestinal antigens during dietary exposure to vomitoxin (deoxynivalenol). *Toxicol Lett* 1990;50:75-84.
17. Pfohl-Leszkowicz A, Manderville RA. Ochratoxin A: An overview on toxicity and carcinogenicity in animals and humans. *Mol Nutr Food Res* 2007;51:61-99.
18. Magoha H, De Meulenaer B, Kimanya M, Hipolite D, Lachat C, Kolsteren P. Fumonisin B1 contamination in breast milk and its exposure in infants under 6 months of age in Rombo, Northern Tanzania. *Food Chem Toxicol* 2014;74:112-116.
19. Rubert J, Leon N, Saez C, Martins CP, Godula M, Yusa V, Manes J, Soriano JM, Soler C. Evaluation of mycotoxins and their metabolites in human breast milk using liquid chromatography coupled to high resolution mass spectrometry. *Anal Chim Acta* 2014;820:39-46.
20. Hidalgo IJ, Raub TJ, Borchardt RT. Characterization of the human colon carcinoma cell line (Caco-2) as a model system for intestinal epithelial permeability. *Gastroenterology* 1989;96:736-749.
21. Sambuy Y, De Angelis I, Ranaldi G, Scarino ML, Stamatii A, Zucco F. The Caco-2 cell line as a model of the intestinal barrier: influence of cell and culture-related factors on Caco-2 cell functional characteristics. *Cell Biol Toxicol* 2005;21:1-26.
22. Sun H, Chow EC, Liu S, Du Y, Pang KS. The Caco-2 cell monolayer: usefulness and limitations. *Expert Opin Drug Metab Toxicol* 2008;4:395-411.
23. Blikslager AT, Moeser AJ, Gookin JL, Jones SL, Odle

- J. Restoration of barrier function in injured intestinal mucosa. *Physiol Rev* 2007;87:545-564.
24. Blikslager AT. Mucosal epithelial barrier repair to maintain pig health. *Livest Sci* 2010;133:194-199.
25. Vos AP, M'Rabet L, Stahl B, Boehm G, Garssen J. Immune-modulatory effects and potential working mechanisms of orally applied nondigestible carbohydrates. *Crit Rev Immunol* 2007;27:97-140.
26. Vulevic J, Drakoularakou A, Yaqoob P, Tzortzis G, Gibson GR. Modulation of the fecal microflora profile and immune function by a novel trans-galactooligosaccharide mixture (B-GOS) in healthy elderly volunteers. *Am J Clin Nutr* 2008;88:1438-1446.
27. Ben XM, Zhou XY, Zhao WH, Yu WL, Pan W, Zhang WL, Wu SM, Van Beusekom CM, Schaafsma A. Supplementation of milk formula with galacto-oligosaccharides improves intestinal micro-flora and fermentation in term infants. *Chin Med J (Engl)* 2004;117:927-931.
28. Fanaro S, Marten B, Bagna R, Vigi V, Fabris C, Pena-Quintana L, Arguelles F, Scholz-Ahrens KE, Sawatzki G, Zelenka R, *et al.* Galacto-oligosaccharides are bifidogenic and safe at weaning: a double-blind randomized multicenter study. *J Pediatr Gastroenterol Nutr* 2009;48:82-88.
29. Fanaro S, Boehm G, Garssen J, Knol J, Mosca F, Stahl B, Vigi V. Galacto-oligosaccharides and long-chain fructo-oligosaccharides as prebiotics in infant formulas: a review. *Acta Paediatr* 2005;94:22-26.
30. Ishikawa H, Matsumoto S, Ohashi Y, Imaoka A, Setoyama H, Umesaki Y, Tanaka R, Otani T. Beneficial effects of probiotic bifidobacterium and galacto-oligosaccharide in patients with ulcerative colitis: a randomized controlled study. *Digestion* 2011;84:128-133.
31. Bracarense AP, Luciola J, Grenier B, Drociunas Pacheco G, Moll WD, Schatzmayr G, Oswald IP. Chronic ingestion of deoxynivalenol and fumonisin, alone or in interaction, induces morphological and immunological changes in the intestine of piglets. *Br J Nutr* 2012;107:1776-1786.
32. Keshavarzian A, Fusunyan RD, Jacyno M, Winship D, MacDermott RP, Sanderson IR. Increased interleukin-8 (IL-8) in rectal dialysate from patients with ulcerative colitis: evidence for a biological role for IL-8 in inflammation of the colon. *Am J Gastroenterol* 1999;94:704-712.
33. Fusunyan RD, Quinn JJ, Ohno Y, MacDermott RP, Sanderson IR. Butyrate enhances interleukin (IL)-8 secretion by intestinal epithelial cells in response to IL-1beta and lipopolysaccharide. *Pediatr Res* 1998;43:84-90.
34. Rossi O, Karczewski J, Stolte EH, Brummer RJ, van Nieuwenhoven MA, Meijerink M, van Neerven JR, van Ijzendoorn SC, van Baarlen P, Wells JM. Vectorial secretion of interleukin-8 mediates autocrine signalling in intestinal epithelial cells via apically located CXCR1. *BMC Res Notes* 2013;6:431.
35. Zenhom M, Hyder A, de Vrese M, Heller KJ, Roeder T, Schrezenmeir J. Prebiotic Oligosaccharides Reduce Proinflammatory Cytokines in Intestinal Caco-2 Cells via Activation of PPAR gamma and Peptidoglycan Recognition Protein 3. *J Nutr* 2011;141:971-977.
36. Varasteh S, Braber S, Garssen J, Fink-Gremmels J. Galacto-oligosaccharides exert a protective effect against heat stress in a Caco-2 cell model. *J Funct Foods* 2015;16:265-277.
37. Akbari P, Braber S, Alizadeh A, Verheijden KA, Schoterman MH, Kraneveld AD, Garssen J, Fink-Gremmels J. Galacto-oligosaccharides Protect the Intestinal Barrier by Maintaining the Tight Junction Network and Modulating the Inflammatory Responses after a Challenge with the Mycotoxin Deoxynivalenol in Human Caco-2 Cell Monolayers and B6C3F1 Mice. *J Nutr* 2015;145:1604-1613.
38. Bhatia S, Prabhu PN, Benefiel AC, Miller MJ, Chow J, Davis SR, Gaskins HR. Galacto-oligosaccharides may directly enhance intestinal barrier function through the modulation of goblet cells. *Mol Nutr Food Res* 2015;59:566-573.
39. Boehm G, Moro G. Structural and functional aspects of prebiotics used in infant nutrition. *J Nutr*

- 2008;138:S1818-S1828.
40. Sanz ML, Cote GL, Gibson GR, Rastall RA. Influence of glycosidic linkages and molecular weight on the fermentation of maltose-based oligosaccharides by human gut bacteria. *J Agric Food Chem* 2006;54:9779-9784.
41. Pompei A, Cordisco L, Raimondi S, Amaretti A, Pagnoni UM, Matteuzzi D, Rossi M. *In vitro* comparison of the prebiotic effects of two inulin-type fructans. *Anaerobe* 2008;14:280-286.
42. Ladirat SE, Schols HA, Nauta A, Schoterman MHC, Schuren FHJ, Gruppen H. *In vitro* fermentation of galacto-oligosaccharides and its specific size-fractions using non-treated and amoxicillin-treated human inoculum. *Bioact Carbohydr Dietary Fibre* 2014;3:59-70.
43. Boehm G, Stahl B. Oligosaccharides from milk. *J Nutr* 2007;137:S847-S849.
44. Bode L, Jantscher-Krenn E. Structure-function relationships of human milk oligosaccharides. *Adv Nutr* 2012;3:S383-S391.
45. Pichery M, Mirey E, Mercier P, Lefrancais E, Dujardin A, Ortega N, Girard JP. Endogenous IL-33 is highly expressed in mouse epithelial barrier tissues, lymphoid organs, brain, embryos, and inflamed tissues: in situ analysis using a novel IL-33-LacZ gene trap reporter strain. *J Immunol* 2012;188:3488-3495.
46. Cayrol C, Girard JP. IL-33: an alarmin cytokine with crucial roles in innate immunity, inflammation and allergy. *Curr Opin Immunol* 2014;31:31-37.
47. Miller AM. Role of IL-33 in inflammation and disease. *J Inflamm* 2011;8:22.
48. Arslanoglu S, Moro GE, Boehm G. Early supplementation of prebiotic oligosaccharides protects formula-fed infants against infections during the first 6 months of life. *J Nutr* 2007;137:2420-2424.
49. van Hoffen E, Ruiter B, Faber J, M'Rabet L, Knol EF, Stahl B, Arslanoglu S, Moro G, Boehm G, Garssen J. A specific mixture of short-chain galacto-oligosaccharides and long-chain fructo-oligosaccharides induces a beneficial immunoglobulin profile in infants at high risk for allergy. *Allergy* 2009;64:484-487.
50. Jeong HS, Kwon HK, Choi JS. High-purity galactooligosaccharides and uses thereof. Patents US 20110189342 A1; 2011.





# *Chapter 9*



General discussion



The interplay between an individual, human or animal, with the environment is a pivotal key to health and well-being. A major unit in this interaction is the gastrointestinal (GI) tract due to its large surface area (approximately 400 m<sup>2</sup> in an adult human) and its role as interface between nutritional and harmful substances, including natural antigens, pathogens and toxins. To protect the body from these potentially hazardous stressors, a physical barrier between the intestinal lumen and the underlying tissue, including the gut-associated immune system, is formed by a monolayer of tightly adhered intestinal epithelial cells (IEC) (1-3).

The intestinal epithelium contains not only enterocytes, but also mucus-secreting goblet cells, contributing to a chemical barrier, as well as Paneth cells that actively secrete functional anti-microbial peptides (4, 5). The second line of defense is the lamina propria of the intestinal wall, which hosts the majority of mucosal immune cells of the body. The major challenge for the immune system is to develop tolerance against nutritional substances and commensal non-dangerous bacterial population, while recognizing and attacking invading pathogens (2, 6).

Permeability of the intestinal barrier is facilitated by two main routes: transcellular and paracellular pathways. The transcellular permeability is generally related to the passage of soluble nutrients, such as minerals, amino acids, fatty acids, sugars and water, through epithelial cells, which is often mediated by specific transporters (7-9). The paracellular permeability is associated with transport across an epithelium by passing through the intercellular space between epithelial cells. This is controlled by a dynamic multiprotein network, sealing the apical and apical-lateral sites of the epithelial cells, composed of tight junctions (TJs), adherens junctions and desmosomes (for details see **Chapter 2**).

### **Mycotoxins as food contaminants and their potential to impair gut barrier functions**

Mycotoxins are the most frequent natural contaminants present in the daily diets of humans as well as animals. While previously, mycotoxins have been mainly considered as being of public health concern due to the mutagenic, genotoxic and probably pro-carcinogenic properties, recent interest focuses on the direct effects of certain mycotoxins on the innate and acquired immune system and on gut health in general (as reviewed in **Chapter 3**) (10-12). In this context, special attention has been given to the deoxynivalenol (DON), which is produced by various *Fusarium* species at the pre-harvest stage. DON occurs in many staple foods such as cereals and grains, in particularly wheat and wheat-based products. DON resists the technical processes of milling and food processing and can be detected in ready-to-consume food commodities (10, 13, 14). The high incidence of human exposure to DON is confirmed by the analysis of human urine samples demonstrating that the exposure incidence exceeds in many cases 90% of the tested population. Human exposure to DON can cover all age groups, even the developing fetus, as it also transfers the placental barrier (15, 16).

In experimental studies with high DON concentrations, DON exerts a variety of toxic effects, but the intestinal epithelium and the gut immune system are generally believed

to be the main target organs for DON (17-20). We already demonstrated in piglets, that even after low-level exposure to DON, which has been generally considered as acceptable in animal feeds, clinically relevant changes are measurable in markers of gut health and integrity (21).

In the presented investigations, DON was applied as a relevant model substance to study the impairment of the intestinal barrier function. The choice was made in consideration of its above-mentioned role as food contaminant, qualifying it as a substance that also in real life challenges the intestinal barrier (in contrast to many other models), as demonstrated by *in vitro* as well as *in vivo* studies (10, 13, 22). In this study, special emphasis was given to the effect of DON on the expression and cellular distribution of TJ proteins. It was demonstrated that the increased paracellular permeability induced by DON is associated with a derangement of the cellular distribution of TJ proteins (for details see **Chapter 4**). Conflicting results are described related to mechanisms behind the DON effects on the TJ network. Pinton *et al.* (23) described that the DON-induced activation of the mitogen-activated protein kinase (MAPK) extracellular signal-regulated kinase 1 and 2 (ERK1/2) signaling pathway correlates with a reduction in barrier function observed by a decrease in transepithelial resistance, increase in paracellular permeability and decrease in CLDN4 protein expression, whereas others pointed out that MAPK ERK1/2, c-Jun N-terminal kinase, and NF- $\kappa$ B pathways were not involved (24).

It is known that DON activates MAPK via a mechanism that has been termed the “ribotoxic stress response” (13). It has been proposed that DON inhibit protein synthesis by binding to the peptidyl transferase region of the ribosome and interfering with initiation and elongation steps of protein translation. Furthermore, DON can also activate ribosome-associated kinase known as double-stranded RNA-associated protein kinase (PKR) by altering the tertiary structure of 28S ribosomal-RNA. Promoting the degradation of 28S ribosomal RNA via an apoptosis associated pathway, DON impairs the ribosome function resulting in an inhibition of the translation step in protein synthesis (25-28). In addition, DON seems to prolong the usually transient expression of genes related to activation of signaling cascades by transcriptional enhancement and/or transcript stabilization (29). These mechanisms might explain the findings in our studies, where the derangement of the cellular localization of TJ proteins, was accompanied by an increase in gene expression, but a decrease in protein levels of various TJ proteins.

Due to the DON-induced translational impairment, *de novo* synthesis of TJ proteins could be delayed, and hence might cause a long-lasting impairment of barrier function, particularly after multiple exposures as common for food-born toxins. The exact molecular targets for DON in the TJ complex still remains to be elucidated, but the functional alterations that could be measured clearly indicate the clinical relevance of these findings, identifying DON as risk factor for intestinal barrier breakdown.

**Clinical manifestation of epithelial damage: chronic inflammatory responses**

TJ proteins form a continuous belt-like structure encircling epithelial cells at the border between the apical and lateral membrane regions and efficiently control paracellular permeability. The metabolic pathways involved in the regulation of TJ homeostasis are still largely unknown. Under pathophysiological conditions, different cytokines such as IFN- $\gamma$ , TNF- $\alpha$ , IL-1 $\beta$ , IL-4, IL-6 and IL-13 can affect the function of TJ proteins and as a consequence contribute to barrier impairment (8, 30, 31). In this aspect, T cells and mast cells play a crucial role in immune regulation of intestinal barrier function as well. T cell-derived IFN- $\gamma$  and TNF- $\alpha$  induce phosphorylation of epithelial myosin light chain (MLC), leading to disruption of TJ structures (32). Mast cells release a variety of inflammatory mediators ranging from cytokines to proteases, which have been shown to impair intestinal barrier function. For example, mast cell protease-1 (MCPT-1) degrades the TJ proteins, altering barrier function (8, 33).

The model compound DON used in the current studies, is known to induce a pro-inflammatory response as evidenced by increased serum levels of IFN- $\gamma$ , IL-2, IL-4 and IL-6 levels in DON-exposed mice (34) as well as by the induction of inflammation- and immune-regulated genes after DON exposure *in vitro* (35, 36). In the current experiments, the DON-induced increase in CXCL1 as well as CXCL2 expression (murine CXCL8 homologs) *in vivo* and CXCL8 expression *in vitro* could serve as markers for the pro-inflammatory effects. Basolateral secretion of CXCL8 plays a role in the recruitment of circulating neutrophils from the bloodstream to site of tissue injury or infection, while it is speculated that apically secreted CXCL8 may initiate or augment the pathway responses in epithelial restitution prior to any potential loss of barrier integrity because of toxin production (37-40). It is prudent to assume that the secretion of these chemokines are important factors driving the regulation of TJs and the loss of barrier function. Both MAPK p38 and NF- $\kappa$ B pathways have been identified to play a role in the DON-induced CXCL8 secretion (41, 42).

Derangement of the TJ protein complex increases the paracellular permeability and may trigger the translocation of allergens and pathogens into the sub-epithelial space resulting in activation of the immune system. The final outcome is an accelerating inflammatory response that further fuels barrier disintegration and is further thought to be important in the initiation and/or development of allergies and several chronic inflammatory diseases, such as inflammatory bowel disease and celiac diseases (8, 43-45). We therefore hypothesized in the related publication (**Chapter 4**) that DON-exposure might contribute to the prevalence of these diseases.

**Clinical manifestation of epithelial damage: allergic responses**

Epithelial damage may contribute to the development of allergic manifestations and it has been previously shown that disruption of the airway epithelial barrier as well as epidermal barrier could induce allergic sensitization. The proteolytic activity of inhaled allergens, such as house dust mite (HDM), pollen or fungi (particularly *Aspergillus*

*fumigatus*) can disrupt the TJ network in the lung epithelium. Subsequently, this epithelial damage results in activation of dendritic cells (DC) and the release of cytokines and alarmins (endogenous danger signals) important for a Th2 cell skewing in immune responses, as well as the IgE synthesis by B cells (46–48). Also in the skin, Strid *et al.* (49, 50) found that even mild epidermal damage results in production of alarmins and cytokines, which initiate migration and activation of epidermal  $\gamma\delta$  T cells required for the induction of specific cytokines associated with Th2 responses leading to a systemic IgE response. In line with these observations in lung and skin, intestinal epithelial damage and subsequent release of alarmins may also be essential requisites for the initiation and development of allergic sensitization and ultimately Th2-mediated immune responses (51, 52).

Local protective and tolerogenic immune responses towards the luminal content depend on antigen sampling by the gut epithelial layer (53). Recent investigations by our group showed that DON facilitates allergic sensitization to food proteins, suggesting a potential role of DON and possible other food contaminants in allergic sensitization in humans (54). In this study, the DON-induced epithelial damage resulted in a rapid increase of intestinal IL-33 and its receptor ST2 in serum, which was associated with changes in intestinal cell subsets, including elevated numbers of ILC2 and DC (54).

Among the different alarmins that are produced in response to tissue damage, special attention has been devoted recently to IL-33, a member of the IL-1 cytokine family. IL-33 delivers an important danger signal in the cellular response to the epithelial damage (55) and it has been shown that the epithelial inflammatory response is largely regulated by IL-33 and its receptor ST2 (56). This epithelial cell-derived IL-33 can induce an allergic response, even in the absence of the B and T cells, which suggest the potential involvement of type 2 innate lymphoid cells (ILC2) in this response (57, 58). ILC2 produce IL-5, IL-9 and IL-13 in response to IL-33 and therefore, serve as an important signal that orchestrates the type 2 response to allergens (58, 59).

Our and previous findings demonstrated that IL-33 and ST2 are both associated with the development and maintenance of allergic asthma (60, 61), whereas treatments with anti-IL-33 or anti-ST2 antibodies abrogated the Th2-mediated inflammatory response (62, 63). Besides the involvement of IL-33 in allergies, IL-33 is also related to an impaired barrier function as observed in mice treated with exogenous IL-33, IL-33<sup>-/-</sup> mice and in patients with Crohn's disease and ulcerative colitis (64–67). In **Chapter 7**, we described an increase in IL-33 and ST2 mRNA expression in the mouse distal small intestine after a DON gavage and even the IL-33 production in the distal small intestine was augmented by DON as demonstrated by immunohistochemistry.

## **Intervention strategies to preserve losses of barrier integrity**

### **1. Direct effects of galacto-oligosaccharides on TJ proteins**

Dietary application of non-digestible oligosaccharides, such as galacto-oligosaccharides (GOS) and fructo-oligosaccharides (FOS), is commonly used in infant formula to mimic the gut health- promoting effects of human milk oligosaccharides (HMOs), and have been associated with a reduced risk of inflammatory diseases as well as allergic responses. Initially, oligosaccharides have been selected due to their prebiotic activity, since they shape the intestinal microbiota and promote the development of desirable microorganisms, such as *Bifidobacterium* and *Lactobacillus* spp., thereby supporting both digestive and immune health (68-71).

Importantly, in this thesis we described the direct, microbiota-independent effects of selected oligosaccharides on the TJ network and the corresponding barrier integrity. The first evidence was obtained by demonstrating the capability of GOS to promote the reassembly of TJ proteins after a calcium-deprivation period (see **Chapter 5** for details). Furthermore, we showed that GOS can prevent the DON-induced intestinal barrier disruption mainly through direct stabilization of the expression and cellular distribution of CLDN3 (**Chapter 5**). It has been previously demonstrated that the Ras GTPase superfamily (including Rho and Rab13), protein kinase C (PKC) and AMP-activated protein kinase (AMPK) regulate the assembly of epithelial TJ proteins, and therefore these are interesting targets to be evaluated in the future (72-74). Rho GTPase-dependent regulation of the actin cytoskeleton is very important for processes requiring the assembly of TJ proteins (73, 75), whereas Rab13 plays a role in early junctional formation and is involved in endocytic recycling and regulating the transport of transmembrane proteins, including claudins and occludin, to the plasma membrane (76-78). Furthermore, PKC is known to regulate the subcellular localization, phosphorylation states, and transcription of several TJ proteins, including claudins, occludin and ZO proteins (31, 74), whereas AMPK maintains the cellular energy balance. It has been shown that the level of AMPK phosphorylation increases during calcium-induced TJs assembly and expression of a kinase-dead mutant of AMPK inhibits TJs assembly (72, 79).

Besides TJ proteins, adherens junctions (AJ) are also involved in intestinal epithelial integrity and homeostasis. AJ consist of transmembrane proteins, including E-cadherin and nectin, as well as associated cytoplasmic proteins, the catenins, which are directly connected to the actin cytoskeleton (80-82). In contrast to TJ proteins, the intercellular space does not completely disappear at the level of adherens junctions (83). Considering that in particular E-cadherin plays a role in initiation and stabilization of cell-cell contacts through a  $\text{Ca}^{2+}$  dependent mechanism, it can be hypothesized that the acceleration of the TJs reassembly in the calcium switch assay as well as the functional losses observed in our transcellular transport experiments, are also associated with changes in E-cadherin expression (which was not measured in these studies). Indeed, in other experiments of our group we could show that GOS prevented the protein disruption as well as the delocalization of E-cadherin, related to the loss of barrier function under the conditions

of heat stress (84). In the same study, GOS prevented the heat-induced increase in haem oxygenase-1 (HO-1) mRNA levels, a sensitive marker of oxidative stress. Possibly GOS, like other glycans, have a macromolecule-stabilizing character that protect cells against oxidative stress (85). Numerous studies have reported that oxidative stress is also an important mechanism in the toxicity of tricothecenes, like DON (86-89).

## 2. Immunomodulatory effects of galacto-oligosaccharides on the intestinal barrier

Numerous studies have addressed the potential immunomodulatory effect of dietary oligosaccharides in human and animals focusing on their effects of the intestinal flora (68, 90, 91). However, when studying the microbiota-independent effects of GOS on intestinal barrier integrity, we could demonstrate that GOS have the ability to modulate the DON-induced epithelial CXCL8 release (**Chapter 5**). We further demonstrated that dietary intervention with GOS mitigates the alarmin IL-33 in mouse intestines, observed in a murine model for intestinal barrier dysfunction and in murine lungs in the HDM-induced asthma model (**Chapter 7**). These promising effects may open new avenues to use GOS not only as a prebiotic in infant nutrition, but also as a functional ingredient that targets inflammatory and allergic responses.

The currently available preclinical experiments warrant studies to further unravel the mechanism behind this effect and clinical studies would be the next approach to evaluate our findings in experimental animals. Dietary intervention studies with GOS and other oligosaccharides related to diseases with intestinal barrier breakdown, like inflammatory bowel disease and celiac disease, would be a valuable addition to the clinical studies that are already conducted in infants as well as in adults (92-94). In addition, our findings suggest that also animals would benefit from the addition of GOS and other oligosaccharides to their diet. Typical indications for such an application are neonatal animals, piglets around weaning experiencing a loss of barrier function due to drastic dietary changes, animals exposed to mycotoxin-contaminated diets (pigs show the highest sensitivity to DON), as well as heat-exposed chickens (21, 95, 96).

Only a few studies have recently described direct immunomodulatory effects of oligosaccharides with different cell types during both steady-state and inflammatory conditions (97-100).

For example, incubation of unstimulated Caco-2 cells either with FOS or  $\alpha$ 3-sialyllactos can inhibit the expression of pro-inflammatory cytokines (CXCL8, IL-12 and TNF- $\alpha$ ) and the nuclear translocation of NF- $\kappa$ B. These immunomodulatory effects of oligosaccharides might be related to the induction of the nuclear receptor peroxisome proliferator-activated receptor  $\gamma$  (PPAR $\gamma$ ), which regulates the peptidoglycan recognition protein 3 (PGlyRP3) (98). Badia *et al.* (101) reported that plant-derived oligosaccharides are able to attenuate *Salmonella*-induced IL-6 and CXCL8 secretion in porcine intestinal epithelial cells. In addition, oligosaccharides may also act as molecular receptor decoys or antiadhesives that can competitively inhibit the adherence of pathogens to the host

epithelial cell surface (102).

Various investigations hypothesize an interaction with TLR4 receptors as the GOS/lcFOS-induced IL-10 release by DCs is impaired by addition of a TLR4 antagonist (103). Comparable results were described by our group showing that PBMCs derived from GOS-treated foals were less responsive to a LPS challenge (97) and Ortega-Gonzalez *et al.* (104) suggested that oligosaccharides are TLR4 ligands in intestinal epithelial cells. While this is certainly a valid hypothesis, the fact that Caco-2 cells, used in current experiments, do not express TLR4 receptors, points towards alternative molecular targets.

Epithelial cells express proteins involved in the recognition of carbohydrate (glycan) structures, so called lectins that may be involved in the recognition of non-digestible oligosaccharides. One family of the soluble type lectins expressed by IEC that contain carbohydrate recognition domains, are galectins, which exhibit binding specificity for  $\beta$ -galactosides (105). To date, IEC were found to express galectin-2, -3, -4, -6, -7 and a specific long isoform of galectin-9 (105, 106). Although it has not been confirmed, HMOs or related oligosaccharides like GOS and FOS, may bind to galectins, resulting in modulation of the immune response in the intestine. de Kivit *et al.* (100) showed that galectin-9 is expressed and secreted by IEC upon activation of TLR9 and exposure to GOS/lcFOS, which supports a tolerogenic DC-mediated Th1/Treg response. Due to the importance of the crosstalk between IEC and the underlying immune system, application of co-culture models with IEC and different immune cells (100, 107) may provide additional insights into the direct targets and immunomodulatory properties of GOS and other oligosaccharides.

### **3. Structure-activity relationships of galacto-oligosaccharides**

Commercially available GOS are produced by enzymatic digestion of the milk sugar lactose. This fermentation process results in a complex mixture of oligosaccharides with different degrees of polymerization (DP) (for details see **Chapter 6**). When comparing these GOS mixtures with plant-derived oligosaccharides, such as FOS and Inulin (used as a reference), it appeared that the GOS mixture was more effective in the experimental model with Caco-2 cells, in which TEER and paracellular transport of marker molecules were used as main functional parameters to assess their effect on DON-induced intestinal barrier breakdown.

The comparison with individual DP fractions again revealed that the mixture of different fractions was more potent than individual fractions. Also an additive effect of various DP fractions present in the mixture can be assumed. The further results showed that particularly the lower DP fractions (like DP2 and DP3) present in Vivinal® GOS syrup were more effective compared to the higher DP fractions. However, the DP concentration as present in Vivinal® GOS syrup may be crucial for the observed protective effects. Compared to GOS, more complex oligosaccharides with higher degree of polymerization, like Inulin, did not affect the intestinal barrier integrity as well as the corresponding CXCL8 release. This is not entirely unexpected, as with a higher DP and an increased molecular size,



membrane attachment and/or transport will be hampered.

It has been speculated for a long time, whether any of the oligosaccharides that are dietary applied, could pass the intestinal barrier. However, the presence of HMOs in the circulation (plasma and urine) of breastfed infants is recently reported (108). In addition, recent investigations by our group provided clear evidence for a – albeit limited – absorption from the intestinal lumen, as dietary applied oligosaccharide structures could be detected in the blood and urine of piglets (109).

The discovery of prebiotic oligosaccharides in the body fluid highlights the importance of a further evaluation of the systemic effects of oligosaccharides in humans and the molecular targets of GOS as discussed above.

### **Other potential molecular targets for dietary oligosaccharides at the intestinal barrier**

Besides the TJ network, a healthy gut barrier function is further acquired by other structural elements, such as the physical barrier (mucus layer), the biochemical barrier (anti-microbial peptides) and the immunological barrier (secretory immunoglobulin A, sIgA), each of which contributes in a unique way to the maintenance of barrier integrity (3, 5, 110). Improved mucosal immunity and barrier function induced by prebiotic supplementation has been previously attributed to specific changes in the gut microbiota, particularly the stimulation of *Lactobacillus* and *Bifidiobacterium* spp. growth, which are known to increase the expression and secretion of mucus, human  $\beta$ -defensin 2 and sIgA (111-113). However, direct, microbiota-independent, effects of GOS and other oligosaccharides on the physical, biochemical and immunological barriers awaits further clarification.

An important, but often neglected part of gut barrier, is the mucus layer produced by goblet cells. In addition to forming of physical barrier against pathogens, intestinal mucus contributes to the establishment of the symbiosis between the host and the commensal bacteria (114, 115). The major components of the mucus are called mucins, and the most prominent mucin alongside the small as well as the large intestine is mucin-2 (MUC-2). MUC-2 is densely packed within mucus granules of goblet cells and is released via exocytosis (5, 116). Bhatia *et al.* (117) described that GOS may enhance mucosal barrier function through direct stimulation of intestinal goblet cell secretory products, such as MUC-2, trefoil factor-3 and resistin-like molecule  $\beta$ . In addition, GOS also enhance specific Golgi sulfotransferases, which contribute to the production of barrier-enhancing sulfomucins. Interestingly, it is known that DON inhibits the expression of intestinal mucins, produced by goblet cells, through a PKR and MAPK dependent repression of the resistin-like molecule  $\beta$ , increasing the susceptibility of an enteric infection following DON exposure (118).

Secretory IgA (sIgA), produced by lamina propria plasma cells, is the major mucosal antibody secreted into the gut and it has been recognized as a first line of innate immunological protection against mucosal antigens. Immune exclusion generally refers

to the process of agglutinating of antigens or microbial pathogens by crosslinking them with sIgA, trapping them in the mucus layer, and clearing them through peristalsis (110). Apical exposure of *Shigella flexneri* to Caco-2 cells, for example, causes disruption of the TJ network, actin depolymerization and cell death, which could be prevented by agglutinating sIgA (119, 120). We recently investigated the effects of GOS on the mucosal immune system by measuring sIgA in saliva of piglets and we observed that the addition of GOS in the diet significantly increased the salivary IgA levels (121). We speculated that promoting the abundance of specific intestinal *Bifidobacterium* spp. by dietary GOS as observed in the same study, might contribute to this elevated sIgA concentration in saliva (121-123). However, a direct effect on the microbiome in the oral cavity could not be entirely excluded. Since formula-fed infants lack the transfer of protective maternal sIgA (124), they would potentially benefit from dietary ingredients that support the production of endogenous sIgA, hence it is important to unravel the exact mechanism behind this effect.

## Conclusions

The current studies have focused on the identification of microbiota-independent effects of oligosaccharides. To demonstrate their potential protective effects, the intestinal barrier function was challenged by DON, a mycotoxin that occurs in the daily diet. The main conclusion derived from our recent work is that a DON-induced disruption of the TJ network and the corresponding epithelial inflammatory response could be prevented by GOS, in addition to the well-known prebiotic effect of these non-digestible carbohydrates. These findings clearly indicate that various molecular targets have to be considered when evaluating the clinical efficacy of GOS. The presented experiments were conducted with cultures of colonic epithelial cells (Caco-2 cells) in the absence of immune cells. Although the results of various experimental approaches were confirmed in *in vivo* experiments in mice, the number of test-parameters remained limited, focusing on the TJs, as a novel approach in assessment of barrier protecting effects of galacto-oligosaccharides. Therefore, the important finding that galacto-oligosaccharides indeed exert microbiota-independent effects should stimulate further investigation into other functional aspects of the intestinal barrier and associated disease conditions. This may result in the identification of new indications for the utilization of their protective effects against bacterial and fungal toxins and other environmental stressors that can jeopardize gut health.

## References

1. Bischoff SC, Barbara G, Buurman W, Ockhuizen T, Schulzke JD, Serino M, Tilg H, Watson A, Wells JM. Intestinal permeability-a new target for disease prevention and therapy. *BMC Gastroenterol* 2014;14:189.
2. Peterson LW, Artis D. Intestinal epithelial cells: regulators of barrier function and immune homeostasis. *Nat Rev Immunol* 2014;14:141-153.
3. Pastorelli L, De Salvo C, Mercado JR, Vecchi M, Pizarro TT. Central role of the gut epithelial barrier in the pathogenesis of chronic intestinal inflammation: lessons learned from animal models and human genetics. *Front Immunol* 2013;4:280.
4. Bevins CL, Salzman NH. Paneth cells, antimicrobial peptides and maintenance of intestinal homeostasis. *Nat Rev Microbiol* 2011;9:356-368.
5. Kim YS, Ho SB. Intestinal goblet cells and mucins in health and disease: recent insights and progress. *Curr Gastroenterol Rep* 2010;12:319-330.
6. Schenk M, Mueller C. The mucosal immune system at the gastrointestinal barrier. *Best Pract Res Clin Gastroenterol* 2008;22:391-409.
7. Kunzelmann K, Mall M. Electrolyte transport in the mammalian colon: mechanisms and implications for disease. *Physiol Rev* 2002;82:245-289.
8. Groschwitz KR, Hogan SP. Intestinal barrier function: molecular regulation and disease pathogenesis. *J Allergy Clin Immunol* 2009;124:3-20.
9. Broer S. Amino acid transport across mammalian intestinal and renal epithelia. *Physiol Rev* 2008;88:249-286.
10. Wu F, Groopman JD, Pestka JJ. Public health impacts of foodborne mycotoxins. *Annu Rev Food Sci Technol* 2014;5:351-372.
11. Bhat R, Rai RV, Karim AA. Mycotoxins in Food and Feed: Present Status and Future Concerns. *Compr Rev Food Sci Food Saf* 2010;9:57-81.
12. Bennett JW, Klich M. Mycotoxins. *Clin Microbiol Rev* 2003;16:497-516.
13. Pestka JJ. Deoxynivalenol: mechanisms of action, human exposure, and toxicological relevance. *Arch Toxicol* 2010;84:663-679.
14. Sobrova P, Adam V, Vasatkova A, Beklova M, Zeman L, Kizek R. Deoxynivalenol and its toxicity. *Interdiscip Toxicol* 2010;3:94-99.
15. Danicke S, Brussow KP, Goyarts T, Valenta H, Ueberschar KH, Tiemann U. On the transfer of the *Fusarium* toxins deoxynivalenol (DON) and zearalenone (ZON) from the sow to the full-term piglet during the last third of gestation. *Food Chem Toxicol* 2007;45:1565-1574.
16. Nielsen JK, Vikstrom AC, Turner P, Knudsen LE. Deoxynivalenol transport across the human placental barrier. *Food Chem Toxicol* 2011;49:2046-2052.
17. Hepworth SJ, Hardie LJ, Fraser LK, Burley VJ, Mijal RS, Wild CP, Azad R, McKinney PA, Turner PC. Deoxynivalenol exposure assessment in a cohort of pregnant women from Bradford, UK. *Food Addit Contam Part A Chem Anal Control Expo Risk Assess* 2012;29:269-276.
18. Sarkanj B, Warth B, Uhlig S, Abia WA, Sulyok M, Klapac T, Krska R, Banjari I. Urinary analysis reveals high deoxynivalenol exposure in pregnant women from Croatia. *Food Chem Toxicol* 2013;62:231-237.
19. Turner PC, Ji BT, Shu XO, Zheng W, Chow WH, Gao YT, Hardie LJ. A biomarker survey of urinary deoxynivalenol in China: the Shanghai Women's Health Study. *Food Addit Contam Part A Chem Anal Control Expo Risk Assess* 2011;28:1220-1223.
20. Warth B, Sulyok M, Fruhmann P, Berthiller F, Schuhmacher R, Hametner C, Adam G, Frohlich J, Krska R. Assessment of human deoxynivalenol exposure using an LC-MS/MS based biomarker method. *Toxicol Lett* 2012;211:85-90.
21. Alizadeh A, Braber S, Akbari P, Garssen J, Fink-Gremmels J. Deoxynivalenol Impairs Weight Gain and Affects Markers of Gut Health after Low-Dose, Short-Term Exposure of Growing Pigs. *Toxins* 2015;7:2071-2095.
22. Pinton P, Oswald IP. Effect of deoxynivalenol and

other Type B trichothecenes on the intestine: a review. *Toxins* 2014;6:1615-1643.

23. Pinton P, Braicu C, Nougayrede JP, Laffitte J, Taranu I, Oswald IP. Deoxynivalenol impairs porcine intestinal barrier function and decreases the protein expression of claudin-4 through a mitogen-activated protein kinase-dependent mechanism. *J Nutr* 2010;140:1956-1962.

24. De Walle JV, Sergent T, Piront N, Toussaint O, Schneider YJ, Larondelle Y. Deoxynivalenol affects *in vitro* intestinal epithelial cell barrier integrity through inhibition of protein synthesis. *Toxicol Appl Pharmacol* 2010;245:291-298.

25. Gray JS, Bae HK, Li JC, Lau AS, Pestka JJ. Double-stranded RNA-activated protein kinase mediates induction of interleukin-8 expression by deoxynivalenol, Shiga toxin 1, and ricin in monocytes. *Toxicol Sci* 2008;105:322-330.

26. Pestka JJ. Deoxynivalenol-induced proinflammatory gene expression: mechanisms and pathological sequelae. *Toxins* 2010;2:1300-1317.

27. Li M, Pestka JJ. Comparative induction of 28S ribosomal RNA cleavage by ricin and the trichothecenes deoxynivalenol and T-2 toxin in the macrophage. *Toxicol Sci* 2008;105:67-78.

28. Pierron A, Mimoun S, Murate LS, Loiseau N, Lippi Y, Bracarense AF, Liaubet L, Schatzmayr G, Berthiller F, Moll WD, *et al.* Intestinal toxicity of the masked mycotoxin deoxynivalenol-3-beta-D-glucoside. *Arch Toxicol* 2015.

29. Azcona-Olivera JI, Ouyang YL, Warner RL, Linz JE, Pestka JJ. Effects of vomitoxin (deoxynivalenol) and cycloheximide on IL-2, 4, 5 and 6 secretion and mRNA levels in murine CD4+ cells. *Food Chem Toxicol* 1995;33:433-441.

30. Suzuki T. Regulation of intestinal epithelial permeability by tight junctions. *Cell Mol Life Sci* 2013;70:631-659.

31. Hu YJ, Wang YD, Tan FQ, Yang WX. Regulation of paracellular permeability: factors and mechanisms. *Mol Biol Rep* 2013;40:6123-6142.

32. Clayburgh DR, Barrett TA, Tang Y, Meddings JB, Van Eldik LJ, Watterson DM, Clarke LL, Mrsny RJ, Turner JR. Epithelial myosin light chain kinase-dependent barrier dysfunction mediates T cell activation-induced diarrhea *in vivo*. *J Clin Invest* 2005;115:2702-2715.

33. McDermott JR, Bartram RE, Knight PA, Miller HR, Garrod DR, Grecis RK. Mast cells disrupt epithelial barrier function during enteric nematode infection. *Proc Natl Acad Sci U S A* 2003;100:7761-7766.

34. Islam MR, Roh YS, Kim J, Lim CW, Kim B. Differential immune modulation by deoxynivalenol (vomitoxin) in mice. *Toxicol Lett* 2013;221:152-163.

35. Wan LY, Turner PC, El-Nezami H. Individual and combined cytotoxic effects of Fusarium toxins (deoxynivalenol, nivalenol, zearalenone and fumonisins B1) on swine jejunal epithelial cells. *Food Chem Toxicol* 2013;57:276-283.

36. Maresca M, Yahi N, Younes-Sakr L, Boyron M, Caporiccio B, Fantini J. Both direct and indirect effects account for the pro-inflammatory activity of enteropathogenic mycotoxins on the human intestinal epithelium: stimulation of interleukin-8 secretion, potentiation of interleukin-1beta effect and increase in the transepithelial passage of commensal bacteria. *Toxicol Appl Pharmacol* 2008;228:84-92.

37. Rossi O, Karczewski J, Stolte EH, Brummer RJ, van Nieuwenhoven MA, Meijerink M, van Neerven JR, van Ijzendoorn SC, van Baarlen P, Wells JM. Vectorial secretion of interleukin-8 mediates autocrine signalling in intestinal epithelial cells via apically located CXCR1. *BMC Res Notes* 2013;6:431.

38. Fusunyan RD, Quinn JJ, Ohno Y, MacDermott RP, Sanderson IR. Butyrate enhances interleukin (IL)-8 secretion by intestinal epithelial cells in response to IL-1beta and lipopolysaccharide. *Pediatr Res* 1998;43:84-90.

39. Keshavarzian A, Fusunyan RD, Jacyno M, Winship D, MacDermott RP, Sanderson IR. Increased interleukin-8 (IL-8) in rectal dialysate from patients with ulcerative colitis: evidence for a biological role for IL-8 in inflammation of the colon. *Am J Gastroenterol*

- 1999;94:704-712.
40. Sturm A, Baumgart DC, d'Heureuse JH, Hotz A, Wiedenmann B, Dignass AU. CXCL8 modulates human intestinal epithelial cells through a CXCR1 dependent pathway. *Cytokine* 2005;29:42-48.
  41. Islam Z, Gray JS, Pestka JJ. p38 Mitogen-activated protein kinase mediates IL-8 induction by the ribotoxin deoxynivalenol in human monocytes. *Toxicol Appl Pharmacol* 2006;213:235-244.
  42. Van De Walle J, Romier B, Larondelle Y, Schneider YJ. Influence of deoxynivalenol on NF-kappaB activation and IL-8 secretion in human intestinal Caco-2 cells. *Toxicol Lett* 2008;177:205-214.
  43. Drago S, El Asmar R, Di Pierro M, Grazia Clemente M, Tripathi A, Sapone A, Thakar M, Iacono G, Carroccio A, D'Agate C, *et al.* Gliadin, zonulin and gut permeability: Effects on celiac and non-celiac intestinal mucosa and intestinal cell lines. *Scand J Gastroenterol* 2006;41:408-419.
  44. Vetrano S, Rescigno M, Cera MR, Correale C, Rumio C, Doni A, Fantini M, Sturm A, Borroni E, Repici A, *et al.* Unique role of junctional adhesion molecule-a in maintaining mucosal homeostasis in inflammatory bowel disease. *Gastroenterology* 2008;135:173-184.
  45. Prasad S, Mingrino R, Kaukinen K, Hayes KL, Powell RM, MacDonald TT, Collins JE. Inflammatory processes have differential effects on claudins 2, 3 and 4 in colonic epithelial cells. *Lab Invest* 2005;85:1139-1162.
  46. Lambrecht BN, Hammad H. The airway epithelium in asthma. *Nat Med* 2012;18:684-692.
  47. Chen JC, Chuang JG, Su YY, Chiang BL, Lin YS, Chow LP. The protease allergen Pen c 13 induces allergic airway inflammation and changes in epithelial barrier integrity and function in a murine model. *J Biol Chem* 2011;286:26667-26679.
  48. Runswick S, Mitchell T, Davies P, Robinson C, Garrod DR. Pollen proteolytic enzymes degrade tight junctions. *Respirology* 2007;12:834-842.
  49. Strid J, Roberts SJ, Filler RB, Lewis JM, Kwong BY, Schpero W, Kaplan DH, Hayday AC, Girardi M. Acute upregulation of an NKG2D ligand promotes rapid reorganization of a local immune compartment with pleiotropic effects on carcinogenesis. *Nat Immunol* 2008;9:146-154.
  50. Strid J, Sobolev O, Zafirova B, Polic B, Hayday A. The intraepithelial T cell response to NKG2D-ligands links lymphoid stress surveillance to atopy. *Science* 2011;334:1293-1297.
  51. Kong J, Chalcraft K, Mandur TS, Jimenez-Saiz R, Walker TD, Goncharova S, Gordon ME, Naji L, Flader K, Larche M, *et al.* Comprehensive metabolomics identifies the alarmin uric acid as a critical signal for the induction of peanut allergy. *Allergy* 2015;70:495-505.
  52. Bol-Schoenmakers M, Marcondes Rezende M, Bleumink R, Boon L, Man S, Hassing I, Fiechter D, Pieters RH, Smit JJ. Regulation by intestinal gammadelta T cells during establishment of food allergic sensitization in mice. *Allergy* 2011;66:331-340.
  53. Menard S, Cerf-Bensussan N, Heyman M. Multiple facets of intestinal permeability and epithelial handling of dietary antigens. *Mucosal Immunol* 2010;3:247-259.
  54. Bol-Schoenmakers M, Braber S, Akbari P, de Graaff P, van Roest M, Kruijssen L, Smit JJ, van Esch BCAM, Jeurink PV, Garssen J, Fink-Gremmels J, Pieters RHH. The mycotoxin deoxynivalenol facilitates allergic sensitization to whey in mice. *Mucosal Immunol* 2016.
  55. Cayrol C, Girard JP. IL-33: an alarmin cytokine with crucial roles in innate immunity, inflammation and allergy. *Curr Opin Immunol* 2014;31:31-37.
  56. Garcia-Miguel M, Gonzalez MJ, Quera R, Hermoso MA. Innate immunity modulation by the IL-33/ST2 system in intestinal mucosa. *Biomed Res Int* 2013;2013:142492.
  57. Kondo Y, Yoshimoto T, Yasuda K, Futatsugi-Yumikura S, Morimoto M, Hayashi N, Hoshino T, Fujimoto J, Nakanishi K. Administration of IL-33 induces airway hyperresponsiveness and goblet cell hyperplasia in the lungs in the absence of adaptive immune system. *Int Immunol* 2008;20:791-800.
  58. Licona-Limon P, Kim LK, Palm NW, Flavell RA.

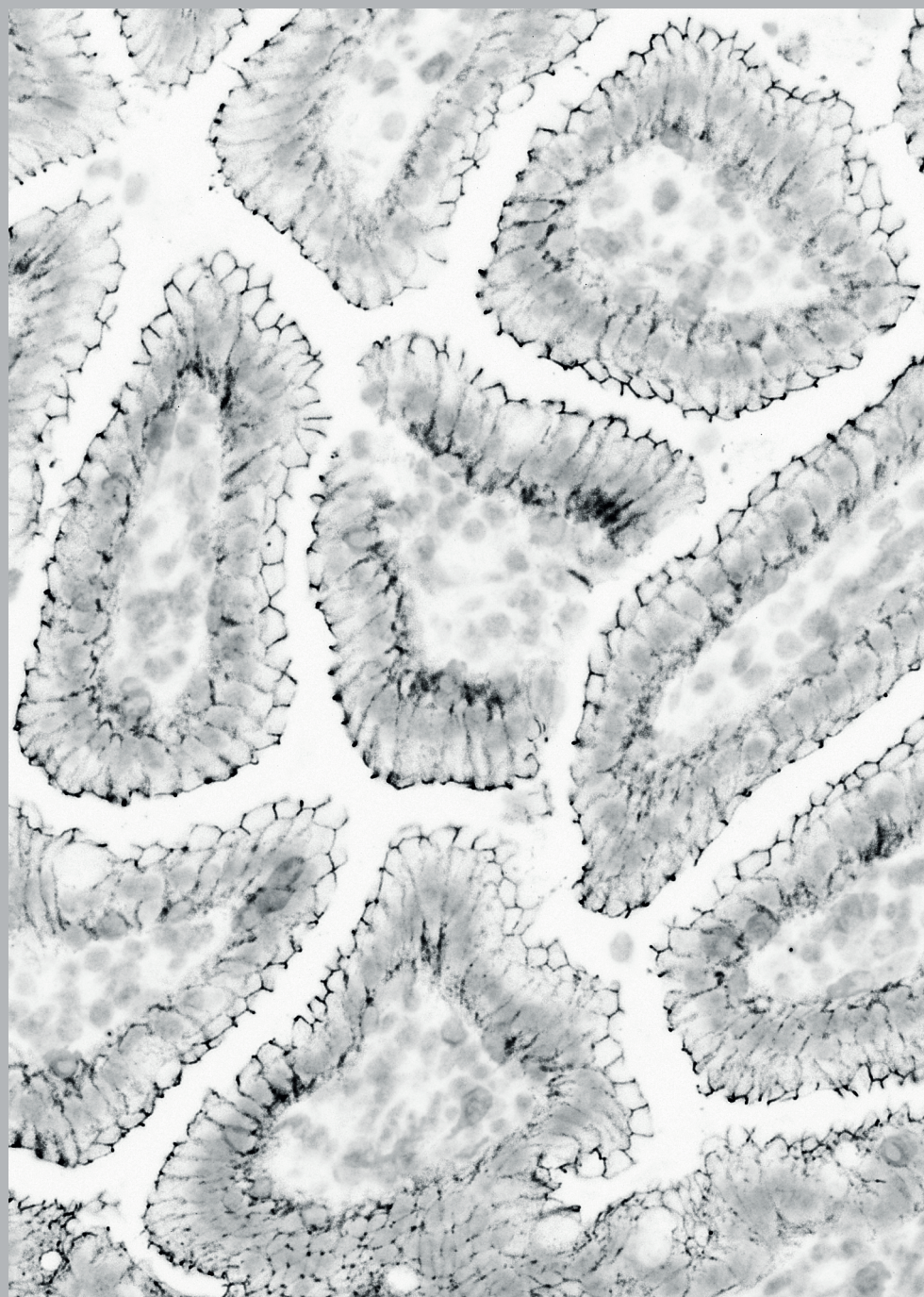
- TH2, allergy and group 2 innate lymphoid cells. *Nat Immunol* 2013;14:536-542.
59. Halim TY, Steer CA, Matha L, Gold MJ, Martinez-Gonzalez I, McNagny KM, McKenzie AN, Takei F. Group 2 innate lymphoid cells are critical for the initiation of adaptive T helper 2 cell-mediated allergic lung inflammation. *Immunity* 2014;40:425-435.
60. Hamzaoui A, Berraies A, Kaabachi W, Haifa M, Ammar J, Kamel H. Induced sputum levels of IL-33 and soluble ST2 in young asthmatic children. *J Asthma* 2013;50:803-809.
61. Verheijden KA, Akbari P, Willemsen LE, Kraneveld AD, Folkerts G, Garssen J, Fink-Gremmels J, Braber S. Inflammation-induced expression of the alarmin interleukin 33 can be suppressed by galactooligosaccharides. *Int Arch Allergy Immunol* 2015;167:127-136.
62. Mizutani N, Nabe T, Yoshino S. Interleukin-33 and alveolar macrophages contribute to the mechanisms underlying the exacerbation of IgE-mediated airway inflammation and remodelling in mice. *Immunology* 2013;139:205-218.
63. Coyle AJ, Lloyd C, Tian J, Nguyen T, Eriksson C, Wang L, Ottoson P, Persson P, Delaney T, Lehar S, *et al*. Crucial role of the interleukin 1 receptor family member T1/ST2 in T helper cell type 2-mediated lung mucosal immune responses. *J Exp Med* 1999;190:895-902.
64. Imaeda H, Andoh A, Aomatsu T, Uchiyama K, Bamba S, Tsujikawa T, Naito Y, Fujiyama Y. Interleukin-33 suppresses Notch ligand expression and prevents goblet cell depletion in dextran sulfate sodium-induced colitis. *Int J Mol Med* 2011;28:573-578.
65. Sedhom MA, Pichery M, Murdoch JR, Foligne B, Ortega N, Normand S, Mertz K, Sanmugalingam D, Brault L, Grandjean T, *et al*. Neutralisation of the interleukin-33/ST2 pathway ameliorates experimental colitis through enhancement of mucosal healing in mice. *Gut* 2013;62:1714-1723.
66. Seidelin JB, Bjerrum JT, Coskun M, Widjaya B, Vainer B, Nielsen OH. IL-33 is upregulated in colonocytes of ulcerative colitis. *Immunol Lett* 2010;128:80-85.
67. Oboki K, Ohno T, Kajiura N, Arae K, Morita H, Ishii A, Nambu A, Abe T, Kiyonari H, Matsumoto K, *et al*. IL-33 is a crucial amplifier of innate rather than acquired immunity. *Proc Natl Acad Sci U S A* 2010;107:18581-18586.
68. Boehm G, Moro G. Structural and functional aspects of prebiotics used in infant nutrition. *J Nutr* 2008;138:S1818-S1828.
69. Arslanoglu S, Moro GE, Boehm G. Early supplementation of prebiotic oligosaccharides protects formula-fed infants against infections during the first 6 months of life. *J Nutr* 2007;137:2420-2424.
70. Arslanoglu S, Moro GE, Schmitt J, Tandoi L, Rizzardi S, Boehm G. Early dietary intervention with a mixture of prebiotic oligosaccharides reduces the incidence of allergic manifestations and infections during the first two years of life. *J Nutr* 2008;138:1091-1095.
71. Moro G, Arslanoglu S, Stahl B, Jelinek J, Wahn U, Boehm G. A mixture of prebiotic oligosaccharides reduces the incidence of atopic dermatitis during the first six months of age. *Arch Dis Child* 2006;91:814-819.
72. Zhang L, Li J, Young LH, Caplan MJ. AMP-activated protein kinase regulates the assembly of epithelial tight junctions. *Proc Natl Acad Sci U S A* 2006;103:17272-17277.
73. Walsh SV, Hopkins AM, Chen J, Narumiya S, Parkos CA, Nusrat A. Rho kinase regulates tight junction function and is necessary for tight junction assembly in polarized intestinal epithelia. *Gastroenterology* 2001;121:566-579.
74. Matter K, Balda MS. Signalling to and from tight junctions. *Nat Rev Mol Cell Biol* 2003;4:225-236.
75. Terry S, Nie M, Matter K, Balda MS. Rho signaling and tight junction functions. *Physiology* 2010;25:16-26.
76. Marzesco AM, Dunia I, Pandjaitan R, Recouvreur M, Dauzonne D, Benedetti EL, Louvard D, Zahraoui A. The small GTPase Rab13 regulates assembly of

- functional tight junctions in epithelial cells. *Mol Biol Cell* 2002;13:1819-1831.
77. Kohler K, Louvard D, Zahraoui A. Rab13 regulates PKA signaling during tight junction assembly. *J Cell Biol* 2004;165:175-180.
78. Sheth B, Fontaine JJ, Ponza E, McCallum A, Page A, CitiS, Louvard D, Zahraoui A, Fleming TP. Differentiation of the epithelial apical junctional complex during mouse preimplantation development: a role for rab13 in the early maturation of the tight junction. *Mech Dev* 2000;97:93-104.
79. Zheng B, Cantley LC. Regulation of epithelial tight junction assembly and disassembly by AMP-activated protein kinase. *Proc Natl Acad Sci U S A* 2007;104:819-822.
80. Niessen CM. Tight junctions/adherens junctions: basic structure and function. *J Invest Dermatol* 2007;127:2525-2532.
81. Schnoor M. E-cadherin Is Important for the Maintenance of Intestinal Epithelial Homeostasis Under Basal and Inflammatory Conditions. *Dig Dis Sci* 2015;60:816-818.
82. Balda MS, Matter K. Epithelial cell adhesion and the regulation of gene expression. *Trends Cell Biol* 2003;13:310-318.
83. Tsukita S, Furuse M, Itoh M. Multifunctional strands in tight junctions. *Nat Rev Mol Cell Biol* 2001;2:285-293.
84. Varasteh S, Braber S, Garssen J, Fink-Gremmels J. Galacto-oligosaccharides exert a protective effect against heat stress in a Caco-2 cell model. *J Funct Foods* 2015;16:265-277.
85. Cray JA, Russell JT, Timson DJ, Singhal RS, Hallsworth JE. A universal measure of chaotropy and kosmotropy. *Environ Microbiol* 2013;15:287-296.
86. Krishnaswamy R, Devaraj SN, Padma VV. Lutein protects HT-29 cells against Deoxynivalenol-induced oxidative stress and apoptosis: prevention of NF-kappaB nuclear localization and down regulation of NF-kappaB and Cyclo-Oxygenase-2 expression. *Free Radic Biol Med* 2010;49:50-60.
87. Fang H, Wu Y, Guo J, Rong J, Ma L, Zhao Z, Zuo D, Peng S. T-2 toxin induces apoptosis in differentiated murine embryonic stem cells through reactive oxygen species-mediated mitochondrial pathway. *Apoptosis* 2012;17:895-907.
88. Yang W, Yu M, Fu J, Bao W, Wang D, Hao L, Yao P, Nussler AK, Yan H, Liu L. Deoxynivalenol induced oxidative stress and genotoxicity in human peripheral blood lymphocytes. *Food Chem Toxicol* 2014;64:383-396.
89. Wu QH, Wang X, Yang W, Nussler AK, Xiong LY, Kuca K, Dohnal V, Zhang XJ, Yuan ZH. Oxidative stress-mediated cytotoxicity and metabolism of T-2 toxin and deoxynivalenol in animals and humans: an update. *Arch Toxicol* 2014;88:1309-1326.
90. Moro G, Minoli I, Mosca M, Fanaro S, Jelinek J, Stahl B, Boehm G. Dosage-related bifidogenic effects of galacto- and fructooligosaccharides in formula-fed term infants. *J Pediatr Gastroenterol Nutr* 2002;34:291-295.
91. Fanaro S, Marten B, Bagna R, Vigi V, Fabris C, Pena-Quintana L, Arguelles F, Scholz-Ahrens KE, Sawatzki G, Zelenka R, *et al.* Galacto-oligosaccharides are bifidogenic and safe at weaning: a double-blind randomized multicenter study. *J Pediatr Gastroenterol Nutr* 2009;48:82-88.
92. Ishikawa H, Matsumoto S, Ohashi Y, Imaoka A, Setoyama H, Umesaki Y, Tanaka R, Otani T. Beneficial effects of probiotic bifidobacterium and galacto-oligosaccharide in patients with ulcerative colitis: a randomized controlled study. *Digestion* 2011;84:128-133.
93. Silk DB, Davis A, Vulevic J, Tzortzis G, Gibson GR. Clinical trial: the effects of a trans-galactooligosaccharide prebiotic on faecal microbiota and symptoms in irritable bowel syndrome. *Aliment Pharmacol Ther* 2009;29:508-518.
94. Fanaro S, Boehm G, Garssen J, Knol J, Mosca F, Stahl B, Vigi V. Galacto-oligosaccharides and long-chain fructo-oligosaccharides as prebiotics in infant



- formulas: a review. *Acta Paediatr* 2005;94:22-26.
95. Varasteh S, Braber S, Akbari P, Garssen J, Fink-Gremmels J. Differences in Susceptibility to Heat Stress along the Chicken Intestine and the Protective Effects of Galacto-Oligosaccharides. *PLoS One* 2015;10:e0138975.
96. Wang H, Zhang C, Wu G, Sun Y, Wang B, He B, Dai Z, Wu Z. Glutamine enhances tight junction protein expression and modulates corticotropin-releasing factor signaling in the jejunum of weanling piglets. *J Nutr* 2015;145:25-31.
97. Vendrig JC, Coffeng LE, Fink-Gremmels J. Effects of orally administered galacto-oligosaccharides on immunological parameters in foals: a pilot study. *BMC Vet Res* 2014;10:278.
98. Zenhom M, Hyder A, de Vrese M, Heller KJ, Roeder T, Schrezenmeir J. Prebiotic oligosaccharides reduce proinflammatory cytokines in intestinal Caco-2 cells via activation of PPARgamma and peptidoglycan recognition protein 3. *J Nutr* 2011;141:971-977.
99. Johnson-Henry KC, Pinnell LJ, Waskow AM, Irrazabal T, Martin A, Hausner M, Sherman PM. Short-chain fructo-oligosaccharide and inulin modulate inflammatory responses and microbial communities in Caco2-bbe cells and in a mouse model of intestinal injury. *J Nutr* 2014;144:1725-1733.
100. de Kivit S, Kraneveld AD, Knippels LM, van Kooyk Y, Garssen J, Willemsen LE. Intestinal epithelium-derived galectin-9 is involved in the immunomodulating effects of nondigestible oligosaccharides. *J Innate Immun* 2013;5:625-638.
101. Badia R, Lizardo R, Martinez P, Brufau J. Oligosaccharide structure determines prebiotic role of beta-galactomannan against *Salmonella enterica* ser. Typhimurium *in vitro*. *Gut Microbes* 2013;4:72-75.
102. Shoaf K, Mulvey GL, Armstrong GD, Hutkins RW. Prebiotic galactooligosaccharides reduce adherence of enteropathogenic *Escherichia coli* to tissue culture cells. *Infect Immun* 2006;74:6920-6928.
103. Lehmann S, Hiller J, van Bergenhenegouwen J, Knippels LM, Garssen J, Traidl-Hoffmann C. *In Vitro* Evidence for Immune-Modulatory Properties of Non-Digestible Oligosaccharides: Direct Effect on Human Monocyte Derived Dendritic Cells. *PLoS One* 2015;10:e0132304.
104. Ortega-Gonzalez M, Ocon B, Romero-Calvo I, Anzola A, Guadix E, Zarzuelo A, Suarez MD, Sanchez de Medina F, Martinez-Augustin O. Nondigestible oligosaccharides exert nonprebiotic effects on intestinal epithelial cells enhancing the immune response via activation of TLR4-NFkappaB. *Mol Nutr Food Res* 2014;58:384-393.
105. de Kivit S, Kraneveld AD, Garssen J, Willemsen LE. Glycan recognition at the interface of the intestinal immune system: target for immune modulation via dietary components. *Eur J Pharmacol* 2011;668:S124-S132.
106. Nio-Kobayashi J, Takahashi-Iwanaga H, Iwanaga T. Immunohistochemical localization of six galectin subtypes in the mouse digestive tract. *J Histochem Cytochem* 2009;57:41-50.
107. de Kivit S, van Hoffen E, Korthagen N, Garssen J, Willemsen LE. Apical TLR ligation of intestinal epithelial cells drives a Th1-polarized regulatory or inflammatory type effector response *in vitro*. *Immunobiology* 2011;216:518-527.
108. Goehring KC, Kennedy AD, Prieto PA, Buck RH. Direct evidence for the presence of human milk oligosaccharides in the circulation of breastfed infants. *PLoS One* 2014;9:e101692.
109. Difilippo E, Bettonvil M, Willems HA, Braber S, Fink-Gremmels J, Jeurink PV, Schoterman M, Gruppen H, Schols HA. Oligosaccharides in urine, blood, and feces of piglets fed on milk replacer containing galacto-oligosaccharides. *J Agric Food Chem* 2015.
110. Mantis NJ, Rol N, Corthesy B. Secretory IgA's complex roles in immunity and mucosal homeostasis in the gut. *Mucosal Immunol* 2011;4:603-611.
111. O'Flaherty S, Saulnier DM, Pot B, Versalovic J. How can probiotics and prebiotics impact mucosal immunity? *Gut Microbes* 2010;1:293-300.
112. Hardy H, Harris J, Lyon E, Beal J, Foey AD. Probiotics,

- prebiotics and immunomodulation of gut mucosal defences: homeostasis and immunopathology. *Nutrients* 2013;5:1869-1912.
113. Caballero-Franco C, Keller K, De Simone C, Chadee K. The VSL#3 probiotic formula induces mucin gene expression and secretion in colonic epithelial cells. *Am J Physiol Gastrointest Liver Physiol* 2007;292:G315-G322.
  114. Juge N. Microbial adhesins to gastrointestinal mucus. *Trends Microbiol* 2012;20:30-39.
  115. Bergstrom KS, Xia L. Mucin-type O-glycans and their roles in intestinal homeostasis. *Glycobiology* 2013;23:1026-1037.
  116. Johansson ME, Larsson JM, Hansson GC. The two mucus layers of colon are organized by the MUC2 mucin, whereas the outer layer is a legislator of host-microbial interactions. *Proc Natl Acad Sci U S A* 2011;108:S4659-S4665.
  117. Bhatia S, Prabhu PN, Benefiel AC, Miller MJ, Chow J, Davis SR, Gaskins HR. Galacto-oligosaccharides may directly enhance intestinal barrier function through the modulation of goblet cells. *Mol Nutr Food Res* 2015;59:566-573.
  118. Pinton P, Graziani F, Pujol A, Nicoletti C, Paris O, Ernouf P, Di Pasquale E, Perrier J, Oswald IP, Maresca M. Deoxynivalenol inhibits the expression by goblet cells of intestinal mucins through a PKR and MAP kinase dependent repression of the resistin-like molecule beta. *Mol Nutr Food Res* 2015;59:1076-1087.
  119. Boullier S, Tanguy M, Kadaoui KA, Caubet C, Sansonetti P, Corthesy B, Phalipon A. Secretory IgA-mediated neutralization of *Shigella flexneri* prevents intestinal tissue destruction by down-regulating inflammatory circuits. *J Immunol* 2009;183:5879-5885.
  120. Mathias A, Longet S, Corthesy B. Agglutinating secretory IgA preserves intestinal epithelial cell integrity during apical infection by *Shigella flexneri*. *Infect Immun* 2013;81:3027-3034.
  121. Alizadeh A, Akbari P, Difilippo E, Schols HA, Ulfman LH, Schoterman MHC, Garssen J, Fink-Gremmels J, Braber S. The piglet as a model for studying dietary components in infant diets: effects of galacto-oligosaccharides on intestinal functions. *Br J Nutr* 2015.
  122. Cebra JJ. Influences of microbiota on intestinal immune system development. *Am J Clin Nutr* 1999;69: S1046-S1051.
  123. Moreau MC, Gaboriau-Routhiau V. Influence of Resident Intestinal Microfora on the Development and Functions of the Gut-Associated Lymphoid Tissue. *Microb Ecol Health Dis* 2001;13:65-86.
  124. Walker WA, Iyengar RS. Breast milk, microbiota, and intestinal immune homeostasis. *Pediatr Res* 2015;77:220-228.



# *Appendices*



Nederlandse samenvatting

Acknowledgements

Curriculum Vitae

List of publications & Awards





## Nederlandse samenvatting



---

Het darmstelsel bevat een enorm groot aantal micro-organismen, gezamenlijk de microbiota genoemd. De kolonisatie van de darm begint al tijdens de 1<sup>e</sup> levensuren en de bacteriën waarmee de pasgeborene in de eerste periode in aanraking komt, bepalen grotendeels de uiteindelijke samenstelling van de microbiota. Een gezonde darm- en vaginale flora van de moeder ondersteund door de functionele ingrediënten in moedermelk zijn de eerste aanzet voor een gezonde darmflora van het kind. Deze darmflora is direct betrokken bij de ontwikkeling van het immuunsysteem en steeds meer onderzoeken wijzen uit dat de eerste kolonisatie van de darm cruciaal is voor reactiviteit van het immuunsysteem later in het leven. De “goede” bacteriën in de darm kunnen het immuunsysteem ondersteunen en werken dus beschermend tegen allergieën, ontstekingen of auto-immuun ziekten.

Ons darmkanaal wordt voortdurend blootgesteld aan binnendringende, potentieel schadelijke elementen, zoals natuurlijke antigenen, pathogenen, en toxinen. Mycotoxinen, de door schimmels geproduceerde chemische stoffen, zijn veel voorkomende natuurlijke voedselcontaminanten die in het dagelijkse dieet voorkomen en geassocieerd worden met (acute en chronische) ziekteverschijnselen bij mens en dier. Het mycotoxine deoxynivalenol (DON), een toxine geproduceerd door verschillende soorten van het genus *Fusarium*, komt voor op granen, zoals tarwe, en maïs. DON is een zeer stabiel molecuul en kan niet door verhitting geneutraliseerd worden en is daarom ook vaak aanwezig in verwerkte graanproducten. De negatieve effecten van het mycotoxine DON op mens en dier komen steeds meer aan het licht en recent is gebleken dat DON de darmbarrière kan beïnvloeden. De darmbarrière is een van de eerste verdedigingslinies van het lichaam en zorgt ervoor dat ziekteverwekkers en schadelijke stoffen uit de omgeving en de voeding het lichaam niet binnendringen. De intrinsieke component van de darmbarrière bestaat uit een laag epitheelcellen, die door tight junctions met elkaar verbonden zijn. Tight junctions zijn eiwitten die het “cement” tussen de darmepitheelcellen vormen om te voorkomen dat antigenen, pathogenen en toxinen uit het lumen in de bloedbaan terecht komen. Tevens spelen mucus (slijm) en antimicrobiële peptiden geproduceerd door Goblet cellen (slijmbekercellen) en Paneth cellen een rol bij het beschermen van de darm tegen ziekteverwekkers.

Baby's (en pasgeboren dieren) hebben een functioneel immatuur (onrijp) en immuno-naïef darmstelsel bij de geboorte en zijn door de verhoogde doorlaatbaarheid van de darm zeer gevoelig voor potentieel schadelijke stoffen. Blootstelling aan toxinen kan direct leiden tot malabsorptie van nutriënten en lokale ontstekingsreacties. Deze verhoogde doorlaatbaarheid van het epitheel tijdens de vroege levensfasen kan zelfs leiden tot een verhoogde kans op chronische ontstekingsreacties later in het leven, zoals allergieën en auto-immuunziekten.

Bij de postnatale ontwikkeling van de microbiota en het immuunsysteem lijken oligosacchariden, complexe suikers die in grote mate voorkomen in moedermelk, een



essentiële rol te spelen. Helaas is het geven van borstvoeding niet altijd mogelijk voor alle vrouwen, en is het zoeken naar alternatieven voor deze prebiotische oligosacchariden een uitdaging. Een veel gebruikt alternatief of aanvulling van moedermelk zijn producten met toegevoegde galacto- and fructo-oligosacchariden (GOS en FOS), die ook prebiotische activiteit vertonen en de samenstelling van de microbiota in de darm van kinderen die borstvoeding krijgen, kunnen evenaren. Eerdere onderzoeken hebben deze positieve effecten op de microbiota en het gerelateerde immuunsysteem in de darm veelvuldig bevestigd. Het hier gerepresenteerde onderzoek richt zich dan ook op andere, microbiota-onafhankelijke effecten van deze oligosacchariden en beschrijft hun werking op de darmepitheelbarrière en functie. De verschillende *in vitro* en *in vivo* modellen, die ontwikkeld zijn om deze effecten duidelijk te maken, zijn beschreven in dit proefschrift.

### **Doel en overzicht van het proefschrift**

Het doel van dit proefschrift is het uitbreiden van de huidige kennis betreffende effecten van niet verteerbare oligosacchariden op een verstoorde darmbarrière en het darm-gerelateerde immuunsysteem. Om dit doel te bereiken zijn de volgende subdoelen behandeld in het proefschrift:

1. Het opzetten van reproduceerbare *in vitro* en *in vivo* modellen, die gebruikt kunnen worden om de effecten van niet verteerbare oligosacchariden op de beschadiging van de darmbarrière te testen.
2. Het bepalen en vergelijken van de directe, microbiota-onafhankelijke effecten van niet verteerbare oligosacchariden op darmbarrière verstoringen in epitheelcellen en meer kennis vergaren betreffende de invloed van de structuur en grootte van deze oligosacchariden op dit beschermende effect.
3. Het onderzoeken van het effect van niet verteerbare oligosacchariden op het immuun systeem na darmbarrière verstoringen met de nadruk op cytokines geproduceerd door epitheelcellen (CXCL8) en T helper 2 gemedieerde cytokines (IL-33/ST2 systeem).

**Hoofdstuk 2** geeft een overzicht van de verschillende tight junctions, die een rol spelen in het handhaven van de darmbarrière functie, gericht op de moleculaire structuur, het voorkomen in de darm en hun klinische relevantie. Tight junctions zijn opgebouwd uit transmembraaneiwitten (o.a. occludine en claudine), die interageren met intracellulaire eiwitten (scaffolding eiwitten), zoals zona occludens 1 (ZO-1), die transmembraan eiwitten verankeren aan het actinecytoskelet. De meest belangrijke functie van de tight junctions tussen de aangrenzende cellen is het voorkomen van een paracellulair transport van antigenen, pathogenen en toxinen uit het lumen. De interactie tussen verschillende tight junction eiwitten is van groot belang voor het behouden van een goede darmintegriteit en een goed gereguleerde barrière is cruciaal voor de homeostase in de darm. Verstoring van de darmbarrière kan leiden tot de ontwikkeling van verschillende chronische ontstekingsprocessen, zoals inflammatory bowel disease (ziekte van Crohn en colitis

---

ulcerosa), coeliakie en andere allergische reacties tegen antigenen uit de voeding.

In **Hoofdstuk 3** wordt op de betekenis van mycotoxinen in de humane voeding ingegaan. De contaminatie van (humane en dierlijke) voeding met mycotoxinen is een wereldwijd probleem en verdient steeds meer aandacht door de verhoogde prevalentie van deze natuurlijke toxines in granen en graanproducten. Uit recente onderzoeken is gebleken, dat verschillende mycotoxinen ook schadelijke effecten teweeg kunnen brengen in de darm, omdat ze het darmepitheel direct aantasten. In **Hoofdstuk 3** worden de effecten van verschillende mycotoxinen op de darmbarrière beschreven gebaseerd op *in vitro* en *in vivo* data. Blootstelling aan deoxynivalenol (DON), T-2/HT-2 toxin, patulin, ochratoxin A, fumonisin B<sub>1</sub> of aflatoxins kan in verschillende mate de darmbarrière functie verstoren. Door de mogelijke aanwezigheid van mycotoxinen in moedermelk en de onvolgroeide darmbarrière bij pasgeborenen, zijn kinderen bijzonder gevoelig voor blootstelling aan deze toxinen. Het meest bekende voorbeeld van een mycotoxine die de darmbarrière verstoort, is het *Fusarium* toxine DON, dat tevens bekend is geworden door zijn pro-inflammatoire en immuun-modulatoire eigenschappen.

In **Hoofdstuk 4** ligt de focus op de opheldering van de cascade van schadelijke effecten geïnduceerd door het mycotoxine DON en deze cascade leidt uiteindelijk tot een beschadiging van de darmbarrière. Een van de typische effecten van DON, gemeten in een *in vitro* model met Caco-2 cellen, een wel bekende epitheliale cellijn afkomstig van het menselijke colon, is het verlies van de barrière integriteit. Dit is gemeten door bepaling van de elektrische weerstand van de cellaag. Een interessante bevinding bij deze proeven is het feit, dat de verstoring van de barrierefunctie niet alleen afhankelijk is van de mycotoxine concentratie en tijd van blootstelling, maar de mate van verstoring wordt ook bepaald door de blootstellingsroute, waarbij de volgende rangorde in de ernst van het effect bepaald is: apicaal en basolateraal  $\geq$  basolateraal  $>$  apicaal. Tevens is de paracellulaire transport van markermoleculen verhoogd in epitheelcellen gestimuleerd met DON en in muizen die een orale gavage met DON hebben gehad. Zowel de *in vitro* experimenten met de darmepitheelcellen blootgesteld aan DON, als de *in vivo* experimenten met muizen blootgesteld aan DON, laten zien dat het tight junction network verstoord is. DON heeft ook een negatief effect op de histomorfologie van de dunne darm, want zowel de villus lengte als de oppervlakte van de villus zijn afgenomen.

In **Hoofdstuk 5** zijn experimenten beschreven, die laten zien, dat de door DON verstoorde integriteit van de darmbarrière, voor een groot gedeelte kan worden voorkomen, indien de Caco-2 cellen van tevoren worden "beschermd" door GOS, het prototype van niet-verteerbare oligosacchariden. GOS staat bekend om zijn potentiële anti-inflammatoire en immuun-modulatoire effecten in de darm. De hier gepresenteerde onderzoeken laten zien, dat GOS niet alleen een prebiotische werking heeft (invloed op de samenstelling van de microbiota), maar kan ook direct de darmbarrière ondersteunen door de vorming van

tight junctions te bevorderen. Deze werking van GOS, i.e. het herstel van de verstoring in het tight junction netwerk werd zowel *in vitro* alsmede *in vivo* in experimenten met muizen aangetoond. Met betrekking tot het immuunsysteem is bewezen dat de synthese en release van interleukine-8 (CXCL8) en CXCL1 (muis homoloog voor CXCL8), een belangrijke mediator bij ontstekingsprocessen, geïnduceerd wordt door DON. Ook dit effect van DON kan worden onderdrukt door voorbehandeling met GOS. Ook de veranderingen in de structuur van de darm, zoals de veranderingen in de villus architectuur na DON blootstelling zijn verminderd na toediening van een GOS dieet voorafgaand aan de orale gavage met DON.

In **Hoofdstuk 6** worden onderzoeken naar de actieve structuren in GOS beschreven. GOS is een fermentatieproduct dat bestaat uit een mengsel van oligosacchariden met verschillende moleculaire structuren (degree of polymerization, DP). Het werd gepostuleerd dat mogelijk de structuur en grootte van individuele oligosacchariden een rol spelen bij de beschermende effecten op darmbarrière. In het *in vitro* testsysteem met humane darmepitheelcellen blootgesteld aan DON zijn daarom verschillende oligosacchariden getest: GOS (Vivinal® GOS siroop en gezuiverde GOS, gemaakt uit lactose), FOS (fructo-oligosacchariden) en Inuline (gemaakt uit planten). De effecten van deze verschillende oligosacchariden op epitheelbarrière integriteit en CXCL8 release zijn vergeleken. Duidelijke onderlinge verschillen tussen de oligosacchariden zijn waargenomen met betrekking tot de effecten op epitheelbarrière functie. Vivinal® GOS siroop vertoont de meest duidelijke beschermende effecten op epitheelbarrière integriteit, en gezuiverd GOS, FOS en Inuline zijn minder potent. Naast de effecten op barrière functie, remt alleen Vivinal® GOS siroop de ontstekingsreactie (CXCL8 release) geïnduceerd door DON. Er kan niet worden uitgesloten met deze experimenten, dat andere resultaten zullen worden verkregen indien er rekening gehouden wordt met de aanwezigheid van de microbiota. De geobserveerde verschillen tussen de oligosacchariden en de potentiële beschermende effecten van Vivinal® GOS siroop zijn dus blijkbaar afhankelijk van de oligosaccharide structuur, molecuulgrootte en mate van polymerisatie.

In **Hoofdstuk 7** wordt dieper ingegaan op het immuun-modulatorische effect van GOS op de T helper 2-geïnduceerde cytokine interleukine-33 (IL-33). IL-33 en zijn receptor ST2 spelen een belangrijke rol in mucosale weefsels, zoals de darm en de long, waar zij functioneren als alarmsignaal in reactie op weefselschade. Het IL-33/ST2 systeem is cruciaal voor het induceren van T helper 2 immuunreacties in verschillende ontstekingsziekten, zoals auto-immuunziekten, IBD en allergieën. Uit voorgaande onderzoeken is gebleven dat GOS niet alleen effect heeft op een verstoorde darmbarrière (zoals bediscussieerd in **Hoofdstuk 5** en **Hoofdstuk 6**), maar toevoeging van GOS/FOS aan zuigelingenvoeding lijkt ook het risico op allergische ziekten en infecties te verminderen. Daarom wordt in **Hoofdstuk 7** onderzocht of een dieet met GOS invloed heeft op IL-33 en zijn receptor ST2 in de darmen van muizen met een verstoorde darmbarrière en in de longen van muizen

---

met allergisch astma. GOS vermindert de verhoogde IL-33 expressie in de dunne darm geïnduceerd door DON en verlaagt de IL-33 eiwit niveaus en ST2 expressie in de longen van astmatische muizen. Deze veel belovende resultaten suggereren dat GOS niet alleen gebruikt kan worden als prebioticum in zuigelingenvoeding, maar tevens als functioneel ingrediënt om inflammatoire en allergische reacties te onderdrukken.

**In conclusie, de verschillende hoofdstukken uit dit proefschrift hebben de volgende belangrijke resultaten opgeleverd:**

- GOS heeft naast zijn eigenschappen als prebioticum, een microbiota-onafhankelijk effect op de darmbarrière integriteit, voornamelijk op het tight junction network.
- De directe, microbiota-onafhankelijke effecten van de verschillende oligosacchariden zijn niet alleen afhankelijk van de oligosaccharide structuur en concentratie, maar ook van de mate van polymerisatie.
- Een beschermend effect van (voornamelijk) GOS op de schadelijke effecten van het mycotoxine DON, een veel voorkomende voedselcontaminant.
- Een anti-inflammatoir effect van GOS op gestimuleerde darmepitheelcellen, aangetoond door de vermindering van CXCL8 productie.
- Een beschermend effect van GOS op de T helper 2 immuunreacties geïnduceerd door epitheelschade, aangetoond door een verlaging van de IL-33 expressie.

In de literatuur werden de effecten van GOS tot nu toe voornamelijk toegeschreven aan de prebiotische werking en dus de verandering in samenstelling van de microbiota van de darm. De resultaten in dit proefschrift betreffende de directe interactie van GOS met de darmepitheelcellen geven aanwijzingen voor andere moleculaire werkingsmechanismen van oligosacchariden en ruimere toepassingsmogelijkheden in de preventie van allergische en immuun-gemedieerde ontstekingsprocessen.



## Acknowledgements



---

What an adventure it has been doing this PhD project! But of course, the work done during the past four and a half years would not have been possible without the support of many people inside and outside the lab.

Firstly, I would like to thank you, Prof. Fink-Gremmels, dear promoter, for your fruitful input, for not letting the project fall off the main path. Somehow, you always found the time in the middle of your busy schedule. It was not all about science, I also have learned quite a lot from you outside the academic world. Our recent trip to Iran was a good chance for me to realize that you have a big heart and great personality. Thank you so much for all support, consideration and care. Thank you making my dream to become true, thank you for everything!

Prof. Garssen, my dear promoter, finding an elegant word to appreciate all you have done for me seems impossible. Words fail me to describe your kindness, dignity and generosity. I have been always treated so well by you and you have very much helped me not to fall down when I was stumbling. Thank you Prof. Garssen for being such a great gentleman.

I would like to thank my co-promoter Saskia, who supported me so immensely during these years of my PhD time. Dear Saskia, thank you for being very much involved in the project with practical and sound advice, valuable support and for teaching me how to think analytically and work independently. Whenever my heart was heavy, you patiently listened to me and helped me to stay positive and strong even in the darkest of life's moments. Thank you for being such a unique co-promoter.

Dear Aletta, my second co-promoter, I really appreciate your super-positive attitude that made me believe there is always a way and that an impasse does not exist. You kept paying me compliments on my research, which helped me a lot to stay motivated. Thank you for your all kindness.

I greatly appreciate the personal support of the Nutricia Research. This generosity has made my life so much easier.

And a word of gratitude to my UIPS colleagues: Frank, Linette, Paula, Caroline, Laura, Atanaska, Astrid, Gerard, Mojtaba, Betty, Pim, Gemma, Mara, Marga, Marlotte, Suzan, Kirsten, Suzanne and Jelle. Thank you all that you made the lab a friendly environment for working. I have always enjoyed chatting with you.

Dear Gert, I would like to thank you for being such a lovely person. We have had very great time with together during different meetings and few lab-day out. I always enjoyed talking with you about Iran and Iranian culture.

Dear Paul, as a coordinator of the PhD program, you have always patiently answered my numerous questions and helped me a lot. Dankje wel Paul!

A special thanks goes to Kim, thank you for all the guidance and your patience when I had questions. Without your help, I would have been definitely lost in the maze of PhD.

Bart, your valuable comments and suggestions helped me a lot throughout my PhD. You are truly deserved to be entitled as *a King of the lab*. I do appreciate your kind support.

My deepest thanks to Lidija for being such a kind and helpful person.

And a word of gratitude also to my IRAS colleagues and friends: Aneliya, Jan, Louska, Xueqing, Aida, Amos, Nynke, Regiane, Cyrina, Dax, Laura W, Laura K, Manon, Fiona, Floris, Jort, Hester P, Karin, Sandra, Evelyn, Sefanne, Veerle, Adrienne, Maarke, Stephan, Theo, Steven and Joris: I really had a great time working with you. Thank you for being such friendly colleagues.

Lilian, Marjolein and Felice, looking back at the time spent in the lab remind me of the great help that you always offered to everybody - among whom I certainly was not an exception. Dank je wel!

Joost, I had a good time chatting and working with you. I appreciate your friendly attention and recommendation for my future career.

Marianne, I have enjoyed our recent collaboration very much. Thanks for a unique opportunity; I learned a lot from that project.

Majorie, Remco and Martin, it was a great pleasure for me to have known you. I always enjoyed taking with you during our several coffee breaks.

Dear Raymond and Dear Joop, your humbleness have always surprised me. You were always interested to talk about history, culture and tradition of Iran with me and I truly liked our friendly conversations. Thanks for being such lovely persons.

Rob, I do appreciate your time helping me to make wonderful immunofluorescence images for my thesis and your help with my cover image.

Niels and Giulio, I really enjoyed the time we spent together. Sometimes talking for hours and eating food all-day-long with you guys and sometimes hanging out till midnight! I liked it all.



---

I would like to thank all friendly and helpful colleagues from CCC project. Prescilla, Paul, Margriet, Dianne, Laurien, Henk, Elisabetta and Rianne, it was a pleasure working with you.

Hendrik, I really appreciate our chats, your helpful attitude, the nice figure you made for our paper, and your positive energy.

Conny, thanks for making those wonderful illustrations for my thesis. I do appreciate your proficiency and patience.

I would like to express my sincere gratitude to my “paranymphs”, Saskia and Niels, for their unconditional and sincere friendship and generosity. Thank you both for being such kind and loyal friends.

***And there are so many other colleagues and friends that supported me in finding my way in my profession and my life:***

Dear Prof. Malekinejad, I have no words to express my gratitude to you. If my dreams are becoming true, it is because of you. I still do remember December 2010, when you surprised me by telling that I may have a chance to do my PhD at Utrecht University. I had mixed feelings that day, full of happiness, excitement and fear - but your words motivated me enough to start this PhD journey. I had such fantastic times with you also outside the lab while playing football, watching movies or eating out plus awesome memories during different conferences. Thanks for trusting in me, Thanks for believing in me, Thanks for everything and I hope that I will never disappoint you.

Dear Prof. Keshavarzian, words fail me to appreciate what you have done for me. You were trying so hard to find a job for me and all your efforts made me feel as if a close member of my family is helping me. Thanks for being such a unique and lovely person.

Dear Prof. Van Miert, thank you very much for your dignity and generosity. You helped me a lot when the life looked gloomy for me in my first year in The Netherlands. It was great to have tea and cake together mixed with relaxed conversations with you.

Lucas, I feel so lucky to have known someone like you. You took a good care of me during my first year living in The Netherlands. I had such a great time with you whether it was just sipping a cappuccino, making a tasty food or having sympathizing conversations we had as good brothers.

Farshad daei, you are one of the best person I've ever met. Those were the days we had together. Merci monsieur!

Apart from research, I enjoyed spending time with my Iranian friends. Nahid, Hamed, Mehrnoosh, Ali A, Mohadeseh, Ali S, Vida, Kamal, Sulmaz, Hamid, Fariba, Amir A, Neda S, Yaser, Shima, Neda K, Negar and Amir R. Thanks for the nice chats and great moments, we had together.

I was so lucky to have known few great Iranian families in The Netherlands. Sara and Ardalan, Atefeh and Sina, Maryam and Mojtaba, We had a great time together and I will never forget you and those wonderful days we spent all together. Thanks a lot for awesome memories.

Dear Farokh, thank you for being there when things were going wrong. Your special way of making things easy helped me a lot. Thanks for being such a kind and supportive person.

Farshad and Mazda, how great it has been to get to know you since I moved to The Netherlands! Without your optimism and your help, I might have not got over some of the obstacles on my way during the first year of my PhD.

Ali, Seyedhamed, Ehsan, Hamed, Hussein, Meisam and Ramin, thank you for all the wonderful and crazy times we had all together. Without you the life in Urmia would have been quiet difficult.

Dear Hojat, I can talk about you and our friendship for hours. A great friend who is more like a close member of my family. We grew up together and have had an awesome time spending next to each other. A famous phrase “out of sight, out of mind” was not definitely true for us. Thank you for being such a unique and loyal friend.

Arash, Soheil and Nafiseh, how can I appreciate 10 years of friendship? I am so glad that living in The Netherlands gave me the opportunity to get to know you more. It was really hard to be far away from my family and I would be definitely lost without you. Like a family, we spent all good periods and challenging ones next to each other. Thank you for all your absolute support, care and to make me feel home again.

Dear Shahla, although we haven't known each other for very long, but ever since that time, I've thoroughly enjoyed spending time together with you. Thank you very much for your kindness, care and calm attitude.

Nazanin, you deserve my sincere gratitude with lots of cordiality and respect. I hope we keep learning from each other. I truly admire your humble, kind and caring nature. Thank you for putting up with me when I am being impossible and grumpy.

---

I would like to thank my wonderful parents for their never ending love, care and support from close-by or far-away. Reza, پدر عزیزم, thank you very much for always encouraging me to leap further and even further! Your strong character has always inspired me to grow up. Shahnaz, مادر مهربانم, your warm smile, your limitless caring attitude, and incredible love have made my life so amazing. You both are the most special persons in my heart now and forever.

همیشه وجود شما مفهوم فداکاری و گذشت رو برام تداعی کرده و امیدوارم روزی شایستگی جبران ذره ای از دریای بی کران محبتتون رو داشته باشم. دوستتون دارم

My wonderful sister “لیلا جان” thank you very much for our inspiring discussions, your honest realistic opinions, and for the great times we have had since childhood. Dear Saeid, my dear brother-in-law, I do appreciate your wise advice and great understanding and thank you for being such a rational, patient and nice person.

Last but not least, my cute little nephew “نیمای عزیزم” on this day three years ago, you were born and brought so much happiness and joy to the family. Seeing you online and talking with you, even if it was few words, have always made my day so great. All my tiredness just goes away when you say “دائی جون خسته نباشی”. Thanks Nima for being such a sweet nephew.

*Peyman*



# Curriculum Vitae





Peyman Akbari was born on the 17<sup>th</sup> of September 1985 in Tabriz, Iran. After finishing high school, he participated in the National University Entrance Exam and was selected to study Veterinary Medicine at Urmia University, Iran. He successfully obtained his DVM degree in 2010 with a Grade Point Average (GPA) of 8.7/10. In 2011, he got a PhD position at Utrecht University, The Netherlands. His PhD program was a joint project between Utrecht Institute for Pharmaceutical Sciences (UIPS), Division of Immunopharmacology, and the Institute for Risk Assessment Sciences (IRAS) under the supervision of Prof. Dr. J. Garssen, Prof. Dr. J. Fink-Gremmels, Dr. S. Braber and Dr. A.D. Kraneveld. His research aimed to expand the current knowledge regarding the gut health promoting effects of non-digestible oligosaccharides focusing on the protection of the intestinal barrier integrity and subsequent modulation of the epithelial immune responses. He was trained in the Drug Innovation PhD program of the Graduate School of Life Sciences, Utrecht University. During his PhD training, Peyman received several awards including the Young Scientist Award of the European Association of Veterinary Pharmacology and Toxicology (EAVPT) in 2012, the Rudy Rabbinge Award of the Carbohydrate Competence Center (CCC) in 2013 and the Young Researcher Award of the Iranian International Congress of Toxicology (IRTOXICO) in 2015.



## List of publications & Awards



---

## List of publications

Bol-Schoenmakers M, Braber S, **Akbari P**, De Graaff P, Van Roest M, Kruijssen L, Smit JJ, Van Esch BCAM, Jeurink PV, Garssen J, Fink-Gremmels J, Pieters RHH. The mycotoxin deoxynivalenol facilitates allergic sensitization to whey in mice. *Mucosal Immunol* 2016; in press.

Alizadeh A, **Akbari P**, Difilippo E, Schols H, Ulfman LLH, Schoterman MHC, Garssen J, Fink-Gremmels J, Braber S. The piglet as a model for studying dietary components in infant diets: effects of galacto-oligosaccharides on intestinal functions. *Br J Nutr* 2016; 115 (4): 605-618.

Grozdanovic MM, Cavic M, Andjelković U, **Akbari P**, Smit JJ, Gavrovic-Jankulovic M. Kiwifruit cysteine protease actinidin compromises the intestinal barrier by disrupting tight junctions. *Biochim Biophys Acta* 2016; 1860 (3): 516-526.

Givi ME, **Akbari P**, Boon L, Puzovic VS, Bezemer GFG, Ricciardolo FLM, Folkerts G, Redegeld FA, Mortaz E. Dendritic cells inversely regulate airway inflammation in cigarette smoke-exposed mice. *Am J Physiol Lung Cell Mol Physiol* 2016; 310 (1): 95-102.

Varasteh S, Braber S, **Akbari P**, Garssen J, Fink-Gremmels J. Differences in susceptibility to heat stress along the chicken intestine and the protective effects of galacto-oligosaccharides. *PLoS ONE* 2015; 10(9): e0138975.

**Akbari P**, Verheijden KAT, Willemsen LEM, Kraneveld AD, Folkerts G, Garssen J, Fink-Gremmels J, Braber S. Inflammation-induced expression of the alarmin interleukin 33 can be suppressed by galacto-oligosaccharides. *Int Arch Allergy Immunol* 2015; 167(2): 127-136.

**Akbari P**, Braber S, Alizadeh A, Verheijden KAT, Schoterman MHC, Kraneveld AD, Garssen J, Fink-Gremmels J. Galacto-oligosaccharides protect the intestinal barrier by maintaining the tight junction network and modulating the inflammatory responses after a challenge with the mycotoxin deoxynivalenol in human Caco-2 cell monolayers and B6C3F<sub>1</sub> mice. *J Nut* 2015; 145(7): 1604-1613.

Rezaei A, Malekinejad H, Asri-Rezaei S, Farshid AB, **Akbari P**. Hawthorn ethanolic extracts with triterpenoids and flavonoids exert hepatoprotective effects and suppress the hypercholesterolemia-induced oxidative stress in rats. *Iran J Basic Med Sci* 2015; 18(7): 691-699.



Alizadeh A, Braber S, **Akbari P**, Garssen J, Fink-Gremmels J. Deoxynivalenol impairs weight gain and affects markers of gut health after low-dose, short-term exposure of growing pigs. *Toxins* 2015; 7(6): 2071-2095.

**Akbari P**, Braber S, Gremmels H, Koelink PJ, Verheijden KAT, Garssen J, Fink-Gremmels J. Deoxynivalenol: a trigger for intestinal integrity breakdown. *FASEB J* 2014; 28(6): 2414-2429.

**Akbari P**, Malekinejad H, Rahmani F, Rezabakhsh A, Fink-Gremmels J. Cyclopiazonic acid attenuates the serum level of divalent cations and augments the nitric oxide content and mRNA level of iNOS in the liver and kidneys of broiler chickens. *World Mycotoxin J* 2012; 5(2): 153-161.

Malekinejad H, **Akbari P**, Allymehr M, Hobbenaghi R, Rezaie A. Cyclopiazonic acid augments the hepatic and renal oxidative stress in broilers. *Hum Exp Toxicol* 2011; 30(8): 910-919.

**Akbari P**, Fink-Gremmels J, Willems HAM, Difilippo E, Schols H, Schoterman MHC, Garssen J, Braber S. Characterizing microbiota-independent effects of oligosaccharides on intestinal epithelial cells: insight into the role of structure and size. Submitted for publication.

**Akbari P**, Braber S, Varasteh S, Alizadeh A, Garssen J, Fink-Gremmels J. The intestinal barrier as an emerging target in the toxicological assessment of mycotoxins: a review. Submitted for publication.

## Awards

**1<sup>st</sup> Young Scientist Award** of 12<sup>th</sup> International Congress of the European Association for Veterinary Pharmacology and Toxicology (EAVPT), July 2012, Noordwijkerhout, The Netherlands.

**1<sup>st</sup> Rudy Rabbinge Award** for giving the best oral presentation at the Carbohydrate Competence Center (CCC), April 2013, Groningen, The Netherlands.

**1<sup>st</sup> Young Researcher Award** of 13<sup>th</sup> Iranian International Congress of Toxicology (IRTOXICO), May 2015, Urmia, Iran.





Education is what remains after one has forgotten  
what one has learned in school.

*Albert Einstein*